frontiers | Research Topics

Personalized medicine of diabetes retinopathy: from bench to bedside

Edited by
Kai Jin, Wenbin Wei, Honghua Yu and Andrzej Grzybowski

Published in
Frontiers in Endocrinology
Frontiers in Public Health

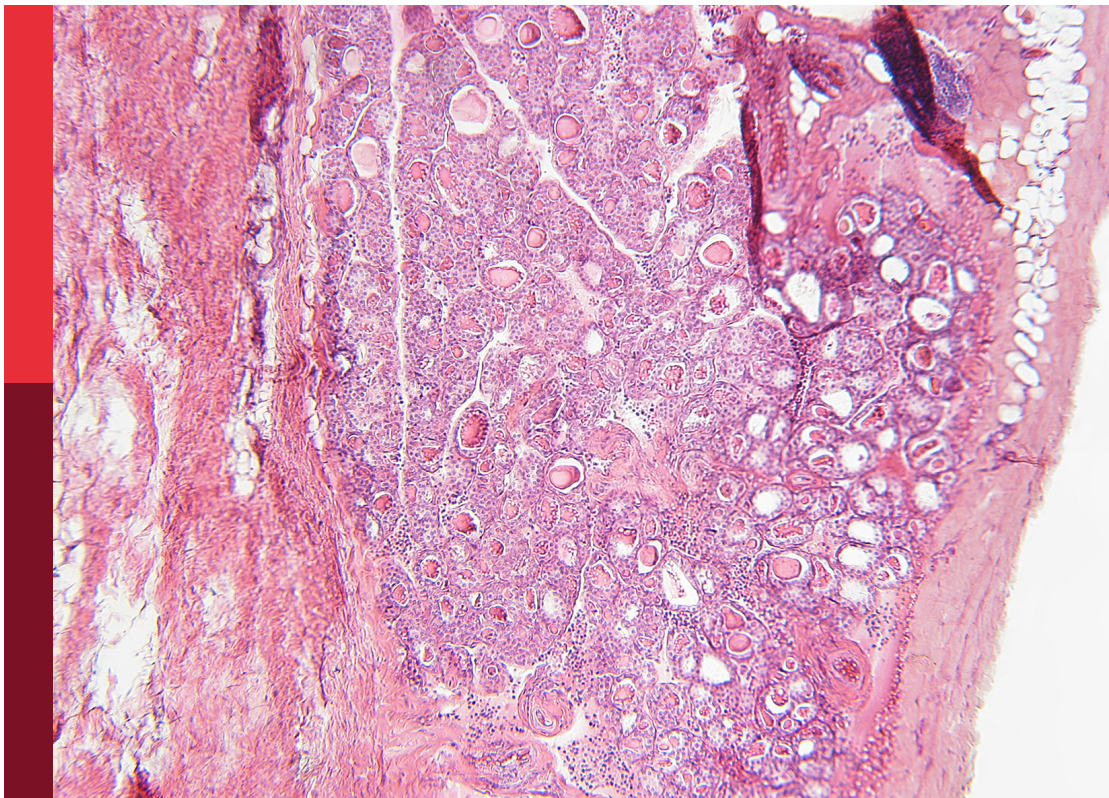

ISSN 1664-8714
ISBN 978-2-8325-6240-6
DOI 10.3389/978-2-8325-6240-6

About Frontiers

Frontiers is more than just an open access publisher of scholarly articles: it is a pioneering approach to the world of academia, radically improving the way scholarly research is managed. The grand vision of Frontiers is a world where all people have an equal opportunity to seek, share and generate knowledge. Frontiers provides immediate and permanent online open access to all its publications, but this alone is not enough to realize our grand goals.

Frontiers journal series

The Frontiers journal series is a multi-tier and interdisciplinary set of open-access, online journals, promising a paradigm shift from the current review, selection and dissemination processes in academic publishing. All Frontiers journals are driven by researchers for researchers; therefore, they constitute a service to the scholarly community. At the same time, the *Frontiers journal series* operates on a revolutionary invention, the tiered publishing system, initially addressing specific communities of scholars, and gradually climbing up to broader public understanding, thus serving the interests of the lay society, too.

Dedication to quality

Each Frontiers article is a landmark of the highest quality, thanks to genuinely collaborative interactions between authors and review editors, who include some of the world's best academicians. Research must be certified by peers before entering a stream of knowledge that may eventually reach the public - and shape society; therefore, Frontiers only applies the most rigorous and unbiased reviews. Frontiers revolutionizes research publishing by freely delivering the most outstanding research, evaluated with no bias from both the academic and social point of view. By applying the most advanced information technologies, Frontiers is catapulting scholarly publishing into a new generation.

What are Frontiers Research Topics?

Frontiers Research Topics are very popular trademarks of the *Frontiers journals series*: they are collections of at least ten articles, all centered on a particular subject. With their unique mix of varied contributions from Original Research to Review Articles, Frontiers Research Topics unify the most influential researchers, the latest key findings and historical advances in a hot research area.

Find out more on how to host your own Frontiers Research Topic or contribute to one as an author by contacting the Frontiers editorial office: frontiersin.org/about/contact

Personalized medicine of diabetes retinopathy: from bench to bedside

Topic editors

Kai Jin — Zhejiang University, China

Wenbin Wei — Capital Medical University, China

Honghua Yu — Guangdong Eye Institute, Department of Ophthalmology, Guangdong Provincial People's Hospital, China

Andrzej Grzybowski — University of Warmia and Mazury in Olsztyn, Poland

Citation

Jin, K., Wei, W., Yu, H., Grzybowski, A., eds. (2025). *Personalized medicine of diabetes retinopathy: from bench to bedside*. Lausanne: Frontiers Media SA. doi: 10.3389/978-2-8325-6240-6

Table of contents

frontiers | Frontiers in Endocrinology

TYPE Editorial
PUBLISHED 01 April 2025
DOI 10.3389/fendo.2025.1597332

OPEN ACCESS

EDITED AND REVIEWED BY
Åke Sjöholm,
Gävle Hospital, Sweden

*CORRESPONDENCE
Kai Jin
jinkai@zju.edu.cn

RECEIVED 21 March 2025
ACCEPTED 21 March 2025
PUBLISHED 01 April 2025

CITATION
Jin K, Yu H, Wei W and Grzybowski A (2025) Editorial: Personalized medicine of diabetes retinopathy: from bench to bedside.
Front. Endocrinol. 16:1597332.
doi: 10.3389/fendo.2025.1597332

Editorial: Personalized medicine of diabetes retinopathy: from bench to bedside

Kai Jin[1,2,3,4]*, Honghua Yu[5], Wenbin Wei[6] and Andrzej Grzybowski[7,8]

[1]Zhejiang University, Eye Center of Second Affiliated Hospital, School of Medicine, Hangzhou, China, [2]Zhejiang Provincial Key Laboratory of Ophthalmology, Zhejiang University, Hangzhou, China, [3]Zhejiang Provincial Clinical Research Center for Eye Diseases, Zhejiang University, Hangzhou, China, [4]Zhejiang Provincial Engineering Institute on Eye Diseases, Zhejiang University, Hangzhou, China, [5]Guangdong Eye Institute, Department of Ophthalmology, Guangdong Provincial People's Hospital, Southern Medical University, Guangzhou, China, [6]Beijing Tongren Eye Center, Beijing Tongren Hospital, Capital Medical University, Beijing, China, [7]Institute for Research in Ophthalmology, Foundation for Ophthalmology Development, Poznan, Poland, [8]Department of Ophthalmology, University of Warmia and Mazury, Olsztyn, Poland

KEYWORDS

diabetes retinopathy, etiology, biomarker, diagnosis, treatment

Editorial on the Research Topic
Personalized medicine of diabetes retinopathy: from bench to bedside

Introduction

Diabetic retinopathy (DR) stands as a prevalent complication of diabetes mellitus, imposing a substantial burden on individuals worldwide and serving as a leading cause of vision impairment among the middle-aged and elderly populations (1). The progression of DR encompasses various stages, ranging from the initial microvascular alterations to advanced manifestations such as proliferative DR and diabetic macular edema, which significantly compromise visual function (2). Traditionally conceived as primarily a microvascular disorder, emerging evidence underscores the intricate involvement of retinal neurodegeneration in the pathogenesis of DR.

Pathophysiological insights: beyond microvasculature

DR is a multifaceted disease driven by a persistent hyperglycemic environment characteristic of diabetes. Beyond microvascular alterations, the pathophysiological mechanisms orchestrating DR onset and progression are diverse and interconnected (3). Genetic predisposition, epigenetic modifications, oxidative stress-induced free radical generation, accumulation of advanced glycosylation end products, inflammatory mediators, and dysregulated vascular endothelial growth factor (VEGF) signaling collectively contribute to the intricate landscape of DR pathogenesis (4). This intricate

interplay of molecular pathways underscores the heterogeneous nature of DR, posing a significant challenge in devising tailored therapeutic strategies for individual patients.

Advancements in personalized medicine

The identification of distinct phenotypes of DR, characterized by unique molecular signatures and varying risks for vision-threatening complications, represents a significant breakthrough in patient stratification (5). Molecular profiling techniques, including genomics, proteomics, and metabolomics, have provided valuable insights into the underlying pathophysiological mechanisms of DR (6). By tailoring treatment strategies to match individual patient profiles, personalized medicine holds promise for optimizing therapeutic outcomes and minimizing treatment-related adverse effects.

Optimization of current treatment strategies

While anti-VEGF therapy and laser photocoagulation remain the mainstays of treatment for diabetic macular edema and proliferative DR, respectively, personalized medicine offers the opportunity to refine and optimize these approaches. Targeted therapies, guided by the specific molecular characteristics of each patient's disease, have the potential to enhance treatment efficacy and improve long-term visual outcomes (7, 8). By minimizing treatment burden and maximizing therapeutic benefit, personalized approaches aim to improve patient adherence and quality of life.

Challenges and opportunities

Despite the significant progress made in personalized medicine for DR, several challenges remain. Integration of omics technologies into clinical practice presents logistical and technical hurdles, including standardization of methodologies and interpretation of complex data sets (9). Additionally, the cost-effectiveness and accessibility of personalized approaches must be carefully considered to ensure equitable access to care for all patients (10). However, with continued advancements in technology and collaboration between researchers, clinicians, and industry partners, personalized medicine holds the promise of revolutionizing the management of DR and improving outcomes for patients worldwide.

Conclusions

In conclusion, the journey towards personalized medicine in DR represents a transformative paradigm shift, poised to revolutionize our approach to patient care and therapeutic decision-making. By embracing the principles of precision medicine and harnessing the power of molecular profiling and biomarker-driven strategies, we can strive towards optimizing visual outcomes and enhancing the quality of life for individuals afflicted with this sight-threatening complication of diabetes.

Author contributions

KJ: Writing – review & editing, Writing – original draft. HY: Writing – review & editing. WW: Writing – review & editing. AG: Writing – review & editing.

Conflict of interest

The authors declare that the research was conducted in the absence of any commercial or financial relationships that could be construed as a potential conflict of interest.

Generative AI statement

The author(s) declare that no Generative AI was used in the creation of this manuscript.

Publisher's note

References

1. Teo ZL, Tham YC, Yu M, Chee ML, Rim TH, Cheung N, et al. Global prevalence of diabetic retinopathy and projection of burden through 2045: systematic review and meta-analysis. *Ophthalmology*. (2021) 128:1580–91. doi: 10.1016/j.ophtha.2021.04.027

2. Sabanayagam C, Banu R, Chee ML, Lee R, Wang YX, Tan G, et al. Incidence and progression of diabetic retinopathy: a systematic review. *Lancet Diabetes Endocrinol*. (2019) 7:140–9. doi: 10.1016/S2213-8587(18)30128-1

3. Yue T, Shi Y, Luo S, Weng J, Wu Y, Zheng X. The role of inflammation in immune system of diabetic retinopathy: Molecular mechanisms, pathogenetic role and therapeutic implications. *Front Immunol*. (2022) 13:1055087. doi: 10.3389/fimmu.2022.1055087

4. Yamaguchi M, Nakao S. Identifying hyperreflective foci in diabetic retinopathy via VEGF-induced local self-renewal of CX3CR1+ Vitreous resident macrophages. *Diabetes*. (2022) 71:2685–701. doi: 10.2337/db21-0247

5. Li L, Cheng WY, Glicksberg BS, Gottesman O, Tamler R, Chen R, et al. Identification of type 2 diabetes subgroups through topological analysis of patient similarity. *Sci Trans Med*. (2015) 7:311ra174. doi: 10.1126/scitranslmed.aaa9364

6. Wang N, Ding L, Liu D, Zhang Q, Zheng G, Xia X, et al. Molecular investigation of candidate genes for pyroptosis-induced inflammation in diabetic retinopathy. *Front Endocrinol*. (2022) 13:918605. doi: 10.3389/fendo.2022.918605

7. Van Hove I, Hu TT, Beets K, Van Bergen T, Etienne I, Stitt AW, et al. Targeting RGD-binding integrins as an integrative therapy for diabetic retinopathy and neovascular age-related macular degeneration. *Prog retinal eye Res*. (2021) 85:100966. doi: 10.1016/j.preteyeres.2021.100966

8. Silva M, Peng T, Zhao X, Li S, Farhan M, Zheng W. Recent trends in drug-delivery systems for the treatment of diabetic retinopathy and associated fibrosis. *Advanced Drug delivery Rev*. (2021) 173:439–60. doi: 10.1016/j.addr.2021.04.007

9. Du X, Yang L, Kong L, Sun Y, Shen K, Cai Y, et al. Metabolomics of various samples advancing biomarker discovery and pathogenesis elucidation for diabetic retinopathy. *Front Endocrinol*. (2022) 13:1037164. doi: 10.3389/fendo.2022.1037164

10. Pasquel FJ, Hendrick AM, Ryan M, Cason E, Ali MK, Narayan KM. Cost-effectiveness of different diabetic retinopathy screening modalities. *J Diabetes Sci Technol*. (2015) 10:301–7. doi: 10.1177/1932296815624109

frontiers | Frontiers in Endocrinology

TYPE Original Research
PUBLISHED 25 August 2023
DOI 10.3389/fendo.2023.1218442

OPEN ACCESS

EDITED BY
Wenbin Wei,
Capital Medical University, China

REVIEWED BY
Claudio Bucolo,
University of Catania, Italy
Changzheng Chen,
Renmin Hospital of Wuhan University, China

*CORRESPONDENCE
Hong Wang
dr.wanghong@163.com

†These authors have contributed equally to this work

RECEIVED 07 May 2023
ACCEPTED 10 August 2023
PUBLISHED 25 August 2023

CITATION
Si M, Tao Y, Zhang Z, Zhao H, Cui W, Yang M and Wang H (2023) Retinal vein changes in patients with high-risk proliferative diabetic retinopathy treated with conbercept and panretinal photocoagulation co-therapy: a cohort study.
Front. Endocrinol. 14:1218442.
doi: 10.3389/fendo.2023.1218442

Retinal vein changes in patients with high-risk proliferative diabetic retinopathy treated with conbercept and panretinal photocoagulation co-therapy: a cohort study

Mingwei Si[1†], Yuan Tao[2†], Ziniu Zhang[3], Hui Zhao[1], Wenxuan Cui[1], Mengyao Yang[1] and Hong Wang[1*]

[1]Department of Ophthalmology, Qilu Hospital of Shandong University, Jinan, China, [2]Department of Ophthalmology, The Second People's Hospital of Jinan, Jinan, China, [3]Department of Acupuncture and Moxibustion, Dongzhimen Hospital, Beijing University of Chinese Medicine, Beijing, China

Objective: This study aimed to observe and compare retinal vein diameter changes and other essential indicators in patients with high-risk proliferative diabetic retinopathy (PDR) treated with intravitreal injection of conbercept (IVC) combined with panretinal photocoagulation (PRP) versus PRP monotherapy.

Methods: A retrospective analysis was conducted on data from patients with high-risk PDR who received specific treatment and were followed up for 24 months. Among 82 patients with high-risk PDR, 50 eyes received PRP combined with IVC, whereas 32 eyes received PRP alone. During the 24-month follow-up period, changes in best-corrected visual acuity (BCVA), central foveal thickness (CFT), retinal vein diameter, number of microaneurysms (MA), neovascularization (NV) area, hard exudate (HE) area, size of the foveal avascular zone (FAZ), superficial capillary plexus (SCP) blood flow density, and adverse effects were recorded and compared between the two groups at baseline and at 6, 12, 18, and 24 months after treatment. The relationship between each observation index and vein diameter was also analyzed.

Results: During the 24-month follow up, significant improvements in the BCVA, CFT, retinal vein diameter, number of MAs, NV area, HE area, FAZ, and SCP were observed in the IVC+PRP group after treatment. The PRP group only showed significant reductions in NV and HE areas. The IVC+PRP group showed significant superiority over the PRP group in improving the vein diameter, number of MA, and HE area. However, no statistically significant difference in NV area reduction was found between the groups.

Conclusion: In the treatment of high-risk PDR, IVC+PRP therapy has a significant advantage over PRP monotherapy. IVC+PRP therapy may reverse diabetes-induced retinal vein changes, restoring morphology and function.

KEYWORDS

high-risk proliferative diabetic retinopathy, conbercept, panretinal photocoagulation, therapeutic effect, retinal vein diameter

1 Introduction

Diabetic retinopathy (DR) is diabetes-induced microvascular damage to the retina, and it is currently the primary cause of avoidable blindness among the working-age population (1, 2). In 2020, 103.12 million people globally had DR, and it is projected to escalate to 160.50 million by 2045 (3). The duration of diabetes and severity of hyperglycemia are primary risk factors associated with DR (4). In addition, changes in retinal venous vessels can be observed in the early stages of diabetes, and a broader diameter of the retinal vein was identified as an independent risk factor for DR progression (5).

Proliferative DR (PDR) is an advanced stage of DR, and its diagnosis is based on the presence of retinal neovascularization (NV) or vitreous hemorrhage, which is caused by progressive damage to the retinal microvascular network (6, 7). PDR can be further defined based on the location and severity of NV, and a high-risk PDR is a more severe classification characterized by severe retinal ischemia and poor visual outcomes (8).

Panretinal photocoagulation (PRP) is still considered the conventional treatment for PDR (4). PRP involves destroying the non-perfused and ischemic areas of the peripheral retina, which results in retinal NV regression. This method aids in preserving central vision and decreasing the possibility of blindness in patients (6). The Early Treatment Diabetic Retinopathy Study (ETDRS) standard recommends early PRP in patients with high-risk PDR to effectively reduce the progression of retinal NV and PDR (9).

Anti-vascular endothelial growth factor (anti-VEGF) drugs, including ranibizumab, aflibercept, brolucizumab, faricima, conbercept, have been approved for the treatment of patients with DME, have changed the previous treatment paradigm of high-risk PDR with DME, which has demonstrated a crucial role in enhancing the best-corrected visual acuity (BCVA), lowering central foveal thickness (CFT), regulating exudation, and curbing NV (4, 10, 11). Conbercept is a recombinant soluble VEGF receptor decoy, like aflibercept. Both can fuse with the second immunoglobulin (Ig) domain of VEGF receptor 1 (VEGFR1), the third Ig domains of VEGFR2, the Fc region of human IgG and P1GF (12). Conbercept has an additional fourth Ig domain of VEGFR2 than aflibercept, which is critical for the receptor dimerization and the enhancement of the association rate of VEGF to the receptor (12). The SAILING study showed that using a pro re nata (PRN) IVC improved BCVA in patients with macular edema, and its efficacy was superior to laser photocoagulation therapy (13).

A meta-analysis reported that compared with PRP monotherapy, the combination therapy of IVC and PRP (IVC+PRP) had a more substantial effect on functional outcomes, such as bettering patient vision and decreasing macular edema (14). Moreover, previous retrospective studies have suggested the possibility of using anti-VEGF drugs to reverse DR by inducing changes in retinal pathology and physiology through reperfusion (15). Our previous study confirmed the efficacy of anti-VEGF drugs in patients with DR and observed a regression in vein diameter and venous beading after anti-VEGF therapy combined with PRP (16–18). However, no previous studies have focused on the changes in retinal vein diameter after IVC +PRP therapy. Current long-term research on the efficacy of IVC +PRP therapy in patients with high-risk PDR is limited, and changes in retinal pathology and physiology after anti-VEGF therapy and their significance need further exploration. Thus, in this retrospective cohort study, we aimed to compare and analyze the efficacy and changes in retinal vein diameter of the IVC+PRP group and PRP group in patients with high-risk PDR.

2 Materials and methods

2.1 Study design

This retrospective cohort study was conducted in compliance with the principles outlined in the Declaration of Helsinki. All patients gave informed consent for diagnosis and clinical procedures. Before treatment, all patients received detailed information about the potential risks involved, and they provided informed consent by signing a consent form for both IVC and PRP. The Medical Ethics Committee of Qilu Hospital of Shandong University approved this study (KYLL-2019-091).

2.2 Patients

Data of 82 patients with high-risk PDR (82 eyes) treated at Shandong University Qilu Hospital between January 2018 and December 2019 were retrospectively analyzed. In this study, high-risk PDR is defined based on the presence of NV accompanied by vitreous hemorrhage or NV without vitreous hemorrhage but occupying 1/3 to 1/4 of the optic disc area (8). Patients were divided into the IVC+PRP and PRP groups according to the treatment they received. The inclusion criteria were as follows: (1) patients with high-risk PDR diagnosed by fundus examination, fluorescein angiography (FFA), and optical coherence tomography (OCT); (2) patients with well-controlled blood glucose, glycated hemoglobin (GHb) <10%, and blood pressure <160/90 mmHg; (3) patients who received IVC+PRP or PRP monotherapy, and (4) patients followed up for a minimum of 24 months. The exclusion criteria were as follows: (1) Patients with diabetes types other than type 2 diabetes; (2) patients with other retinal diseases; (3) patients who underwent other types of intraocular therapies, including but not limited to intravitreal injection of other anti-VEGF agents or corticosteroids; and (4) patients with poor picture quality for various reasons including, but not limited to, refractive media opacities or proliferative membranes.

2.3 Data collection and follow up

The age, sex, eyes involved, disease duration, BCVA, CFT, retinal vein diameter, number of microaneurysms (MA), hard exudate (HE) area, NV area, size of the foveal avascular zone (FAZ), and superficial capillary plexus (SCP) blood flow density were collected by reviewing medical records. Adverse reactions during treatment were also recorded.

General information and medical history of patients were collected at the initial diagnosis. BCVA, color fundus photography (CFP), OCT, OCT angiography (OCTA), and FFA were performed on all patients at the initial diagnosis and at 6, 12, 18, and 24 months. The differences in each index before and after treatment and between groups at the above five time points were compared.

The primary efficacy analysis was based on changes in BCVA, CFT, and vein diameter. Other outcomes were considered secondary efficacy analyses.

BCVA was assessed using the ETDRS visual acuity chart. ZEISS Cirrus HD-OCT was used to acquire OCT images, and the built-in image processing software was used to measure CFT, which was the sum of subretinal fluid and neuroepithelial layer thickness. The Heidelberg Spectralis HRA fundus camera and video angiography were employed to measure the vein diameter, MA number, HE area, and NV area after image processing of the FFA. All vein measurements were taken from the photographs of the edge of 1–1.5 disc diameters centered on the optic disc. The maximum projected diameter of the largest six veins was manually measured, and the values were averaged to obtain the vein diameter using the proposed formula (19). For obtaining accurate and precise FFA results, images with a distinct outline of the retinal vein during the venous phase were used to eliminate the potential effect of neovascular leakage on the measurements. Following PRP, the examination of the peripheral retina was affected; therefore, the MA, HE area, and NV area were measured from FFA images of the retina within a 30-degree range centered on the fovea at 1 min. OCTA images were obtained using the ZEISS Cirrus HD-OCTA in the "HD Angio Retina 6 × 6 mm" mode, and FAZ and SCP were automatically measured. Two professional ophthalmologists reviewed all examination results.

In both groups, PRP was performed on patients by the same experienced ophthalmologist following the guidelines established by the DR Study Group (17). A frequency-doubled 532-nm laser (Lumenis Novus Omni, Lumenis Be, Inc., San Jose, USA) was used, with the patient's eye fully dilated before treatment. The laser reaction was grade III, and the spot size was set to 200 μm, pulse width to 200 ms, and power to 230 mW. Laser therapy started from the posterior pole and extended to two disc diameters (PD) from the temporal side of the macula and superior and inferior vascular arcades, and one PD from the nasal side of the optic disc to the peripheral retina. The distance between laser spots was one spot diameter. PRP was performed in four sessions, with 300–400 laser spots applied in each session.

In the PRP group, the above treatment was employed at the initial diagnosis. If NV did not regress during follow up, additional laser therapy was performed.

The IVC+PRP group received an additional three + PRN regimen of the IVC based on the PRP mentioned above. All patients received IVC once a month for the first three months (0.05 mL/0.5 mg; Chengdu Kanghong Pharmaceutical Group Co., Ltd., China). All injections were performed by the same experienced physician.

The IVC+PRP group underwent the first PRP 1 week after the initial IVC injection, and if NV persisted or recurred after three injections, IVC+PRP therapy was repeated.

2.4 Statistical analysis

The IBM SPSS Statistics version 25.0 (IBM Corp., Armonk, NY, USA) was utilized to conduct the statistical analyses. Continuous variables are presented as means ± standard deviations, whereas categorical variables are presented as percentages (%). Paired t-tests were employed for normally distributed data, whereas non-parametric tests were employed for non-normally distributed ones. Count data were compared using chi-square tests. Statistical significance was established at $P < 0.05$. In the correlation analysis, $|r| \leq 0.3$ indicated no linear correlation between variables.

3 Results

3.1 Baseline information

The baseline characteristics of the participants are shown in Table 1. This study included a total of 82 patients (82 eyes), of which 50 patients (50 eyes) were assigned to the IVC+PRP group and 32 patients (32 eyes) to the PRP group. The IVC+PRP and PRP groups did not exhibit any statistically significant differences in terms of age, sex, history of diabetes, number of MA, vein diameter, NV area, and HE area ($P > 0.05$; Table 1). However, significant differences were observed in BCVA and CFT ($P < 0.01$; Table 1).

3.2 BCVA and CFT

As significant differences in BCVA and CFT were found between the two groups at baseline, only BCVA and CFT changes in the IVC+PRP group were analyzed.

The BCVA of the IVC+PRP group exhibited the superiority of the measurement at 6, 12, 18, and 24 months post-treatment over pretreatment measurement ($P < 0.01$, respectively, Table 2, Figure 1A). The CFT measurements at 6, 12, 18, and 24 months post-treatment were lower than pretreatment measurements ($P < 0.01$, respectively, Table 2, Figure 1B). BCVA and CFT improved significantly in the first 6 months, and the therapeutic effect was maintained in the subsequent treatment.

3.3 Retinal vein diameter

Changes in the mean vein diameter in the two groups during the follow up are shown in Table 3, Figure 1C. At baseline, no significant difference was observed in the vein diameter between the two groups ($P > 0.05$). After IVC+PRP therapy, the retinal vein diameter in both groups was lower than that before treatment, and the diameter had a decreasing trend at 6 months of treatment, but without statistical significance ($P > 0.05$). At 12, 18, and 24 months of treatment, the decreasing trend of the retinal vein diameter continued at a slower rate, and the differences between the mean vein diameter and baseline were statistically significant ($P < 0.01$). No statistically significant difference in vein diameter changes was noted during the four follow up visits in the PRP group ($P > 0.05$).

10.3389/fendo.2023.1218442

TABLE 1 Baseline information.

	IVC+PRP (n = 50)	PRP (n = 32)	$t,\chi 2$	*P*
Sex, n (%)				
Male	26 (52.0%)	16 (50.0%)	0.03	0.86
Female	24 (48.0%)	16 (50.0%)		
Age (years)	62.12 ± 5.37	63.86 ± 6.03	1.37	0.18
Eyes				
Right eye	27 (54.0%)	15 (46.9%)	0.40	0.53
Left eye	23 (46.0%)	17 (53.1%)		
BCVA (LogMAR)	0.65 ± 0.15	0.46 ± 0.13	5.97	< 0.01
CFT (μm)	470.91 ± 44.14	295.43 ± 32.09	19.43	< 0.01
Duration of diabetes (years)	6.66 ± 2.14	7.58 ± 1.73	2.04	0.04

BCVA, best-corrected visual acuity; CFT, central foveal thickness.

TABLE 2 Changes in BCVA (logMAR) and CFT (μm) at baseline *vs.* different time points post-treatment in the IVC+PRP group.

BCVA	Baseline	6 m	12 m	18 m	24 m	CFT	Baseline	6 m	12 m	18 m	24 m
n = 50	0.65 ± 0.15	0.53 ± 0.15	0.52 ± 0.13	0.49 ± 0.15	0.55 ± 0.14		470.91 ± 44.14	303.77 ± 37.54	306.62 ± 35.86	297.63 ± 30.71	307.35 ± 32.17
t		4.30	4.70	5.29	3.75			20.40	20.43	22.79	21.18
P		< 0.01	< 0.01	< 0.01	< 0.01			< 0.01	< 0.01	< 0.01	< 0.01

BCVA, best-corrected visual acuity; CFT, central foveal thickness; m, months.

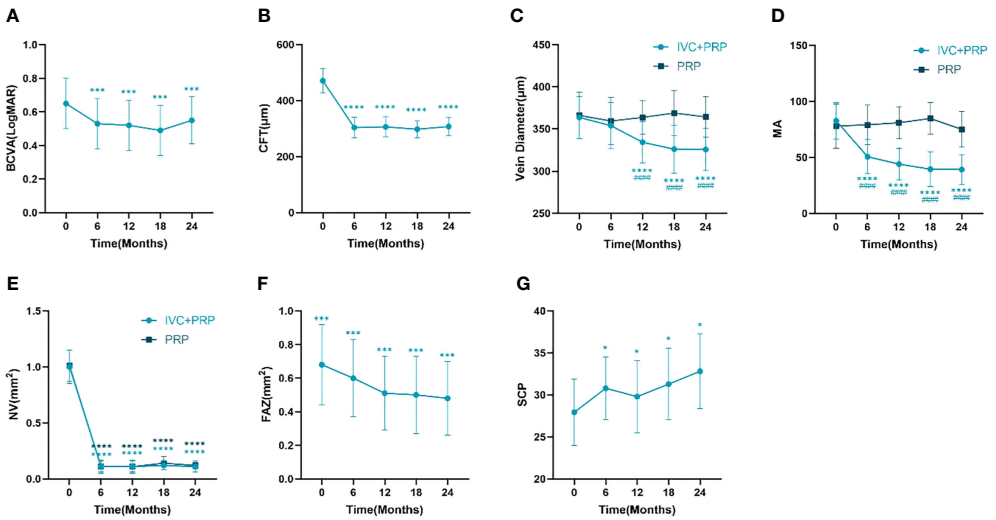

FIGURE 1
Changes in the BCVA (logMAR) **(A)**, CFT (mm) **(B)**, retinal vein diameter (mm) **(C)**, number of MA **(D)**, NV (mm^2) **(E)**, FAZ (mm^2) **(F)**, and vessel density of the SCP **(G)** at different time points between the IVC+PRP group and the PRP group. BCVA, best-corrected visual acuity. CFT, central foveal thickness. MA, microaneurysm. NV, neovascularization. FAZ, foveolar avascular zone. SCP, superficial retinal capillary plexus. **P* < 0.05 *vs.* pretreatment, ****P* < 0.001 *vs.* pretreatment, *****P* < 0.0001 *vs.* pretreatment, $^{\#\#\#\#}P$ < 0.0001 *vs.* PRP group.

TABLE 3 Changes in vein diameter (μm) at baseline *vs.* different time points post-treatment between the IVC+PRP group and the PRP group.

	Baseline	6m	*t*	*P*	12 m	*t*	*P*	18 m	*t*	*P*	24 m	*t*	*P*
IVC+PRP (n = 50)	363.79 ± 24.95	354.01 ± 27.23	1.87	0.06	334.23 ± 24.71	5.95	< 0.01	326.05± 28.28	7.08	< 0.01	325.6 ± 25.16	7.61	< 0.01
PRP (n = 32)	366.11 ± 27.67	359.49± 27.89	0.95	0.34	363.81 ± 19.77	0.38	0.70	368.99± 26.71	0.42	0.67	364.34± 24.10	0.27	0.79
t	0.39	0.88			5.70			6.85			6.90		
P	0.70	0.38			< 0.01			< 0.01			< 0.01		

m, months.

Compared with the PRP group, the IVC+PRP group showed significant vein diameter regression 12, 18, and 24 months after treatment ($P < 0.01$).

3.4 MA, NV, and HE

Changes in MA, NV area, and HE area are shown in Tables 4–6, respectively.

For MA, the IVC+PRP group showed a decreasing trend throughout the treatment process, and the rate of decrease slowed down with the extension of treatment time (Figure 1D). The decrease in the number of MA at each follow-up visit was statistically significant when compared with the number before treatment ($P < 0.01$). The change in the PRP group was not significant ($P > 0.05$), and the difference between the two groups was significant ($P < 0.01$).

For the NV area, no statistically significant difference was found between the IVC+PRP and PRP groups at baseline ($P > 0.05$). Both groups showed a significant decrease in the NV area in the first 6 months of treatment, followed by a stable trend (Figure 1E). The NV area decreased significantly in both groups at each follow-up point after treatment ($P < 0.01$), and no significant difference was found between the two groups ($P > 0.05$).

For HE, both groups demonstrated a statistically significant reduction in the number of patients with different sizes of HE areas before and after treatment ($P < 0.05$). However, no significant statistical difference was observed between the two groups. The number of patients with no HE after treatment in the IVC+PRP group significantly increased, whereas in the PRP group, more patients had HE <0.5 mm^2 after treatment than those with larger HE areas.

3.5 FAZ and SCP

Changes in the FAZ and SCP of the IVC+PRP group are shown in Table 7 and Figure 1. Throughout treatment, the change in the FAZ showed a downward trend, with a significant downward trend in the first 12 months and a slowing trend from 12 to 24 months (Figure 1F). Compared with baseline, the FAZ was significantly reduced at 6, 12, 18, and 24 months of treatment ($P < 0.01$). Moreover, the SCP improved, with a rise at 6 months, a slight rebound at 12 months, and a continued upward trend in subsequent treatments (Figure 1G). Compared with baseline, the SCP also showed significant improvement at 6, 12, 18, and 24 months of treatment ($P < 0.05$).

3.6 Correlation coefficients

Correlation analysis was performed for the significant parameters in the IVC+PRP group before and after treatment. All values showed good statistical significance. Only a weak positive correlation was discovered between the vein diameter and CFT (r = 0.37215446, $P < 0.01$).

3.7 Adverse effects

No severe adverse effects were reported. Four patients in the combination group experienced subconjunctival hemorrhage after injection, which resolved spontaneously.

TABLE 4 Changes in numbers of MA at baseline *vs.* different time points post-treatment between the IVC+PRP group and the PRP group.

	Baseline	6m	*t*	*P*	12 m	*t*	*P*	18 m	*t*	*P*	24 m	*t*	*P*
IVC+PRP (n = 50)	82.82 ± 16.47	50.66 ± 15.19	10.15	< 0.01	44.07 ± 14.29	12.57	< 0.01	39.50 ± 15.65	13.49	< 0.01	39.16 ± 13.39	14.54	< 0.01
PRP (n = 32)	78.04 ± 19.77	79.15 ± 17.68	0.24	0.81	80.95 ± 14.40	0.67	0.50	84.79 ± 14.10	1.57	0.12	75.09 ± 15.93	0.66	0.51
t	1.19	7.77			11.37			13.28			13.28		
P	0.24	< 0.01			< 0.01			< 0.01			< 0.01		

MA, microaneurysm; m, months.

10.3389/fendo.2023.1218442

TABLE 5 Changes in NV (mm^2) at baseline *vs.* different time points post-treatment between the IVC+PRP group and the PRP group.

	Baseline	6 m	*t*	*P*	12 m	*t*	*P*	18 m	*t*	*P*	24 m	*t*	*P*
IVC+PRP (n = 50)	1.00 ± 0.15	0.11 ± 0.06	40.12	< 0.01	0.11 ± 0.06	40.34	< 0.01	0.12 ± 0.04	41.22	< 0.01	0.11 ± 0.05	40.54	< 0.01
PRP (n = 32)	1.01 ± 0.14	0.11 ± 0.05	35.25	< 0.01	0.11 ± 0.05	35.51	< 0.01	0.14 ± 0.06	33.25	< 0.01	0.12 ± 0.03	35.82	< 0.01
t	0.34	0.02			0.23			1.78			0.28		
P	0.73	0.98			0.82			0.08			0.78		

NV, neovascularization; m, months.

4 Discussion

This study aimed to observe the efficacy and changes in the retinal vein of patients with high-risk PDR treated with IVC+PRP and PRP therapy. To our knowledge, this is the first study to quantify changes in the retinal vein diameter after treatment with conbercept. Moreover, the combined use of conbercept and PRP exerted a significant effect on high-risk PDR, and this combination therapy may reverse the DR-induced changes in the retinal vein.

During the 2-year follow up, anti-VEGF combined with PRP for patients with high-risk PDR significantly improved the BCVA and reduced the CFT, which is consistent with previous reports (20). A study compared the efficacy of ranibizumab combined with PRP versus PRP alone in treating patients with high-risk PDR. The results showed that within 48 weeks, both groups had significantly reduced fluorescein angiography leakage; however, the combination group showed greater improvements in visual acuity, central macular thickness, and vascular leakage (21). In our previous retrospective study, we evaluated whether anti-VEGF treatment combined with PRP could reverse DR within a short treatment period. That study included 52 patients with high-risk PDR (72 eyes), which were divided into an aflibercept combination group and a PRP group. In the 6-month follow up, the combination group had significantly improved BCVA and CFT compared with the PRP group, with statistically significant differences in efficacy (17).

Improvement in the BCVA may be related to the degree of macular edema after treatment, and IVC+PRP therapy can alleviate macular edema and exudation by suppressing VEGF expression and improving vascular permeability, thereby improving macular morphology and function. The SAILING study and its extension study evaluated the safety and efficacy of aflibercept in patients with diabetic macular edema and observed the average change in BCVA in patients with diabetic macular edema from baseline to 24 months. The experimental group received aflibercept therapy and sham laser therapy at baseline, whereas the control group received sham injections or laser therapy at baseline, and both groups had repeated treatments based on monthly evaluations. The aflibercept therapy was more effective than traditional ETDRS laser photocoagulation therapy in improving vision and reducing CFT (13). In treating high-risk PDR, protecting the macula may be critical for improving BCVA.

Regarding changes in the retinal vein diameter, our results showed that in the 24-month follow up, IVC+PRP therapy effectively reduced the retinal vein diameter in patients with high-risk PDR, whereas no significant change was found in the vein diameter of the PRP group.

The change in the retinal vein diameter was consistent with our team's previous observations in 59 patients with high-risk PDR (59 eyes) treated with 2-year aflibercept combined with PRP. After treatment, the BCVA and CFT significantly improved, and a statistically significant change in retinal vein diameter was found in

TABLE 6 Changes in the number of patients with different sizes of HE areas at baseline *vs.* different time points post-treatment between the IVC+PRP group and the PRP group.

		Baseline	6 m	χ^2	*P*	12 m	χ^2	*P*	18 m	χ^2	*P*	24 m	χ^2	*P*
IVC+PRP (n = 50)	No HE	1	2	2.73	0.43	4	7.81	0.05	5	13.79	< 0.01	9	18.88	< 0.01
	<0.5 mm^2	11	15			19			22			21		
	0.5 mm^2–2.5 mm^2	20	22			19			18			16		
	>2.5 mm^2	18	11			8			5			4		
PRP (n = 32)	No HE	1	1	0.34	0.95	1	3.36	0.34	2	5.59	0.13	2	6.31	0.10
	<0.5 mm^2	7	9			12			14			15		
	0.5 mm^2–2.5 mm^2	12	11			13			11			10		
	>2.5 mm^2	12	11			6			5			5		
χ^2		0.14	1.63			0.88			0.84			3.15		
P		0.99	0.65			0.83			0.83			0.37		

HE, hard exudate; m, months.

TABLE 7 Changes in FAZ (mm^2) and vessel density of SCP at baseline *vs*. different time points post-treatment in the IVC+PRP group.

FAZ	Baseline	6 m	12 m	18 m	24 m	SCP	Baseline	6 m	12 m	18 m	24 m
N = 50	0.68 ± 0.24	0.60 ± 0.23	0.51 ± 0.22	0.50 ± 0.23	0.48 ± 0.22		27.94 ± 3.95	30.79 ± 3.71	29.79 ± 4.31	31.29 ± 4.26	32.82 ± 4.46
t		1.57	3.61	3.66	4.23			3.7162	2.2356	4.0710	5.78
P		0.12	< 0.01	< 0.01	< 0.01			< 0.01	0.03	< 0.01	< 0.01

FAZ, foveolar avascular zone; SCP, superficial retinal capillary plexus; m, months.

the late stage of treatment. Notably, a regression of the vein bead was observed in the 18th month. Aflibercept intravitreal injection and PRP may reverse the retinal vein diameter and vein bead in the morphology of high-risk PDR (18).

A 12-month prospective cohort study reported that the retinal venous caliber decreased following treatment of diabetic macular edema with intravitreal anti-VEGF agents. Moreover, this decrease remained unchanged even when the injection regimen was switched from monthly treatment to a PRN regimen. Even in eyes that did not receive PRN aflibercept therapy exhibited persistent venous constriction at 12 months (22). The CLARITY study also observed changes in the retinal venous caliber and venous beading during treatment, and our results were consistent with their findings, demonstrating an improvement in BCVA, CFT, and intravitreal microvascular abnormalities at week 52 of aflibercept injection. Over 1 year of observation, the mean venous caliber and venous beading decreased; however, the decrease was not statistically significant (23). Fonseca believed that venous dilation and venous beading formation were chronic reactive dilations of the retinal veins to retinal ischemia, inflammatory response, or other abnormal conditions (24). We speculate that the retinal ischemia, hypoxia, and inflammation worsen with DR progression, causing the veins to reactively dilate to obtain more oxygen supply. Increased blood flow leads to an elevated venous hydrostatic pressure, and the vascular wall structure becomes fragile because of the apoptosis of vascular pericytes and thickening of the basement membrane caused by ischemia, hypoxia, and inflammation. The dilated venous vessels lose their elasticity and cannot recover, which may lead to a vicious cycle of further retinal vessel dilation caused by the burden of increased intravenous pressure. In the present study, the vein diameter of patients with PDR in the combined group changed significantly, and this may be due to the relief of retinal ischemia, leading to reductions in the hydrostatic pressure and pathological dilation of the vein diameter restored to a normal level. In addition, the anti-inflammatory effects of anti-VEGF drugs may also be a factor in vein diameter regression, new results showed the anti-inflammatory action of aflibercept in the retina damaged with high glucose *via* the PlGF/ERK pathway (25). Over time, retinal veins recovered their functions, and anatomical structure remodeling occurred. The results of the CLARITY study regarding changes in veins appear different from ours; however, our observation period was longer than that of the CLARITY study, and we found that venous changes appeared in the later stage of the 2-year treatment period. This may also indicate that anatomical changes in the retinal veins require sufficient time for venous remodeling.

Regarding secondary outcomes, we found that after 6 months of combined IVC and PRP, the NV area, number of MA, and HE area reduced in the treated eyes. The PRP group only showed improvement in the NV area.

Many studies have shown that both combination therapy and PRP monotherapy can eliminate NV. In our previous study on the use of aflibercept in combination with PRP to treat patients with high-risk PDR, the combination and PRP groups had statistically significant reductions in NV compared with baseline data during the 6-month observation period. However, no statistical difference was found between the two groups, and the combination group had a faster reduction in NV than the PRP group. Furthermore, we observed statistically significant improvements in BCVA, CFT, and MA in the combination group (17). Subgroup analysis from the CLARITY study revealed that during the 52-week observation period, 78.9% of the cases in the PRP group displayed partial regression of NV, with an average reduction in the NV area of 75.5% compared with the baseline. By contrast, all eyes in the anti-VEGF group exhibited complete regression of NV by week 12. Although both groups demonstrated significant NV regression, the combination group achieved earlier and more complete benefits (26). Sun also included two groups, i.e., IVC+PRP and PRP groups, followed up for 12 months. In addition, 70.88%, 29.12%, and 0% of eyes in the combination group had complete regression, partial regression, no regression, or NV progression, respectively, and in the PRP group, these were observed in 15.12%, 58.14%, 26.74% of eyes respectively, indicating better and earlier benefits in the combination therapy group (27). Preventing further vitreous hemorrhage and leakage is always our primary treatment goal in the prevention and treatment of NV. The efficacy of both IVC+PRP and PRP alone in improving NV regression was statistically significant after 24 months of treatment, indicating that both methods can achieve optimal efficacy by improving NV regression in patients with high-risk PDR. The combination therapy showed an earlier onset of efficacy compared with PRP monotherapy, which was also demonstrated in our previous study (17).

In our study, the combination group had reduced MA and HE area and was superior to the PRP group in all five observation points. Early studies have suggested that MA formation in patients with DR is caused by fragile vascular walls and vascular dilation, increased proliferation of endothelial cells, thickening of the basement membrane, and loss of pericytes (28). Animal experiments have shown that increased VEGF concentration in the vitreous body is related to MA formation (29), and the injection of anti-VEGF drugs can reduce VEGF concentration and other cytokines in the vitreous body (30). We speculate that MA and HE reductions in our study are caused by the loss of support for proliferating endothelial cells after the VEGF concentration decreased, which may lead to the cessation of

proliferation or even apoptosis and ultimately result in DR regression. However, the influence of changes in the concentrations of other factors after injection cannot be excluded, and further experiments are needed to explore the relationship between each factor and MAs.

HE is primarily composed of dilated capillaries and lipids and proteins that leak into the interstitial space, mainly from MAs. The ETDRS reported that persistent central macular edema can progress to subretinal fibrosis with irreversible vision loss (31). A recent experiment suggested that HE can be an early predictive biomarker for HEs in DR (32). Previous studies have shown that HE significantly decreased after injections of anti-VEGF drugs (33), and our previous study also yielded similar results (17). In this study, the reduction in the HE in the combination group was superior to that in the PRP group. Therefore, because the injections of anti-VEGF drugs significantly reduce MAs, improve vascular permeability, and relatively restore lipid metabolism, HE is significantly reduced. The reduction in the HE area after anti-VEGF therapy may be related to MA reduction and the restoration of retinal vascular health after ischemia and hypoxia improved.

Quantitative indicators of FAZ and SCP in OCTA are related to the severity of DR (34–36). In this study, changes in the FAZ and SCP in the IVC+PRP group are consistent with previous research (37, 38), indicating that IVC+PRP therapy has a positive effect on macular perfusion status. These results suggest that IVC+PRP therapy can prevent the progression of DR-related non-perfusion.

Our trial is mainly limited by its retrospective design and a more restricted sample. Therefore, more prospective multicenter studies with larger sample sizes are warranted to comprehensively compare the effects of the two treatments. Our imaging results were all manually averaged over multiple measurements, which may introduce bias; thus, more professional equipment, targeted image processing software, and formulas are needed to provide more accurate results. Given the damage to the peripheral retina after PRP, we could not observe the condition of the peripheral retina. To monitor the treatment effect for a longer period, the first follow up was set at 6 months after treatment, which may not be suitable for observing the speed of onset between the two groups.

In summary, the combination therapy of IVC and PRP has advantages in BCVA improvement, CFT reduction, vein diameter restoration, reduction of the number of MAs, HE area, and FAZ, and improvement of SCP. Although the baseline BCVA and CFT of the PRP group are better than those of the IVC+PRP group, only the change in NV during treatment showed statistical significance compared with before treatment. The comparison between the two groups indicates the advantages of IVC+PRP therapy.

In the treatment of high-risk PDR, IVC+PRP therapy has a significant advantage over PRP monotherapy. Intravitreal injection of conbercept combined with PRP may reverse the retinal vein changes caused by diabetes in terms of morphology and function in DR.

Data availability statement

The original contributions presented in the study are included in the article/supplementary material. Further inquiries can be directed to the corresponding author.

Ethics statement

The studies involving human participants were reviewed and approved by The Medical Ethics Committee of Qilu Hospital of Shandong University. The patients/participants provided their written informed consent to participate in this study.

Author contributions

MS, YT, and HZ contributed to conception and design of the study. MS wrote the manuscript. YT performed the statistical analysis. ZZ explained and visualized the data. WC and MY participated in the acquisition of data. HW performed the screening diagnosis and treatment of high-risk PDR. All authors contributed to manuscript revision, read, and approved the submitted version.

Conflict of interest

The authors declare that the research was conducted in the absence of any commercial or financial relationships that could be construed as a potential conflict of interest.

Publisher's note

References

1. Cheung N, Mitchell P, Wong TY. Diabetic retinopathy. *Lancet* (2010) 376 (9735):124–36. doi: 10.1016/S0140-6736(09)62124-3

2. Chen L, Cheng CY, Choi H, Ikram MK, Sabanayagam C, Tan GSW, et al. Plasma metabonomic profiling of diabetic retinopathy. *Diabetes* (2016) 65(4):1099–108. doi: 10.2337/db15-0661

3. Teo ZL, Tham YC, Yu M, Chee ML, Rim TH, Cheung N, et al. Global prevalence of diabetic retinopathy and projection of burden through 2045: systematic review and meta-analysis. *Ophthalmology* (2021) 128(11):1580–91. doi: 10.1016/j.ophtha.2021.04.027

4. Martinez-Zapata MJ, Salvador I, Marti-Carvajal AJ, Pijoan JI, Cordero JA, Ponomarev D, et al. Anti-vascular endothelial growth factor for proliferative diabetic

retinopathy. *Cochrane Database Syst Rev* (2023) 3(3):CD008721. doi: 10.1002/14651858.CD008721.pub2

5. Klein R, Myers CE, Lee KE, Gangnon R, Klein BEK. Changes in retinal vessel diameter and incidence and progression of diabetic retinopathy. *Arch Ophthalmol* (2012) 130(6):749–55. doi: 10.1001/archophthalmol.2011.2560

6. Moutray T, Evans JR, Lois N, Armstrong DJ, Peto T, Azuara-Blanco A. Different lasers and techniques for proliferative diabetic retinopathy. *Cochrane Database Systematic Rev* (2018) 3(3):CD012314. doi: 10.1002/14651858.CD012314.pub2/full

7. Lee R, Wong TY, Sabanayagam C. Epidemiology of diabetic retinopathy, diabetic macular edema and related vision loss. *Eye Vis (Lond)* (2015) 2:17. doi: 10.1186/s40662-015-0026-2

8. Flaxel CJ, Adelman RA, Bailey ST, Fawzi A, Lim JI, Vemulakonda GA, et al. Diabetic retinopathy preferred practice pattern. *Ophthalmology* (2020) 127(1):P66–145. doi: 10.1016/j.ophtha.2019.09.025

9. The Diabetic Retinopathy Study Research Group. Indications for photocoagulation treatment of diabetic retinopathy: Diabetic Retinopathy Study Report no. 14. *Int Ophthalmol Clin* (1987) 27(4):239–53. doi: 10.1097/00004397-198702740-00004

10. Sun JK, Glassman AR, Beaulieu WT, Stockdale CR, Bressler NM, Flaxel C, et al. Rationale and application of the protocol S anti-vascular endothelial growth factor algorithm for proliferative diabetic retinopathy. *Ophthalmology* (2019) 126(1):87–95. doi: 10.1016/j.ophtha.2018.08.001

11. Wang X, He X, Qi F, Liu J, Wu J. Different anti-vascular endothelial growth factor for patients with diabetic macular edema: A network meta-analysis. *Front Pharmacol* (2022) 13:876386. doi: 10.3389/fphar.2022.876386

12. Huang J, Li X, Li M, Li S, Xiao W, Chen X, et al. Effects of intravitreal injection of KH902, a vascular endothelial growth factor receptor decoy, on the retinas of streptozotocin-induced diabetic rats. *Diabetes Obes Metab* (2012) 14(7):644–53. doi: 10.1111/j.1463-1326.2012.01584.x

13. Liu K, Wang H, He W, Ye J, Song Y, Wang Y, et al. Intravitreal conbercept for diabetic macular oedema: 2-year results from a randomised controlled trial and open-label extension study. *Br J Ophthalmol* (2022) 106(10):1436–43. doi: 10.1136/bjophthalmol-2020-318690

14. Huang C, Ji H, Han X. The effectiveness of conbercept combined with panretinal photocoagulation vs. Panretinal photocoagulation in the treatment of diabetic retinopathy: A meta-analysis. *J Ophthalmol* (2021) 2021:5591719. doi: 10.1155/2021/5591719

15. Levin AM, Rusu I, Orlin A, Gupta MP, Coombs P, D'Amico DJ, et al. Retinal reperfusion in diabetic retinopathy following treatment with anti-VEGF intravitreal injections. *Clin Ophthalmol* (2017) 11:193–200. doi: 10.2147/OPTH.S118807

16. Wang J, Jiang PF, Liu M, Kou MR, Lei JY, Yu XT, et al. Efficacy of intravitreal injection of conbercept on non-proliferative diabetic retinopathy: a retrospective study. *J Int Med Res* (2020) 48(4):300060519893176. doi: 10.1177/0300060519893176

17. Tao Y, Jiang P, Zhao Y, Song L, Ma Y, Li Y, et al. Retrospective study of aflibercept in combination therapy for high-risk proliferative diabetic retinopathy and diabetic maculopathy. *Int Ophthalmol* (2021) 41(6):2157–65. doi: 10.1007/s10792-021-01773-6

18. Zhao H, Wang J, Li S, Bao Y, Zheng X, Tao Y, et al. Retinal vein changes after treatment with aflibercept and PRP in high-risk proliferative diabetic retinopathy. *Front Med* (2023) 10:1090964. doi: 10.3389/fmed.2023.1090964

19. Knudtson MD, Lee KE, Hubbard LD, Wong TY, Klein R, Klein BEK. Revised formulas for summarizing retinal vessel diameters. *Curr Eye Res* (2003) 27(3):143–9. doi: 10.1076/ceyr.27.3.143.16049

20. Zhang W, Geng J, Sang A. Effectiveness of panretinal photocoagulation plus intravitreal anti-VEGF treatment against PRP alone for diabetic retinopathy: A systematic review with meta-analysis. *Front Endocrinol (Lausanne)* (2022) 13:807687. doi: 10.3389/fendo.2022.807687

21. Filho JAR, Messias A, Almeida FPP, Ribeiro JAS, Costa RA, Scott IU, et al. Panretinal photocoagulation (PRP) versus PRP plus intravitreal ranibizumab for high-risk proliferative diabetic retinopathy. *Acta Ophthalmol* (2011) 89(7):e567–572. doi: 10.1111/j.1755-3768.2011.02184.x

22. Blindbaek SL, Peto T, Grauslund J. Alterations in retinal arteriolar microvascular structure associate with higher treatment burden in patients with diabetic macular oedema: results from a 12-month prospective clinical trial. *Acta Ophthalmol* (2020) 98(4):353–9. doi: 10.1111/aos.14278

23. Sivaprasad S, Prevost AT, Vasconcelos JC, Riddell A, Murphy C, Kelly J, et al. Clinical efficacy of intravitreal aflibercept versus panretinal photocoagulation for best corrected visual acuity in patients with proliferative diabetic retinopathy at 52 weeks (CLARITY): a multicentre, single-blinded, randomised, controlled, phase 2b, non-inferiority trial. *Lancet* (2017) 389(10085):2193–203. doi: 10.1016/S0140-6736(17)31193-5

24. Fonseca RA, Dantas MA. Retinal venous beading associated with recurrent branch vein occlusion. *Can J Ophthalmol* (2002) 37(3):182–3. doi: 10.1016/S0008-4182(02)80062-X

25. Lazzara F, Fidilio A, Platania CBM, Giurdanella G, Salomone S, Leggio GM, et al. Aflibercept regulates retinal inflammation elicited by high glucose *via* the PlGF/ERK pathway. *Biochem Pharmacol* (2019) 168:341–51. doi: 10.1016/j.bcp.2019.07.021

26. Nicholson L, Crosby-Nwaobi R, Vasconcelos JC, Prevost AT, Ramu J, Riddell A, et al. Mechanistic evaluation of panretinal photocoagulation versus aflibercept in proliferative diabetic retinopathy: CLARITY substudy. *Invest Ophthalmol Vis Sci* (2018) 59(10):4277–84. doi: 10.1167/iovs.17-23509

27. Sun Y, Qi H. A comparison between the therapeutic effects of Conbercept combined with panretinal photocoagulation and panretinal photocoagulation monotherapy for high-risk proliferative diabetic retinopathy. *Front Endocrinol (Lausanne)* (2022) 13:1038757. doi: 10.3389/fendo.2022.1038757

28. Frank RN. Diabetic retinopathy. *N Engl J Med* (2004) 350(1):48–58. doi: 10.1056/NEJMra021678

29. Tolentino MJ, McLeod DS, Taomoto M, Otsuji T, Adamis AP, Lutty GA. Pathologic features of vascular endothelial growth factor-induced retinopathy in the nonhuman primate. *Am J Ophthalmol* (2002) 133(3):373–85. doi: 10.1016/S0002-9394(01)01381-2

30. Mastropasqua R, D'Aloisio R, Di Nicola M, Di Martino G, Lamolinara A, Di Antonio L, et al. Relationship between aqueous humor cytokine level changes and retinal vascular changes after intravitreal aflibercept for diabetic macular edema. *Sci Rep* (2018) 8(1):16548. doi: 10.1038/s41598-018-35036-9

31. Fong DS, Segal PP, Myers F, Ferris FL, Hubbard LD, Davis MD. Subretinal fibrosis in diabetic macular edema. ETDRS report 23. Early Treatment Diabetic Retinopathy Study Research Group. *Arch Ophthalmol* (1997) 115(7):873–7. doi: 10.1001/archopht.1997.01100160043006

32. Shen Y, Wang H, Fang J, Liu K, Xu X. Novel insights into the mechanisms of hard exudate in diabetic retinopathy: Findings of serum lipidomic and metabolomics profiling. *Heliyon* (2023) 9(4):e15123. doi: 10.1016/j.heliyon.2023.e15123

33. Domalpally A, Ip MS, Ehrlich JS. Effects of intravitreal ranibizumab on retinal hard exudate in diabetic macular edema: findings from the RIDE and RISE phase III clinical trials. *Ophthalmology* (2015) 122(4):779–86. doi: 10.1016/j.ophtha.2014.10.028

34. Sun Z, Tang F, Wong R, Lok J, Szeto SKH, Chan JCK, et al. OCT angiography metrics predict progression of diabetic retinopathy and development of diabetic macular edema: A prospective study. *Ophthalmology* (2019) 126(12):1675–84. doi: 10.1016/j.ophtha.2019.06.016

35. Tang FY, Chan EO, Sun Z, Wong R, Lok J, Szeto S, et al. Clinically relevant factors associated with quantitative optical coherence tomography angiography metrics in deep capillary plexus in patients with diabetes. *Eye Vis (Lond)* (2020) 7:7. doi: 10.1186/s40662-019-0173-y

36. Lee H, Lee M, Chung H, Kim HC. Quantification of retinal vessel tortuosity in diabetic retinopathy using optical coherence tomography angiography. *Retina* (2018) 38(5):976–85. doi: 10.1097/IAE.0000000000001618

37. Lin W, Feng M, Liu T, Wang Q, Wang W, Xie X, et al. Microvascular changes after conbercept intravitreal injection of PDR with or without center-involved diabetic macular edema analyzed by OCTA. *Front Med (Lausanne)* (2022) 9:797087. doi: 10.3389/fmed.2022.797087

38. Zhu Z, Liang Y, Yan B, Meng Z, Long K, Zhang Y, et al. Clinical effect of conbercept on improving diabetic macular ischemia by OCT angiography. *BMC Ophthalmol* (2020) 20(1):382. doi: 10.1186/s12886-020-01648-x

frontiers | Frontiers in Endocrinology

TYPE Review
PUBLISHED 28 September 2023
DOI 10.3389/fendo.2023.1276225

OPEN ACCESS

EDITED BY
Kai Jin,
Zhejiang University, China

REVIEWED BY
Yin Wang,
First People's Hospital of Kunshan, China
Li Xiao,
University of Virginia, United States

*CORRESPONDENCE
Qin Jiang
jqin710@vip.sina.com
Keran Li
kathykeran860327@126.com

†These authors share first authorship

RECEIVED 11 August 2023
ACCEPTED 07 September 2023
PUBLISHED 28 September 2023

CITATION
Yao Y, Li J, Zhou Y, Wang S, Zhang Z, Jiang Q and Li K (2023) Macrophage/microglia polarization for the treatment of diabetic retinopathy. *Front. Endocrinol.* 14:1276225. doi: 10.3389/fendo.2023.1276225

Macrophage/microglia polarization for the treatment of diabetic retinopathy

Yujia Yao[1,2†], Jiajun Li[1,2†], Yunfan Zhou[1,2†], Suyu Wang[1,2], Ziran Zhang[1,2], Qin Jiang[1,2*] and Keran Li[1,2*]

[1]Department of Ophthalmology, The Affiliated Eye Hospital of Nanjing Medical University, Nanjing, China, [2]The Fourth School of Clinical Medicine, Nanjing Medical University, Nanjing, China

Macrophages/microglia are immune system defense and homeostatic cells that develop from bone marrow progenitor cells. According to the different phenotypes and immune responses of macrophages (Th1 and Th2), the two primary categories of polarized macrophages/microglia are those conventionally activated (M1) and alternatively activated (M2). Macrophage/microglial polarization is a key regulating factor in the development of inflammatory disorders, cancers, metabolic disturbances, and neural degeneration. Macrophage/microglial polarization is involved in inflammation, oxidative stress, pathological angiogenesis, and tissue healing processes in ocular diseases, particularly in diabetic retinopathy (DR). The functional phenotypes of macrophages/microglia affect disease progression and prognosis, and thus regulate the polarization or functional phenotype of microglia at different DR stages, which may offer new concepts for individualized therapy of DR. This review summarizes the involvement of macrophage/microglia polarization in physiological situations and in the pathological process of DR, and discusses the promising role of polarization in personalized treatment of DR.

KEYWORDS

diabetic retinopathy, immune system, macrophages, microglia, ocular diseases, polarization

1 Introduction

A crucial part of innate and acquired immunity is the immune cell class known as macrophages/microglia, which are produced by bone marrow progenitor cells. In response to certain stimuli from the ecological environment, macrophages undergo a process called macrophage polarization in which they develop distinct functional features (1). In different microenvironments macrophages/microglia may be phenotypically polarized to mount specific functional programs. M1 (classically activated macrophages) and M2 (alternatively activated macrophages) are the primary subcategories of polarized macrophages/microglia (2). Furthermore, polarized macrophages/microglia can affect local immunological

responses in many ways (3–5). They are essential for the regulation of infectious and metabolic diseases, tumors, and neurodegenerative disorders (6–9).

In both healthy and unhealthy conditions, macrophages/microglia are crucial for physiological homeostasis. Physically, macrophages/microglia are highly tiled and ramified, and are characterized by a tiny soma with many branches and fine cellular processes. They incessantly, randomly, and repetitively expand and contract in all directions, serving as immunological surveillance. Phagocytosis, external antigen presentation, and management via cytokine and growth factor production are the main functions of macrophages and microglia in the pathological state. They can be activated by pattern recognition receptors to promote phagocytosis of cellular debris. In addition to their phagocytic functions, activated microglia can serve as antigen-presenting cells. They release pro-inflammatory cytokines and stimulate the immune system through direct cell-cell interaction. Furthermore, they upregulate induced nitric oxide synthase (iNOS) upon activation, which increases local nitric oxide concentrations, damages peripheral neurons, and promotes local capillary leakage.

Major causes of blindness, including diabetic retinopathy (DR), oxygen-induced retinopathy (OIR), age-related macular degeneration (AMD), uveitis, and tumors (uveal melanoma), are closely related to inflammation and immunity (10–13). The polarization of macrophages/microglia has recently been found to be associated with the onset of ocular diseases (14, 15). As a result of retinal ischemia and hypoxia, inflammatory cells such as macrophages and monocytes gather around the vessels (16). Macrophages are polarized in response to environmental stimuli. The majority of pro-angiogenic substances (including vascular endothelial growth factor [VEGF]) required for ocular neovascularization are secreted by these cells. Vascular endothelial cells and smooth muscle cells proliferate, differentiate, and migrate as a result of this process, bringing about the formation of harmed vessels and eventually retinal/vitreous hemorrhage (17). This association substantially influences the progression and prognosis of ocular diseases (Figure 1).

Diabetes mellitus is a metabolic disease featured with hyperglycemia caused by improper insulin production and insulin resistance. Microvascular complications occur most commonly in

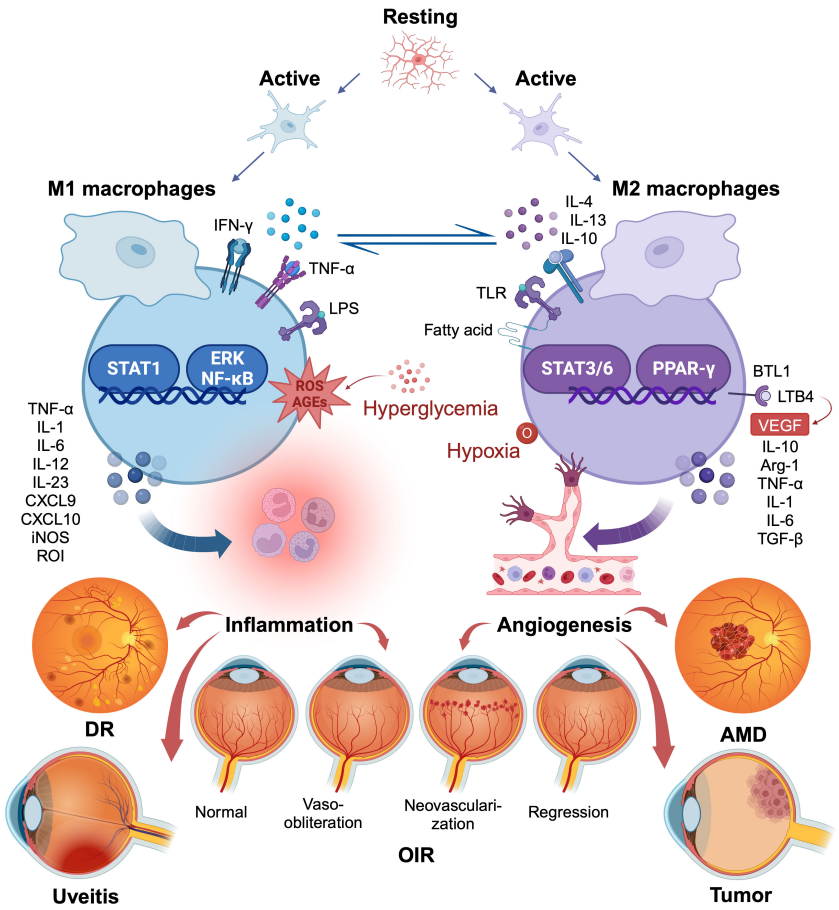

FIGURE 1
Macrophage/microglia polarization in several ocular disorders. The two polar opposites of the changed state of macrophage/microglia activation are M1 and M2. They are kinetically reversible; type M1 can shift to type M2 when microenvironmental conditions change, and vice versa. M1 macrophages produce pro-inflammatory chemicals that, although engulfing many pathogens, may also accelerate inflammatory processes that are detrimental. M2 macrophages, in contrast, lessen such harm, clear away necrotic cell debris, encourage tissue repair and remodeling, along with revascularization. The figure illustrates the common role of macrophage/microglia polarization in several ocular diseases. Created with BioRender.com. M1, conventionally activated macrophages; M2, alternatively activated macrophages.

patients with DR and their prevalence is rapidly increasing worldwide (18). DR is subdivided into non-proliferative DR (NPDR) and proliferative diabetic retinopathy (PDR) decided by whether the retina undergoes neovascularization (19). The main factor that causes permanent blindness in working-age individuals is DR, particularly PDR (20). Damage to the neurovascular unit is currently considered an important pathogenic mechanism of diabetic retinopathy (21). Neurons, glial cells, basement membranes, pericytes, and endothelial cells comprise the retinal neurovascular unit (22). Increased neural activity results in greater blood flow to meet metabolic needs. Neuronal stress and apoptosis in the early stages of DR cause microglial activation and aggravate vascular damage. Vascular abnormalities further affect neuronal cell growth, metabolism, and function, making neural damage more severe. The neurovascular unit is gradually damaged, and eventually forms a microvascular lesion (23–25). A key player in the pathophysiology of DR is VEGF. Thus, anti-VEGF medications are currently the main DR treatment (26). Anti-VEGF medications are efficient in clinically inhibiting the development of neovascularization however they have no effect on angiogenic agents other than VEGF. Other treatment modalities, such as laser photocoagulation and vitrectomy, are often accompanied by significant side effects, including damage to healthy tissues, postoperative cataracts, and neuronal apoptosis (27–29). Therefore, new treatments for DR need to be developed.

In this review, the major duties of polarized microglia and macrophages in DR are examined, their research status and prospects for DR treatment are discussed.

2 Macrophage/microglia origin, classical activation, and functions

The current view is that during embryonic development, precursor cells from the yolk sac or embryo infiltrate organs and differentiate into tissue-resident macrophages (30, 31). Tissue-resident macrophages permanently survive and constantly self renew during adulthood and peripherally derived macrophages from monocytes also exist (32). Monocyte-derived macrophages mainly differentiate from blood monocytes produced from bone marrow hematopoietic stem cells. They are stimulated by multi-colony stimulating factor (CSF) and granulocyte-macrophage CSF to develop into monocytes, pre-monocytes, and mature monocytes. Subsequently, they spread throughout the epidermal and submucosal tissues of the body where they are vital for immunological surveillance, self-stabilization, and infection resistance (33). Macrophages can be further classified into microglia, osteoblasts, and within areas, such as lung macrophages, based on their anatomical location and function type. Microglia, a type of central nervous system tissue-resident macrophages, can engulf apoptotic neurons and trigger synaptic remodeling to maintain central nervous system homeostasis (34).

Macrophages and microglia are remarkably plastic, heterogeneous cells with multiple immunological functions. They are generally classified into two groups based on their function following activation: cc or M2 and caM or M1 type (35). However, continuous in-depth research on macrophage polarization indicates this process is constantly evolving. M1 and M2 are the two extreme states of macrophages, and the phenotypes of macrophages are altered under numerous normal and pathogenic conditions (1, 36).

M1 macrophages, whose surface markers include HLA-DR, CD80, CD86, and CD197, produce pro-inflammatory cytokines (37, 38). Typically, Th1 (interferon [IFN]-gamma, tumor necrosis factor-[TNF]-alpha) or bacterial lipopolysaccharide (LPS) can induce and activate M1 polarization, causing them to release large amounts of pro-inflammatory cytokines, including TNF-alpha, interleukin (IL)-1, IL-6, IL-12, IL-18, IL-23, and the chemokine ligands CXCL-9 and CXCL-10. They also generate significant amounts of iNOS, reactive oxygen intermediates (ROI), nitric oxide, and reactive oxygen species (ROS) (39, 40). Therefore, they are effector cells in the Th1 immune response, killing intracellular pathogens, removing foreign substances, and participating in the acute pro-inflammatory response (41–43). As a result, M1 macrophages may intensify inflammatory processes that are detrimental to tissue while eliminating pathogens.

M2 macrophages secrete anti-inflammatory molecules to mitigate this damage. They generate angiogenic mediators, including transforming growth factor (TGF-beta), VEGF, and epidermal growth factor, which reduce inflammation and accelerate wound healing. However, precisely because of the secretion of these factors and their overactivation, aberrant hyperplasia may result, such as pathological angiogenesis. Four distinct populations of M2 macrophages may be identified based on the multiple activation signals they receive: M2a, M2b, M2c, and M2d, whose surface markers include CD206, CD209, CD301, and CD163 (40, 44). Type II cytokines, IL-4 or IL-13, activate M2a macrophages, which then secrete several pro-inflammatory cytokines, including IL-10 and arginase 1, and receptors, such as mannose receptor CD206 and macrophage galactose type C lectin (MGL; CD301) (40). They are insensitive to inflammatory stimuli, however, they eliminate pathogens, remove debris, stimulate angiogenesis, and aid in tissue regeneration, thus promoting Th2 immunity. Immune complexes, toll-like receptors (TLR), IL-1R ligands, and LPS can trigger M2b macrophages. These cells secrete high levels of IL-10 and low levels of IL-12. In addition, they notably release several inflammatory cytokines such as TNF-alpha, IL-1, and IL-6, which reduce acute inflammation brought on by bacterial endotoxins and promote Th2 differentiation and humoral immunity (45). IL-10, TGF-beta, glucocorticoids, or open-loop steroid hormones (such as vitamin D) can activate M2c macrophages, also referred to as inactivated macrophages. They generate large amounts of TGF-beta and IL-10, which inhibit immunological inflammation (46).

M2d macrophages, also known as tumor-associated macrophages (TAM), are dominant in tumors. IL-6 and adenosine induce them to generate a lot of IL-10 and VEGF. Evidence suggests that macrophages can inhibit immunity, promote tumor cell proliferation, and stimulate angiogenesis (47, 48). TAM release more mannose receptor and scavenger receptor A than M1 macrophages, and fewer pro-inflammatory chemicals, such as IL-1beta, IL-6, IL-12, TNF-alpha, and ROI (47).

Simultaneously, the levels of several macrophage differentiation markers in TAM, including F4/80, CD11b, CD68, and CD115, are lower than those in typical M2 macrophages. Therefore, more researches are of the opinion that TAM have traits common to both M1 and M2 polarization types and are in a stage of transition between them (49, 50). Thus, the ratio of the two polarization types is influenced by the tumor microenvironment, which promotes or inhibits tumor growth (51) (Table 1).

Nevertheless, a disadvantage of this typing system is that it ignores macrophages undergoing positive division. Macrophage CSF-1 and IL-34 interact with the CSF receptor (CSF-1R) to induce macrophage proliferation and influence their differentiation, survival, and function (52). Studies have revealed that CSF-1-treated mouse microglia do not exhibit conventional M1 or M2 polarization, in contrast to earlier theories that macrophage CSF stimulation causes M2 polarization (53, 54). Therefore, the possibility of establishing M3 typing has been proposed (55). The diverse phenotypes and functions of macrophages enable them to play important roles in inflammation, pathogen resistance, tissue remodeling and repair, autoimmune regulation, and tumor suppression.

3 Retinal macrophages/microglia origin, distribution and functions

Microglia are macrophages assumed to be inherent in the central nervous system and fundamental for neuronal regeneration and immunological homeostasis (56). Primitive yolk sac macrophages are the source of microglia (57–59). In addition to tissue-resident microglia and monocyte-derived microglia in the bone marrow can penetrate the blood-retinal barrier under specific circumstances and show morphology and function similar to those of endogenous microglia in the retinal environment (60). After complete eradication of indigenous microglia in the retina, additional microglia recharge and originate from two different ways: macrophages in the ciliary body and iris, which arise peripherally (minority), and the optic nerve, which develop in the center (majority) (61, 62). This phenomenon confirms the presence of macrophage-derived microglia in the retinal periphery.

Microglia are mostly found in the inner layers of the retina in healthy individuals, including the nerve fiber layer (NFL), ganglion cell layer (GCL), inner plexiform layer (IPL), and outer plexiform layer (OPL) (25). At the age of 10-week-gestation, microglia have been found in the human retina (63). Moreover, their distribution is almost identical to that in mature retinas during development (64). Using immunocytochemistry and tomato lectin histochemistry, microglia are shown to be present in mouse retinas of 11.5-day-old embryos, distributed in the neuroblastic layer, IPL, and GCL just prior to birth, and with similar distribution as adult retinas from postnatal day 14 on (65). Microglia are also present in the OPL, ONL, IPL, GCL, and NFL of the primate retinas, resembling those of the human retinas (66). Microglia migrate to the retina in two ways. Before vascularization, most microglia migrate to the peripheral retina from nearby ocular tissues through the ciliary epithelium, primarily from the developing ciliary body and iris blood vessels. However, after vascularization, microglia originally derived from retinal blood vessels appear to migrate to the retina through the optic nerve head (67).

Conventional studies have assumed that microglia are dormant in healthy adult retinas and respond only when damaged. However, more recent studies indicate microglia have been found to be dynamic, constantly surveying the neural environment and performing tissue surveillance and intercellular communication functions (68–70). Using *in vitro* preparations, gradual and ongoing expansion and contraction of microglial processes may be observed, which suggest a key role in maintaining normal retinal function (71, 72). Anatomically, microglia are in direct contact with pericytes, which are strongly related to other components of the neurovascular unit nearby, to keep the normal function of the neurovascular unit and blood-retina barrier (BRB) integrity (73). Activated microglial cells are thought to play a crucial role in pathogenic situations, such as inflammation and traumatic and degenerative nerve injury. In response to damage, microglia upregulate process motility, reorient their shape and promote migratory activity (74). However, when frequently activated by alarm signals from both external and endogenous sources, microglial cells may become chronically hyperactive and secrete massive amounts of pro-inflammatory cytokines, which can result in an imbalance between the protective and injurious effects (75). Pericyte loss and endothelial cell damage result from the production of such inflammatory mediators (76). These mechanisms are present throughout DR development, and understanding the control of microglial polarization may lead to new perspectives for the development of individualized DR therapies.

TABLE 1 Phenotypes, stimulations, secretions, and markers of M1 and M2 macrophages.

Phenotype	Stimulation	Secretion	Marker
M1	IFN-γ, LPS	TNF-α, IL-1, IL-6, IL-12, IL-18, IL-23	HLA-DR, CD80, CD86, CD197
M2a	IL-4, IL-13	IL-10, TGF-β, Arg-1	CD206, CD209, CD301, CD163
M2b	TLR, IL-1R, LPS	IL-1, IL-6, IL-10, TNF-α	
M2c	IL-10, TGF-β, glucocorticoids, open-loop steroid hormones	IL-10, TGF-β	
TAM	IL-6, adenosine	VEGF, IL-1β, IL-6, IL-10, IL-12, TNF-α	

IFN-γ, interferon-gamma; IL, interleukin; LPS, lipopolysaccharide; M1, conventionally activated; M2, alternatively activated; TAM, tumor-associated macrophages; TGF-β, transforming growth factor-beta; TNF-α, tumor necrosis factor-alpha; TLR, toll-like receptors; VEGF, vascular endothelial growth factor.

4 Macrophage/microglia polarization in DR

4.1 Polarization in DR metabolism

Changes in blood glucose levels are a characteristic of diabetes mellitus. Altered glucose levels affect macrophage polarization and inflammatory cytokine secretion. Glucose transporter 1 has been reported to govern glycolysis, a process that is necessary for the generation of inflammatory cytokines and regulation of pro-inflammatory genes in microglia, indicating the participation of polarization in the pathological process (77). M1/M2 macrophage polarization is balanced in healthy human circulation. In contrast, deficiency in anti-inflammatory cells causes a significant reduction in M2 macrophage polarization, leading to an increase in M1/M2 polarization in the peripheral blood of patients with type 2 diabetes (78). Central obesity, insulin resistance, and abnormal glycemic control are typical characteristics of patients with type 2 diabetes and are all associated with a polarization imbalance. Chen et al. (79) obtained similar results. They observed that microglia stimulated by high glucose was initially polarized to the M2a phenotype, which protects against damaged tissues. However, over time, M1 pro-inflammatory factor production increases, M2 anti-inflammatory factor production decreases, and macrophages gradually tend to have the M2b phenotype (likely an intermediate phenotype between M2a and M1). In the late stage, microglia display an M1-like phenotype with pro-inflammatory effects. Furthermore, increased pro-inflammatory M1 monocyte-macrophages in the peripheral blood have been observed in individuals with preclinical diabetes, for instance impaired fasting glucose and/or impaired glucose tolerance patients (80). Similar findings were observed in the circulation of db/db mice, where pro-inflammatory cytokines (M1) and anti-inflammatory cytokines (M2) increased early (5 weeks), and by 20 weeks, db/db mice had considerably greater levels of pro-inflammatory cytokines compared to db/+ controls (81)..

Moreover, diabetes often coexists with hyperlipidemia, which is directly correlated with the onset of diabetic complications, such as DR, and accelerates progression (82). Research has shown that when TLR are activated by LPS, glucose absorption increases and glucose is oxidized to induce acetyl-CoA production, a precursor for the production of fatty acids. During inflammatory reactions, glucose metabolism is activated to promote *de novo* lipogenesis. Sterol regulatory element binding transcription factor 1a, which controls the production of inflammatory cytokines, is also expressed as a result of TLR activation (83). Compared to healthy people, patients with hypercholesterolemia had higher levels of pro-inflammatory $CD68^{(+)}$ $CCR2^{(+)}$ M1 monocyte macrophages, although anti-inflammatory $CX3CR1^{(+)}$ $CD163^{(+)}$/$CD206^{(+)}$ M2 monocyte macrophages are decreased (84). Overall, a predominance of M1 macrophage polarization and increased secretion of pro-inflammatory cytokines have been observed in the peripheral blood of patients with diabetes.

According to recent studies, one of the most promising treatment options for diabetes may be to boost the polarization of the macrophage M2 phenotype to reduce insulin resistance and stabilize glucose/lipid metabolism (85–87). Additionally, this therapy may assist patients with diabetes in diminishing endothelial dysfunction and preventing complications of diabetes (88–90).

4.2 Microglia activation and polarization in animal models and patients with DR

An important characteristic of retinas with DR in both animals and humans is the migratory tendency of microglia. The retinal glia cells undergo alterations in both the early and late phases of DR development. A number of animal models have been created to comprehend the pathophysiology of DR. In DR model rats, M1 polarization increased, while M2 polarization decreased, and microglia were more prone to M1 polarization as the glucose concentration increased (91, 92). The iNOS (M1 marker) and arginase-1 (M2 marker) levels in the retinas of db/db mice were high at five-week-old; however, by eight-week-old, iNOS continued to rise, while arginase-1 returned to baseline levels. Retinal M1 and M2 proteins were also differentially distributed. M1-like proteins are mostly found in the outer segment, OPL, inner nuclear layer, and GCL, whereas M2-like proteins are primarily produced in the inner nuclear layer and GCL (81). Chen et al. (93) observed the activation and distribution of microglia in rats with hyperglycemia induced by Streptozotocin through OX-42 staining. The percentage of activated microglia considerably increased in the retinas of four-week-old rats with diabetes and remained high in eight- and twelve-week-old rats with diabetes. Twelve weeks following the initiation of diabetes, there appeared to be a redistribution of retinal microglia, with more in the NFL/GCL and fewer in the IPL, whereas there was no difference in the distribution of microglia in the NFL/GCL and IPL layers at 4 and 8 weeks. This demonstrates the motility of the microglia. The study by Omri et al. (94) seems to explain this phenomenon. In a Goto-Kakizaki rat model for spontaneous type 2 diabetes, the number of retinal pigment epithelium pores increased during the prophase of hyperglycemia (5 months). After long-term exposure to hyperglycemia (12 months), fewer retinal pigment epithelium pores remained, causing activated microglia/macrophages to accumulate subretinally and promote retinal injury (21, 94).

Similarly, clinical studies have demonstrated that microglia are significantly more prevalent in eyes with DR and display a hypertrophic pattern distinct from the ramified form during the resting state. The quantity of activated microglia, which are more common in the perivascular areas of the microaneurysms, slightly increases during NPDR. The number of activated microglia, which accumulate in cotton wool areas and the surrounding dilated arteries, significantly increases from NPDR to PDR. An abnormally high number of activated microglia develop in the GCL, surrounding newly formed juvenile arteries in the NFL and in the optic nerve head in PDR (95). These results imply that microglia in the retinas of DR patients are distributed similarly to 12-week-old diabetic mice. Thus, activated microglia are tightly associated with blood vessels that are closely connected geographically and promote microangiopathy in DR. Microglia/macrophages accumulate in the retina under the prolonged effects of hyperglycemia, indicating their contribution to the development

of the disease. Optical coherence tomography angiography revealed that patients with PDR had significantly more macrophage-like cells surrounding their retinal vessels than healthy individuals, diabetics without DR, and patients with NPDR (96); diabetic macular edema was the most relevant factor contributing to the increase in macrophage-like cells (97). Moreover, macrophages near the vitreoretinal interface, mainly microglia, may act as biomarkers for inflammation (98). The emergence of diabetic complications, including microangiopathy, may be associated with a decrease in M2 polarization and a rise in the M1/M2 proportion. In pathological angiogenic ecology, retinal myeloid cells, especially macrophages/microglia, which are located close to endothelial cells in pathological angiogenic ecosystems, are highly glycolytic, express M1 and M2 markers more frequently, and produce more pro-inflammatory and pro-angiogenic cytokines (99). Angiogenic ability increases because of the interaction between macrophages and endothelial cells. Macrophages promote endothelial cell glycolysis and the lactate produced by glycolysis promotes macrophage activation, creating a positive feedback loop. Compared with normal retinas, patients with PDR have considerably more M1 and M2 macrophages in their fibrovascular membranes, and fibrovascular membranes development may be associated with M2 macrophages (100, 101).

The results mentioned in this section have led to the hypothesis that more than one type of polarized macrophage participate in retinal neovascularization. We can infer that in the early stages of DR, both pro-inflammatory (M1) and anti-inflammatory (M2) microglia are activated, and retinal adaptations increase to maintain their dynamic balance. Nevertheless, as the disease progresses, the number of M1 macrophages is maintained, whereas that of M2 macrophages gradually declines, favoring an inflammatory environment that causes retinal degeneration and loss of visual function.

5 Mechanisms of polarization in DR

Chronic hyperglycemia may cause gliosis by promoting the synthesis of advanced glycation end products (AGEs), which are macromolecules that are exposed to high blood glucose levels for a long period and become excessively glycated (102). Accumulated AGEs can trigger pro-inflammatory reactions via receptor (RAGE)-dependent or-independent mechanisms. In contrast to RAGE activation, which causes glial activation and the release of inflammatory cytokines, AGEs can cause endothelial cells to overexpress adhesion molecules (such as intercellular cell adhesion molecule-1) and subsequently activate leukocytes. Furthermore, oxidizing conditions and ROS generation connect retinal neuroinflammation with AGEs accumulation and create a positive feedback loop (103). Thus, inflammation and oxidative stress are the two main mechanisms involved in DR development and are closely related to macrophage polarization. Current research has mainly focused on the relationship among M1 polarization, oxidative stress, and inflammation. Both clinical and fundamental studies have shown that M2 polarization occurs in DR. Given that VEGF matters in retinal neovascularization and is a marker of M2 polarization, we also need to discuss the possible role of M2 polarization in pathological neovascularization in DR. We summarized the main signaling pathways related to polarization in Table 2.

5.1 Inflammation

Inflammation is one of the core pathological processes in DR. The expression of various inflammatory chemicals, including cytokines, chemokines, and growth factors is enhanced in the retina as a result of diabetes. The retina is already in a systemic pro-inflammatory environment before any clinical signs of DR manifest (118).

Macrophages/microglia located close to the vitreoretinal interface have been identified as possible indicators of inflammation in retinal vascular disease (98). M1 polarization and the generation of pro-inflammatory cytokines are both increased by activated NF-κB-related signaling pathways (104–106). Glucose fluctuations have been found to promote macrophage TLR4/IRF5 pathway activation, which in turn activate M1 macrophages and enhances the secretion of pro-inflammatory cytokines (108). A20, also called TNF-alpha-induced protein 3, negatively regulates M1 microglia. Glucose stimulation lowers ALKBH5 by m6A modification, resulting in reduced microglial A20 expression and promotion of M1 polarization in microglia (91). The mouse macrophage line Raw264.7 that was stimulated with high glucose levels showed that glucose primarily activates macrophages via the ROCK/JNK and ROCK/ERK pathways, promotes the conversion of the pro-inflammatory phenotype, and increases TNF-alpha expression (109). Aldose reductase, an enzyme linked to the pathophysiology of DR and strongly connected to LPS-induced M1 polarization, promotes microglial cell activation (119).

The communication between microglial cells has also been investigated. Exosomes produced from activated microglia boost microglial activation by sending polarized signals to M0 microglia via miR-155-5p (107). Inhibiting suppressor of cytokine signaling 1 and activating the NF-κB pathway, miR-155-5p eventually triggers an inflammatory cascade and intensifies the angiogenesis impact (107). In addition, studies have been conducted to determine how microglia interact with macroglia like Müller cells and astrocytes. Müller cells are susceptible to M1-polarized microglia and secrete more pro-inflammatory cytokines including IL-1beta, IL-6, and iNOS. Bidirectional signaling between the two cell types further boosts microglial activation and migration. Müller cells promote inflammatory responses throughout the retinal layer in chemotactic and sticky cell interactions, boosting microglia mobilization (120). Hyperglycemia affects retinal astrocyte proliferation, adhesion, and migration by producing inflammatory mediators (121). Translocator protein (TSPO), a microglial and astrocyte gliosis biomarker in cerebral deterioration, is acutely and selectively increased in the retinal microglia in an inflammatory environment. Likewise, astrocytes have increased levels of their endogenous ligand, diazepam-binding inhibitor (DBI). Microglial activation is adversely regulated by TSPO-mediated signaling via DBI-derived ligands (122). A network of well-coordinated

TABLE 2 Signaling pathways related to polarization:.

Pathological process	Polarization phenotype	Signaling pathway	Authors
Inflammation	M1	NF-κB	Tang et al. (104) Fang et al. (105) Liu et al. (106) Chen et al. (107)
		TLR4/IRF5	Al-Rashed et al. (108)
		ROCK/JNK ROCK/ERK	Cheng et al. (109)
Oxidative stress	M1	ERK NF-κB	Khalid et al. (110) Yu et al. (111) Zhang et al. (112)
		TLR4/IRF5	Al-Rashed et al. (108)
Angiogenesis	M2	HIF-1α/VEGF/VEGFR2	Xu et al. (113) Liu et al. (114)
		histone acetyltransferase p300/spliced X-box binding protein 1/homocysteine-inducible endoplasmic reticulum protein with ubiquitin-like domain 1	Li et al. (115)
		CSF1/CSF-1R	Zhou et al. (116)
		prostaglandin E2/E-prostanoid 1 receptor/protein kinase C axis	Zhan et al. (117)

M1, conventionally activated macrophages; M2, alternatively activated macrophages; NF-κB, nuclear factor kappa-B; TLR, toll-like receptors; IRF, interferon regulatory factor; ROCK, Rho-associated coiled-coil containing protein kinase; JNK, c-Jun N-terminal kinase; ERK, extracellular regulated protein kinases; HIF, hypoxia inducible factor; VEGF, vascular endothelial growth factor; CSF, colony-stimulating factor.

astrocyte-microglial contacts is revealed by the inducibility and consequences of retinal DBI-TSPO signaling.

5.2 Oxidative stress

Free radicals are continually created in cells during metabolism under physiological conditions. Antioxidants are produced to neutralize these free radicals, ensuring a balance between them to support normal body functions. However, several metabolic issues can alter the ratio of free radicals to antioxidants, leading to an abundance of free radicals. Diabetes mellitus is a major metabolic disorder. Diabetes presents the retina with a double blow because it increases the formation of free radicals while simultaneously impairing their ability to be neutralized because of a dysfunctional antioxidant system (123). Cytosolic ROS damage the mitochondria, and mitochondrial damage enhances capillary cell death, which in turn causes diabetic retinopathy. This vicious cycle of ROS generation is further exacerbated by mitochondrial damage and continues to spread.

ERK and NF-κB signaling is activated by increased ROS levels and AGEs accumulation induced by hyperglycemia (110). Additionally, hyperglycemia stimulates HIF-1alpha-mediated VEGF production, which promotes neovascularization and serves a similar function by activating the ERK1/2-NF-κB signaling pathway in microglia (111, 112). The activation of TLR4/IRF5 signaling promotes M1 polarization and the production of matrix metalloproteinases (MMP)-9 at the same time (108). MMP-2 and MMP-9 are activated by increased ROS production, and with the aid of the heat shock protein 60, these MMPs penetrate the mitochondria. Subsequently, the mitochondrial membrane is damaged, which causes cytochrome c to leak into the cytoplasm and initiates apoptosis (124). Oxidative stress causes macrophages to polarize into the M1 form, which in turn promotes inflammation. Simultaneously, inflammatory cytokines are increased by oxidative stress and ROS may also be increased by inflammatory cytokines, forming a vicious cycle (125). Therefore, microglial polarization induces inflammation related to oxidative stress, which fosters DR emergence and progression.

Neurodegeneration and breakdown of the BRB are typical changes in the early DR stages. Before the development of clinical symptoms, the retinal neurons start decaying, and neuroretinal function is impaired prior to vascular lesions (25). Abnormal neural cell function, as well as pericyte and endothelial cell damage, are

caused by the production of neurotoxic substances, including glutamate, oxidative stress, caspase-3, MMPs, and nitrous oxide (126). In the retinas of diabetic rats, activated microglia phagocytosed endothelial cells, increasing acellular capillaries and albumin leakage (127). Ding et al. (128) observed that LPS-activated M1 microglia may induce pericyte apoptosis in co-cultures. Increased levels of ROS secreted by M1 microglia may be the main reason for disruption of the inner BRB.

5.3 Angiogenesis

As mentioned in this section, fibrovascular membranes in DR formation may be associated with M2 macrophages. Recent research on DR has mostly focused on M1 polarization; studies of M2 polarization in DR are still lacking. Therefore, we summarized the role of M2 polarization in different retinal neovascular disorders to penetrate the similar potential roles and mechanisms of M2 polarization in DR.

Retinopathy of prematurity is a severe vasoproliferative disease caused by preterm birth or postnatal hyperoxia. OIR in animal models of retinopathy of prematurity are commonly used to study retinal neovascularization. Macrophages polarize toward the M2 phenotype throughout the course of retinal neovascularization, as evidenced by the fact that M1 macrophage levels change from considerably high levels at postnatal day 13 to nearly normal levels at postnatal day 21, whereas M2 macrophage levels rise from postnatal day 13 to day 21 (129). Moreover, M2 macrophages encircle emerging vessels and connect vascular sprouts. Co-culturing of human umbilical vein endothelial cells with M1- or M2-like macrophage supernatants has revealed that M2 macrophages are more effective in promoting proliferation and tube formation (130). M2 macrophage depletion by mannosylated clodronate liposomes inhibits pathological neovascularization, whereas intravitreally injecting M2 macrophages derived from the bone marrow has enhanced pathological neovascularization in OIR mice models (131). According to Wang et al. (132), increased retinal neovascularization is the outcome of M2 macrophages' ability to attract and differentiate bone marrow-derived cells in response to stromal cell-derived factor-1 and VEGF. Furthermore, by stimulating signal transduction and activator of transcription 3, myeloid cells from circulation, particularly M2 macrophages, can travel through the lingual vascular system to the immature retina, which is ischemic and induces neovascularization (133).

Other investigations have looked into how M2 polarization influences neovascularization in AMD, which is a complicated, progressive, and degenerative disease influenced by several hereditary and environmental variables (134, 135). Two types of AMD manifest clinically: non-exudative senile macular degeneration, also called dry AMD, characterized by macular vitreous warts, pigmentary disorders, and map-like atrophy, and exudative senile macular degeneration, also called wet AMD, characterized mainly by choroidal neovascularization. The preponderance of M2 macrophages has been observed in both the mouse laser-induced choroidal neovascularization model and the atrial fluid of patients with wet AMD (136, 137). There may be a pathogenic change in the early AMD phases from pro-inflammatory M1 activity to protective M2 activity. M2 macrophages, in contrast, could serve a detrimental role by promoting fibrosis and angiogenesis. Macrophages stimulate VEGF production in laser- and AMD-associated choroidal neovascularization (138, 139). Activation of the HIF-1alpha/VEGF/VEGFR2 pathway has also been observed (113, 114). M2 macrophages are closely associated with VEGF production (132, 140). The histone acetyltransferase p300/spliced X-box binding protein 1/homocysteine-inducible endoplasmic reticulum protein with ubiquitin-like domain 1 (115), CSF1/CSF-1R (116) and prostaglandin E2/E-prostanoid 1 receptor/protein kinase C axis (117) can all, when hypoxic circumstances exist, stimulate M2 macrophage polarization, hence increase choroidal vascular endothelial cell proliferation, migration, and tube formation. M2 macrophages express leukotriene B4 (LTB4) receptor 1 (BLT1) which is drawn to the LTB to generate VEGF-A in a BLT1-dependent manner, inducing choroidal neovascularization formation (141). According to these investigations, M2 polarization is thought to be crucial for the growth of retinal neovascularization and to have a similar function in DR.

However, the specific role of M2 polarization in retinal neovascularization is still controversial. M2 macrophages are considered to play a protective function in tissue repair and remodeling (142). In a study of phase changes following OIR, in the late phase after postnatal day 17, IL-4/STAT6/PPAR-gamma signaling activity is heightened, activating M2 macrophages and peaks at postnatal day 20, causing the reduction of inflammation and the naturally occurring regression of neovascularization clusters (143). Due to a change in macrophage polarization towards an M2 phenotype, the OIR model that administered IL-17A neutralizing antibody had noticeably less retinal neovascularization than normal mice (144). Injecting umbilical cord blood-derived $CD14^{(+)}$ cells into OIR eyes stabilizes retinal ischemia-damaged vessels after subdivision into M2 macrophages (145). By controlling the inflammatory response, promoting tissue repair, accelerating nutritional recovery, enhancing the clearance of apoptotic cellular debris, and becoming tolerant instead of autoimmune, M2 macrophages aid in the normalization of the retinal vasculature. These effects are reinforced by the fact that M2 macrophages participate in downstream vascular anastomosis of VEGF-activated endothelial tip cells (146).

In summary, microglial polarization affects inflammation and oxidative stress caused by sustained tissue stress caused by hyperglycemia in DR, during which M1 macrophages play a critical role. The two processes interact with each other and promote the pathological alterations in DR. Pericyte loss occurs followed by endothelial cell injury due to chronic inflammation, eventually the BRB is destroyed and neoangiogenesis arises. M1 polarization has been the main subject of the majority of recent investigations on microglia polarization in DR. Other ocular neovascular disorders have been found to be related to both the pro-angiogenic and protective effects of M2 macrophages. Since DR is a typical retinal neovascularization disease caused by increased VEGF levels, the specific role of M2 macrophages in the pathogenesis of DR needs further study. Additionally, we have

integrated some currently recognized polarization pathways linked to ophthalmic diseases (Figure 2). Whether the same mechanisms that cause polarization in other diseases also play a role in DR requires further investigation.

6 New strategies for DR treatment targeting polarization

Considering the dominant role of M1 polarization in DR, current therapeutic approaches mainly focus on inhibiting the pro-inflammatory response to M1 polarization and promoting the switch of M1 to M2 polarization. Studies about the treatments related to polarization were summarized in Table 3.

6.1 Signaling inhibition related therapy

We can draw the conclusion that NF-κB signaling pathway really matters in M1-type polarization from the previously mentioned mechanisms. In order to effectively treat DR by targeting polarization, more attention is given to NF-κB signaling inhibitors. Melatonin (104) and pyrrolidinedithiocarbamate (149) injection into the vitreous cavity and Asiatic acid (105), cyanidin 3-O-glucoside (150) and ferulic acid (151) oral administration were reported to decrease NF-κB signaling, reduce inflammatory lesion and M1 polarization, and promote M2 polarization in the retina of rats with DR, therefore minimizing the lesions. They may simultaneously maintain BRB integrity by controlling the expression of proteins associated with barriers. The sp^2-iminosugar glycolipid (sp^2-IGL) family, (S_S,1R)-1-docecylsulfiny-5N,6O-oxomethylidenenojirimycin ((Ss)-DS-ONJ), increases the expression of heme oxygenase-1 and IL-10 in endotoxin-stimulated microglia, thereby exerting anti-inflammatory effects by inducing arginase-1 to boost M2 responses (152). Other members of the sp^2-IGL family, such as 1-dodecylsulfonyl-5N, 6O-oxomethylidenenojirimycin (DSO_2-ONJ) (153) and the sp_2-iminosugar dodecylsulfoxide derivative R-DS-ONJ (81) have also been shown to perform a similar function, alleviating DR. In addition, DBI-TSPO signaling in the retina is regulated by VEGF, which can alleviate the severity of inflammation, promote the production of neurotrophic factors, polarize M2 macrophages, and relieve neovascular retinopathy (154). Considering the role of aldose reductase in M1 polarization, pharmacological inhibition of aldose reductase could relieve M1 polarization induced by LPS, decelerate optic nerve degeneration, and decrease the capacity of activated microglia to induce apoptosis in retinal pigment epithelium cells, thus protecting the integrity of the BRB (119, 155–157).

6.2 Stem cell related therapy

Macrophages/microglial cells differentiate and develop from bone marrow hematopoietic cells. Based on different macrophage phenotypes and the conversion of phenotypes, a rising variety of researches have concentrated on the underlying value of bone marrow stem cell transplantation for the treatment of intravenous pathological neovascularization and retinal neurodegenerative diseases (166, 168–170). Numerous studies have demonstrated that intravenously injected stem cells or local transplantation can enhance function in ischemic regions (171–173). Stem cells can develop into endothelial (174, 175), neuronal (176, 177), and mature myeloid cells (such as, monocytes, macrophages, and dendritic cells) *in vitro*. According to recent studies, distinct tissue microenvironments subject myeloid cells to various stimuli and determine whether they differentiate into inflammatory macrophages (M1 and M2), endothelial cells, or dendritic cells (41, 178–180). Therefore, various myeloid cell subpopulations may have opposing effects on angiogenesis; one population may support

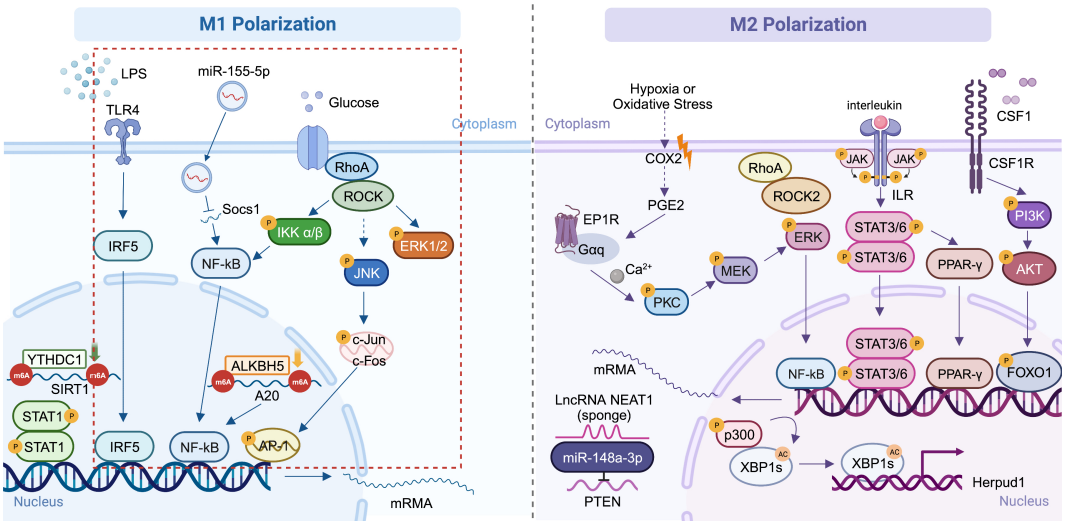

FIGURE 2
Mechanisms of macrophage polarization in ocular diseases. The main DR-related mechanisms are circled in red (91, 108, 109, 115–117, 134, 147, 148). Created with BioRender.com. M1, conventionally activated macrophages; M2, alternatively activated macrophages; DR, diabetic retinopathy.

TABLE 3 Treatments associated with polarization:.

Treatment	Detailed name	Administration	Pharmacological effect	Authors
medication	Melatonin	Intravitreal injection	Inhibit NF-κB signaling	Tang et al. (104)
	Pyrrolidinedithiocarbamate			Sui et al. (149)
	Asiatic acid	Oral administration		Fang et al. (105)
	Cyanidin 3-O-glucoside			Zhao et al. (150)
	Ferulic acid			Sun et al. (151)
	(S_S,1R)-1-docecylsulfiny-5N,6O-oxomethylidenenojirimycin ((Ss)-DS-ONJ)	*In vitro* experiment	Boost M2 responses	Cano-Cano et al. (152)
	1-dodecylsulfonyl-5N, 6O-oxomethylidenenojirimycin (DSO_2-ONJ)			Alcalde-Estévez et al. (153)
	sp_2-iminosugar dodecylsulfoxide derivative R-DS-ONJ			Arroba et al. (81)
	Anti-VEGF agent	Intravitreal injection	Regulate DBI-TSPO signaling	Gao et al. (154)
	Sorbinil, β-glucogallin	*In vitro* experiment	Inhibit aldose reductase	Chang et al. (119)
	Sorbinil	Intraperitoneal injection		Chang et al. (155) Rao et al. (156)
	Sorbinil	*In vitro* experiment		Huang et al. (157)
Stem cell therapy	Human umbilical cord blood	Intravitreal injection	Phenotypic transition from M1 to M2	Marchetti et al. (145) El Kasmi et al. (158) Panopoulos et al. (159) Ritter et al. (160) Xu et al. (161)
	Mesenchymal stem cells	*In vitro* experiment		An et al. (162) Jaimes et al. (163) Teixeira-Pinheiro et al. (164) Honda et al. (165)
	Bone marrow-derived precursor cells			Medina et al. (166) Nakagawa et al. (167)

M1, conventionally activated macrophages; M2, alternatively activated macrophages; NF-κB, nuclear factor kappa-B; DBI, diazepam-binding inhibitor; TSPO, translocator protein.

angiogenesis in tumors (181), whereas another may suppress tip cell numbers and vascular sprouting (182).

Mesenchymal stem cells (MSCs) are found in various tissues and can differentiate in several directions. MSCs are a potential therapy for inflammatory illnesses because a significant body of research has shown that they are potent immunomodulators. They often influence microglial polarization via paracrine actions (183). MSCs inhibit NF-κB activation and excretion of TNF-alpha stimulated protein 6 in human umbilical vein endothelial cells co-stimulated by hyperglycemia and megadose of palmitic acid, thereby suppressing inflammation (162). After co-culturing with MSC-derived microvesicles, increased levels of M2 markers and fewer LPS-induced pro-inflammatory cytokines were detected in BV-2 cells, indicating their role in the phenotypic transition from M1 to M2 (163). To observe the role of MSCs in the retina, MSCs obtained from human umbilical cords were co-cultured with complete adult rat retinal explants and kept apart using a transwell membrane (164). Due to a decline in M1 markers and a raise in M2 markers, paracrine signaling of hMSC altered the microglial phenotype and the production of anti-inflammatory proteins in the retina (164). In neurological studies, MSCs have been found to induce M2 polarization in macrophages and facilitate their migration into MSCs *in vitro* (165). Therefore, it is conceivable that injecting MSCs into the vitreous cavity may be a potential therapeutic approach for treating DR since it may increase the number of microglia with anti-inflammatory phenotypes and help preserve the retina.

According to Marchetti et al. (145) injecting the human umbilical cord blood into the vitreous cavity has a significant curative effect, creating abundant myeloid progenitor $CD14^{(+)}$ cells. $CD14^{(+)}$ cells can stop abnormal neovascularization and polarize into M2 macrophages. For the sake of managing cell proliferation, differentiation, and the resolution of inflammation, $CD14^{(+)}$ cells develop into a macrophage oriented M2 type, inducing the production of genes participating in cellular signals such as IFI6, IFI1631, BCL2A1, AKT1, NF-κB1, and TGF-beta1. They not only ease oxidative stress, apoptosis, inflammation, and angiogenesis (145, 158, 159) but also stabilize the retinal vasculature (160, 161). Furthermore, transcriptome sequencing has validated the biological functions of $CD14^{(+)}$ cells.

Nakagawa et al. (167) also confirmed that bone marrow-derived precursor cells can migrate to the retinal vascular network, differentiate

into glial cells, and promote the steady state of the blood vessels of the retina, which plays an essential role in retinal vascular reconstruction and stabilization. Therefore, they hypothesized that this protective effect may be intimately linked to macrophage/microglia polarization. To determine whether myeloid angiogenic cells exhibit pro-angiogenic characteristics, Medina et al. (166) employed a 3D Matrigel tube formation assay and discovered that myeloid angiogenic cells might cause endothelial tube development *in vitro* in a paracrine manner. Additional research focusing on M1/M2 markers and pro-angiogenic genes revealed that myeloid angiogenic cells significantly expressed M2 macrophage markers, such as IL-10, transforming growth factor beta 2, CD163, macrophage scavenger receptor 1, and mannose receptor C type 1. However, pro-inflammatory M1 macrophage markers, such as TNF, IL-1, IL-6, IL-12, and cytochrome c oxidase subunit II were almost undetected. The pro-angiogenic genes VEGF-beta, connective tissue growth factor, platelet-derived growth factor beta polypeptide, neuropilin 1, and MMP-9 were also strongly expressed. This study demonstrated that M1 macrophage markers were downregulated, whereas pro-angiogenic genes and M2 macrophage markers were highly upregulated.

Overall, stem cells are a promising treatment for DR because of their pluripotency. More critically, DR development may be significantly slowed by the promotion of stem cell differentiation into M2 macrophages with anti-inflammatory capabilities.

7 Discussion

As important immunoregulatory cells, the extensive distribution and function of macrophages and microglia have become a research hotspot. Recently, researches have focused more on polarization and differentiation in cancer, cardiovascular diseases, obesity, and neovascularization. In ocular diseases, macrophage/microglia polarization is associated with the onset of illness, especially DR. The inflammatory stage appears to be dominated by M1 polarization, which is also correlated with the beginning of inflammation and the onset of early tissue damage. Disease relief and tissue healing are highly correlated with M2 polarization. However, it is also crucial to remember that increased M2 polarization may play a role in several aberrant healing processes, including fibrosis and angiogenesis. Phenotype conversion not only reflects the tissue microenvironment inflammatory state but also suggests the severity of pathological neovascularization, which affects the outcome and prognosis of the disease.

The present review demonstrated that early DR, even at the preclinical stage, is accompanied by both M1 and M2 polarization, whereas only M1 polarization is effective in the latter phases. The classic change in the latter phase of DR (PDR) is the secretion of large quantities of VEGF, which results in retinal neovascularization. However, M2 polarization is often considered to result in excessive VEGF release. Therefore, further research is needed to explore whether M2 polarization continues to play a significant role in the later DR stages so that more precise treatment can be realized. Moreover, the target of current treatments is to convert M1 polarization to M2 polarization. It is still doubtful whether such medication will boost VEGF output and aggravate the lesion, despite the possibility that it will reduce inflammation. Inflammation and neovascularization signaling pathways often crosstalk, and persistent chronic inflammation can result in neovascularization. The M2 macrophages are mostly anti-inflammatory and pro-neovascular cells. If M2 macrophages encourage the formation of structurally and functionally intact neovascularization to replace pathogenic neovascularization in DR, this may represent a potential therapeutic strategy. A better approach is to focus more on the transformation of resting M0 macrophages, which should be further investigated. Stem cell therapy deserves more attention as a personalized treatment. Depending on its pluripotency, they may differentiate into various macrophage states, including M1, M2, and even quiescent M0, thereby opening up more treatment options. Depending on an individual patient's retinal microenvironment, different measures can be implemented on a case-by-case basis, thus maximizing personalization.

Given that the current research is not in-depth, further exploration of the internal mechanisms of macrophage/microglial polarization is important for understanding ocular diseases. The "double" polarization of macrophages/microglia remains controversial, its plasticity and diversity need to be further studied and assessed. It is still being determined whether some functional categories reflect different populations because macrophage polarization characteristics are not unique. It is also possible to reverse polarization imbalances, thus intervening in disease development. These findings will likely provide new therapeutic strategies for DR and bring up new therapy options for ocular disorders.

Author contributions

YY: Writing – original draft, Visualization. JL: Writing – original draft, Writing – review & editing. YZ: Writing – original draft, Writing – review & editing. SW: Writing – original draft. ZZ: Writing – original draft. QJ: Writing – review & editing, Supervision. KL: Writing – review & editing, Supervision, Funding acquisition.

Funding

The authors declare financial support was received for the research, authorship, and/or publication of this article. The study was funded by the National Natural Science Foundation of China (82171080, 82101155), and Postgraduate Research & Practice Innovation Program of Jiangsu Province (JX10413973).

Acknowledgments

The authors would like to express their gratitude to the Affiliated Eye Hospital of Nanjing Medical University for funding the study. The study was funded by the National Natural Science Foundation of China (82171080, 82101155), and Postgraduate

Research & Practice Innovation Program of Jiangsu Province (JX10413973).

Conflict of interest

The authors declare that the research was conducted in the absence of any commercial or financial relationships that could be construed as a potential conflict of interest.

Publisher's note

References

1. Murray PJ. Macrophage polarization. *Annu Rev Physiol* (2017) 79:541–66. doi: 10.1146/annurev-physiol-022516-034339

2. Hu X. Microglia/macrophage polarization: Fantasy or evidence of functional diversity? *J Cereb Blood Flow Metab* (2020) 40(1_suppl):S134–s6. doi: 10.1177/0271678x20963405

3. Pérez S, Rius-Pérez S. Macrophage polarization and reprogramming in acute inflammation: A redox perspective. *Antioxid (Basel)* (2022) 11(7):1394. doi: 10.3390/antiox11071394

4. Ahamada MM, Jia Y, Wu X. Macrophage polarization and plasticity in systemic lupus erythematosus. *Front Immunol* (2021) 12:734008. doi: 10.3389/fimmu.2021.734008

5. Garnier M, Gibelin A, Mailleux AA, Leçon V, Hurtado-Nedelec M, Laschet J, et al. Macrophage polarization favors epithelial repair during acute respiratory distress syndrome. *Crit Care Med* (2018) 46(7):e692–701. doi: 10.1097/ccm.0000000000003150

6. Dong B, Wang C, Zhang J, Zhang J, Gu Y, Guo X, et al. Exosomes from human umbilical cord mesenchymal stem cells attenuate the inflammation of severe steroid-resistant asthma by reshaping macrophage polarization. *Stem Cell Res Ther* (2021) 12(1):204. doi: 10.1186/s13287-021-02244-6

7. Wu HM, Ni XX, Xu QY, Wang Q, Li XY, Hua J. Regulation of lipid-induced macrophage polarization through modulating peroxisome proliferator-activated receptor-gamma activity affects hepatic lipid metabolism via a Toll-like receptor 4/NF-κB signaling pathway. *J Gastroenterol Hepatol* (2020) 35(11):1998–2008. doi: 10.1111/jgh.15025

8. Zhang W, Zheng X, Yu Y, Zheng L, Lan J, Wu Y, et al. Renal cell carcinoma-derived exosomes deliver lncARSR to induce macrophage polarization and promote tumor progression via STAT3 pathway. *Int J Biol Sci* (2022) 18(8):3209–22. doi: 10.7150/ijbs.70289

9. Hsieh SW, Huang LC, Chang YP, Hung CH, Yang YH. M2b macrophage subset decrement as an indicator of cognitive function in Alzheimer's disease. *Psychiatry Clin Neurosci* (2020) 74(7):383–91. doi: 10.1111/pcn.13000

10. Behnke V, Wolf A, Langmann T. The role of lymphocytes and phagocytes in age-related macular degeneration (AMD). *Cell Mol Life Sci* (2020) 77(5):781–8. doi: 10.1007/s00018-019-03419-4

11. Rathi S, Jalali S, Patnaik S, Shahulhameed S, Musada GR, Balakrishnan D, et al. Abnormal complement activation and inflammation in the pathogenesis of retinopathy of prematurity. *Front Immunol* (2017) 8:1868. doi: 10.3389/fimmu.2017.01868

12. Okunuki Y, Mukai R, Nakao T, Tabor SJ, Butovsky O, Dana R, et al. Retinal microglia initiate neuroinflammation in ocular autoimmunity. *Proc Natl Acad Sci U S A* (2019) 116(20):9989–98. doi: 10.1073/pnas.1820387116

13. García-Mulero S, Alonso MH, Del Carpio LP, Sanz-Pamplona R, Piulats JM. Additive role of immune system infiltration and angiogenesis in uveal melanoma progression. *Int J Mol Sci* (2021) 22(5):2669. doi: 10.3390/ijms22052669

14. Yu J, Chai P, Xie M, Ge S, Ruan J, Fan X, et al. Histone lactylation drives oncogenesis by facilitating m(6)A reader protein YTHDF2 expression in ocular melanoma. *Genome Biol* (2021) 22(1):85. doi: 10.1186/s13059-021-02308-z

15. Qu R, Zhou M, Qiu Y, Peng Y, Yin X, Liu B, et al. Glucocorticoids improve the balance of M1/M2 macrophage polarization in experimental autoimmune uveitis through the P38MAPK-MEF2C axis. *Int Immunopharmacol* (2023) 120:110392. doi: 10.1016/j.intimp.2023.110392

16. Zeng Y, Wen F, Mi L, Ji Y, Zhang X. Changes in macrophage-like cells characterized by en face optical coherence tomography after retinal stroke. *Front Immunol* (2022) 13:987836. doi: 10.3389/fimmu.2022.987836

17. Gao F, Hou H, Liang H, Weinreb RN, Wang H, Wang Y. Bone marrow-derived cells in ocular neovascularization: contribution and mechanisms. *Angiogenesis* (2016) 19(2):107–18. doi: 10.1007/s10456-016-9497-6

18. Teo ZL, Tham YC, Yu M, Chee ML, Rim TH, Cheung N, et al. Global prevalence of diabetic retinopathy and projection of burden through 2045: systematic review and meta-analysis. *Ophthalmology* (2021) 128(11):1580–91. doi: 10.1016/j.ophtha.2021.04.027

19. Cheung N, Mitchell P, Wong TY. Diabetic retinopathy. *Lancet* (2010) 376(9735):124–36. doi: 10.1016/s0140-6736(09)62124-3

20. Crabtree GS, Chang JS. Management of complications and vision loss from proliferative diabetic retinopathy. *Curr Diabetes Rep* (2021) 21(9):33. doi: 10.1007/s11892-021-01396-2

21. Mills SA, Jobling AI, Dixon MA, Bui BV, Vessey KA, Phipps JA, et al. Fractalkine-induced microglial vasoregulation occurs within the retina and is altered early in diabetic retinopathy. *Proc Natl Acad Sci U.S.A.* (2021) 118(51):e2112561118. doi: 10.1073/pnas.2112561118

22. Newman EA. Functional hyperemia and mechanisms of neurovascular coupling in the retinal vasculature. *J Cereb Blood Flow Metab* (2013) 33(11):1685–95. doi: 10.1038/jcbfm.2013.145

23. Garhöfer G, Chua J, Tan B, Wong D, Schmidl D, Schmetterer L. Retinal neurovascular coupling in diabetes. *J Clin Med* (2020) 9(9):2829. doi: 10.3390/jcm9092829

24. Kinuthia UM, Wolf A, Langmann T. Microglia and inflammatory responses in diabetic retinopathy. *Front Immunol* (2020) 11:564077. doi: 10.3389/fimmu.2020.564077

25. Altmann C, Schmidt MHH. The role of microglia in diabetic retinopathy: inflammation, microvasculature defects and neurodegeneration. *Int J Mol Sci* (2018) 19(1):110. doi: 10.3390/ijms19010110

26. Berrocal MH, Acaba LA, Chenworth ML. Surgical innovations in the treatment of diabetic macular edema and diabetic retinopathy. *Curr Diabetes Rep* (2019) 19(10):106. doi: 10.1007/s11892-019-1210-x

27. Everett LA, Paulus YM. Laser therapy in the treatment of diabetic retinopathy and diabetic macular edema. *Curr Diabetes Rep* (2021) 21(9):35. doi: 10.1007/s11892-021-01403-6

28. Berrocal MH, Acaba-Berrocal L. Early pars plana vitrectomy for proliferative diabetic retinopathy: update and review of current literature. *Curr Opin Ophthalmol* (2021) 32(3):203–8. doi: 10.1097/icu.0000000000000760

29. Duh EJ, Sun JK, Stitt AW. Diabetic retinopathy: current understanding, mechanisms, and treatment strategies. *JCI Insight* (2017) 2(14):e93751. doi: 10.1172/jci.insight.93751

30. Bian Z, Gong Y, Huang T, Lee CZW, Bian L, Bai Z, et al. Deciphering human macrophage development at single-cell resolution. *Nature* (2020) 582(7813):571–6. doi: 10.1038/s41586-020-2316-7

31. Masuda T, Amann L, Prinz M. Novel insights into the origin and development of CNS macrophage subsets. *Clin Transl Med* (2022) 12(11):e1096. doi: 10.1002/ctm2.1096

32. Silvin A, Uderhardt S, Piot C, Da Mesquita S, Yang K, Geirsdottir L, et al. Dual ontogeny of disease-associated microglia and disease inflammatory macrophages in aging and neurodegeneration. *Immunity* (2022) 55(8):1448–65.e6. doi: 10.1016/j.immuni.2022.07.004

33. Perdiguero EG, Geissmann F. The development and maintenance of resident macrophages. *Nat Immunol* (2016) 17(1):2–8. doi: 10.1038/ni.3341

34. Wang X, Zhao L, Zhang J, Fariss RN, Ma W, Kretschmer F, et al. Requirement for microglia for the maintenance of synaptic function and integrity in the mature retina. *J Neurosci* (2016) 36(9):2827–42. doi: 10.1523/jneurosci.3575-15.2016

35. Yunna C, Mengru H, Lei W, Weidong C. Macrophage M1/M2 polarization. *Eur J Pharmacol* (2020) . 877:173090. doi: 10.1016/j.ejphar.2020.173090

36. Guo S, Wang H, Yin Y. Microglia polarization from M1 to M2 in neurodegenerative diseases. *Front Aging Neurosci* (2022) 14:815347. doi: 10.3389/fnagi.2022.815347

37. Costantini A, Viola N, Berretta A, Galeazzi R, Matacchione G, Sabbatinelli J, et al. Age-related M1/M2 phenotype changes in circulating monocytes from healthy/

unhealthy individuals. *Aging (Albany NY)* (2018) 10(6):1268–80. doi: 10.18632/aging.101465

38. Orihuela R, McPherson CA, Harry GJ. Microglial M1/M2 polarization and metabolic states. *Br J Pharmacol* (2016) 173(4):649–65. doi: 10.1111/bph.13139

39. Zhou T, Liu Y, Yang Z, Ni B, Zhu X, Huang Z, et al. IL-17 signaling induces iNOS+ microglia activation in retinal vascular diseases. *Glia* (2021) 69(11):2644–57. doi: 10.1002/glia.24063

40. Zhou L, Wang D, Qiu X, Zhang W, Gong Z, Wang Y, et al. DHZCP Modulates Microglial M1/M2 Polarization via the p38 and TLR4/NF-κB Signaling Pathways in LPS-Stimulated Microglial Cells. *Front Pharmacol* (2020) 11:1126. doi: 10.3389/fphar.2020.01126

41. Shapouri-Moghaddam A, Mohammadian S, Vazini H, Taghadosi M, Esmaeili SA, Mardani F, et al. Macrophage plasticity, polarization, and function in health and disease. *J Cell Physiol* (2018) 233(9):6425–40. doi: 10.1002/jcp.26429

42. Geng P, Zhu H, Zhou W, Su C, Chen M, Huang C, et al. Baicalin inhibits influenza A virus infection via promotion of M1 macrophage polarization. *Front Pharmacol* (2020) 11:1298. doi: 10.3389/fphar.2020.01298

43. Wang X, Li H, Chen S, He J, Chen W, Ding Y, et al. P300/CBP-associated factor (PCAF) attenuated M1 macrophage inflammatory responses possibly through KLF2 and KLF4. *Immunol Cell Biol* (2021) 99(7):724–36. doi: 10.1111/imcb.12455

44. Topf MC, Tuluc M, Harshyne LA, Luginbuhl A. Macrophage type 2 differentiation in a patient with laryngeal squamous cell carcinoma and metastatic prostate adenocarcinoma to the cervical lymph nodes. *J Immunother Cancer* (2017) 5(1):60. doi: 10.1186/s40425-017-0264-z

45. Fan W, Huang W, Chen J, Li N, Mao L, Hou S. Retinal microglia: Functions and diseases. *Immunology* (2022) 166(3):268–86. doi: 10.1111/imm.13479

46. Mantovani A, Sozzani S, Locati M, Allavena P, Sica A. Macrophage polarization: tumor-associated macrophages as a paradigm for polarized M2 mononuclear phagocytes. *Trends Immunol* (2002) 23(11):549–55. doi: 10.1016/S1471-4906(02)02302-5

47. Pan Y, Yu Y, Wang X, Zhang T. Tumor-associated macrophages in tumor immunity. *Front Immunol* (2020) 11:583084. doi: 10.3389/fimmu.2020.583084

48. Zhu C, Kros JM, Cheng C, Mustafa D. The contribution of tumor-associated macrophages in glioma neo-angiogenesis and implications for anti-angiogenic strategies. *Neuro Oncol* (2017) 19(11):1435–46. doi: 10.1093/neuonc/nox081

49. Jackaman C, Yeoh TL, Acuil ML, Gardner JK, Nelson DJ. Murine mesothelioma induces locally-proliferating IL-10(+)TNF-α(+)CD206(-)CX3CR1(+) M3 macrophages that can be selectively depleted by chemotherapy or immunotherapy. *Oncoimmunology* (2016) 5(6):e1173299. doi: 10.1080/2162402x.2016.1173299

50. Helm O, Held-Feindt J, Grage-Griebenow E, Reiling N, Ungefroren H, Vogel I, et al. Tumor-associated macrophages exhibit pro- and anti-inflammatory properties by which they impact on pancreatic tumorigenesis. *Int J Cancer* (2014) 135(4):843–61. doi: 10.1002/ijc.28736

51. Zhou J, Tang Z, Gao S, Li C, Feng Y, Zhou X. Tumor-associated macrophages: recent insights and therapies. *Front Oncol* (2020) 10:188. doi: 10.3389/fonc.2020.00188

52. Lin H, Lee E, Hestir K, Leo C, Huang M, Bosch E, et al. Discovery of a cytokine and its receptor by functional screening of the extracellular proteome. *Science* (2008) 320(5877):807–11. doi: 10.1126/science.1154370

53. Martinez FO, Gordon S. The M1 and M2 paradigm of macrophage activation: time for reassessment. *F1000Prime Rep* (2014) 6:13. doi: 10.12703/p6-13

54. De I, Nikodemova M, Steffen MD, Sokn E, Maklakova VI, Watters JJ, et al. CSF1 overexpression has pleiotropic effects on microglia in vivo. *Glia* (2014) 62(12):1955–67. doi: 10.1002/glia.22717

55. Walker DG, Lue LF. Immune phenotypes of microglia in human neurodegenerative disease: challenges to detecting microglial polarization in human brains. *Alzheimers Res Ther* (2015) 7(1):56. doi: 10.1186/s13195-015-0139-9

56. Eyo UB, Wu LJ. Microglia: Lifelong patrolling immune cells of the brain. *Prog Neurobiol* (2019) 179:101614. doi: 10.1016/j.pneurobio.2019.04.003

57. Gomez Perdiguero E, Klapproth K, Schulz C, Busch K, Azzoni E, Crozet L, et al. Tissue-resident macrophages originate from yolk-sac-derived erythro-myeloid progenitors. *Nature* (2015) 518(7540):547–51. doi: 10.1038/nature13989

58. O'Koren EG, Yu C, Klingeborn M, Wong AYW, Prigge CL, Mathew R, et al. Microglial function is distinct in different anatomical locations during retinal homeostasis and degeneration. *Immunity* (2019) 50(3):723–37.e7. doi: 10.1016/j.immuni.2019.02.007

59. Ginhoux F, Prinz M. Origin of microglia: current concepts and past controversies. *Cold Spring Harb Perspect Biol* (2015) 7(8):a020537. doi: 10.1101/cshperspect.a020537

60. McPherson SW, Heuss ND, Lehmann U, Roehrich H, Abedin M, Gregerson DS. The retinal environment induces microglia-like properties in recruited myeloid cells. *J Neuroinflammation* (2019) 16(1):151. doi: 10.1186/s12974-019-1546-9

61. Tay TL, Mai D, Dautzenberg J, Fernández-Klett F, Lin G, Sagar, et al. A new fate mapping system reveals context-dependent random or clonal expansion of microglia. *Nat Neurosci* (2017) 20(6):793–803. doi: 10.1038/nn.4547

62. Heuss ND, Pierson MJ, Roehrich H, McPherson SW, Gram AL, Li L, et al. Optic nerve as a source of activated retinal microglia post-injury. *Acta Neuropathol Commun* (2018) 6(1):66. doi: 10.1186/s40478-018-0571-8

63. Diaz-Araya CM, Provis JM, Penfold PL, Billson FA. Development of microglial topography in human retina. *J Comp Neurol* (1995) 363(1):53–68. doi: 10.1002/cne.903630106

64. Asare-Bediako B, Adu-Agyeiwaah Y, Abad A, Li Calzi S, Floyd JL, Prasad R, et al. Hematopoietic cells influence vascular development in the retina. *Cells* (2022) 11(20):3207. doi: 10.3390/cells11203207

65. Santos AM, Calvente R, Tassi M, Carrasco MC, Martín-Oliva D, Marín-Teva JL, et al. Embryonic and postnatal development of microglial cells in the mouse retina. *J Comp Neurol* (2008) 506(2):224–39. doi: 10.1002/cne.21538

66. Singaravelu J, Zhao L, Fariss RN, Nork TM, Wong WT. Microglia in the primate macula: specializations in microglial distribution and morphology with retinal position and with aging. *Brain Struct Funct* (2017) 222(6):2759–71. doi: 10.1007/s00429-017-1370-x

67. Li F, Jiang D, Samuel MA. Microglia in the developing retina. *Neural Dev* (2019) 14(1):12. doi: 10.1186/s13064-019-0137-x

68. Stevens B, Schafer DP. Roles of microglia in nervous system development, plasticity, and disease. *Dev Neurobiol* (2018) 78(6):559–60. doi: 10.1002/dneu.22594

69. Kierdorf K, Prinz M. Microglia in steady state. *J Clin Invest* (2017) 127(9):3201–9. doi: 10.1172/jci90602

70. Castanos MV, Zhou DB, Linderman RE, Allison R, Milman T, Carroll J, et al. Imaging of macrophage-like cells in living human retina using clinical OCT. *Invest Ophthalmol Vis Sci* (2020) 61(6):48. doi: 10.1167/iovs.61.6.48

71. Phipps JA, Vessey KA, Brandli A, Nag N, Tran MX, Jobling AI, et al. The role of angiotensin II/AT1 receptor signaling in regulating retinal microglial activation. *Invest Ophthalmol Vis Sci* (2018) 59(1):487–98. doi: 10.1167/iovs.17-22416

72. Vidal-Itriago A, Radford RAW, Aramideh JA, Maurel C, Scherer NM, Don EK, et al. Microglia morphophysiological diversity and its implications for the CNS. *Front Immunol* (2022) 13:997786. doi: 10.3389/fimmu.2022.997786

73. Nian S, Lo ACY, Mi Y, Ren K, Yang D. Neurovascular unit in diabetic retinopathy: pathophysiological roles and potential therapeutical targets. *Eye Vis (Lond)* (2021) 8(1):15. doi: 10.1186/s40662-021-00239-1

74. Lee JE, Liang KJ, Fariss RN, Wong WT. Ex vivo dynamic imaging of retinal microglia using time-lapse confocal microscopy. *Invest Ophthalmol Vis Sci* (2008) 49(9):4169–76. doi: 10.1167/iovs.08-2076

75. Huang Z, Zhou T, Sun X, Zheng Y, Cheng B, Li M, et al. Necroptosis in microglia contributes to neuroinflammation and retinal degeneration through TLR4 activation. *Cell Death Differ* (2018) 25(1):180–9. doi: 10.1038/cdd.2017.141

76. Spencer BG, Estevez JJ, Liu E, Craig JE, Finnie JW. Pericytes, inflammation, and diabetic retinopathy. *Inflammopharmacology* (2020) 28(3):697–709. doi: 10.1007/s10787-019-00647-9

77. Wang L, Pavlou S, Du X, Bhuckory M, Xu H, Chen M. Glucose transporter 1 critically controls microglial activation through facilitating glycolysis. *Mol Neurodegener* (2019) 14(1):2. doi: 10.1186/s13024-019-0305-9

78. Fadini GP, de Kreutzenberg SV, Boscaro E, Albiero M, Cappellari R, Kränkel N, et al. An unbalanced monocyte polarisation in peripheral blood and bone marrow of patients with type 2 diabetes has an impact on microangiopathy. *Diabetologia* (2013) 56(8):1856–66. doi: 10.1007/s00125-013-2918-9

79. Chen C, Wu S, Hong Z, Chen X, Shan X, Fischbach S, et al. Chronic hyperglycemia regulates microglia polarization through ERK5. *Aging (Albany NY)* (2019) 11(2):697–706. doi: 10.18632/aging.101770

80. Fadini GP, Cappellari R, Mazzucato M, Agostini C, Vigili de Kreutzenberg S, Avogaro A. Monocyte-macrophage polarization balance in pre-diabetic individuals. *Acta Diabetol* (2013) 50(6):977–82. doi: 10.1007/s00592-013-0517-3

81. Arroba AI, Alcalde-Estevez E, García-Ramírez M, Cazzoni D, de la Villa P, Sánchez-Fernández EM, et al. Modulation of microglia polarization dynamics during diabetic retinopathy in db/db mice. *Biochim Biophys Acta* (2016) 1862(9):1663–74. doi: 10.1016/j.bbadis.2016.05.024

82. Eid S, Sas KM, Abcouwer SF, Feldman EL, Gardner TW, Pennathur S, et al. New insights into the mechanisms of diabetic complications: role of lipids and lipid metabolism. *Diabetologia* (2019) 62(9):1539–49. doi: 10.1007/s00125-019-4959-1

83. Yan J, Horng T. Lipid metabolism in regulation of macrophage functions. *Trends Cell Biol* (2020) 30(12):979–89. doi: 10.1016/j.tcb.2020.09.006

84. Fadini GP, Simoni F, Cappellari R, Vitturi N, Galasso S, Vigili de Kreutzenberg S, et al. Pro-inflammatory monocyte-macrophage polarization imbalance in human hypercholesterolemia and atherosclerosis. *Atherosclerosis* (2014) 237(2):805–8. doi: 10.1016/j.atherosclerosis.2014.10.106

85. Sun J, Huang Q, Li S, Meng F, Li X, Gong X. miR-330-5p/Tim-3 axis regulates macrophage M2 polarization and insulin resistance in diabetes mice. *Mol Immunol* (2018) 95:107–13. doi: 10.1016/j.molimm.2018.02.006

86. Gao J, Cheng Y, Hao H, Yin Y, Xue J, Zhang Q, et al. Decitabine assists umbilical cord-derived mesenchymal stem cells in improving glucose homeostasis by modulating macrophage polarization in type 2 diabetic mice. *Stem Cell Res Ther* (2019) 10(1):259. doi: 10.1186/s13287-019-1338-2

87. Chen X, Zhuo S, Zhu T, Yao P, Yang M, Mei H, et al. Fpr2 deficiency alleviates diet-induced insulin resistance through reducing body weight gain and inhibiting inflammation mediated by macrophage chemotaxis and M1 polarization. *Diabetes* (2019) 68(6):1130–42. doi: 10.2337/db18-0469

88. Sha W, Zhao B, Wei H, Yang Y, Yin H, Gao J, et al. Astragalus polysaccharide ameliorates vascular endothelial dysfunction by stimulating macrophage M2 polarization via potentiating Nrf2/HO-1 signaling pathway. *Phytomedicine* (2023) 112:154667. doi: 10.1016/j.phymed.2023.154667

89. Zhu X, Xing P, Zhang P, Zhang M, Shen H, Chen L, et al. Fine-tuning of microglia polarization prevents diabetes-associated cerebral atherosclerosis. *Front Immunol* (2022) 13:948457. doi: 10.3389/fimmu.2022.948457

90. Sood A, Fernandes V, Preeti K, Khot M, Khatri DK, Singh SB. Fingolimod Alleviates Cognitive Deficit in Type 2 Diabetes by Promoting Microglial M2 Polarization via the pSTAT3-jmjd3 Axis. *Mol Neurobiol* (2023) 60(2):901–22. doi: 10.1007/s12035-022-03120-x

91. Chen T, Zhu W, Wang C, Dong X, Yu F, Su Y, et al. ALKBH5-mediated mA modification of A20 regulates microglia polarization in diabetic retinopathy. *Front Immunol* (2022) 13:813979. doi: 10.3389/fimmu.2022.813979

92. Lv K, Ying H, Hu G, Hu J, Jian Q, Zhang F. Integrated multi-omics reveals the activated retinal microglia with intracellular metabolic reprogramming contributes to inflammation in STZ-induced early diabetic retinopathy. *Front Immunol* (2022) 13:942768. doi: 10.3389/fimmu.2022.942768

93. Chen X, Zhou H, Gong Y, Wei S, Zhang M. Early spatiotemporal characterization of microglial activation in the retinas of rats with streptozotocin-induced diabetes. *Graefes Arch Clin Exp Ophthalmol* (2015) 253(4):519–25. doi: 10.1007/s00417-014-2727-y

94. Omri S, Behar-Cohen F, de Kozak Y, Sennlaub F, Verissimo LM, Jonet L, et al. Microglia/macrophages migrate through retinal epithelium barrier by a transcellular route in diabetic retinopathy: role of PKCζ in the Goto Kakizaki rat model. *Am J Pathol* (2011) 179(2):942–53. doi: 10.1016/j.ajpath.2011.04.018

95. Zeng HY, Green WR, Tso MO. Microglial activation in human diabetic retinopathy. *Arch Ophthalmol* (2008) 126(2):227–32. doi: 10.1001/archophthalmol.2007.65

96. Ong JX, Nesper PL, Fawzi AA, Wang JM, Lavine JA. Macrophage-like cell density is increased in proliferative diabetic retinopathy characterized by optical coherence tomography angiography. *Invest Ophthalmol Vis Sci* (2021) 62(10):2. doi: 10.1167/iovs.62.10.2

97. Zhang NT, Nesper PL, Ong JX, Wang JM, Fawzi AA, Lavine JA. Macrophage-like cells are increased in patients with vision-threatening diabetic retinopathy and correlate with macular edema. *Diagnostics* (2022) 12(11):2793. doi: 10.3390/diagnostics12112793

98. Rajesh A, Droho S, Lavine JA. Macrophages in close proximity to the vitreoretinal interface are potential biomarkers of inflammation during retinal vascular disease. *J Neuroinflammation* (2022) 19(1):203. doi: 10.1186/s12974-022-02562-3

99. Liu Z, Xu J, Ma Q, Zhang X, Yang Q, Wang L, et al. Glycolysis links reciprocal activation of myeloid cells and endothelial cells in the retinal angiogenic niche. *Sci Transl Med* (2020) 12(555):eaay1371. doi: 10.1126/scitranslmed.aay1371

100. Meng Z, Chen Y, Wu W, Yan B, Meng Y, Liang Y, et al. Exploring the immune infiltration landscape and M2 macrophage-related biomarkers of proliferative diabetic retinopathy. *Front Endocrinol (Lausanne)* (2022) 13:841813. doi: 10.3389/fendo.2022.841813

101. Yoshida S, Kobayashi Y, Nakama T, Zhou Y, Ishikawa K, Arita R, et al. Increased expression of M-CSF and IL-13 in vitreous of patients with proliferative diabetic retinopathy: implications for M2 macrophage-involving fibrovascular membrane formation. *Br J Ophthalmol* (2015) 99(5):629–34. doi: 10.1136/bjophthalmol-2014-305860

102. Xu J, Chen LJ, Yu J, Wang HJ, Zhang F, Liu Q, et al. Involvement of advanced glycation end products in the pathogenesis of diabetic retinopathy. *Cell Physiol Biochem* (2018) 48(2):705–17. doi: 10.1159/000491897

103. Bianco L, Arrigo A, Aragona E, Antropoli A, Berni A, Saladino A, et al. Neuroinflammation and neurodegeneration in diabetic retinopathy. *Front Aging Neurosci* (2022) . 14:937999. doi: 10.3389/fnagi.2022.937999

104. Tang L, Zhang C, Lu L, Tian H, Liu K, Luo D, et al. Melatonin maintains inner blood-retinal barrier by regulating microglia via inhibition of PI3K/Akt/Stat3/NF-κB signaling pathways in experimental diabetic retinopathy. *Front Immunol* (2022) 13:831660. doi: 10.3389/fimmu.2022.831660

105. Fang M, Wan W, Li Q, Wan W, Long Y, Liu H, et al. Asiatic acid attenuates diabetic retinopathy through TLR4/MyD88/NF-κB p65 mediated modulation of microglia polarization. *Life Sci* (2021) 277:119567. doi: 10.1016/j.lfs.2021.119567

106. Liu T, Zhang L, Joo D, Sun SC. NF-κB signaling in inflammation. *Signal Transduct Target Ther* (2017) 2:17023–. doi: 10.1038/sigtrans.2017.23

107. Chen X, Wang X, Cui Z, Luo Q, Jiang Z, Huang Y, et al. M1 microglia-derived exosomes promote activation of resting microglia and amplifies proangiogenic effects through Irf1/miR-155-5p/Socs1 axis in the retina. *Int J Biol Sci* (2023) 19(6):1791–812. doi: 10.7150/ijbs.79784

108. Al-Rashed F, Sindhu S, Arefanian H, Al Madhoun A, Kochumon S, Thomas R, et al. Repetitive intermittent hyperglycemia drives the M1 polarization and inflammatory responses in THP-1 macrophages through the mechanism involving the TLR4-IRF5 pathway. *Cells* (2020) 9(8):1892. doi: 10.3390/cells9081892

109. Cheng CI, Chen PH, Lin YC, Kao YH. High glucose activates Raw264.7 macrophages through RhoA kinase-mediated signaling pathway. *Cell Signal* (2015) 27(2):283–92. doi: 10.1016/j.cellsig.2014.11.012

110. Khalid M, Petroianu G, Adem A. Advanced glycation end products and diabetes mellitus: mechanisms and perspectives. *Biomolecules* (2022) 12(4):542. doi: 10.3390/biom12040542

111. Yu Z, Zhang T, Gong C, Sheng Y, Lu B, Zhou L, et al. Erianin inhibits high glucose-induced retinal angiogenesis via blocking ERK1/2-regulated HIF-1α-VEGF/VEGFR2 signaling pathway. *Sci Rep* (2016) 6:34306. doi: 10.1038/srep34306

112. Zhang T, Ouyang H, Mei X, Lu B, Yu Z, Chen K, et al. Erianin alleviates diabetic retinopathy by reducing retinal inflammation initiated by microglial cells via inhibiting hyperglycemia-mediated ERK1/2-NF-κB signaling pathway. *FASEB J* (2019) 33 (11):11776–90. doi: 10.1096/fj.201802614RRR

113. Xu J, Tu Y, Wang Y, Xu X, Sun X, Xie L, et al. Prodrug of epigallocatechin-3-gallate alleviates choroidal neovascularization via down-regulating HIF-1α/VEGF/VEGFR2 pathway and M1 type macrophage/microglia polarization. *BioMed Pharmacother* (2020) 121:109606. doi: 10.1016/j.biopha.2019.109606

114. Liu X, Guo A, Tu Y, Li W, Li L, Liu W, et al. Fruquintinib inhibits VEGF/VEGFR2 axis of choroidal endothelial cells and M1-type macrophages to protect against mouse laser-induced choroidal neovascularization. *Cell Death Dis* (2020) 11 (11):1016. doi: 10.1038/s41419-020-03222-1

115. Li W, Wang Y, Zhu L, Du S, Mao J, Wang Y, et al. The P300/XBP1s/Herpud1 axis promotes macrophage M2 polarization and the development of choroidal neovascularization. *J Cell Mol Med* (2021) 25(14):6709–20. doi: 10.1111/jcmm.16673

116. Zhou Y, Zeng J, Tu Y, Li L, Du S, Zhu L, et al. CSF1/CSF1R-mediated crosstalk between choroidal vascular endothelial cells and macrophages promotes choroidal neovascularization. *Invest Ophthalmol Vis Sci* (2021) 62(3):37. doi: 10.1167/iovs.62.3.37

117. Zhan P, Cui Y, Cao Y, Bao X, Wu M, Yang Q, et al. PGE2 promotes macrophage recruitment and neovascularization in murine wet-type AMD models. *Cell Commun Signal* (2022) 20(1):155. doi: 10.1186/s12964-022-00973-6

118. Joussen AM, Poulaki V, Le ML, Koizumi K, Esser C, Janicki H, et al. A central role for inflammation in the pathogenesis of diabetic retinopathy. *FASEB J* (2004) 18 (12):1450–2. doi: 10.1096/fj.03-1476fje

119. Chang KC, Ponder J, Labarbera DV, Petrash JM. Aldose reductase inhibition prevents endotoxin-induced inflammatory responses in retinal microglia. *Invest Ophthalmol Vis Sci* (2014) 55(5):2853–61. doi: 10.1167/iovs.13-13487

120. Wang M, Ma W, Zhao L, Fariss RN, Wong WT. Adaptive Müller cell responses to microglial activation mediate neuroprotection and coordinate inflammation in the retina. *J Neuroinflammation* (2011) 8:173. doi: 10.1186/1742-2094-8-173

121. Shin ES, Huang Q, Gurel Z, Sorenson CM, Sheibani N. High glucose alters retinal astrocytes phenotype through increased production of inflammatory cytokines and oxidative stress. *PloS One* (2014) 9(7):e103148. doi: 10.1371/journal.pone.0103148

122. Wang M, Wang X, Zhao L, Ma W, Rodriguez IR, Fariss RN, et al. Macroglia-microglia interactions via TSPO signaling regulates microglial activation in the mouse retina. *J Neurosci* (2014) 34(10):3793–806. doi: 10.1523/jneurosci.3153-13.2014

123. Kowluru RA. Cross talks between oxidative stress, inflammation and epigenetics in diabetic retinopathy. *Cells* (2023) 12(2):300. doi: 10.3390/cells12020300

124. Kowluru RA, Mishra M. Regulation of matrix metalloproteinase in the pathogenesis of diabetic retinopathy. *Prog Mol Biol Transl Sci* (2017) 148:67–85. doi: 10.1016/bs.pmbts.2017.02.004

125. Kowluru RA, Kowluru A, Mishra M, Kumar B. Oxidative stress and epigenetic modifications in the pathogenesis of diabetic retinopathy. *Prog Retin Eye Res* (2015) 48:40–61. doi: 10.1016/j.preteyeres.2015.05.001

126. Qiu AW, Huang DR, Li B, Fang Y, Zhang WW, Liu QH. IL-17A injury to retinal ganglion cells is mediated by retinal Müller cells in diabetic retinopathy. *Cell Death Dis* (2021) 12(11):1057. doi: 10.1038/s41419-021-04350-y

127. Xie H, Zhang C, Liu D, Yang Q, Tang L, Wang T, et al. Erythropoietin protects the inner blood-retinal barrier by inhibiting microglia phagocytosis via Src/Akt/cofilin signalling in experimental diabetic retinopathy. *Diabetologia* (2021) 64(1):211–25. doi: 10.1007/s00125-020-05299-x

128. Ding X, Zhang M, Gu R, Xu G, Wu H. Activated microglia induce the production of reactive oxygen species and promote apoptosis of co-cultured retinal microvascular pericytes. *Graefes Arch Clin Exp Ophthalmol* (2017) 255(4):777–88. doi: 10.1007/s00417-016-3578-5

129. Zhu Y, Zhang L, Lu Q, Gao Y, Cai Y, Sui A, et al. Identification of different macrophage subpopulations with distinct activities in a mouse model of oxygen-induced retinopathy. *Int J Mol Med* (2017) 40(2):281–92. doi: 10.3892/ijmm.2017.3022

130. Gao S, Li C, Zhu Y, Wang Y, Sui A, Zhong Y, et al. PEDF mediates pathological neovascularization by regulating macrophage recruitment and polarization in the mouse model of oxygen-induced retinopathy. *Sci Rep* (2017) 7:42846. doi: 10.1038/srep42846

131. Zhou Y, Yoshida S, Nakao S, Yoshimura T, Kobayashi Y, Nakama T, et al. M2 macrophages enhance pathological neovascularization in the mouse model of oxygen-induced retinopathy. *Invest Ophthalmol Vis Sci* (2015) 56(8):4767–77. doi: 10.1167/iovs.14-16012

132. Wang Y, Chang T, Wu T, Xu W, Dou G, Wang Y, et al. M2 macrophages promote vasculogenesis during retinal neovascularization by regulating bone marrow-derived cells via SDF-1/VEGF. *Cell Tissue Res* (2020) 380(3):469–86. doi: 10.1007/s00441-019-03166-9

133. Hombrebueno JR, Lynch A, Byrne EM, Obasanmi G, Kissenpfennig A, Chen M, et al. Hyaloid vasculature as a major source of STAT3 (Signal transducer and activator of transcription 3) myeloid cells for pathogenic retinal neovascularization in oxygen-induced retinopathy. *Arterioscler Thromb Vasc Biol* (2020) 40(12):e367–e79. doi: 10.1161/ATVBAHA.120.314567

134. Zhang P, Lu B, Zhang Q, Xu F, Zhang R, Wang C, et al. LncRNA NEAT1 Sponges MiRNA-148a-3p to Suppress Choroidal Neovascularization and M2 macrophage polarization. *Mol Immunol* (2020) 127:212–22. doi: 10.1016/j.molimm.2020.08.008

135. Lai K, Li Y, Li L, Gong Y, Huang C, Zhang Y, et al. Intravitreal injection of triptolide attenuates subretinal fibrosis in laser-induced murine model. *Phytomedicine* (2021) 93:153747. doi: 10.1016/j.phymed.2021.153747

136. Yang Y, Liu F, Tang M, Yuan M, Hu A, Zhan Z, et al. Macrophage polarization in experimental and clinical choroidal neovascularization. *Sci Rep* (2016) 6:30933. doi: 10.1038/srep30933

137. Lai K, Gong Y, Zhao W, Li L, Huang C, Xu F, et al. Triptolide attenuates laser-induced choroidal neovascularization via M2 macrophage in a mouse model. *BioMed Pharmacother* (2020) 129:110312. doi: 10.1016/j.biopha.2020.110312

138. Song J, Lee K, Park SW, Chung H, Jung D, Na YR, et al. Lactic acid upregulates VEGF expression in macrophages and facilitates choroidal neovascularization. *Invest Ophthalmol Vis Sci* (2018) 59(8):3747–54. doi: 10.1167/iovs.18-23892

139. Wang Y, Xie L, Zhu M, Guo Y, Tu Y, Zhou Y, et al. Shikonin alleviates choroidal neovascularization by inhibiting proangiogenic factor production from infiltrating macrophages. *Exp Eye Res* (2021) 213:108823. doi: 10.1016/j.exer.2021.108823

140. Lai YS, Wahyuningtyas R, Aui SP, Chang KT. Autocrine VEGF signalling on M2 macrophages regulates PD-L1 expression for immunomodulation of T cells. *J Cell Mol Med* (2019) 23(2):1257–67. doi: 10.1111/jcmm.14027

141. Sasaki F, Koga T, Ohba M, Saeki K, Okuno T, Ishikawa K, et al. Leukotriene B4 promotes neovascularization and macrophage recruitment in murine wet-type AMD models. *JCI Insight* (2018) 3(18):e96902. doi: 10.1172/jci.insight.96902

142. Mantovani A, Biswas SK, Galdiero MR, Sica A, Locati M. Macrophage plasticity and polarization in tissue repair and remodelling. *J Pathol* (2013) 229(2):176–85. doi: 10.1002/path.4133

143. Li J, Yu S, Lu X, Cui K, Tang X, Xu Y, et al. The phase changes of M1/M2 phenotype of microglia/macrophage following oxygen-induced retinopathy in mice. *Inflammation Res* (2021) 70(2):183–92. doi: 10.1007/s00011-020-01427-w

144. Zhu Y, Tan W, Demetriades AM, Cai Y, Gao Y, Sui A, et al. Interleukin-17A neutralization alleviated ocular neovascularization by promoting M2 and mitigating M1 macrophage polarization. *Immunology* (2016) 147(4):414–28. doi: 10.1111/imm.12571

145. Marchetti V, Yanes O, Aguilar E, Wang M, Friedlander D, Moreno S, et al. Differential macrophage polarization promotes tissue remodeling and repair in a model of ischemic retinopathy. *Sci Rep* (2011) 1:76. doi: 10.1038/srep00076

146. Fantin A, Vieira JM, Gestri G, Denti L, Schwarz Q, Prykhozhij S, et al. Tissue macrophages act as cellular chaperones for vascular anastomosis downstream of VEGF-mediated endothelial tip cell induction. *Blood* (2010) 116(5):829–40. doi: 10.1182/blood-2009-12-257832

147. Xu Y, Cui K, Li J, Tang X, Lin J, Lu X, et al. Melatonin attenuates choroidal neovascularization by regulating macrophage/microglia polarization via inhibition of RhoA/ROCK signaling pathway. *J Pineal Res* (2020) 69(1):e12660. doi: 10.1111/jpi.12660

148. Zhou H, Xu Z, Liao X, Tang S, Li N, Hou S. Low expression of YTH domain-containing 1 promotes microglial M1 polarization by reducing the stability of sirtuin 1 mRNA. *Front Cell Neurosci* (2021) 15:774305. doi: 10.3389/fncel.2021.774305

149. Sui A, Chen X, Demetriades AM, Shen J, Cai Y, Yao Y, et al. Inhibiting NF-κB signaling activation reduces retinal neovascularization by promoting a polarization shift in macrophages. *Invest Ophthalmol Vis Sci* (2020) 61(6):4. doi: 10.1167/iovs.61.6.4

150. Zhao F, Gao X, Ge X, Cui J, Liu X. Cyanidin-3-o-glucoside (C3G) inhibits vascular leakage regulated by microglial activation in early diabetic retinopathy and neovascularization in advanced diabetic retinopathy. *Bioengineered* (2021) 12 (2):9266–78. doi: 10.1080/21655979.2021.1996512

151. Sun X, Ma L, Li X, Wang J, Li Y, Huang Z. Ferulic acid alleviates retinal neovascularization by modulating microglia/macrophage polarization through the ROS/NF-κB axis. *Front Immunol* (2022) 13:976729. doi: 10.3389/fimmu.2022.976729

152. Cano-Cano F, Alcalde-Estévez E, Gómez-Jaramillo L, Iturregui M, Sánchez-Fernández EM, García Fernández JM, et al. Anti-inflammatory (M2) response is induced by a sp-iminosugar glycolipid sulfoxide in diabetic retinopathy. *Front Immunol* (2021) 12:632132. doi: 10.3389/fimmu.2021.632132

153. Alcalde-Estévez E, Arroba AI, Sánchez-Fernández EM, Mellet CO, García Fernández JM, Masgrau L, et al. The sp-iminosugar glycolipid 1-dodecylsulfonyl-5N,6O-oxomethylidenenojirimycin (DSO-ONJ) as selective anti-inflammatory agent by modulation of hemeoxygenase-1 in Bv.2 microglial cells and retinal explants. *Cells Food Chem Toxicol* (2018) 111:454–66. doi: 10.1016/j.fct.2017.11.050

154. Gao S, Li N, Wang Y, Lin Z, Zhu Y, Xu J, et al. Inhibition of vascular endothelial growth factor alleviates neovascular retinopathy with regulated neurotrophic/proinflammatory cytokines through the modulation of DBI-TSPO signaling. *FASEB J* (2022) 36(7):e22367. doi: 10.1096/fj.202101294RRR

155. Chang KC, Shieh B, Petrash JM. Aldose reductase mediates retinal microglia activation. *Biochem Biophys Res Commun* (2016) 473(2):565–71. doi: 10.1016/j.bbrc.2016.03.122

156. Rao M, Huang YK, Liu CC, Meadows C, Cheng HC, Zhou M, et al. Aldose reductase inhibition decelerates optic nerve degeneration by alleviating retinal microglia activation. *Sci Rep* (2023) 13(1):5592. doi: 10.1038/s41598-023-32702-5

157. Huang YK, Liu CC, Wang S, Cheng HC, Meadows C, Chang KC. The role of aldose reductase in beta-amyloid-induced microglia activation. *Int J Mol Sci* (2022) 23 (23):15088. doi: 10.3390/ijms232315088

158. El Kasmi KC, Holst J, Coffre M, Mielke L, de Pauw A, Lhocine N, et al. General nature of the STAT3-activated anti-inflammatory response. *J Immunol (Baltimore Md: 1950)* (2006) 177(11):7880–8. doi: 10.4049/jimmunol.177.11.7880

159. Panopoulos AD, Zhang L, Snow JW, Jones DM, Smith AM, El Kasmi KC, et al. STAT3 governs distinct pathways in emergency granulopoiesis and mature neutrophils. *Blood* (2006) 108(12):3682–90. doi: 10.1182/blood-2006-02-003012

160. Ritter MR, Banin E, Moreno SK, Aguilar E, Dorrell MI, Friedlander M. Myeloid progenitors differentiate into microglia and promote vascular repair in a model of ischemic retinopathy. *J Clin Invest* (2006) 116(12):3266–76. doi: 10.1172/jci29683

161. Xu W, Cheng W, Cui X, Xu G. Therapeutic effect against retinal neovascularization in a mouse model of oxygen-induced retinopathy: bone marrow-derived mesenchymal stem cells versus Conbercept. *BMC Ophthalmol* (2020) 20(1):7. doi: 10.1186/s12886-019-1292-x

162. An X, Li L, Chen Y, Luo A, Ni Z, Liu J, et al. Mesenchymal stem cells ameliorated glucolipotoxicity in HUVECs through TSG-6. *Int J Mol Sci* (2016) 17 (4):483. doi: 10.3390/ijms17040483

163. Jaimes Y, Naaldijk Y, Wenk K, Leovsky C, Emmrich F. Mesenchymal stem cell-derived microvesicles modulate lipopolysaccharides-induced inflammatory responses to microglia cells. *Stem Cells* (2017) 35(3):812–23. doi: 10.1002/stem.2541

164. Teixeira-Pinheiro LC, Toledo MF, Nascimento-Dos-Santos G, Mendez-Otero R, Mesentier-Louro LA, Santiago MF. Paracrine signaling of human mesenchymal stem cell modulates retinal microglia population number and phenotype in vitro. *Exp Eye Res* (2020) 200:108212. doi: 10.1016/j.exer.2020.108212

165. Honda N, Watanabe Y, Tokuoka Y, Hanajima R. Roles of microglia/macrophage and antibody in cell sheet transplantation in the central nervous system. *Stem Cell Res Ther* (2022) . 13(1):470. doi: 10.1186/s13287-022-03168-5

166. Medina RJ, O'Neill CL, O'Doherty TM, Knott H, Guduric-Fuchs J, Gardiner TA, et al. Myeloid angiogenic cells act as alternative M2 macrophages and modulate angiogenesis through interleukin-8. *Mol Med* (2011) 17(9-10):1045–55. doi: 10.2119/molmed.2011.00129

167. Nakagawa Y, Masuda H, Ito R, Kobori M, Wada M, Shizuno T, et al. Aberrant kinetics of bone marrow-derived endothelial progenitor cells in the murine oxygen-induced retinopathy model. *Invest Ophthalmol Visual Sci* (2011) 52(11):7835–41. doi: 10.1167/iovs.10-5880

168. Tzameret A, Sher I, Belkin M, Treves AJ, Meir A, Nagler A, et al. Epiretinal transplantation of human bone marrow mesenchymal stem cells rescues retinal and vision function in a rat model of retinal degeneration. *Stem Cell Res* (2015) 15(2):387–94. doi: 10.1016/j.scr.2015.08.007

169. Di Pierdomenico J, García-Ayuso D, Rodríguez González-Herrero ME, García-Bernal D, Blanquer M, Bernal-Garro JM, et al. Bone marrow-derived mononuclear cell transplants decrease retinal gliosis in two animal models of inherited photoreceptor degeneration. *Int J Mol Sci* (2020) 21(19):7252. doi: 10.3390/ijms21197252

170. Di Pierdomenico J, Gallego-Ortega A, Martínez-Vacas A, García-Bernal D, Vidal-Sanz M, Villegas-Pérez MP, et al. Intravitreal and subretinal syngeneic bone marrow mononuclear stem cell transplantation improves photoreceptor survival but does not ameliorate retinal function in two rat models of retinal degeneration. *Acta Ophthalmol* (2022) 100(6):e1313–e31. doi: 10.1111/aos.15165

171. Fang IM, Yang CM, Yang CH, Chiou SH, Chen MS. Transplantation of induced pluripotent stem cells without C-Myc attenuates retinal ischemia and reperfusion injury in rats. *Exp Eye Res* (2013) 113:49–59. doi: 10.1016/j.exer.2013.05.007

172. Goldenberg-Cohen N, Avraham-Lubin BC, Sadikov T, Goldstein RS, Askenasy N. Primitive stem cells derived from bone marrow express glial and neuronal markers and support revascularization in injured retina exposed to ischemic and mechanical damage. *Stem Cells Dev* (2012) 21(9):1488–500. doi: 10.1089/scd.2011.0366

173. Dreixler JC, Poston JN, Balyasnikova I, Shaikh AR, Tupper KY, Conway S, et al. Delayed administration of bone marrow mesenchymal stem cell conditioned medium significantly improves outcome after retinal ischemia in rats. *Invest Ophthalmol Vis Sci* (2014) 55(6):3785–96. doi: 10.1167/iovs.13-11683

174. Wang C, Li Y, Yang M, Zou Y, Liu H, Liang Z, et al. Efficient differentiation of bone marrow mesenchymal stem cells into endothelial cells in vitro. *Eur J Vasc Endovasc Surg* (2018) 55(2):257–65. doi: 10.1016/j.ejvs.2017.10.012

175. McDonald CA, Penny TR, Paton MCB, Sutherland AE, Nekkanti L, Yawno T, et al. Effects of umbilical cord blood cells, and subtypes, to reduce neuroinflammation following perinatal hypoxic-ischemic brain injury. *J Neuroinflammation* (2018) 15 (1):47. doi: 10.1186/s12974-018-1089-5

176. Mishra A, Mohan KV, Nagarajan P, Iyer S, Kesarwani A, Nath M, et al. Peripheral blood-derived monocytes show neuronal properties and integration in immune-deficient rd1 mouse model upon phenotypic differentiation and induction with retinal growth factors. *Stem Cell Res Ther* (2020) 11(1):412. doi: 10.1186/s13287-020-01925-y

177. Bellon A, Wegener A, Lescallette AR, Valente M, Yang SK, Gardette R, et al. Transdifferentiation of human circulating monocytes into neuronal-like cells in 20 days and without reprograming. *Front Mol Neurosci* (2018) 11:323. doi: 10.3389/fnmol.2018.00323

178. Tacke F, Randolph GJ. Migratory fate and differentiation of blood monocyte subsets. *Immunobiology* (2006) 211(6-8):609–18. doi: 10.1016/j.imbio.2006.05.025

179. Sanberg PR, Park DH, Kuzmin-Nichols N, Cruz E, Hossne NA Jr., Buffolo E, et al. Monocyte transplantation for neural and cardiovascular ischemia repair. *J Cell Mol Med* (2010) 14(3):553–63. doi: 10.1111/j.1582-4934.2009.00903.x

180. Zhu Z, Zheng L, Li Y, Huang T, Chao YC, Pan L, et al. Potential immunotherapeutic targets on myeloid cells for neurovascular repair after ischemic stroke. *Front Neurosci* (2019) 13:758. doi: 10.3389/fnins.2019.00758

181. Protopsaltis NJ, Liang W, Nudleman E, Ferrara N. Interleukin-22 promotes tumor angiogenesis. *Angiogenesis* (2019) 22(2):311–23. doi: 10.1007/s10456-018-9658-x

182. Haupt F, Krishnasamy K, Napp LC, Augustynik M, Limbourg A, Gamrekelashvili J, et al. Retinal myeloid cells regulate tip cell selection and vascular branching morphogenesis via Notch ligand Delta-like 1. *Sci Rep* (2019) 9(1):9798. doi: 10.1038/s41598-019-46308-3

183. Liu YY, Li Y, Wang L, Zhao Y, Yuan R, Yang MM, et al. Mesenchymal stem cell-derived exosomes regulate microglia phenotypes: a promising treatment for acute central nervous system injury. *Neural Regener Res* (2023) 18(8):1657–65. doi: 10.4103/1673-5374.363819

10.3389/fendo.2023.1276225

Glossary

M1	Classically activated macrophages
M2	Alternatively activated macrophages
DR	Diabetic retinopathy
OIR	Oxygen-induced retinopathy
AMD	Age-related macular degeneration
VEGF	Vascular endothelial growth factor
NPDR	Non-proliferative diabetic retinopathy
PDR	Proliferative diabetic retinopathy
CSF	Colony stimulating factor
IFN	Interferon
TNF	Tumor necrosis factor
LPS	Lipopolysaccharide
IL	Interleukin
iNOS	Inducible nitric oxide synthase
ROI	Reactive oxygen intermediates
TGF	Transforming growth factor
TLR	Toll-like receptor
TAM	Tumor-associated macrophage
NFL	Nerve fiber layer
GCL	Ganglion cell layer
IPL	Inner plexiform layer
OPL	Outer plexiform layer
BRB	Blood-retina barrier
AGEs	Advanced glycation end products
ROS	Reactive oxygen species
TSPO	Translocator protein
DBI	Diazepam-binding inhibitor
MMP	Matrix metalloproteinases
LTB4	Leukotriene B4
BLT1	Leukotriene B4 receptor 1
MSCs	Mesenchymal stem cells
NF-κB	Nuclear factor kappa-B
IRF	Interferon regulatory factor
ROCK	Rho-associated coiled-coil containing protein kinase
JNK	c-Jun N-terminal kinase
ERK	Extracellular regulated protein kinases
HIF	Hypoxia inducible factor

frontiers | Frontiers in Endocrinology

TYPE Original Research
PUBLISHED 22 November 2023
DOI 10.3389/fendo.2023.1307468

OPEN ACCESS

EDITED BY
Kai Jin,
Zhejiang University, China

REVIEWED BY
Zhongming Wu,
Tianjin Medical University, China
Dan-Qian Chen,
Northwest University, China

*CORRESPONDENCE
Meihua Bao
mhbao78@163.com
Sen Li
senli@connect.hku.hk
Qiuhong Wang
qiuhongfortune@126.com

†These authors have contributed equally to this work and share first authorship

RECEIVED 04 October 2023
ACCEPTED 27 October 2023
PUBLISHED 22 November 2023

CITATION
Chen R, Xu S, Ding Y, Li L, Huang C, Bao M, Li S and Wang Q (2023) Dissecting causal associations of type 2 diabetes with 111 types of ocular conditions: a Mendelian randomization study.
Front. Endocrinol. 14:1307468.
doi: 10.3389/fendo.2023.1307468

Dissecting causal associations of type 2 diabetes with 111 types of ocular conditions: a Mendelian randomization study

Rumeng Chen[1†], Shuling Xu[1†], Yining Ding[1†], Leyang Li[2], Chunxia Huang[3], Meihua Bao[4,5*], Sen Li[1*] and Qiuhong Wang[2*]

[1]School of Life Sciences, Beijing University of Chinese Medicine, Beijing, China, [2]Department of Endocrinology, Guang'anmen Hospital, China Academy of Chinese Medical Sciences, Beijing, China, [3]School of Stomatology, Changsha Medical University, Changsha, China, [4]The Hunan Provincial Key Laboratory of the TCM Agricultural Biogenomics, Changsha Medical University, Changsha, China, [5]Hunan Key Laboratory of the Research and Development of Novel Pharmaceutical Preparations, School of Pharmaceutical Science, Changsha Medical University, Changsha, China

Background: Despite the well-established findings of a higher incidence of retina-related eye diseases in patients with diabetes, there is less investigation into the causal relationship between diabetes and non-retinal eye conditions, such as age-related cataracts and glaucoma.

Methods: We performed Mendelian randomization (MR) analysis to examine the causal relationship between type 2 diabetes mellitus (T2DM) and 111 ocular diseases. We employed a set of 184 single nucleotide polymorphisms (SNPs) that reached genome-wide significance as instrumental variables (IVs). The primary analysis utilized the inverse variance-weighted (IVW) method, with MR-Egger and weighted median (WM) methods serving as supplementary analyses.

Results: The results revealed suggestive positive causal relationships between T2DM and various ocular conditions, including "Senile cataract" (OR= 1.07; 95% CI: 1.03, 1.11; P=7.77×10^{-4}), "Glaucoma" (OR= 1.08; 95% CI: 1.02, 1.13; P=4.81×10^{-3}), and "Disorders of optic nerve and visual pathways" (OR= 1.10; 95% CI: 0.99, 1.23; P=7.01×10^{-2}).

Conclusion: Our evidence supports a causal relationship between T2DM and specific ocular disorders. This provides a basis for further research on the importance of T2DM management and prevention strategies in maintaining ocular health.

KEYWORDS

type 2 diabetes, ocular diseases, diabetes complications, Mendelian randomization, causal association

Introduction

Type 2 diabetes mellitus (T2DM) accounts for approximately 90% of the global population of 537 million individuals with diabetes mellitus (DM), predominantly affecting individuals over the age of 55 (1). The prevalence of T2DM is rising due to accelerated global aging, and it is projected that the worldwide diabetic population will reach 783 million by 2045 (2). DM can give rise to a range of complications, characterized by elevated disability and mortality rates (3–8). Visual impairment stands out as a particularly severe complication (9).

A systematic review and meta-analysis of global population-based eye disease surveys conducted from 1990 to 2020 established that cataract, glaucoma, age-related macular degeneration (AMD), and diabetic retinopathy (DR) are the primary causes of blindness. Importantly, early detection and timely intervention can prevent these conditions (10). It is widely recognized that there is a strong association between DM and the development of DR, with approximately one-third of diabetic patients affected by this condition (11). Furthermore, DM has been linked to several other significant visual impairments worldwide, including cataract, AMD, and glaucoma (12). For instance, a meta-analysis indicated that DM was associated with an increased risk of AMD (13), while two other studies reported a 50% reduction in AMD prevalence among patients with DM (14, 15). Moreover, there are conflicting reports regarding the association between diabetes and glaucoma. While a meta-analysis suggested that diabetes increased the prevalence of glaucoma (16), another study revealed that DM conferred a protective effect against the development of glaucomatous optic nerve damage in patients with primary open-angle glaucoma (POAG) (17). Hence, the existing research on DM and ocular-related diseases remains inconclusive. The primary reason for these conflicting findings is that most studies examining the relationship between diabetes and ocular-related diseases are observational, making it difficult to exclude the effects of confounding variables and reverse causality.

Mendelian Randomization (MR) analysis is an epidemiological approach that utilizes genetic variants associated with a specific exposure as instrumental variables (IVs). Its primary objective is to evaluate potential causal relationships between the exposure and outcome measures (18). The methodologies employed in MR analysis are grounded in Mendel's second law, which states that alleles are randomly allocated. This characteristic, irrespective of the individual's illness status, helps mitigate biases induced by confounding factors and reverse causality. The objective of this study is to employ the MR method to examine the causal relationship between T2DM and 111 types of ocular conditions. Furthermore, it seeks to establish a theoretical basis for the prevention and treatment of eye diseases in individuals with diabetes.

Abbreviations: T2DM, type 2 diabetes mellitus; DM, diabetes mellitus; AMD, age-related macular degeneration; DR, diabetic retinopathy; POAG, primary open-angle glaucoma; MR, Mendelian randomization; IVs, instrumental variables; GWAS, genome-wide association study; SNPs, single nucleotide polymorphism; MAF, minor allele frequency; IVW, inverse-variance weighted; WM, weighted median; ORs, odds ratios; CIs, confidence intervals; FDR, false discovery rate; AGEs, advanced glycation end products; ROS, reactive oxygen species; TLR, toll-like receptor; ECM, extracellular matrix; RR, relative risk; AR, aldose reductase; GSH, glutathione.

Methods

Study design

Based on the dataset acquired from the genome-wide association study (GWAS), we identified specific single nucleotide polymorphisms (SNPs) that exhibited significant associations with T2DM as the exposure variable. We utilized these SNPs as IVs and employed a MR analysis to evaluate the causal association between T2DM and the aforementioned ocular diseases.

Data sources

The data for the exposure variable (T2DM) (including 74,124 T2DM cases and 824,006 controls of European ancestry) was obtained from Anubha Mahajan et al.'s study (19), while data for the outcome variables were obtained from all 111 eye-related diseases (detailed information can be found in Supplementary Table 1) available in the FinnGen database, which is a comprehensive biomedical research project conducted in Finland (20).

Selection of IVs

We implemented specific criteria for the selection of IVs in our MR analysis. These criteria included: (1) establishing a significant genomic-level association between the IVs and the exposure ($P < 5.00\times10^{-8}$), (2) ensuring the independent selection of IVs by clumping within a 10 Mb window and minimizing linkage disequilibrium ($R^2 < 0.001$), and (3) setting a minimum minor allele frequency (MAF) threshold of 0.01. We employed F-statistics to evaluate the strength of the IVs, considering values greater than 10 as indicative of a lower probability of weak instrument bias (21).

MR analysis

Among the three MR methods employed in this study, the inverse variance-weighted (IVW) method was the primary approach. IVW primarily evaluates the results by aggregating the MR effect estimates for each individual SNP. For the weighted median (WM) method to be applicable, it is necessary for the valid variable to constitute a minimum of 50%. Furthermore, an intercept term is employed by MR-Egger to assess potential pleiotropy.

Sensitivity analysis

To detect and eliminate potential outliers, we employed pleiotropy-corrected data from MR-PRESSO. We assessed

heterogeneity using Cochrane Q-values. Furthermore, we employed the Leave-one-out method by removing one SNP at a time and reanalyzing whether the remaining SNPs significantly impacted the results. Causal estimates were obtained by calculating odds ratios (ORs) and their corresponding 95% confidence intervals (CIs). To handle multiple comparisons, we applied a false discovery rate (FDR) of 5%. Causal associations were considered significant if they survived FDR correction, but suggestive associations were also discussed in our study. The two-sample MR software package in R was utilized for conducting all MR analyses.

Results

Assessment of the IVs

We identified 184 SNPs from T2DM as IVs, with F statistic values ranging from 29.47 to 1393.78 (Supplementary Table 2).

Results of the MR analysis

The findings of the IVW method indicated a potential causal association between T2DM and various ocular-related diseases, including "Vitreous haemorrhage" (OR= 1.21; 95% CI: 1.06, 1.38; P=3.77×10^{-3}), "Senile cataract" (OR= 1.07; 95% CI: 1.03, 1.11; P=7.77×10^{-4}), "Glaucoma" (OR= 1.08; 95% CI: 1.02, 1.13; P=4.81×10^{-3}), and "Disorders of optic nerve and visual pathways" (OR= 1.10; 95% CI: 0.99, 1.23; P=7.01×10^{-2}) (Figures 1, 2; Supplementary Table 3). Furthermore, significant associations persisted between T2DM and diseases of the eye and adnexa, disorders of choroid and retina, and senile cataract even after adjusting for multiple comparisons. Using the MR-Egger and WM approaches, the relationships between T2DM and these ocular-related diseases had the same direction (Figure 2; Supplementary Table 3). Figure 3 displays the scatter plot illustrating the causal relationships between T2DM and these ocular-related diseases.

Results of the sensitivity analysis

The potential heterogeneity was evaluated (Figure 4; Supplementary Table 4). The findings presented in Supplementary Figure 1 indicate that most individual SNPs had minimal impact on the results during the leave-one-out analysis. The MR-Egger method did not detect the presence of horizontal pleiotropy (Supplementary Table 5). Despite the MR-PRESSO analysis identifying several outliers in the results, it did not significantly alter the outcomes after correction (Supplementary Table 6).

Discussion

In our MR analysis involving 111 ocular diseases, we identified potential causal associations between T2DM and various ocular-related diseases, such as diseases of the eye and adnexa, disorders of choroid and retina, vitreous haemorrhage, senile cataract, glaucoma, and disorders of optic nerve and visual pathways. After applying multiple corrections, the causal relationship between T2DM and diseases of the eye and adnexa, senile cataract, as well as disorders of choroid and retina, remained statistically significant. According to the definition provided by FinnGen, diseases of the eye and adnexa encompass disorders of choroid and retina (including any disease or disorder of the retina), glaucoma (characterized by increased ocular pressure due to impaired outflow), and disorders of optic nerve and visual pathways. Based

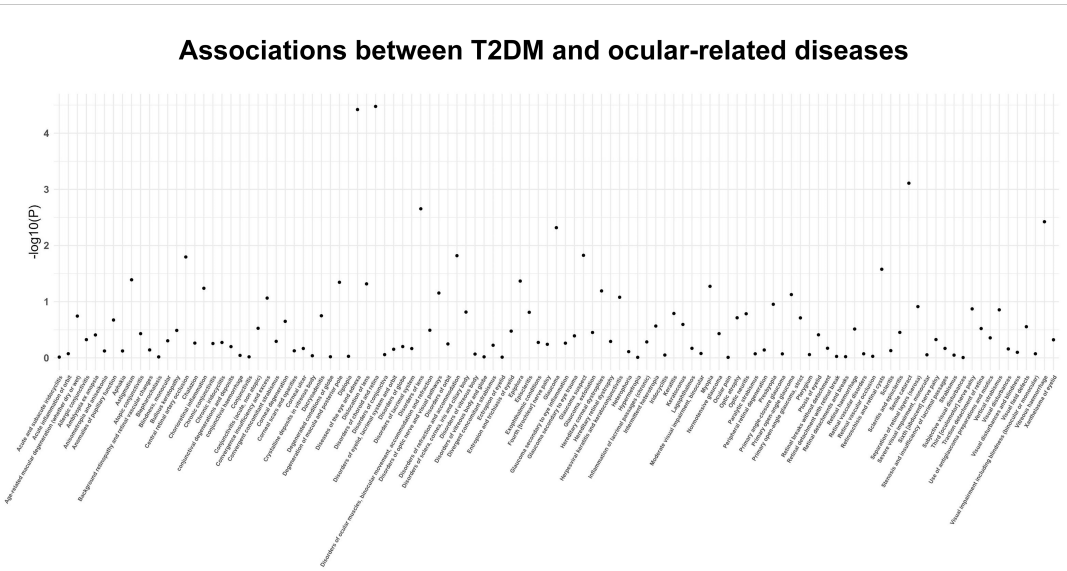

FIGURE 1
The P-value distribution of associations between type 2 diabetes mellitus and 111 ocular-related diseases in the Mendelian randomization analysis.

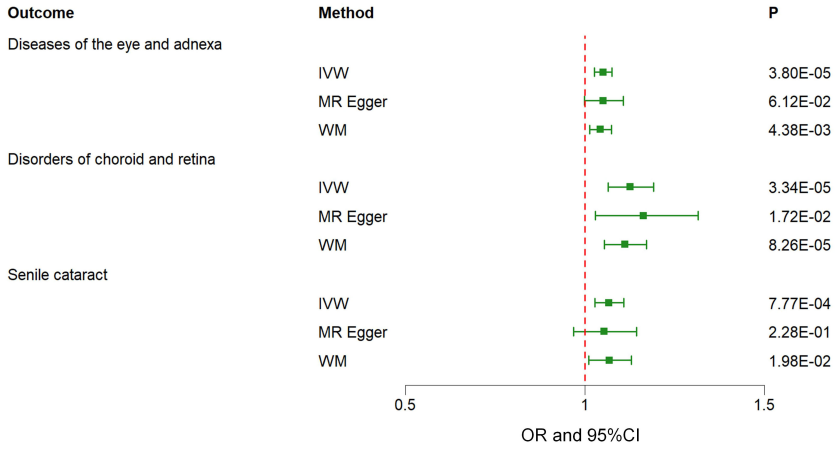

FIGURE 2
Associations between genetically predicted type 2 diabetes mellitus and various ocular-related diseases examined by three MR methods. MR, Mendelian randomization; IVW, inverse-variance weighted; WM, weighted median; CI, confidence interval.

on the preceding content and considering the actual clinical morbidity rate, our discussion will primarily focus on four key aspects.

Disorders of choroid and retina

Our study identified a significant causal relationship between T2DM and disorders of choroid and retina, which is consistent with prior research findings. Previous studies have shown a risk of DR ranging from 50% to 60% in patients diagnosed with T2DM (22). The underlying mechanism of T2DM causing DR may be related to oxidative stress, resulting from the formation of advanced glycation end products (AGEs). Prolonged hyperglycemia can result in the non-enzymatic glycosylation of macromolecules, such as proteins and lipids, leading to a continuous increase in the levels of AGEs (23). Previous studies have demonstrated an association between AGEs and the prevalence of DR across all stages (24). The interaction between AGEs and their receptors on the cell surface activates nicotinamide adenine dinucleotide phosphate-oxidase, promoting the generation of intracellular reactive oxygen species (ROS) (25). In turn, the enhanced ROS levels contribute to the formation of AGEs, thereby exacerbating the damage caused by AGEs (26). Oxidative stress plays a pivotal role in the pathogenesis of diabetic retinopathy. The excessive accumulation of ROS can cause damage to the retinal endovascular and surrounding tissues, leading to the development of diabetic retinopathy (27).

Disorders of optic nerve and visual pathways

The present study uncovered a potential positive causal relationship between T2DM and disorders of optic nerve and visual pathways. This finding is consistent with prior research. A cohort study found optic neuritis intensifies with the duration of diabetes and increasing glucose levels (28). This finding aligns with our research. The pathogenesis of optic nerve and visual pathway diseases in patients with T2DM may be attributed to hyperglycemia-induced oxidative stress. DM is characterized as an inflammatory disease that impacts the optic nerve through the release of inflammatory mediators resulting from oxidative stress (29). Moreover, previous research has demonstrated that elevated blood glucose levels induce the activation of Toll-like receptor 2 (TLR-2) and TLR-4 via reactive ROS, resulting in dysregulated microglial activation (30).

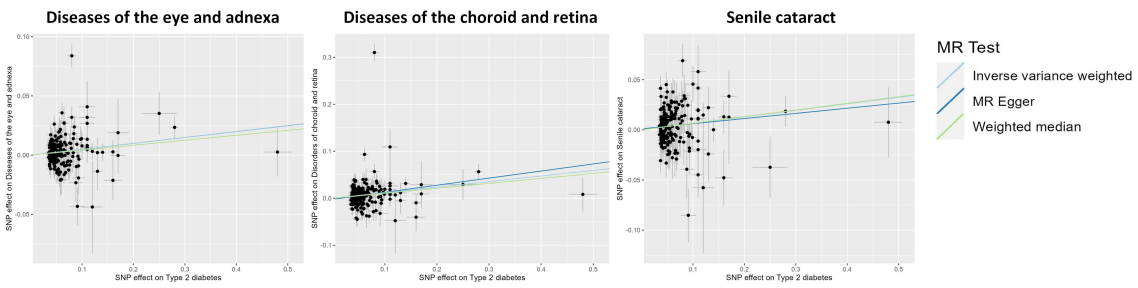

FIGURE 3
Scatter plot showing the causal effects of type 2 diabetes mellitus on various ocular-related diseases. SNP, single nucleotide polymorphism.

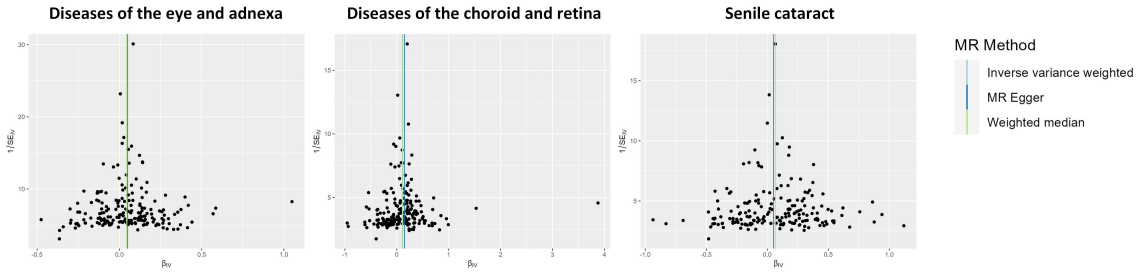

FIGURE 4
Funnel plot indicating the causal associations of type 2 diabetes mellitus on various ocular-related diseases. SNP, single nucleotide polymorphism; IV, instrumental variable; SE, standard error.

Glaucoma

Our study identified a potential positive causal relationship between T2DM and glaucoma. However, a MR study conducted on an East Asian population found no statistically significant association between genetically predicted type 2 diabetes and POAG risk (31). This discrepancy may be attributed to ethnic differences. Nonetheless, a cohort study carried out in South Korea reported a significant association between the incidence of T2DM and open-angle glaucoma (32). Moreover, another cohort study conducted in Korea observed that T2DM was associated with a higher risk of glaucoma incidence (33). Furthermore, another MR study focusing on glaucoma revealed an independent and causal association between T2DM and glaucoma risk (34), which aligns with our own findings. Hyperglycemia may contribute to the increased accumulation of extracellular matrix (ECM) substances, which could be an underlying mechanism of glaucoma in individuals with diabetes. The abnormal accumulation of ECM substances is a key factor contributing to elevated intraocular pressure (35). The ECM primarily consists of fibronectin and glycosaminoglycans. Studies have demonstrated that elevated glucose levels can induce the synthesis of fibronectin in trabecular meshwork cells, which plays a crucial role in regulating aqueous outflow and intraocular pressure (36). Additionally, the stiffening of the cornea due to saccharification in individuals with diabetes also may compromise the flow of aqueous humor (37, 38).

Senile cataracts

Our study has identified a significant causal relationship between T2DM and senile cataract, which is supported by previous research. A cohort study conducted in Sweden involving 35,369 women found that diabetic women had a 43% increased risk of cataract extraction (RR, 1.43; 95% CI, 1.10-1.86) (39). This finding is consistent with a meta-analysis of 20,837 subjects, which also confirmed T2DM as a risk factor for cataract (40). Additionally, Yuan et al. reported a positive correlation between genetic susceptibility to T2DM and senile cataract (41). Moreover, a previous MR study demonstrated that a higher genetic predisposition to T2DM was associated with an elevated risk of senile cataract (41). Kanishk et al. discovered that in diabetics, insufficient blood glucose control leads to increased aldose reductase (AR) levels and decreased glutathione (GSH) activity (42). AR is a critical initiator of sorbitol establishment in the lens, and abnormal sorbitol accumulation poses several risks to the lens, including lens opacity, interruption of the primary location for protein synthesis - the endoplasmic reticulum, ignition of apoptosis in lens epithelial cells, and oxidative stress damage to lens fibers (43–45). Additionally, GSH is one of the essential biochemical factors that maintain oxidative equilibrium in the lens; unusually low GSH levels can potentially affect lens transparency (46). Hence, the potential mechanism by which T2DM contributes to the development of senile cataracts may involve hyperglycemia-induced alterations in the activity of AR and GSH, thereby affecting lens metabolism.

Strengths and limitations

A major strength of this study lies in its systematic analysis using MR to examine the causal relationships between T2DM and multiple ocular-related diseases. Furthermore, our findings were reinforced through rigorous sensitivity analyses, affirming the reliability and stability of our causal conclusions. Finally, by incorporating genetic variations, we minimized confounding interference, thereby upholding the validity of our study.

The MR method itself has inherent limitations and potential problems, such as weak instruments and pleiotropy. Despite our efforts to address these issues through various methods, there are still unavoidable challenges. Firstly, we need to consider the problem of population stratification, which refers to differences in disease incidence (or trait distribution) and allele frequencies among populations. Secondly, there is a possibility of bias due to sample overlap. Although we selected two distinct samples, it is important to note that the data from these samples may not be entirely independent, as both samples consist of European populations. Lastly, while we did not find evidence of horizontal pleiotropy, it is important to acknowledge the presence of residual bias since the precise function of most SNPs remains unknown. Lastly, since our study focused on the European population, the generalizability of our findings to other ethnic groups may be limited.

Conclusion

In summary, the MR analysis results showed a significant positive causal relationship between T2DM and various ocular-related diseases, further demonstrating the adverse impact of diabetes on ocular health. As a corollary, addressing the necessity of maintaining adequate glycemic control becomes critical in protecting the ocular health of diabetics.

Data availability statement

The original contributions presented in the study are included in the article/Supplementary Material. Further inquiries can be directed to the corresponding authors.

Author contributions

RC: Writing - original draft. SX: Writing - original draft. YD: Writing - original draft. LL: Writing - original draft. CH: Writing - original draft. MB: Writing - review & editing. SL: Writing - review & editing. QW: Writing - review & editing.

Funding

The author(s) declare financial support was received for the research, authorship, and/or publication of this article. This study was supported by Young Elite Scientists Sponsorship Program by CAST (Grant No. 2019QNRC001), Special Training Program for Outstanding Young Scientific and Technological Talents (Innovation) of Chinese Academy of Chinese Medical Sciences (Grant No.ZZ14-YQ-010), the Scientific and Technological Innovation Project of China Academy of Chinese Medical Sciences (Grant No.CI2021A01612) and the BUCM Precision Cultivation Program (Grant No. JZPY-202205).

Conflict of interest

The authors declare that the research was conducted in the absence of any commercial or financial relationships that could be construed as a potential conflict of interest.

Publisher's note

All claims expressed in this article are solely those of the authors and do not necessarily represent those of their affiliated organizations, or those of the publisher, the editors and the reviewers. Any product that may be evaluated in this article, or claim that may be made by its manufacturer, is not guaranteed or endorsed by the publisher.

Supplementary material

The Supplementary Material for this article can be found online at: https://www.frontiersin.org/articles/10.3389/fendo.2023.1307468/full#supplementary-material

References

1. Ahmad E, Lim S, Lamptey R, Webb DR, Davies MJ. Type 2 diabetes. *Lancet* (2022) 400(10365):1803–20. doi: 10.1016/S0140-6736(22)01655-5

2. Ogurtsova K, Guariguata L, Barengo NC, Ruiz PL, Sacre JW, Karuranga S, et al. IDF diabetes Atlas: Global estimates of undiagnosed diabetes in adults for 2021. *Diabetes Res Clin Pract* (2022) 183:109118. doi: 10.1016/j.diabres.2021.109118

3. Yang YY, Shi LX, Li JH, Yao LY, Xiang DX. Piperazine ferulate ameliorates the development of diabetic nephropathy by regulating endothelial nitric oxide synthase. *Mol Med Rep* (2019) 19(3):2245–53. doi: 10.3892/mmr.2019.9875

4. Xu Z, Zhang P, Chen Y, Jiang J, Zhou Z, Zhu H. Comparing SARC-calF with SARC-F for screening sarcopenia in adults with type 2 diabetes mellitus. *Front Nutr* (2022) 9:803924. doi: 10.3389/fnut.2022.803924

5. Luo M, Cao Q, Wang D, Tan R, Shi Y, Chen J, et al. The impact of diabetes on postoperative outcomes following spine surgery: A meta-analysis of 40 cohort studies with 2.9 million participants. *Int J Surg* (2022) 104:106789. doi: 10.1016/j.ijsu.2022.106789

6. Yu T, Xu B, Bao M, Gao Y, Zhang Q, Zhang X, et al. Identification of potential biomarkers and pathways associated with carotid atherosclerotic plaques in type 2 diabetes mellitus: A transcriptomics study. *Front Endocrinol (Lausanne)* (2022) 13:981100. doi: 10.3389/fendo.2022.981100

7. Su M, Hu R, Tang T, Tang W, Huang C. Review of the correlation between Chinese medicine and intestinal microbiota on the efficacy of diabetes mellitus. *Front Endocrinol (Lausanne)* (2022) 13:1085092. doi: 10.3389/fendo.2022.1085092

8. Chen J, Li X, Liu H, Zhong D, Yin K, Li Y, et al. Bone marrow stromal cell-derived exosomal circular RNA improves diabetic foot ulcer wound healing by activating the nuclear factor erythroid 2-related factor 2 pathway and inhibiting ferroptosis. *Diabetes Med* (2023) 40(7):e15031. doi: 10.1111/dme.15031

9. Mi W, Xia Y, Bian Y. Meta-analysis of the association between aldose reductase gene (CA)n microsatellite variants and risk of diabetic retinopathy. *Exp Ther Med* (2019) 18(6):4499–509. doi: 10.3892/etm.2019.8086

10. Steinmetz JD, Bourne RRA, Briant PS, Flaxman S, Taylor HR, Jonas JB. Causes of blindness and vision impairment in 2020 and trends over 30 years, and prevalence of avoidable blindness in relation to VISION 2020: the Right to Sight: an analysis for the Global Burden of Disease Study. *Lancet Glob Health* (2021) 9(2):e144–60. doi: 10.1016/S2214-109X(20)30489-7

11. Hou X, Wang L, Zhu D, Guo L, Weng J, Zhang M, et al. Prevalence of diabetic retinopathy and vision-threatening diabetic retinopathy in adults with diabetes in China. *Nat Commun* (2023) 14(1):4296. doi: 10.1038/s41467-023-39864-w

12. Feldman-Billard S, Dupas B. Eye disorders other than diabetic retinopathy in patients with diabetes. *Diabetes Metab* (2021) 47(6):101279. doi: 10.1016/j.diabet.2021.101279

13. Chen X, Rong SS, Xu Q, Tang FY, Liu Y, Gu H, et al. Diabetes mellitus and risk of age-related macular degeneration: a systematic review and meta-analysis. *PloS One* (2014) 9(9):e108196. doi: 10.1371/journal.pone.0108196

14. Bikbov MM, Zainullin RM, Gilmanshin TR, Kazakbaeva GM, Rakhimova EM, Rusakova IA, et al. Prevalence and associated factors of age-related macular degeneration in a Russian population: the ural eye and medical study. *Am J Ophthalmol* (2020) 210:146–57. doi: 10.1016/j.ajo.2019.10.004

15. Chakravarthy U, Bailey CC, Scanlon PH, McKibbin M, Khan RS, Mahmood S, et al. Progression from early/intermediate to advanced forms of age-related macular degeneration in a large UK cohort: rates and risk factors. *Ophthalmol Retina* (2020) 4 (7):662–72. doi: 10.1016/j.oret.2020.01.012

16. Zhao D, Cho J, Kim MH, Friedman DS, Guallar E. Diabetes, fasting glucose, and the risk of glaucoma: a meta-analysis. *Ophthalmology* (2015) 122(1):72–8. doi: 10.1016/j.ophtha.2014.07.051

17. Akkaya S, Can E, Öztürk F. Comparison of the corneal biomechanical properties, optic nerve head topographic parameters, and retinal nerve fiber layer thickness measurements in diabetic and non-diabetic primary open-angle glaucoma. *Int Ophthalmol* (2016) 36(5):727–36. doi: 10.1007/s10792-016-0191-x

18. Burgess S, Butterworth A, Malarstig A, Thompson SG. Use of Mendelian randomisation to assess potential benefit of clinical intervention. *Bmj* (2012) 345: e7325. doi: 10.1136/bmj.e7325

19. Mahajan A, Taliun D, Thurner M, Robertson NR, Torres JM, Rayner NW, et al. Fine-mapping type 2 diabetes loci to single-variant resolution using high-density imputation and islet-specific epigenome maps. *Nat Genet* (2018) 50(11):1505–13. doi: 10.1038/s41588-018-0241-6

20. Kurki MI, Karjalainen J, Palta P, Sipilä TP, Kristiansson K, Donner KM, et al. FinnGen provides genetic insights from a well-phenotyped isolated population. *Nature* (2023) 613(7944):508–18. doi: 10.1038/s41586-022-05473-8

21. Burgess S, Thompson SG. Avoiding bias from weak instruments in Mendelian randomization studies. *Int J Epidemiol* (2011) 40(3):755–64. doi: 10.1093/ije/dyr036

22. He M, Long P, Chen T, Li K, Wei D, Zhang Y, et al. ALDH2/SIRT1 contributes to type 1 and type 2 diabetes-induced retinopathy through depressing oxidative stress. *Oxid Med Cell Longev* (2021) 2021:1641717. doi: 10.1155/2021/1641717

23. Shamsi A, Shahwan M, Husain FM, Khan MS. Characterization of methylglyoxal induced advanced glycation end products and aggregates of human transferrin: Biophysical and microscopic insight. *Int J Biol Macromol* (2019) 138:718–24. doi: 10.1016/j.ijbiomac.2019.07.140

24. Ying L, Shen Y, Zhang Y, Wang Y, Liu Y, Yin J, et al. Association of advanced glycation end products with diabetic retinopathy in type 2 diabetes mellitus. *Diabetes Res Clin Pract* (2021) 177:108880. doi: 10.1016/j.diabres.2021.108880

25. Guimarães ELM, Empsen C, Geerts A, van Grunsven LA. Advanced glycation end products induce production of reactive oxygen species via the activation of NADPH oxidase in murine hepatic stellate cells. *J Hepatol* (2010) 52(3):389–97. doi: 10.1016/j.jhep.2009.12.007

26. Moldogazieva NT, Mokhosoev IM, Mel'nikova TI, Porozov YB, Terentiev AA. Oxidative stress and advanced lipoxidation and glycation end products (ALEs and AGEs) in aging and age-related diseases. *Oxid Med Cell Longev* (2019) 2019:3085756. doi: 10.1155/2019/3085756

27. Kang Q, Yang C. Oxidative stress and diabetic retinopathy: Molecular mechanisms, pathogenetic role and therapeutic implications. *Redox Biol* (2020) 37:101799. doi: 10.1016/j.redox.2020.101799

28. Lee GI, Han K, Park KA, Oh SY. Risk of optic neuritis in type 2 diabetes mellitus: A nationwide cohort study. *J Neurol Sci* (2023) 450:120673. doi: 10.1016/j.jns.2023.120673

29. Sanz-Morello B, Ahmadi H, Vohra R, Saruhanian S, Freude KK, Hamann S, et al. Oxidative stress in optic neuropathies. *Antioxidants (Basel)* (2021) 10(10):1538. doi: 10.3390/antiox10101538

30. Altmann C, Schmidt MHH. The role of microglia in diabetic retinopathy: inflammation, microvasculature defects and neurodegeneration. *Int J Mol Sci* (2018) 19(1):110. doi: 10.3390/ijms19010110

31. Hu Z, Zhou F, Kaminga AC, Xu H. Type 2 diabetes, fasting glucose, hemoglobin A1c levels and risk of primary open-angle glaucoma: A mendelian randomization study. *Invest Ophthalmol Vis Sci* (2022) 63(5):37. doi: 10.1167/iovs.63.5.37

32. Jung Y, Han K, Park HYL, Park CK. Type 2 diabetes mellitus and risk of open-angle glaucoma development in Koreans: An 11-year nationwide propensity-score-matched study. *Diabetes Metab* (2018) 44(4):328–32. doi: 10.1016/j.diabet.2017.09.007

33. Jung Y, Han K, Ohn K, Kim DR, Moon JI. Association between diabetes status and subsequent onset of glaucoma in postmenopausal women. *Sci Rep* (2021) 11 (1):18272. doi: 10.1038/s41598-021-97740-3

34. Wang K, Yang F, Liu X, Lin X, Yin H, Tang Q, et al. Appraising the effects of metabolic traits on the risk of glaucoma: A mendelian randomization study. *Metabolites* (2023) 13(1):109. doi: 10.3390/metabo13010109

35. Pouw AE, Greiner MA, Coussa RG, Jiao C, Han IC, Skeie JM, et al. Cell-matrix interactions in the eye: from cornea to choroid. *Cells* (2021) 10(3):687. doi: 10.3390/cells10030687

36. Sato T, Roy S. Effect of high glucose on fibronectin expression and cell proliferation in trabecular meshwork cells. *Invest Ophthalmol Vis Sci* (2002) 43(1):170–5.

37. Cui Y, Yang X, Zhang G, Guo H, Zhang M, Zhang L, et al. Intraocular pressure in general and diabetic populations from southern China: the dongguan eye study. *Invest Ophthalmol Vis Sci* (2019) 60(2):761–9. doi: 10.1167/iovs.18-25247

38. Gulati V, Ghate DA, Camras CB, Toris CB. Correlations between parameters of aqueous humor dynamics and the influence of central corneal thickness. *Invest Ophthalmol Vis Sci* (2011) 52(2):920–6. doi: 10.1167/iovs.10-5494

39. Lindblad BE, Håkansson N, Philipson B, Wolk A. Metabolic syndrome components in relation to risk of cataract extraction: a prospective cohort study of women. *Ophthalmology* (2008) 115(10):1687–92. doi: 10.1016/j.ophtha.2008.04.004

40. Li L, Wan XH, Zhao GH. Meta-analysis of the risk of cataract in type 2 diabetes. *BMC Ophthalmol* (2014) 14:94. doi: 10.1186/1471-2415-14-94

41. Yuan S, Wolk A, Larsson SC. Metabolic and lifestyle factors in relation to senile cataract: a Mendelian randomization study. *Sci Rep* (2022) 12(1):409. doi: 10.1038/s41598-021-04515-x

42. Khare K, Mendonca T, Rodrigues G, Kamath M, Hegde A, Nayak S, et al. Aldose reductase and glutathione in senile cataract nucleus of diabetics and non-diabetics. *Int Ophthalmol* (2023) 43:3673–80. doi: 10.1007/s10792-023-02776-1

43. Kumamoto Y, Takamura Y, Kubo E, Tsuzuki S, Akagi Y. Epithelial cell density in cataractous lenses of patients with diabetes: association with erythrocyte aldose reductase. *Exp Eye Res* (2007) 85(3):393–9. doi: 10.1016/j.exer.2007.06.007

44. Mulhern ML, Madson CJ, Danford A, Ikesugi K, Kador PF, Shinohara T. The unfolded protein response in lens epithelial cells from galactosemic rat lenses. *Invest Ophthalmol Vis Sci* (2006) 47(9):3951–9. doi: 10.1167/iovs.06-0193

45. Pollreisz A, Schmidt-Erfurth U. Diabetic cataract-pathogenesis, epidemiology and treatment. *J Ophthalmol 2010* (2010) p:608751. doi: 10.1155/2010/608751

46. Fan X, Monnier VM, Whitson J. Lens glutathione homeostasis: Discrepancies and gaps in knowledge standing in the way of novel therapeutic approaches. *Exp Eye Res* (2017) 156:103–11. doi: 10.1016/j.exer.2016.06.018

frontiers | Frontiers in Endocrinology

TYPE Systematic Review
PUBLISHED 07 December 2023
DOI 10.3389/fendo.2023.1302127

OPEN ACCESS

EDITED BY
Kai Jin,
Zhejiang University, China

REVIEWED BY
Fangyu Lin,
Emory University, United States
Lu Yuan,
Zhejiang University, China

*CORRESPONDENCE
Jianlong Zhou
jianlong_zhoumd@163.com

RECEIVED 26 September 2023
ACCEPTED 25 October 2023
PUBLISHED 07 December 2023

CITATION
Zhou J, Zhu L and Li Y (2023) Association between the triglyceride glucose index and diabetic retinopathy in type 2 diabetes: a meta-analysis.
Front. Endocrinol. 14:1302127.
doi: 10.3389/fendo.2023.1302127

Association between the triglyceride glucose index and diabetic retinopathy in type 2 diabetes: a meta-analysis

Jianlong Zhou[1]*, Lv Zhu[2] and Yadi Li[1]

[1]Department of Traditional Chinese Medicine, People's Hospital of Deyang City, Deyang, China, [2]Department of Integrative Medicine, West China Hospital, Sichuan University, Chengdu, China

The triglyceride-glucose (TyG) index is an accessible and reliable surrogate indicator of insulin resistance and is strongly associated with diabetes. However, its relationship with diabetic retinopathy (DR) remains controversial. This meta-analysis aimed to assess the relationship between the TyG index and the prevalence of DR. Initial studies were searched from PubMed, Embase, Web of Science, and China National Knowledge Infrastructure (CNKI) electronic databases. The retrieval time range was from the establishment of the database to June 2023. Pooled estimates were derived using a random-effects model and reported as odds ratio (OR) with 95% confidence intervals (CIs). Two researchers independently assessed the methodological quality of the included studies. The Newcastle-Ottawa Quality Scale (NOS) was utilized to assess cohort studies or case-control studies. The Agency for Healthcare Research and Quality (AHRQ) methodology checklist was applied to assess cross-sectional studies. Ten observational studies encompassing 13716 patients with type 2 diabetes were included in the meta-analysis. The results showed that a higher TyG index increased the risk of DR compared with a low TyG index (OR: 2.34, 95% CI: 1.31-4.19, P < 0.05). When the index was analyzed as a continuous variable, consistent results were observed (OR: 1.48, 95% CI: 1.12-1.97, P < 0.005). There was no significant effect on the results of the sensitivity analyses excluding one study at a time (P all < 0.05). A higher TyG index may be associated with an increased prevalence of DR in patients with type 2 diabetes. However, high-quality cohort or case-control studies are needed to further substantiate this evidence.

Systematic review registration: https://www.crd.york.ac.uk/PROSPERO/, identifier CRD42023432747.

KEYWORDS

triglyceride glucose index, diabetic retinopathy, type 2 diabetes, meta-analysis, observational study

Introduction

Diabetic retinopathy (DR) is a common and serious chronic microvascular complication of diabetes mellitus (DM) (1). It is one of the leading causes of vision loss worldwide (2), as well as the leading cause of vision impairment in patients aged 25-74 (3). A recent meta-analysis of 59 population-based studies has shown that the global prevalence of DR is 22.27% and the prevalence of vision-threatening diabetic retinopathy (VTDR) is 6.17% among people with DM. In 2020, the global number of adults with DR and VTDR was estimated to be 103.12 million and 28.54 million, respectively; by 2045, it is expected to increase to 160.5 million and 44.82 million, respectively (4). DR not only affects patients' visual quality, but it is also associated with patients' health-related quality of life and well-being. As DR progresses, the patient's ability to work and live continues to decline, while some DR patients also experience varying degrees of anxiety or depression (5, 6). Therefore, early diagnosis and prevention are important to reduce the prevalence of DR and the hazard caused by adverse prognosis.

Insulin resistance (IR), referred to as resistance to insulin-stimulated glucose uptake, is an essential feature of aging, vascular disease, obesity, type 2 diabetes mellitus (T2D), dyslipidemia, and other components of the metabolic syndrome (7, 8). It has been found that IR may be an early driver of DR in the absence of significant hyperglycemia (9). The hyperinsulinemic-euglycemic clamp is a gold-standard method for assessing IR, but it is cumbersome, expensive, and not easy to perform in the clinic (10). Interestingly, the triglyceride-glucose (TyG) index, an indicator calculated from fasting triglyceride (TG) and fasting plasma glucose (FPG), is a simple, accurate, and reliable surrogate marker for assessing IR (11).

Previous studies have confirmed that the TyG index was strongly associated with DM (12), diabetic nephropathy (DN) (13), metabolic syndrome (MetS) (14), and atherosclerotic cardiovascular diseases (ASCVDs) (15). Recent studies have shown that the TyG index is a favorable predictor of DR prevalence and incidence (16, 17). Nevertheless, some studies have shown no correlation between the TyG index and DR (18, 19). The different results may be due to differences in factors such as participants, inclusion criteria, and type of study design. However, it still showed that the relationship between the TyG index and DR is controversial. Therefore, we performed this systematic review and meta-analysis aimed at assessing the relationship between the TyG index and DR.

Methods

This study followed the Preferred Reporting Items for Systematic Evaluation and Meta-Analysis (PRISMA) guidelines for meta-analysis. A detailed PRISMA checklist has been provided in Supplementary Material 1. The study was registered on the PROSPERO platform (CRD42023432747).

Sources and methods of data retrieval

The literature search used the following combination of words: (1) "triglyceride glucose index" OR "TyG index" OR "triglyceride and glucose index" OR "triglyceride–glucose index" OR "triglyceride/glucose index" OR "triacylglycerol glucose index;" and (2) "diabetic retinopathy" OR "diabetic retinopathies" OR "diabetes retinopathy" OR "retinopathy, diabetic". The following electronic literature databases will be searched: PubMed, Embase, Web of Science, and CNKI. Literature published in English or Chinese will be included. It was limited to human studies only. The search strategy will be conducted in duplicate and independently. The detailed search strategy for PubMed is described in Supplementary Material 2, and similar search strategies will be used for other electronic databases. Prior to the final analysis, the search will be re-run periodically until June 2023 to retrieve additional eligible studies, excluding unpublished studies.

Study selection and eligible criteria

Studies meeting the following criteria will be included: (1) the research design was observational study; (2) study participants were clearly diagnosed with T2D; (3) the TyG index could be acquired by laboratory examination; (4) DR was definitively diagnosed as the outcome disease; (5) the outcome measures indicating the relationship between TyG index and DR risk were presented as odds ratios (ORs), risk ratios(RRs), or hazard ratios (HRs), along with their corresponding 95% confidence intervals (CIs). Alternatively, complete data that could be used to calculate the effect size was provided; and (6) the effect estimates were obtained after accounting for confounding variables.

Meanwhile, studies meeting the following criteria will be excluded: (1) conference abstracts; (2) *in vitro* or animal experiments; (3) duplicate literature; (4) editorials, reviews, or commentaries; and (5) studies lacking sufficient data.

Date extraction and quality assessment

Two researchers independently conducted a literature search and screening. Subsequently, they performed data extraction and quality assessment of the eligible literature. In case of disagreement, it would be resolved by the third researcher. Based on the included studies, we extracted the following data: first author, year of publication, country of subjects, research design, number of participants, demographics (age, sex), model for TyG index analysis, and confounding variables adjusted in multiple regression analyses. The TyG index was calculated according to the following formula: ln (fasting TG [mg/dL] × fasting glucose [mg/dL]) (20). The estimates of effect were recorded as odds ratios (ORs). OR was defined as odds ratios, RRs, or HRs.

Depending on the type of observational study, the two authors chose different assessment tools to independently assess the quality

and risk of bias of the included studies. The Newcastle-Ottawa Scale (NOS) was used to assess case-control studies and cohort studies (21). For cross-sectional studies, the Agency for Healthcare Research and Quality (AHRQ) methodology checklist was selected for assessment (22). The NOS consisted of eight items categorized into three aspects such as selection, comparability, and outcome or exposure. Based on the number of stars assessed, the quality of the literature was differentiated into low quality (< 5 stars), medium quality (5-7 stars), and high quality (> 7 stars). AHRQ's assessment methodology included the eleven-item assessment component. The quality of the literature was ranked according to the percentage of "yes" received as low quality (< 30%), medium quality (30%-60%), and high quality (> 60%).

Statistical analysis

Statistical analysis was performed using Revman version 5.4, STATA version 12.0 and R version 4.4.1 softwares. For categorical and continuous data, we summarized the OR and the corresponding 95% CI to assess the relationship between the TyG index and the prevalence of DR, respectively. The effect valuation was seen to be statistically significant when the *P*-value was < 0.05. If the TyG index was treated as a categorical variable, we would extract the estimation value from the highest TyG index level. Once the TyG index was assessed as a continuous variable, we would extract the estimation value for each unit increase in the variable. If multiple models were present in the multifactorial analysis, we chose the one with the most adjusted confounders. To evaluate heterogeneity, Cochrane *Q* and I^2 tests were employed (23). When the *P*-value of the *Q*-test was less than 0.1 or $I^2 > 50\%$, it indicated the existence of significant heterogeneity. If $I^2 > 75\%$, it signified the presence of a high degree of heterogeneity. If there was significant heterogeneity, a random effects model was taken. Conversely, a fixed-effects model was employed. To test the stability of the findings, we further undertook sensitivity analyses, in which one study was excluded at a time and the change in the pooled OR of the remaining studies was observed (24).

To assess potential publication bias, we adopted funnel plots and contour-enhanced funnel plots incorporating the "cut-and-fill method" (25). Besides, we also used Egger's test to assess publication bias. If the funnel plot existed asymmetrically and the missing studies were located in regions with no statistical significance, the funnel plot asymmetry may be caused by publication bias. If publication bias was present, the pooled risk estimates were recalculated using the cut-and-fill method. If the funnel plot was asymmetric and the missing studies were distributed in statistically significant areas, this showed that the funnel plot asymmetry could be caused by other reasons rather than publication bias.

Patient and public involvement

Patients and the public were not involved in this study.

Results

Literature search

According to the search strategy, we retrieved a total of 699 literatures. Potentially relevant 514 pieces of literature were retained after the exclusion of duplicates. Then, 448 pieces of literature that were obviously irrelevant were excluded based on their titles or abstracts. Afterward, we assessed the remaining 66 pieces of literature across the full text. Eventually, ten qualified studies were integrated into the meta-analysis. The procedure for a more detailed literature search was illustrated in Figure 1.

Characteristics

In the present meta-analysis, we incorporated ten observational studies that encompassed a substantial sample size of 13,716 individuals in the quantitative synthesis. Among them were three cohorts studies (16, 19, 26), one case-control study (17), and six cross-sectional studies (27–32). These studies were conducted in four different countries such as Iran, Singapore, China, and India. The study primarily involved adults diagnosed with type 2 diabetes, although one study did not provide specific details about the type of diabetes under consideration (29). Nevertheless, considering the mean age of the included patients, it is reasonable to assume that they were type 2 diabetics. The number of participants ranged from 208 to 4721. Furthermore, the mean age of all participants across the studies exceeded 50 years. The percentage of male participants varied from 46.63% to 86.47%. The TyG index was used as the categorical variable in four studies and as the continuous variable in three studies. Another three studies utilized the TyG index as both types of variables. The confounders adjusted were nonidentical among the different studies. Adjusted confounders usually encompassed age, gender, duration of diabetes, body mass index (BMI), glycosylated hemoglobin, blood pressure, high-density lipoprotein (HDL), low-density lipoprotein (LDL), and other factors. However, in one study, adjusted confounders were not clearly identified (27). The information on the baseline characteristics of the included studies was presented graphically in Table 1.

Quality assessment

The AHRQ methodology checklist was used for quality assessment of the six cross-sectional studies, as shown in Table 2. Of these, three studies were evaluated as high quality. Three studies were assessed as medium quality. The NOS was used to assess the literature quality of one case-control study and three cohort studies, as shown in Table 3. There were two studies evaluated as high quality and two studies evaluated as medium quality. Overall, the studies included in this meta-analysis demonstrated a relatively good level of quality.

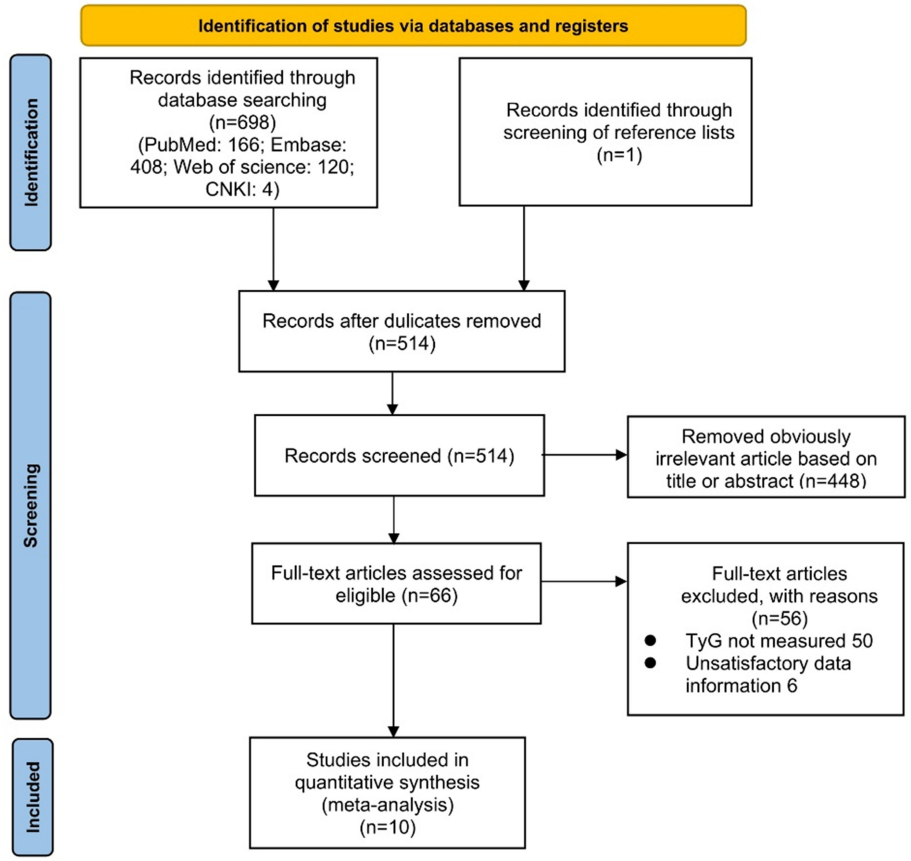

FIGURE 1
PRISMA flow diagram of literature search.

TyG index and prevalence of DR

A meta-analysis of seven studies (17, 26–30, 32) using the TyG index as a categorical variable showed that the highest TyG index group had a significantly increased risk of DR compared with the lowest TyG index group (OR 2.34, 95% CI 1.31- 4.19, I^2 90%, $P < 0.05$) (Figure 2A). A pooled analysis of the six studies (16, 19, 28, 29, 31, 32) in which the TyG index was used as a continuous variable also showed consistent results (OR 1.48, 95% CI 1.12- 1.97, I^2 83%, $P < 0.05$) (Figure 2B). Meanwhile, these analyses also revealed a high degree of heterogeneity among the studies.

Sensitivity analysis

The results of the sensitivity analysis demonstrated that excluding any of the studies had no notable effect on the pooled OR values (ORs for the TyG index as a categorical variable: 2.04-2.78, all $P < 0.05$; ORs for the TyG index as a continuous variable: 1.40-1.57, all $P < 0.05$) (Tables 4, 5). Interestingly, in the sensitivity analysis of the TyG index as a categorical variable, we found that heterogeneity decreased to a medium degree after excluding Yao LT, et al's study (17) (I^2 53%). While, in the sensitivity analysis of the TyG index as a continuous variable, the heterogeneity became insignificant after excluding Pan Y, et al's study (19) (I^2 17%).

Publication bias

By visual inspection, we found asymmetry in funnel plots (Figures 3A, 4A). Further, we investigated the potential publication bias using a contour-enhanced funnel plot combined with the cut-and-fill method. As shown in Figures 3B, 4B, most of the missing studies were distributed in statistically significant regions, while individual studies (Filled 1 and Filled 6 in Figure 4B) were distributed in statistically nonsignificant regions ($P > 0.05$). Therefore, this meta-analysis could not exclude the possibility of publication bias. However, it may also indicate that the observed asymmetry was due to other factors, such as the low number of studies included in the funnel plot analysis, methodological differences in the included studies, and the presence of small sample size studies. Hence, we performed Egger's test. The results still showed possible publication bias (all $P < 0.05$). However, after recalculating the effect sizes using the cut-and-fill method, there were no statistically significant changes in the effect sizes (adjusted OR for TyG index as a categorical variable:

10.3389/fendo.2023.1302127

TABLE 1 Characteristics of the included studies.

Study	Country	Research type	Characteristics of participants	Number of participants	Mean age (years)	Male (%)	TyG index analysis	Variables adjusted
Hameed EK, et al., 2019 (27)	Iraq	Cross-sectional	T2DM patients	416	NDR: 54.56 ± 9.31; DR: 58.98 ± 7.63	46.63%	Q4: Q1	Age, duration of diabetes, FBG, HbA1C, SBP, DBP, TC, TG, HDL, WC, and BMI
Neelam K, et al., 2023 (16)	Singapore	Cohort	T2DM patients	1339	NDR: 56.1 ± 10.7; DR: 56.5 ± 9.4	55.90%	Continuous	Duration of type 2 diabetes, BMI, eGFR, uACR and SBP
Pan Y, et al., 2021 (19)	China	Cohort	T2DM patients	4721	59.56 ± 13.02	53.57%	Continuous	Age, sex, BMI, smoking status
Srinivasan S, et al., 2021 (28)	India	Cross-sectional	T2DM patients	1413	56.30 ± 10	53.01%	Continuous; Categorized	Age, smoking, blood pressure
Yao LT, et al., 2021 (17)	China	Case-control	T2DM patients	2112	56.08 ± 13.85	57.90%	Q4: Q1	Age, sex, duration of diabetes, use of antidiabetic agents, HR, SBP, PP, height, weight, BMI, HbA1c, and TC
Zhou Y, et al., 2023 (29)	China	Cross-sectional	Adults with diabetes mellitus	888	62.2 ± 12.1	50.11%	Continuous; Categorized	Age; gender; race; education; PIR; HDL; LDL; TC; hypertension and retinopathy
Wang J, et al., 2022 (30)	China	Cross-sectional	T2DM patients	1061	NDR: 60.07 ± 8.06; DR: 57.63 ± 8.45	82.09%	Q4: Q1	Gender, age, smoking history, the course of diabetes, HbA1c, SBP, DBP, BMI, and SUA
Pang M, et al., 2020 (31)	China	Cross-sectional	T2DM patients	208	NDR: 53.68 ± 14.39; DR: 54.85 ± 11.37	61.06%	Continuous	Duration of diabetes, SBP, SUA
Li CH, et al., 2022 (26)	China	Cohort	T2DM patients	1153	58.89 ± 8.60	86.47%	Q4: Q1	Age, gender, course of disease, smoking, alcohol consumption, exercise, HDL-C, SBP, BMI, HbA1c, the use of hypoglycemic drugs, and the use of lipid-lowering drugs
Xiao HY, et al., 2022 (32)	China	Cross-sectional	T2DM patients	405	58.9 ± 9.7	56.50%	Continuous; Categorized	Gender, age, Duration of type 2 diabetes, BMI

NDR, no diabetic retinopathy; DR, diabetic retinopathy; FBG, fasting blood glucose; BMI, body mass index; eGFR, estimated glomerular filtration rate; uACR, urinary albumin-to-creatinine ratio; SBP, systolic blood pressure; DBP, diastolic blood pressure; HR, heart rate; PP, pulse pressure; HbA1c, glycated hemoglobin; TC, total cholesterol; PIR, poverty income ratio; HDL, high-density lipoprotein; HDL-C, HDL-cholesterol; LDL, low-density lipoprotein; WC, waist circumference; SUA, serum uric acid.

0.349, 95% CI: -0.208- 0.906, P =0.22, number of cut and fill =3; adjusted OR for TyG index as a continuous variable: 0.158, 95% CI: -0.107- 0.423, P =0.24, number of cut and fill =3), which suggested that publication bias had little effect on the results.

Discussion

Studies have found that more than 60% of patients with type 2 diabetes might develop diabetic retinopathy within 20 years of its onset (33). As a leading cause of vision loss, DR has a serious impact on the daily life and well-being of patients. Previous studies have found that insulin resistance was a major pathogenic factor in type 2 diabetes (34). Current studies have shown that IR was closely associated with DR (35). However, whether the TyG index, a valid predictor of IR, is associated with DR remains controversial. Our meta-analysis demonstrated that a higher TyG index might be more likely to increase the prevalence risk of DR compared to a lower TyG index. To the best of our knowledge, this study is the first meta-analysis to assess the relationship between TyG index and the risk of diabetic retinopathy in type 2 diabetes.

TABLE 2 Quality Assessment of cross-sectional studies with AHRQ methodology checklist.

Domain	Hameed EK, et al., 2019 (27)	Srinivasan S, et al., 2021 (28)	Zhou Y, et al., 2023 (29)	Wang J, et al., 2022 (30)	Pang M, et al., 2020 (31)	Xiao HY, et al., 2022 (32)
1 Define source of information (survey, record review)	Y	Y	Y	Y	Y	Y
2 List inclusion and exclusion criteria for exposed and unexposed subjects (cases and controls) or refer to previous publications	Y	Y	Y	Y	Y	Y
3 Indicate time period used for identifying patients	Y	N	Y	Y	Y	Y
4 Indicate whether or not subjects were consecutive if not population-based	Y	N	U	U	Y	U
5 Indicate if evaluators of subjective components of study were masked to other aspects of the status of the participants	N	N	N	N	N	N
6 Describe any assessments undertaken for quality assurance purposes (e.g., test/retest of primary outcome measurements)	Y	Y	Y	Y	Y	Y
7 Explain any patient exclusions from analysis	Y	U	Y	Y	N	N
8 Describe how confounding was assessed and/or controlled	Y	Y	Y	Y	Y	Y
9 If applicable, explain how missing data were handled in the analysis	U	U	U	U	U	U
10 Summarize patient response rates and completeness of data collection	U	N	Y	Y	U	N
11 Clarify what follow-up, if any, was expected and the percentage of patients for which incomplete data or follow-up was obtained	N	N	N	N	N	N
Number (percentage) of domain agreement	7/11 (64%)	4/11 (36%)	7/11 (64%)	7/11 (64%)	6/11 (55%)	5/11 (45%)

AHRQ, Agency for Healthcare Research and Quality; Y, Yes; N, No; U, Unclear.

Risk factors for DR usually involved age, glycosylated hemoglobin (HbA1c), lipids, obesity, duration of diabetes, smoking, kidney disease, hypertension, and others (36, 37). Currently, DR is mainly diagnosed through funduscopic examination (38). According to the Early Treatment Diabetic Retinopathy Research Study (ETDRS) criteria (39), DR was diagnosed if certain characteristic lesions were present, such as cotton wool spots, hard exudates, macular edema, intraretinal microvascular abnormalities, microaneurysms, hemorrhages, or neovascularization. However, there are no obvious symptoms in the early stage of DR (40), and many patients seek medical treatment only when they experience vision loss and blurred vision, which is already a serious condition and is not conducive to later recovery and prognosis. Therefore, it is of great clinical significance to find a convenient and noninvasive early detection index for early screening of DR patients. Our study provided a potential method for early detection of DR. The TyG index could be used to assess the risk profile of DR in patients with type 2 diabetes. Further, optimizing lipid and glycemic management is an important component of diabetes management, which contributes to obtaining the TyG index. Thus, the TyG index, as an accessible routine indicator, may be a potentially clinically valuable option for early diagnosis and treatment of DR.

Although the actual role of the TyG index in the pathogenesis of DR has been unclear, several potential mechanisms associated with IR have been recognized. Previous studies have found that inflammation, oxidative stress, nitric oxide production, mitochondrial damage, and vascular endothelial dysfunction were involved in the pathogenesis of DR (41–45). The increasing evidence suggested that IR played an important role in the mechanism of DR and might be related to the

TABLE 3 Quality assessment of the Newcastle-Ottawa Scale for cohort and case-control studies.

Author (year)	Selection	Comparability	Outcome/Exposure	NOS score
Neelam K, et al., 2023 (16)	★★★	★★	★★★	8
Pan Y, et al., 2021 (19)	★★★	★★	★★	7
Li CH, et al., 2022 (26)	★★★	★★	★★★	8
Yao LT, et al., 2021 (17)	★★★	★★	★★	7

★: The NOS consists of eight items categorized into three aspects. Each numbered item can score one star if the study is eligible. A maximum of four stars can be awarded for selection, two stars for comparability, and three stars for outcome or exposure.

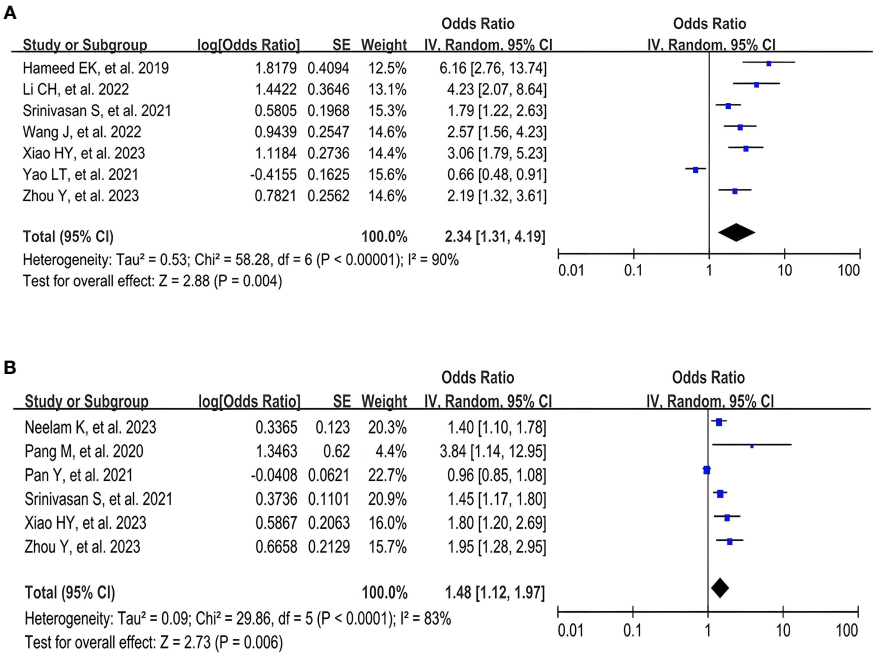

FIGURE 2
Forest plot of the relationship between TyG index and DR risk. **(A)** Forest plot of TyG index as a categorical variable. **(B)** Forest plot of TyG index as a continuous variable.

TABLE 4 Results of the sensitivity analysis when the TyG index was applied as a categorical variable.

Dataset excluded	OR	95% CI	I^2 %	*P* for effect
Hameed EK, et al., 2019 (27)	2.04	1.13, 3.65	90%	0.02
Li CH, et al., 2022 (26)	2.14	1.16, 3.96	90%	0.02
Srinivasan S, et al., 2021 (28)	2.49	1.21, 5.14	91%	0.01
Wang J, et al., 2022 (30)	2.32	1.19, 3.61	91%	0.01
Xiao HY, et al., 2022 (32)	2.25	1.18, 4.30	91%	0.01
Yao LT, et al., 2021 (17)	2.78	2.01, 3.85	53%	< 0.00001
Zhou Y, et al., 2023 (29)	2.39	1.21, 4.71	91%	0.01

TABLE 5 Results of the sensitivity analysis when the TyG index was applied as a continuous variable.

Dataset excluded	OR	95% CI	I^2 %	*P* for effect
Neelam K, et al., 2023 (16)	1.54	1.07, 2.20	85%	0.02
Pang M, et al., 2020 (31)	1.42	1.07, 1.87	85%	0.01
Pan Y, et al., 2021 (19)	1.57	1.33, 1.84	17%	< 0.00001
Srinivasan S, et al., 2021 (28)	1.52	1.06, 2.18	84%	0.02
Xiao HY, et al., 2022 (32)	1.43	1.05, 1.94	84%	0.02
Zhou Y, et al., 2023 (29)	1.40	1.04, 1.89	83%	0.02

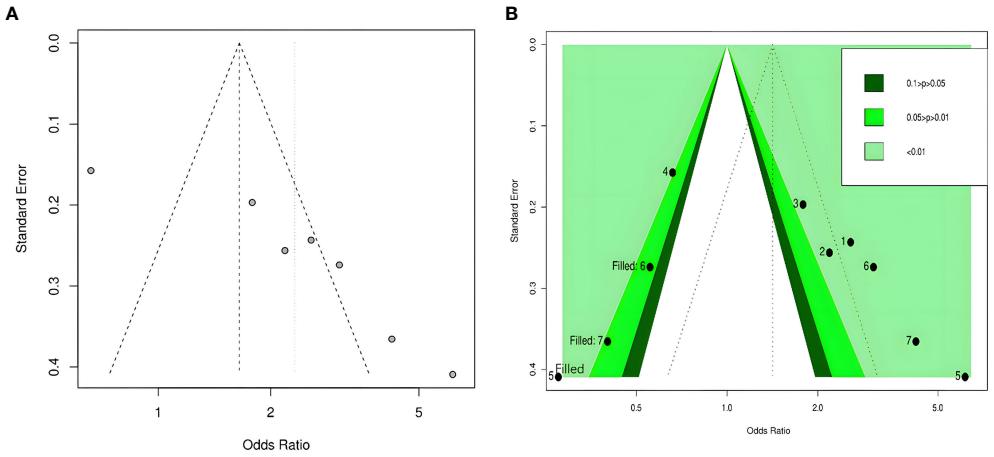

FIGURE 3
Funnel plot of the relationship between the TyG index as a categorical variable and DR. **(A)** Funnel plot; **(B)** Contour-enhanced funnel plot.

pathways mentioned above (35, 46). C-reactive protein (CRP) is an independent predictor of IR (47). IR may increase the release of inflammatory factors such as C-reactive protein and tumor necrosis factor, leading to the adhesion and aggregation of leukocytes, which can cause retinal capillary obstruction and finally local ischemia (48). IR could lead to elevated levels of oxidative stress, increased malondialdehyde (MDA), a product of oxidative stress, and decreased antioxidants such as superoxide dismutase (SOD) and glutathione S-transferase (GSH-ST) (49). There was a close relationship between oxidative stress and endothelial cell dysfunction, which can cause diabetic microangiopathy (50). IR not only could diminish endothelial nitric oxide synthase (eNOS) activity, causing endothelial dysfunction, but also reduce nitric oxide production, which in turn leads to vasodilatory-contractile dysregulation, ultimately resulting in microcirculatory disorders and retinal damage (51–54). Mitochondrial dysfunction was strongly associated with IR and played an important role in the pathogenesis of DR (55). IR may speed up mitochondrial damage and thus promote apoptosis in retinal capillary cells (56, 57). In addition, some limited studies have shown that IR and DR may have a common genetic basis. For example, studies have found that DR was significantly associated with mutations in genes that express vascular endothelial growth factor (VEGF) (58). Additional studies have confirmed that blood VEGF levels were positively correlated with an index of IR (59). This suggested that expression of the VEGF gene may be one of the common genetic bases between IR and DR. Pro12Ala is located at the amino-terminus of the PPAR-γ 2 gene and was found to be associated with higher insulin sensitivity (59). Pro12Ala mutations may affect lipid metabolism, and pancreatic β-cell function, and be associated with the risk of IR (60). Meanwhile, it was also found that the alanine variant of Pro12Ala may be associated with a lower risk of DR (61). This suggested that Pro12Ala may be a common genetic base between IR and DR. Overall, these studies above imply that IR may mediate the mechanism of DR in type 2 diabetes. However, more studies are needed to prove these findings.

A high degree of heterogeneity was noted in our meta-analysis results, which may be due to the presence of many confounding

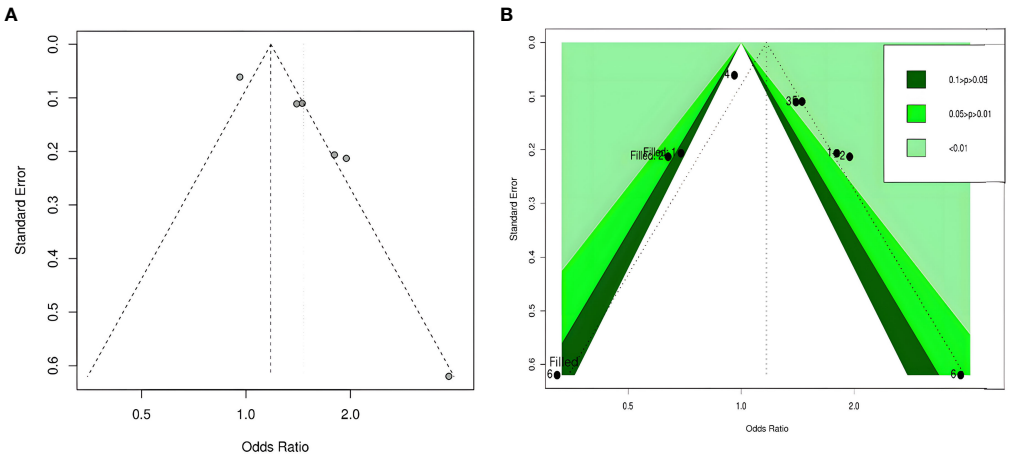

FIGURE 4
Funnel plot of the relationship between the TyG index as a continuous variable and DR. **(A)** Funnel plot; **(B)** Contour-enhanced funnel plot.

variables. Heterogeneity decreased after the exclusion of Yao LT, et al's study (a case-control study) and Pan Y, et al's study (a cohort study), which may be related to the fact that the design type of the included studies was mainly cross-sectional. In addition, it was not excluded that the differences between studies in terms of study populations, number of participants, and adjusted confounders influenced heterogeneity. For example, this study involved populations from four different countries. The lowest number of participants was 208, while the highest was 4721. However, due to the small number of included studies, it was difficult for us to perform further subgroup analyses in this study. Nevertheless, the sensitivity analysis still presented a stable pooled result.

Despite obtaining a positive conclusion, our study still had the following limitations that merit further deliberation. First, the studies included in the analysis were mainly observational studies, with a predominance of cross-sectional studies. Their level of evidence was lower than randomized controlled trials or cohort studies Moreover, these studies were mostly concerned with the analysis of prevalence and lacked investigation of incidence. Second, it was worth considering that the number of studies included was very limited. This meant that the results of the study may not necessarily be applicable to a wider population. Additionally, there was a high degree of heterogeneity in these studies, and more studies were needed to ascertain whether research type, country, sample size, gender, and other study characteristics influenced the results of the analyses. Third, there were many confounding variables affecting the relationship between the TyG index and DR risk. The variables adjusted by different studies were not identical, which may have had an impact on the results. Finally, results based on observational studies could not show a causal relationship between the TyG index and DR risk. Therefore, it is essential to perform more high-quality cohort studies and basic research to obtain more reliable evidence.

Conclusions

In conclusion, the existing evidence based on observational studies suggested that a higher TyG index was a potential predictor of DR risk in patients with type 2 diabetes. Considering the ease of obtaining the TyG index, more cohort studies are needed in the future to further identify the independent predictive role of the TyG index in DR incidence and prevalence, and it may also be compared with other DR risk prediction tools.

Author contributions

JZ: Conceptualization, Data curation, Formal analysis, Investigation, Methodology, Software, Writing – original draft, Writing – review & editing. LZ: Data curation, Formal analysis, Writing – review & editing. YL: Resources, Supervision, Writing – review & editing.

Funding

The author(s) declare that no financial support was received for the research, authorship, and/or publication of this article.

Conflict of interest

The authors declare that the research was conducted in the absence of any commercial or financial relationships that could be construed as a potential conflict of interest.

Publisher's note

Supplementary material

The Supplementary Material for this article can be found online at: https://www.frontiersin.org/articles/10.3389/fendo.2023.1302127/full#supplementary-material

References

1. Jiang T, Chang Q, Cai J, Fan J, Zhang X, Xu G. Protective effects of melatonin on retinal inflammation and oxidative stress in experimental diabetic retinopathy. *Oxid Med Cell Longev* (2016) 2016:3528274. doi: 10.1155/2016/3528274

2. Toto L, D'Aloisio R, Di Nicola M, Di Martino G, Di Staso S, Ciancaglini M, et al. Qualitative and quantitative assessment of vascular changes in diabetic macular edema after dexamethasone implant using optical coherence tomography angiography. *Int J Mol Sci* (2017) 18(6):1181. doi: 10.3390/ijms18061181

3. Zhang X, Saaddine JB, Chou CF, Cotch MF, Cheng YJ, Geiss LS, et al. Prevalence of diabetic retinopathy in the United States, 2005-2008. *Jama* (2010) 304(6):649–56. doi: 10.1001/jama.2010.1111

4. Teo ZL, Tham YC, Yu M, Chee ML, Rim TH, Cheung N, et al. Global prevalence of diabetic retinopathy and projection of burden through 2045: systematic review and meta-analysis. *Ophthalmology* (2021) 128(11):1580–91. doi: 10.1016/j.ophtha.2021.04.027

5. Khoo K, Man REK, Rees G, Gupta P, Lamoureux EL, Fenwick EK. The relationship between diabetic retinopathy and psychosocial functioning: a systematic review. *Qual Life Res* (2019) 28(8):2017–39. doi: 10.1007/s11136-019-02165-1

6. Cooper OAE, Taylor DJ, Crabb DP, Sim DA, McBain H. Psychological, social and everyday visual impact of diabetic macular oedema and diabetic retinopathy: a systematic review. *Diabetes Med* (2020) 37(6):924–33. doi: 10.1111/dme.14125

7. Bernal-Mizrachi C, Xiaozhong L, Yin L, Knutsen RH, Howard MJ, Arends JJ, et al. An afferent vagal nerve pathway links hepatic PPARalpha activation to glucocorticoid-induced insulin resistance and hypertension. *Cell Metab* (2007) 5(2):91–102. doi: 10.1016/j.cmet.2006.12.010

8. Nogiec C, Burkart A, Dreyfuss JM, Lerin C, Kasif S, Patti ME. Metabolic modeling of muscle metabolism identifies key reactions linked to insulin resistance phenotypes. *Mol Metab* (2015) 4(3):151–63. doi: 10.1016/j.molmet.2014.12.012

9. Amoaku WM, Ghanchi F, Bailey C, Banerjee S, Banerjee S, Downey L, et al. Diabetic retinopathy and diabetic macular oedema pathways and management: UK Consensus Working Group. *Eye (Lond)* (2020) 34(Suppl 1):1–51. doi: 10.1038/s41433-020-0961-6

10. Yuan X, Chen R, Zhang Y, Lin X, Yang X, McCormick KL. Gut microbiota of chinese obese children and adolescents with and without insulin resistance. *Front Endocrinol (Lausanne)* (2021) 12:636272. doi: 10.3389/fendo.2021.636272

11. Li L, Yao H, Dai W, Chen Y, Liu H, Ding W, et al. A higher TyG index is related with a higher prevalence of erectile dysfunction in males between the ages 20-70 in the United States, according to a cross-sectional research. *Front Endocrinol (Lausanne)* (2022) 13:988257. doi: 10.3389/fendo.2022.988257

12. Park B, Lee HS, Lee YJ. Triglyceride glucose (TyG) index as a predictor of incident type 2 diabetes among nonobese adults: a 12-year longitudinal study of the Korean Genome and Epidemiology Study cohort. *Transl Res* (2021) 228:42–51. doi: 10.1016/j.trsl.2020.08.003

13. Liu L, Xia R, Song X, Zhang B, He W, Zhou X, et al. Association between the triglyceride-glucose index and diabetic nephropathy in patients with type 2 diabetes: A cross-sectional study. *J Diabetes Investig* (2021) 12(4):557–65. doi: 10.1111/jdi.13371

14. Son DH, Lee HS, Lee YJ, Lee JH, Han JH. Comparison of triglyceride-glucose index and HOMA-IR for predicting prevalence and incidence of metabolic syndrome. *Nutr Metab Cardiovasc Dis* (2022) 32(3):596–604. doi: 10.1016/j.numecd.2021.11.017

15. Ding X, Wang X, Wu J, Zhang M, Cui M. Triglyceride-glucose index and the incidence of atherosclerotic cardiovascular diseases: a meta-analysis of cohort studies. *Cardiovasc Diabetol* (2021) 20(1):76. doi: 10.1186/s12933-021-01268-9

16. Neelam K, Aung KCY, Ang K, Tavintharan S, Sum CF, Lim SC. Association of triglyceride glucose index with prevalence and incidence of diabetic retinopathy in a Singaporean population. *Clin Ophthalmol* (2023) 17:445–54. doi: 10.2147/OPTH.S382336

17. Yao L, Wang X, Zhong Y, Wang Y, Wu J, Geng J, et al. The triglyceride-glucose index is associated with diabetic retinopathy in chinese patients with type 2 diabetes: A hospital-based, nested, case-control study. *Diabetes Metab Syndr Obes* (2021) 14:1547–55. doi: 10.2147/DMSO.S294408

18. Chiu H, Tsai HJ, Huang JC, Wu PY, Hsu WH, Lee MY, et al. Associations between triglyceride-glucose index and micro- and macro-angiopathies in type 2 diabetes mellitus. *Nutrients* (2020) 12(2):328. doi: 10.3390/nu12020328

19. Pan Y, Zhong S, Zhou KX, Tian ZJ, Chen F, Liu ZQ, et al. Association between diabetes complications and the triglyceride-glucose index in hospitalized patients with type 2 diabetes. *J Diabetes Res* (2021) 2021:6. doi: 10.1155/2021/8757996

20. Park K, Ahn CW, Lee SB, Kang S, Nam JS, Lee BK, et al. Elevated tyG index predicts progression of coronary artery calcification. *Diabetes Care* (2019) 42(8):1569–73. doi: 10.2337/dc18-1920

21. Stang A. Critical evaluation of the Newcastle-Ottawa scale for the assessment of the quality of nonrandomized studies in meta-analyses. *Eur J Epidemiol* (2010) 25 (9):603–5. doi: 10.1007/s10654-010-9491-z

22. Rostom A, Dubé C, Cranney A, Saloojee N, Sy R, Garritty C. *Celiac disease. Evidence reports/technology assessments, no. 104. Appendix D*. (Rockville (MD): Quality Assessment Forms: Agency for Healthcare Research and Quality US) (2004). Available at: https://www.ncbi.nlm.nih.gov/books/NBK35156/.

23. Higgins JP, Thompson SG. Quantifying heterogeneity in a meta-analysis. *Stat Med* (2002) 21(11):1539–58. doi: 10.1002/sim.1186

24. Ekelund U, Tarp J, Fagerland MW, Johannessen JS, Hansen BH, Jefferis BJ, et al. Joint associations of accelero-meter measured physical activity and sedentary time with all-cause mortality: a harmonised meta-analysis in more than 44 000 middle-aged and older individuals. *Br J Sports Med* (2020) 54(24):1499–506. doi: 10.1136/bjsports-2020-103270

25. Peters JL, Sutton AJ, Jones DR, Abrams KR, Rushton L. Contour-enhanced meta-analysis funnel plots help distinguish publication bias from other causes of asymmetry. *J Clin Epidemiol* (2008) 61(10):991–6. doi: 10.1016/j.jclinepi.2007.11.010

26. Li CH, Niu LL, Wang J. Relationship between the triglyceride glucose index and diabetic retinopathy in patients with type 2 diabetes mellitus: a cohort study. *Chin J Diabetes Mellitus* (2022) 14(10):1051–6. doi: 10.3760/cma.j.cn115791-20220130-00061

27. Hameed EK, Abdul-Qahar ZH, Kadium TE. The association of triglycerides glucose index with diabetic retinopathy in patients with type 2 diabetes mellitus. *Indian J Public Health Res Dev* (2019) 10(11):1885–90. doi: 10.5958/0976-5506.2019.03828.2

28. Srinivasan S, Singh P, Kulothungan V, Sharma T, Raman R. Relationship between triglyceride glucose index, retinopathy and nephropathy in Type 2 diabetes. *Endocrinol Diabetes Metab* (2021) 4(1):8. doi: 10.1002/edm2.151

29. Zhou Y, Lu Q, Zhang M, Yang L, Shen X. The U-shape relationship between triglyceride-glucose index and the risk of diabetic retinopathy among the US population. *J Pers Med* (2023) 13(3):11. doi: 10.3390/jpm13030495

30. Wang J, Zhang HF, Li CH. Triglyceride and glucose index as a predictive factor for diabetic retinopathy in Type 2 diabetic patients. *Int Eye Science* (2022) 22(08):1385–90. doi: 3980/j.issn.1672-5123.2002.8.29

31. Pang M, Wei Y, Weng XG. Analysis of risk factors of type 2 diabetic retinopathy. *J Xinxiang Med University* (2020) 37(03):270–3. doi: 10.7683/xxyxyxb.2020.03.017

32. Xiao HY. *Patients with type 2 diabetes triglycerides- glucose index and retinopathy correlation studies*. (Nanchang: Nanchang University) (2022).

33. Begum T, Rahman A, Nomani D, Mamun A, Adams A, Islam S, et al. Diagnostic accuracy of detecting diabetic retinopathy by using digital fundus photographs in the peripheral health facilities of Bangladesh: validation study. *JMIR Public Health Surveill* (2021) 7(3):e23538. doi: 10.2196/23538

34. Urakaze M, Kobashi C, Satou Y, Shigeta K, Toshima M, Takagi M, et al. The beneficial effects of astaxanthin on glucose metabolism and modified low-density lipoprotein in healthy volunteers and subjects with prediabetes. *Nutrients* (2021) 13 (12):4381. doi: 10.3390/nu13124381

35. Arıkan S, Erşan İ, Eroğlu M, Yılmaz M, Tufan HA, Gencer B, et al. Does retinal neurodegeneration seen in diabetic patients begin in the insulin resistance stage? *Turk J Ophthalmol* (2016) 46(6):264–9. doi: 10.4274/tjo.68888

36. Aljehani EA, Alhawiti AE, Mohamad RM. Prevalence and determinants of diabetic retinopathy among type 2 diabetic patients in Saudi Arabia: A systematic review. *Cureus* (2023) 15(7):e42771. doi: 10.7759/cureus.42771

37. Lima VC, Cavalieri GC, Lima MC, Nazario NO, Lima GC. Risk factors for diabetic retinopathy: a case-control study. *Int J Retina Vitreous* (2016) 2:21. doi: 10.1186/s40942-016-0047-6

38. Motz CT, Chesler KC, Allen RS, Bales KL, Mees LM, Feola AJ, et al. Novel detection and restorative levodopa treatment for preclinical diabetic retinopathy. *Diabetes* (2020) 69(7):1518–27. doi: 10.2337/db19-0869

39. Patz A, Smith RE. Grading diabetic retinopathy from stereoscopic color fundus photographs–an extension of the modified Airlie House classification. ETDRS report number 10. Early Treatment Diabetic Retinopathy Study Research Group. *Ophthalmology* (1991) 98(5 Suppl):786–806.

40. Platania CBM, Maisto R, Trotta MC, D'Amico M, Rossi S, Gesualdo C, et al. Retinal and circulating miRNA expression patterns in diabetic retinopathy: an in silico and *in vivo* approach. *Br J Pharmacol* (2019) 176(13):2179–94. doi: 10.1111/bph.14665

41. Rubsam A, Parikh S, Fort PE. Role of inflammation in diabetic retinopathy. *Int J Mol Sci* (2018) 19(4):31. doi: 10.3390/ijms19040942

42. Peng JJ, Xiong SQ, Ding LX, Peng J, Xia XB. Diabetic retinopathy: Focus on NADPH oxidase and its potential as therapeutic target. *Eur J Pharmacol* (2019) 853:381–7. doi: 10.1016/j.ejphar.2019.04.038

43. Sharma S, Saxena S, Srivastav K, Shukla RK, Mishra N, Meyer CH, et al. Nitric oxide and oxidative stress is associated with severity of diabetic retinopathy and retinal structural alterations. *Clin Exp Ophthalmol* (2015) 43(5):429–36. doi: 10.1111/ceo.12506

44. Devi TS, Somayajulu M, Kowluru RA, Singh LP. TXNIP regulates mitophagy in retinal Müller cells under high-glucose conditions: implications for diabetic retinopathy. *Cell Death Dis* (2017) 8(5):e2777. doi: 10.1038/cddis.2017.190

45. Tung TH, Shih HC, Tsai ST, Chou P, Chen SJ, Lee FL, et al. A community-based study of the relationship between insulin resistance/beta-cell dysfunction and diabetic retinopathy among type II diabetics in Kinmen, Taiwan. *Ophthalmic Epidemiol* (2007) 14(3):148–54. doi: 10.1080/09286580601139220

46. Chaturvedi N, Sjoelie AK, Porta M, Aldington SJ, Fuller JH, Songini M, et al. Markers of insulin resistance are strong risk factors for retinopathy incidence in type 1 diabetes. *Diabetes Care* (2001) 24(2):284–9. doi: 10.2337/diacare.24.2.284

47. Taniguchi A, Nagasaka S, Fukushima M, Sakai M, Okumura T, Yoshii S, et al. C-reactive protein and insulin resistance in non-obese Japanese type 2 diabetic patients. *Metabolism* (2002) 51(12):1578–81. doi: 10.1053/meta.2002.36312

48. Fain JN. Release of interleukins and other inflammatory cytokines by human adipose tissue is enhanced in obesity and primarily due to the nonfat cells. *Vitam Horm* (2006) 74:443–77. doi: 10.1016/S0083-6729(06)74018-3

49. Zhao Q. *A study on insulin resistance and oxidative stress*. (Tianjin: Nankai University) (2004).

50. Kowluru RA, Tang J, Kern TS. Abnormalities of retinal metabolism in diabetes and experimental galactosemia. VII. Effect of long-term administration of antioxidants on the development of retinopathy. *Diabetes* (2001) 50(8):1938–42. doi: 10.2337/diabetes.50.8.1938

51. Artunc F, Schleicher E, Weigert C, Fritsche A, Stefan N, Häring HU. The impact of insulin resistance on the kidney and vasculature. *Nat Rev Nephrol* (2016) 12 (12):721–37. doi: 10.1038/nrneph.2016.145

52. Sugiyama T, Yamamoto E, Bryniarski K, Xing L, Fracassi F, Lee H, et al. Coronary plaque characteristics in patients with diabetes mellitus who presented with acute coronary syndromes. *J Am Heart Assoc* (2018) 7(14):e009245. doi: 10.1161/JAHA.118.009245

53. van Bommel EJM, Ruiter D, Muskiet MHA, van Baar MJB, Kramer MHH, Nieuwdorp M, et al. Insulin sensitivity and renal hemodynamic function in metformin-treated adults with type 2 diabetes and preserved renal function. *Diabetes Care* (2020) 43(1):228–34. doi: 10.2337/dc19-1651

54. Rojas M, Lemtalsi T, Toque HA, Xu Z, Fulton D, Caldwell RW, et al. NOX2-induced activation of arginase and diabetes-induced retinal endothelial cell senescence. *Antioxidants (Basel)* (2017) 6(2):43. doi: 10.3390/antiox6020043

55. Xu DQ, Li CJ, Jiang ZZ, Wang L, Huang HF, Li ZJ, et al. The hypoglycemic mechanism of catalpol involves increased AMPK-mediated mitochondrial biogenesis. *Acta Pharmacol Sin* (2020) 41(6):791–9. doi: 10.1038/s41401-019-0345-2

56. Kowluru RA. Retinopathy in a diet-induced type 2 diabetic rat model and role of epigenetic modifications. *Diabetes* (2020) 69(4):689–98. doi: 10.2337/db19-1009

57. Kowluru RA, Mishra M, Kowluru A, Kumar B. Hyperlipidemia and the development of diabetic retinopathy: Comparison between type 1 and type 2 animal models. *Metabolism* (2016) 65(10):1570–81. doi: 10.1016/j.metabol.2016.07.012

58. Rong X, Ji Y, Zhu X, Yang J, Qian D, Mo X, et al. Neuroprotective effect of insulin-loaded chitosan nanoparticles/PLGA-PEG-PLGA hydrogel on diabetic retinopathy in rats. *Int J Nanomed* (2019) 14:45–55. doi: 10.2147/IJN.S184574

59. Zaki ME, Basha W, Yousef RN, Awad M. Serum vascular endothelial growth factor in Egyptian obese women with insulin resistance. *Open Access Maced J Med Sci* (2019) 7(8):1330–4. doi: 10.3889/oamjms.2019.156

60. Vales-Villamarín C, de Dios O, Pérez-Nadador I, Gavela-Pérez T, Soriano-Guillén L, Garcés C. PPARγ2 pro12Ala polymorphism is associated in children with traits related to susceptibility to type 2 diabetes. *Front Pharmacol* (2021) 12:763853. doi: 10.3389/fphar.2021.763853

61. Malecki MT, Cyganek K, Mirkiewicz-Sieradzka B, Wolkow PP, Wanic K, Skupien J, et al. Alanine variant of the Pro12Ala polymorphism of the PPARgamma gene might be associated with decreased risk of diabetic retinopathy in type 2 diabetes. *Diabetes Res Clin Pract* (2008) 80(1):139–45. doi: 10.1016/j.diabres.2007.11.001

frontiers | Frontiers in Endocrinology

TYPE Original Research
PUBLISHED 11 January 2024
DOI 10.3389/fendo.2023.1321226

OPEN ACCESS

EDITED BY
Honghua Yu,
Guangdong Provincial People's Hospital, China

REVIEWED BY
Mohd Anul Haq,
Majmaah University, Saudi Arabia
Du Shaolin,
Dongguan Tungwah Hospital, China

*CORRESPONDENCE
Fengmei Zhang
FengmeiZhang1@outlook.com

RECEIVED 13 October 2023
ACCEPTED 19 December 2023
PUBLISHED 11 January 2024

CITATION
Zheng X, Feng L, Xing C, Wang J, Zhao W and Zhang F (2024) Renal impairment may indicate postoperative low vision in young patients with proliferative diabetic retinopathy undergoing vitrectomy.
Front. Endocrinol. 14:1321226.
doi: 10.3389/fendo.2023.1321226

Renal impairment may indicate postoperative low vision in young patients with proliferative diabetic retinopathy undergoing vitrectomy

Xiaorong Zheng[1], Lin Feng[2], Chen Xing[3], Junlan Wang[4], Wei Zhao[5] and Fengmei Zhang[1*]

[1]Clinical Laboratory, Hebei Provincial Key Laboratory of Ophthalmology, Hebei Provincial Clinical Research Center for Eye Diseases, Hebei Eye Hospital, Xingtai, Hebei, China, [2]Diabetic Eye Disease Ward, Hebei Provincial Key Laboratory of Ophthalmology, Hebei Provincial Clinical Research Center for Eye Diseases, Hebei Eye Hospital, Xingtai, Hebei, China, [3]Fundus Imaging and Laser Therapy Department, Hebei Provincial Key Laboratory of Ophthalmology, Hebei Provincial Clinical Research Center for Eye Diseases, Hebei Eye Hospital, Xingtai, Hebei, China, [4]Internal Medicine Department, Hebei Provincial Key Laboratory of Ophthalmology, Hebei Provincial Clinical Research Center for Eye Diseases, Hebei Eye Hospital, Xingtai, Hebei, China, [5]Medical Records Room, Hebei Provincial Key Laboratory of Ophthalmology, Hebei Provincial Clinical Research Center for Eye Diseases, Hebei Eye Hospital, Xingtai, Hebei, China

Objective: To innovatively evaluate the impact of renal impairment in young work age patients with proliferative diabetic retinopathy (PDR) on their visuality after vitrectomy.

Methods: To find out whether it is possible to better predict the improvement of visual acuity after vitrectomy in working-age people without adding additional preoperative testing. In view of the fact that diabetic retinopathy and diabetic nephropathy are common diabetic complications of microvascular damage, it is considered whether preoperative renal function can be used as this evaluation index. This paper studies the design under this theme. This retrospective study included 306 patients (306 eyes) diagnosed with PDR and undergoing vitrectomy in our hospital from January 2016 to June 2023. Relevant baseline data were collected, including age, history of kidney disease and clinical laboratory test results. According to the International Standard Logarithmic Visual Acuity Checklist, the best corrected visual acuity was tested on the first day of admission and one month after surgery, and the difference between the two was subtracted. A difference >0 was defined as "vision improved". Patients were classified as vision-improved group (n=245) and non-improved group (n=61). The differences in baseline serum urea nitrogen, creatinine, uric acid, Cystatin C, estimated glomerular filtration rate (eGFR) and urine protein distribution between the two groups were statistically analyzed, binary regression analysis was performed for meaningful parameters, and random forest model ranked the characteristics in importance.

Results: 1.A higher level of serum cystatin C [1.02(0.80,1.48) mg/L vs 0.86 (0.67,1.12) mg/L, P<0.001] and a lower eGFR [82.3(50.33, 115.11) ml/(min/1.73m^2) vs 107.69(73.9, 126.01) ml/(min/1.73m^2), P=0.002] appeared in the non-(vision-)improved group compared with the vision-improved group. 2.

The occurrence of preoperation proteinuria history of nephropathy take a larger proportion in non-improved group. 3. Univariate regression analysis showed history of nephrology (OR=1.887, P=0.028), preoperative serum urea nitrogen (OR=0.939, P=0.043), cystatin C (Cys-C) concentration (OR=0.75, P=0.024), eGFR (OR=1.011, P=0.003) and proteinuria (OR=3.128, P<0.001) were influencing factors to postoperative visual acuity loss in young working age PDR patients. Excluding other confounding factors, preoperative proteinuria is an independent risk factor for postoperative vision improvement in working-age PDR populations (OR=2.722, P=0.009). 4. The accuracy of the prediction random forst model is 0.81. The model appears to be superior in terms of positive prediction.

Conclusion: In young work aged PDR patients undergoing vitrectomy, preoperative urine protein can be an independent indicator of postoperative visual loss. Aggressive correction of kidney injury before surgery may help improve postoperative vision in patients with PDR.

KEYWORDS

proliferative diabetic retinopathy, renal impairment, vitrectomy, low vision, cystatin C, estimate glomerular filtration rate, urine protein

1 Introduction

Diabetic patients have abnormal blood glucose elevation in the non-intervention state due to the impaired uptake and utilization of glucose, and the body cells are in a state of high glucose for a long time, which eventually leads to damage to multiple tissues and organs. It can manifest as increased permeability of small vessels, vascular occlusion leading to compensatory neovascularization, rupture and bleeding of fragile neovascularization, and exacerbation of the disease process. Diabetic nephropathy(DN) and diabetic retinopathy (DR) are common complications of diabetes. China has currently the largest number of diabetic patients in the world (1), with one DR for every there DM patients (2). DR is the first blinding eye disease in working-age people, which seriously affects the quality of work and life and has become a major public health problem. DR can be clinically divided into non-proliferative DR (NPDR) and proliferative DR (PDR), the latter requiring surgery in severe cases. Whether postoperative vision can be effectively improved is worthy of more attention. Studies have found that the progression of DR is associated with renal pathological changes and the degree of progression of end-stage renal disease (3). The sensitivity and specificity of DR predicting DN in patients with T2DM is 0.65 and 0.75, separately (4). In view of the link between DR and DN, is it possible to predict postoperative visual acuity changes in young patients from the preoperative assessment of renal function status? This article briefly showed the discussion.

2 Methods

2.1 Selection of research subjects

Inclusion criteria: (1) patients with diabetes (type 1, type 2); (2) worhing age people (aged 18-55 years); (3) The diagnosis and staging of PDR conform to the "Guidelines for Clinical Diagnosis and Treatment of Diabetic Retinopathy in China (2022)" (5), and the evidence of fundus imaging examination is clear.

Exclusion criteria: (1) Patients with active infection (bacterial or viral infections), autoimmune diseases (eg, lupus, multiple sclerosis, rheumatoid arthritis and psoriasis) and malignant tumors, pregnant and lactating women; (2) Patients with glaucoma, eye trauma, hypertensive retinopathy and other eye diseases; (3) Special types of diabetes caused by immune-mediated type 1 diabetes, pancreatic diabetes, infection, other endocrine diseases, glucocorticoids, anti-tumor drugs, etc;(4) Have received intraocular surgery (excluding photocoagulation therapy) before the visit;(5) Non-diabetic-related kidney disease, such as congenital renal absence or renal hypoplasia, acute/chronic glomerulonephritis, renal cysts, acute kidney injury, urinary tract infection; (6) High-protein, high-purine diet within half a month before the visit.

According to the above criteria, 306 young PDR patients (aged 20-55 years, 306 eyes) who were hospitalized in our hospital and treated with vitrectomy from January 2016 to June 2023 were continuously enrolled.

2.2 Research methods

Collected relevant baseline data of the patient's hospitalization, including age, gender, previous renal history, preoperative clinical serological tests (renal function) and so on. The visual acuity before and after treatment were recorded, and the difference between the two was made. Preoperative visual acuity examination: The best visual acuity that can be achieved in the affected eye after the patient has adequately corrected the patient's refractive errors (myopia, farsightedness, and astigmatism) before surgery. The International Standard Visual Acuity Chart was used to perform distance visual acuity examination, and the results were recorded using *the Miu method* (5-point expression) (5). Postoperative visual acuity examination: about 1 month after vitrectomy surgery, the gas or liquid to be filled is fully absorbed, and the patient's best corrected visual acuity is measured and recorded. Study postoperative visual acuity and preoperative visual acuity. Patients with the difference >0 were included in the study group, defined as "vision-improved group"; the difference ≤0 were included in the control group named "non-improved group". Statistical methods were used to compare whether there was any difference in the distribution of renal function evaluation indexes between the two groups.

2.3 Statistical analysis

Firstly, we used SPSS25.0 software for statistical analysis. After all continuous variables were tested for normality, data of normal distribution was described as mean ± standard deviation (X ± SD), and the mean difference between two groups was compared by the t-test of two independent samples. Data of nonnormal distributors was represented by *M (P25, P75)*, and the nonparametric test compared the difference between two groups. The chi-square test compared differences in discontinuous variables between groups. Binary Logistic Regression analyzed the influencing factors of postoperative visual acuity decline in young PDR patients. P<0.05 indicates that the difference is statistically significant. In this study, multiple variables such as age, medical history, and renal function tests were included, and the relationship between these variables was complex, and binary regression analysis alone could not meet the research needs. We could try to use machine learning approaches. Nowadays the machine learning and deep learning models have been used in many fields, including agriculture (6), environment (7–9) and medical field (10). We utilized Random Forest machine learning techniques for the multivariate classification analysis.

3 Results

3.1 Baseline data

Three hundred and six eyes from306 young PDR patients were included in the study. As shown in Table 1, there was no difference between the two groups on gender (p=0.779), history of hypertension (p = 0.288), surgical eyes (p=0.587), mean age (p=0.495), diabetes duration (p=0.649), serum glucose level (p=0.975) and Glycosylated hemoglobin (p=0.573). The two groups showed significant differences on history of hypertension (X^2 = 4.896, p = 0.027).

3.2 Renal function

3.2.1 Serology test

All 306 patients underwent vitrectomy and were tested to evaluate their renal function on the early morning fasting on second day in hospital. According to Table 2, the serum Cys-C and urea nitrogen level in non-improved group was separately significantly higher than that of the vision-improved group [1.02 (0.80, 1.48) mg/L vs 0.86 (0.67, 0.1.12) mg/L, P<0.001; 7.71(5.41, 9.69)mmol/L vs 6.08(4.52, 7.95)mmol/L, p=0.005]. The eGFR of the non-improved group [82.30(50.33, 115.11) ml/(min/1.73m^2)] was significantly lower than that of the vision-improved group [103.69 (67.67, 124.87) ml/(min/1.73m^2)], P=0.002. There was no significant difference in creatinine and uric acid levels between the two groups (P >0.05).

TABLE 1 Baseline characteristics according to vision difference (non-improved group ≤ 0, vision-improved group>0).

index	Total observed (n=306)	vision-improved group (n=245)	non-improved group (n=61)	Z value	P value
Gender〔male, n (%)〕	201 (65.7)	160 (65.3)	41 (67.2)	0.079*	0.779
history of nephrology, n (%)	137 (44.8)	102 (41.6)	35 (57.4)	4.896*	0.027
history of hypertension, n (%)	162 (52.9)	126 (51.4)	36 (59.0)	1.129*	0.288
Surgical eye [left, n (%)]	155 (50.7)	119 (48.6)	32 (52.5)	0.295*	0.587
age, years	38 (33, 46)	38 (34, 44)	40 (31,50)	-0.682	0.495
DM duration, year	6.5 (1.5, 12.0)	6.0 (2.0, 12.0)	8.0 (1.5, 13.0)	-0.456	0.649
Glu, mmol/L	6.69 (5.37, 8.62)	6.70 (5.38, 8.62)	6.60 (5.24, 8.65)	-0.031	0.975
HbAlc, %	7.5 (6.6, 8.9)	7.5 (6.6, 9.0)	7.5 (6.6, 8.5)	-0.564	0.573

*stands for X^2value, Glu, glucose; DM, diabetes mellitus.

10.3389/fendo.2023.1321226

TABLE 2 Serology test for renal function according to vision difference (non-improved group ≤ 0, vision-improved group>0).

index	Total observed (n=306)	vision-improved group (n=245)	non-improved group (n=61)	Z value	P value
urea nitrogen, mmol/L	6.30 (4.61, 8.61)	6.08 (4.52, 7.95)	7.71 (5.41, 9.69)	-2.838	0.005
creatinine, μmol/L	75 (59, 113)	74 (60, 105)	96 (57, 132)	-1.632	0.103
uric acid, μmol/L	357 (296, 412)	357 (295, 414)	362 (309, 401)	-0.182	0.856
Cys-C, mg/L	0.88 (0.68, 1.22)	0.86 (0.67, 1.12)	1.02 (0.80, 1.48)	-3.672	<0.001
eGFR, ml/(min/1.73m^2)	103.69 (67.67, 124.87)	107.69 (73.89, 126.01)	82.30 (50.33, 115.11)	-3.031	0.002

3.2.2 Urine test

According to Table 3, in young PDR patients undergoing vitrectomy, the rate of preoperative proteinuria in vision-improved group was significantly lower compared to the non-improved group (47.3% vs 73.8%, P<0.001). There was no significant difference in preoperative haematuria, glycosuria and pyuria between the two groups (P >0.05).

3.3 Logistic regression analysis

As shown in Table 4, univariate regression analysis was performed for all variables, and We selected variables with P<0.1 for inclusion in the next round of multivariate regression analysi, including history of nephrology (OR=1.887, P=0.028), preoperative serum urea nitrogen (OR=0.939, P=0.043), cystatin C concentration (OR=0.75, P=0.024), eGFR (OR=1.011, P=0.003) and proteinuria (OR=3.128, P<0.001). The results showed that only one variable was left for last. Excluding other confounding factors, preoperative proteinuria is an independent risk factor for postoperative vision improvement in working-age PDR populations (OR=2.722, P=0.009).

3.4 Random forest model

All variables were included in the random forest model, and the parameters were adjusted. The importance of each feature is ranked to obtain Figure 1. The constructed random forest model showed that the top five influencing factors for postoperative visual acuity improvement in working-age PDR patients undergoing vitrectomy were age, serum urea nitrogen, serum creatinine, eGFR and serum glucose. The accuracy of the prediction model is 0.81. The model appears to be superior in terms of positive prediction (Figure 2).

4 Discussion

DR is a common fundus lesion of DM which can reduce eye vision and even worsely blind. There is a certain commonality between diabetic retinopathy and many pathological processes of the microvascular system of diabetic nephropathy. Diabetic nephropathy (DN) is the main cause of chronic kidney disease and is significantly associated with the development of diabetic retinopathy. With the improvement of modern living standards and the transformation of working mode, the number of young PDR patients has increased, PDR greatly affects the vision health of the working population, there are currently few studies on young PDR patients, and there is still a great clinical appeal for evaluating the influencing factors of postoperative vision recovery, and clinical treatment measures and effect monitoring need to attract sufficient attention. This study included 306 young PDR patients treated with vitrectomy to explore the effect of baseline renal function on postoperative visual acuity in young PDR patients.

The SN-DREAMS (11) study suggested that DN is associated with visual impairment in DM patients. Patients with chronic kidney injury were more likely to develop visual impairment than those without kidney disease (nonproliferative diabetic retinopathy OR=5.01, proliferative diabetic retinopathy OR=9.7). William S

TABLE 3 Urine test for renal function according to vision difference (non-improved group ≤ 0, vision-improved group>0).

index	Total observed (n=306)	vision-improved group (n=245)	non-improved group (n=61)	x^2value	P value
Urine glucose [positive, n (%)]	72 (23.5)	56 (22.9)	16 (26.2)	0.309	0.578
Urine protein [positive, n (%)]	161 (52.6)	116 (47.3)	45 (73.8)	13.677	<0.001
Urine RBC [positive, n (%)]	91 (29.7)	69 (28.2)	22 (36.1)	1.46	0.227
Urine WBC [positive, n (%)]	25 (8.2)	18 (7.3)	7 (11.5)	0.628	0.428

RBC, red blood cells; WBC, white blood cells.

10.3389/fendo.2023.1321226

TABLE 4 Logistic regression analysis for factors influencing postoperative vision decrease.

Index	Univariate analysis		Multivariate analysis	
	P value	OR (95%CI)	P value	OR (95%CI)
Gender〔male, n (%)〕	0.779	1.089 (0.6, 1.976)		
history of nephrology, n (%)	0.028	1.887 (1.07, 3.329)	0.752	0.881 (0.4, 1.939)
history of hypertension, n (%)	0.289	1.36 (0.77, 2.401)		
Surgical eye [left, n (%)]	0.587	0.856 (0.488, 1.501)		
age, years	0.546	0.99 (0.957, 1.023)		
DM duration, year	0.585	0.988 (0.945, 1.033)		
Glu, mmol/L	0.95	0.997 (0.913, 1.089)		
HbAlc, %	0.514	1.058 (0.893, 1.254)		
Serum urea nitrogen (mmol/L)	0.043	0.939 (0.884, 0.998)	0.567	1.030 (0.93, 1.142)
Serum creatinine (μmol/L)	0.206	0.999 (0.996, 1.001)		
Serum uric acid (μmol/L)	0.984	0.999 (0.997,1.003)		
Serum Cys-C (mg/L)	0.024	0.75 (0.584,0.962)	0.379	0.855 (0.603, 1.212)
eGFR [ml/ (min/1.73m2)]	0.003	1.011 (1.004, 1.019)	0.514	1.005 (0.989, 1.021)
Urine glucose, positive	0.579	1.2 (0.63, 2.284)		
Urine protein, positive	<0.001	3.128 (1.677,5.833)	0.009	2.722 (1.289,5.746)
Urine RBC, positive	0.228	1.439 (0.796,2.601)		
Urine WBC, positive	0.296	1.635 (0.65, 4.111)		

Gange (12) analyzed data from 71817 newly diagnosed T2DM patients aged ≥ 18 years and showed that the incidence of PDR was higher after 5 years in patients with renal disease [OR (95% CI) = 2.68 (2.09~3.42)]. PDR progression in patients with type 2 diabetes is associated with baseline renal dysfunction, including elevated serum creatinine, decreased eGFR, and high urine albumin/creatinine ratio (13). The risk of DR was positively correlated with serum creatinine concentration, [OR (95% CI) = 1.01 (1.002~1.022)] (14). Higher serum UA levels were significantly associated with adverse outcomes in DM (15). In this study,

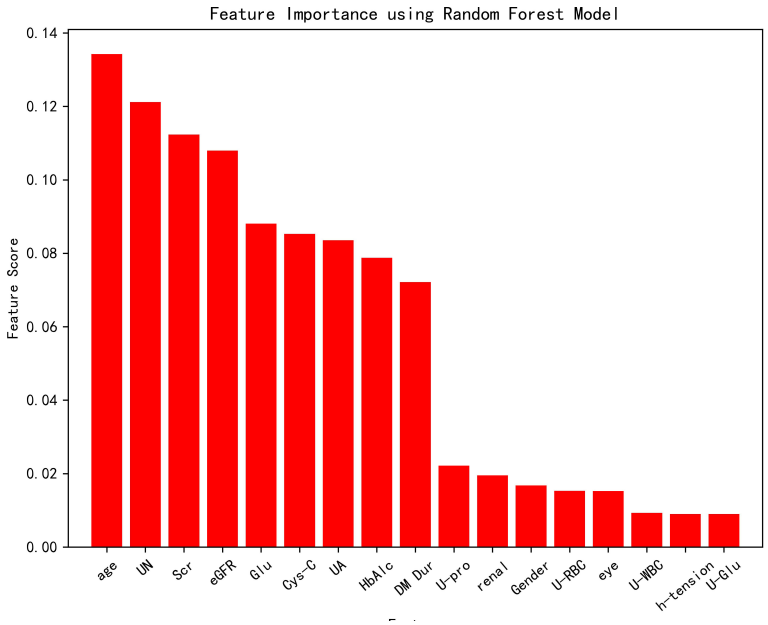

FIGURE 1
Random forest model Feature importance diagram.

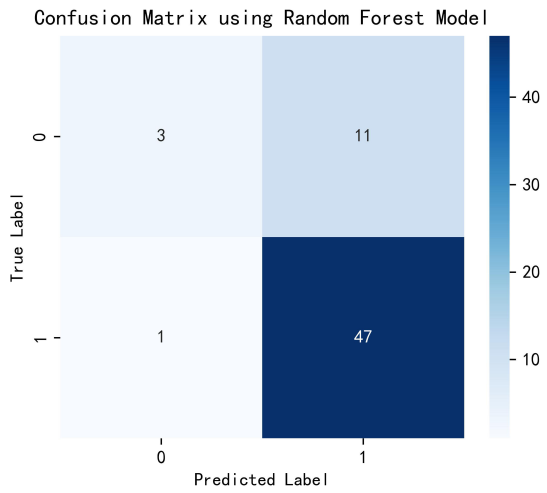

FIGURE 2
Random forest model confusion matrix heat map.

young PDR patients with reduced renal function were more likely to have visual acuity loss after vitrectomy, including high serum Cys-c levels [0.85 (0.68, 1.37) mg/L vs 0.72 (0.58, 0.88) mg/L, P=0.049], and eGFR reduction [105.70(60.67, 122.17)ml/(min/1.73m2) vs 118.99(101.97, 126.67)ml/(min/1.73m2), P=0.04]. In univariate regression analysis, the decrease in baseline eGFR and the increase in serum urea nitrogen, creatinine, and cystatin c before surgery were the contributing factors to the decline of visual acuity after vitrectomy in young PDR patients.

Saini DC (16) noted that DR may be independently associated with the occurrence of microalbuminuria and microalbuminuria is a strong predictor of kidney injury progression in DM patients. Hsieh YT's (17) another study of 576 patients with type 2 diabetes mellitus with microalbuminuria followed for 8 years showed that remission of microalbuminuria (urine albumin/creatinine ratios < 30 mg/g at least two times in there for 6 months) was an independent protective factor for the development of PDR and DME. In this study, individuals with baseline proteinuria and hematuria had a higher rate of visual loss in young PDR patients (25.0% vs 12.9%, P=0.04; 27.1% vs 13.6%, P=0.033). Excluding other confounding factors, the risk of postoperative visual acuity loss in patients with preoperative proteinuria was higher [OR (95% CI) = 5.886 (1.101, 31.474)].

In addition, there is currently no consensus on the impact of renal impairment on the prognosis of surgical vision in PDR patients. Studies have shown that PDR patients with renal impairment are more likely to have complications and a worse prognosis after vitrectomy (18, 19). It has also been suggested that decreased renal function is not significantly associated with worsening PDR and postoperative visual impairment (20, 21). In this study, more attention was paid to young PDR patients, and 180 cases were enrolled, and the relationship between renal function and postoperative vision of PDR patients was innovatively examined from multiple dimensions such as renal history, baseline renal function serological indicators, cystatin C, eGFR and urine protein. At the same time, some limitations of the study were exposed, and follow-up studies of patients will be presented in a subsequent article.

In conclusion, understanding the factors of vision after vitrectomy in young working age PDR patients will help to the clinical therapy choice, preoperative preparation, and postoperative care of patients. Preoperative renal function and urine protein monitoring for PDR patients with risk factors, and active targeted interventions, can improve the visual acuity and quality of life of patients after vitrectomy. It is helpful to find out whether it is possible to better predict the improvement of visual acuity after vitrectomy in working-age people without adding additional preoperative testing. While saving talent and financial resources, it also ensures patient efficacy evaluation and clinical intervention.

Data availability statement

The original contributions presented in the study are included in the article/Supplementary Material. Further inquiries can be directed to the corresponding author.

Ethics statement

The studies involving humans were approved by the Ethic Committee of Hebei Eye Hospital (NO.2022KY29). The studies were conducted in accordance with the local legislation and institutional requirements. The human samples used in this study were acquired from primarily isolated as part of our previous study for which ethical approval was obtained. Written informed consent for participation was not required from the participants or the participants' legal guardians/next of kin in accordance with the national legislation and institutional requirements.

Author contributions

XZ: Conceptualization, Formal analysis, Investigation, Methodology, Project administration, Visualization, Writing – original draft. LF: Conceptualization, Formal analysis, Investigation, Methodology, Project administration, Visualization, Writing – original draft. CX: Data curation, Formal analysis, Software, Writing – original draft. JW: Data curation, Formal analysis, Software, Writing – original draft. WZ: Formal analysis, Supervision, Validation, Writing – original draft. FZ: Funding acquisition, Project administration, Resources, Supervision, Writing – review & editing.

Funding

The author(s) declare financial support was received for the research, authorship, and/or publication of this article. This study

was supported by Medical Science Research Project Plan of Hebei Province (No. 20231996).

Acknowledgments

We thank all the patients who participated in our investigation and those who have helped us in the research but not mentioned as co-authors.

Conflict of interest

The authors declare that the research was conducted in the absence of any commercial or financial relationships that could be construed as a potential conflict of interest.

Publisher's note

Supplementary material

The Supplementary Material for this article can be found online at: https://www.frontiersin.org/articles/10.3389/fendo.2023.1321226/full#supplementary-material

References

1. Sun H, Saeedi P, Karuranga S, Pinkepank M, Ogurtsova K, Duncan BB, et al. IDF Diabetes Atlas: Global, regional and country-level diabetes prevalence estimates for 2021 and projections for 2045. *Diabetes Res Clin Pract* (2022) 183:109–19. doi: 10.1016/j.diabres.2021.109119

2. Tan GS, Cheung N, Simó R, Cheung GC, Wong TY. Diabetic macular oedema. *Lancet Diabetes Endocrinol* (2017) 5(2):143–55. doi: 10.1016/S2213-8587(16)30052-3

3. Yamanouchi M, Mori M, Hoshino J, Kinowaki K, Fujii T, Ohashi K, et al. Retinopathy progression and the risk of end-stage kidney disease: results from a longitudinal Japanese Cohort of 232 patients with type 2 diabetes and biopsy-proven diabetic kidney disease. *BMJ Open Diabetes Res Care* (2019) 7(l):e000726. doi: 10.1136/bmjdrc-2019-000726

4. He F, Xia X, Wu XF, Yu XQ, Huang FX. Diabetic retinopathy in predicting diabetic nephropathy in patients with type 2 diabetes and renal disease: a meta-analysis. *Diabetologia* (2013) 56(3):457–66. doi: 10.1007/s00125-012-2796-6

5. GB/T 11533-2011. *Standard for logarithmic visual acuity charts*. Beijing: Standards Press of China (2011).

6. Haq MA. Planetscope nanosatellites image classification using machine learning. *Comput Syst Sci Eng* (2022) 42(3):1031–46. doi: 10.32604/csse.2022.023221

7. Haq MA, Baral P, Yaragal S, Pradhan B. Bulk processing of multi-temporal modis data, statistical analyses and machine learning algorithms to understand climate variables in the Indian himalayan region. *Sensors* (2021) 21(21):7416. doi: 10.3390/s21217416

8. Haq MA, Baral P. Study of permafrost distribution in Sikkim Himalayas using Sentinel-2 satellite images and logistic regression modelling. *Geomorphology* (2019) 333:123–36. doi: 10.1016/j.geomorph.2019.02.024

9. Baral P, Haq MA. Spatial prediction of permafrost occurrence in Sikkim Himalayas using logistic regression, random forests, support vector machines and neural networks. *Geomorphology* (2020) 371:107331. doi: 10.1016/j.geomorph.2020.107331

10. Lu M, Liao X. Telehealth utilization in U.S. medicare beneficiaries aged 65 years and older during the COVID-19 pandemic. *BMC Public Health* (2023) 23(1):368. doi: 10.1186/s12889-023-15263-0

11. Rani PK, Raman R, Gella L, Kulothungan V, Sharma T. Prevalence of visual impairment and associated risk factors in subjects with type II diabetes mellitus: Sankara Nethralaya diabetic retinopathy epidemiology and molecular genetics study (SN-DREAMS, report 16). *Middle East Afr J Ophthalmol* (2012) 19(1):129–34. doi: 10.4103/0974-9233.92129

12. Gange WS, Lopez J, Xu BY, Lung K, Seabury SA, Toy BC. Incidence of proliferative diabetic retinopathy and other neovascular sequelae at 5 years following diagnosis of type 2 diabetes. *Diabetes Care* (2021) 44(11):2518–26. doi: 10.2337/dc21-0228

13. Hsieh YT, Tsai MJ, Tu ST, Hsieh MC. Association of abnormal renal profiles and proliferative diabetic retinopathy and diabetic macular edema in an Asian population with type 2 diabetes. *JAMA Ophthalmol* (2018) 136(1):68–74. doi: 10.1001/jamaophthalmol.2017.5202

14. Xu J, Xu L, Wang YX, You QS, Jonas JB, Wei WB. Ten-year cumulative incidence of diabetic retinopathy. The Beijing Eye Study 2001/2011. *PLoS One* (2014) 9(10):e111320. doi: 10.1371/journal.pone.0111320

15. Li B, Chen L, Hu X, Tan T, Yang J, Bao W, et al. Association of serum uric acid with all-cause and cardiovascular mortality in diabetes. *Diabetes Care* (2023) 46 (2):425–33. doi: 10.2337/dc22-1339

16. Saini DC, Kochar A, Poonia R. Clinical correlation of diabetic retinopathy with nephropathy and neuropathy. *Indian J Ophthalmol* (2021) 69:3364–8. doi: 10.4103/ijo.IJO_1237_21

17. Hsieh YT, Hsieh MC. Time-sequential correlations between diabetic kidney disease and diabetic retinopathy in type 2 diabetes - an 8-year prospective cohort study. *Acta Ophthalmol* (2021) 99(1):e1–6. doi: 10.1111/aos.14487

18. Kameda Y, Saeki T, Hanai K, Suzuki Y, Uchigata Y, Babazono T, et al. Is chronic kidney disease affecting the postoperative complications of vitrectomy for proliferative diabetic retinopathy? *J Clin Med* (2021) 10:5309. doi: 10.3390/jcm10225309

19. Song YS, Nagaoka T, Omae T, Yokota H, Takahashi A, Yoshida A. SYSTEMIC RISK FACTORS IN BILATERAL PROLIFERATIVE DIABETIC RETINOPATHY REQUIRING VITRECTOMY. *Retina* (2016) 36(7):1309–13. doi: 10.1097/IAE.0000000000000886

20. Larrañaga-Fragoso P, Laviers H, McKechnie C, Zambarakji H. Surgical outcomes of vitrectomy surgery for proliferative diabetic retinopathy in patients with abnormal renal function. *Graefes Arch Clin Exp Ophthalmol* (2020) 258(1):63–70. doi: 10.1007/s00417-019-04532-7

21. Liu J, Zhang W, Xie P, Yuan S, Jiang L, Liu Q, et al. The relationship between renal function and surgical outcomes of patients with proliferative diabetic retinopathy. *Front Endocrinol (Lausanne)* (2022) 13:984561. doi: 10.3389/fendo.2022.984561

frontiers | Frontiers in Endocrinology

TYPE Original Research
PUBLISHED 11 January 2024
DOI 10.3389/fendo.2023.1339374

OPEN ACCESS

EDITED BY
Kai Jin,
Zhejiang University, China

REVIEWED BY
Lin Chen,
Independent Researcher, Fuzhou, China
Dimitrios Ntentakis,
Massachusetts Eye &Ear Infirmary and Harvard Medical School,
United States

*CORRESPONDENCE
Yao Tan
tanyao2000@qq.com

†These authors have contributed equally to this work and share first authorship

RECEIVED 16 November 2023
ACCEPTED 13 December 2023
PUBLISHED 11 January 2024

CITATION
Zou X, Ye S and Tan Y (2024) Potential disease biomarkers for diabetic retinopathy identified through Mendelian randomization analysis. *Front. Endocrinol.* 14:1339374. doi: 10.3389/fendo.2023.1339374

Potential disease biomarkers for diabetic retinopathy identified through Mendelian randomization analysis

Xuyan Zou[1†], Suna Ye[2†] and Yao Tan[3,4*]

[1]Changsha Aier Eye Hospital, Aier Eye Hospital Group, Changsha, China, [2]Senzhen Aier Eye Hospital, Jinan University, Shenzhen, China, [3]Department of Ophthalmology, The Third Xiangya Hospital, Central South University, Changsha, China, [4]Postdoctoral Station of Clinical Medicine, The Third Xiangya Hospital, Central South University, Changsha, China

Background: Diabetic retinopathy (DR), a leading cause of vision loss, has limited options for effective prevention and treatment. This study aims to utilize genomics and proteomics data to identify potential drug targets for DR.

Methods: We utilized plasma protein quantitative trait loci data from the Atherosclerosis Risk in Communities Study and the Icelandic Decoding Genetics Study for discovery and replication, respectively. Genetic associations with DR, including its subtypes, were derived from the FinnGen study. Mendelian Randomization (MR) analysis estimated associations between protein levels and DR risk, complemented by colocalization analysis to examine shared causal variants.

Results: Our MR analysis identified significant associations of specific plasma proteins with DR and proliferative DR (PDR). Elevated genetically predicted levels of WARS (OR = 1.16; 95% CI = 0.095-0.208, FDR = 1.31×10^{-4}) and SIRPG (OR = 1.15; 95% CI = 0.071-0.201, FDR = 1.46×10^{-2}) were associated with higher DR risk, while increased levels of ALDOC (OR = 1.56; 95% CI = 0.246-0.637, FDR = 5.48×10^{-3}) and SIRPG (OR = 1.15; 95% CI = 0.068-0.208, FDR = 4.73×10^{-2}) were associated with higher PDR risk. These findings were corroborated by strong colocalization evidence.

Conclusions: Our study highlights WARS, SIRPG, and ALDOC as significant proteins associated with DR and PDR, providing a basis for further exploration in drug development. Additional studies are needed to validate these proteins as disease biomarkers across diverse populations.

KEYWORDS

diabetic retinopathy, Mendelian randomization, genomics, proteomics, disease biomarkers

1 Introduction

Diabetic retinopathy (DR) is a leading cause of vision loss worldwide, significantly impacting both individual health and public healthcare systems (1). Approximately one-third of people with diabetes develop severe visual impairments due to DR, leading to a substantial proportion suffering from irreversible blindness (2). The progression of DR is primarily driven by prolonged hyperglycemia, oxidative stress, and inflammation, resulting in microvascular damage in the retina (3). Current treatments, particularly anti-vascular endothelial growth factor (anti-VEGF) therapies, have marked a significant advancement in managing DR, effectively slowing its progression in many patients. However, about 40% of patients either resist or respond inadequately to these treatments, underscoring the need for more diverse and effective therapeutic strategies (4). Alongside anti-VEGF, other treatments, including steroid therapies and combination protocols, have been explored (5, 6). While these have shown limited efficacy, they represent important attempts in the ongoing effort to combat DR.

Circulatory proteins have become key targets for therapeutic research in DR, playing critical roles in various molecular processes (7). Previous studies have highlighted several proteins associated with the development of DR, including C-C motif chemokine 5 (CCL5), α-2-antiplasmin (SERPINF2), various adhesion molecules, and C-reactive protein (CRP) (8–10). These findings are significant in understanding the pathogenesis of DR and offer potential avenues for treatment. Advancements in high-throughput proteomics have further enriched our understanding of DR at the molecular level. For example, research by Lu et al. compared plasma proteomes of DR patients and identified key biomarkers like afamin and protein arginine N-methyltransferase 5, which are linked to the progression and development of diabetes (11). Similarly, Gopalakrishnan et al. discovered distinct protein expression profiles between DR and proliferative DR (PDR), with neuroglobin (NGB) standing out as a notable marker for DR development (12). However, these associations, primarily derived from observational studies, necessitate rigorous validation. This is crucial to ensure that the identified protein associations with DR are not confounded by external variables or biased by reverse causality. The pursuit of this validation represents a critical step in translating these proteomic discoveries into practical therapeutic interventions for DR.

Mendelian randomization (MR) utilizes single nucleotide polymorphisms (SNPs) from genome-wide association studies (GWAS) to uncover causal links between genetic factors and health outcomes (13). This method capitalizes on the random distribution of genes at birth, which helps overcome biases and confounding factors often encountered in observational studies (13). MR's integration of advanced genomic and proteomic data has been instrumental in identifying potential disease biomarkers for various diseases (14, 15). Despite its proven utility, the application of MR in DR research remains limited. There is a significant opportunity to expand this approach in DR, particularly by combining insights from GWAS and protein quantitative trait loci (pQTL) datasets. This integration could offer new perspectives and solutions in understanding and treating DR, an area where there is still much to explore and discover.

Our study embarks on a comprehensive proteome-wide MR analysis, augmented by colocalization analysis, to explore potential disease biomarkers for DR and PDR. By integrating genomic and proteomic data, we aim to uncover new pathways and targets, potentially paving the way for innovative treatments for these visually debilitating conditions.

2 Materials and methods

2.1 Study design and ethics

Our research methodology is outlined in Figure 1. We utilized data from three key sources: the large-scale genome-wide blood proteome study (available at https://www.decode.com/summarydata/) (16), the Atherosclerosis Risk in Communities (ARIC) study (http://nilanjanchatterjeelab.org/pwas/) (17), and the FinnGen study (https://www.finngen.fi/en) (18). All the data were sourced from established studies that had already obtained ethical clearance from their respective institutions, eliminating the need for a separate ethical review for our research.

2.2 Data sources

In the discovery stage, plasma protein pQTL data were obtained from the ARIC study, which included a total of 4657 plasma proteins collected from 7213 European Americans (EA) (17). For the replication stage, plasma protein pQTL data were obtained from the Icelandic deCODE genetics study by Ferkingstad et al, which analyzed 4907 plasma proteins from 35,559 Icelanders and reported more than 272 million genetic variants (16). The use of both datasets allowed us to balance the discovery and validation phases of our study effectively. The ARIC dataset provided a detailed platform for initial protein association findings, while the Icelandic dataset enabled us to replicate and validate these findings across a different population, thereby enhancing the generalizability of our study. Proteomics analyses for both studies were performed using the advanced SomaScan technology on the v.4.1 platform, ensuring consistent and high-quality data for our analyses.

We obtained DR and PDR data from the FinnGen study (18). This included 10,413 DR cases and 308,633 controls, and 9,511 PDR cases and 362,581 controls. The participants were all of European descent. We adjusted genetic associations for factors like age, sex, and genetic correlation, along with genotyping batch and the top 10 principal components. We identified cases of DR and PDR using International Classification of Diseases codes, specifically ICD-9

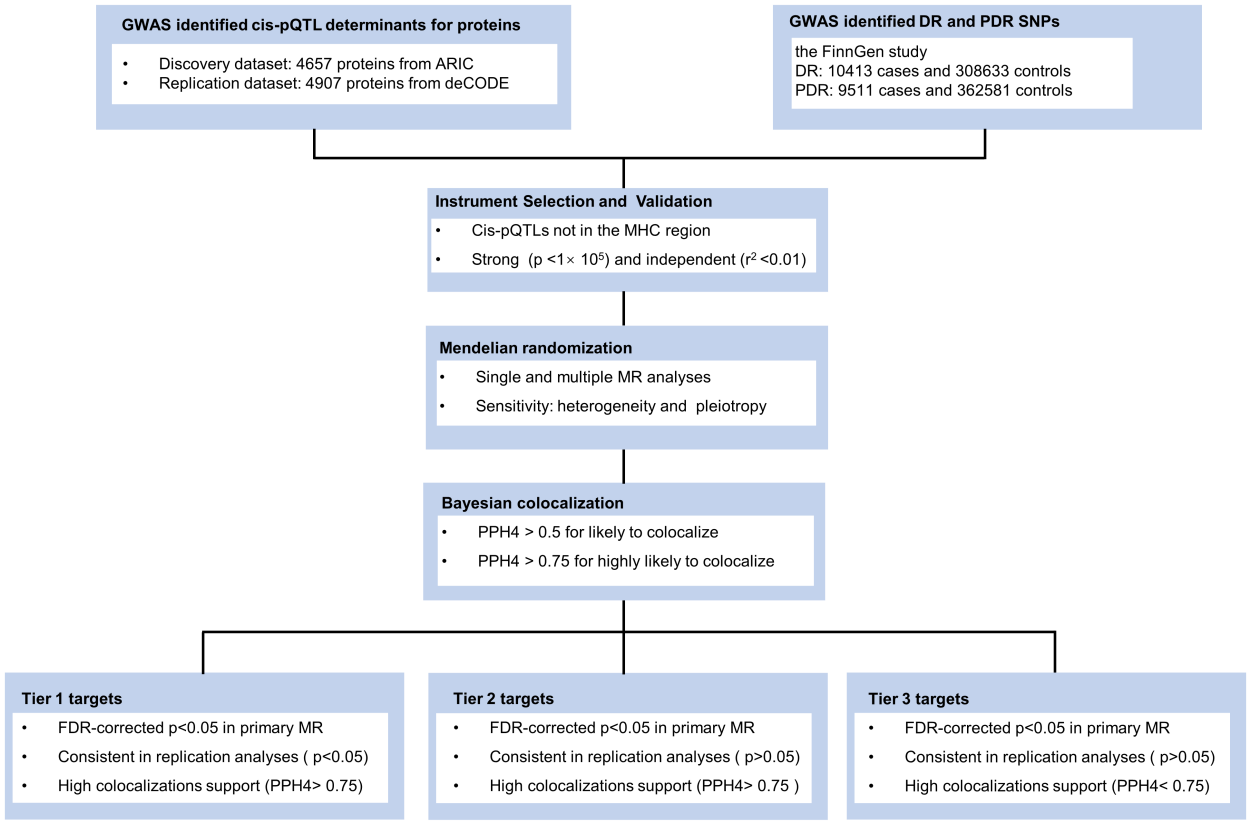

FIGURE 1
Study design. ARIC, the Atherosclerosis Risk in Communities study; deCODE, the Icelandic Decoding Genetics Study; DR, diabetic retinopathy; PDR, proliferative diabetic retinopathy; FDR, false discovery rate; MR, Mendelian Randomization.

(3620) and ICD-10 (H360) for DR, and ICD-10 (H3603) for PDR (18).

2.3 Instrument selection and validation

In conducting our MR analysis, we rigorously derived genetic instrumental variables (IVs) from plasma protein pQTL data, as referenced in our prior research (16, 17). To ensure a substantial association between these IVs and the exposure variable, which in our study is protein abundance, we meticulously selected cis-SNPs positioned within 1 megabase (Mb) of the gene encoding the relevant protein. This selection was based on a stringent p-value threshold of less than 1×10^{-5}, a criterion chosen to balance statistical significance with the likelihood of a genuine biological impact on protein levels. To secure the independence of these SNPs and preclude confounding due to linkage disequilibrium, we employed linkage disequilibrium (LD) clumping using PLINK software. This process involved evaluating SNPs within a 10 Mb window, considering them as independent if their LD values (r^2) was less than 0.01. Our choice of reference panel for this analysis was the genotype data of Europeans from the 1000 Genomes Project, which aligns with the ancestry of the study's participant population. This methodological approach was adopted to ensure the reliability and relevance of the instrumental variables used in our MR analysis.

2.4 Mendelian randomization

All MR analyses were undertaken with the TwoSampleMR package in R. The primary MR analysis was conducted using the inverse-variance weighted (IVW) method to determine the causal effects of plasma proteins on DR. FDR correction was performed using the BH method, and FDR < 0.05 was considered for statistical significance. The MR results were presented as odds ratio (OR) and 95% confidence interval (95% CI) for risk of DR per genetically predicted 1-standard deviation (SD) increase in plasma protein level.

To further identify the associations identified by the primary analyses, we performed multiple MR analyses of the preliminarily identified proteins as replications using an independent blood pQTL database (The Icelandic deCODE genetics study). Multiple MR analytical approaches, including IVW, Egger, weighted median, and weighted mode, were applied for validation, of which IVW was chosen as the primary approach according to the recommendation (19).

To further assess the robustness of the causal relationships identified by the multiple MR analyses, we also conducted

sensitivity analyses, including heterogeneity and horizontal pleiotropy tests. Heterogeneity was assessed using Cochran's Q statistic (20). The Cochran's Q test followed a chi-square distribution with IV number minus one degree of freedom. MR-Egger regression intercept was employed as a measure of directional pleiotropy (20). Proteins with only one IV are not suitable for the above sensitivity analyses. Heterogeneity tests require at least two IVs to be analyzed and MR-Egger regression requires at least three IVs to be analyzed. For the multiple MR and sensitivity analyses, p-value < 0.05 was considered significant.

2.5 Bayesian colocalization

Colocalization analysis serves as an indispensable complement to cis-MR, crucial for assessing the validity of IV assumptions (21). This analysis is pivotal in differentiating whether the same genetic variants are influencing both the exposure (plasma protein levels) and the outcome (DR risk). By conducting colocalization analysis using the coloc.abf function in the R package coloc, we aimed to determine if the identified proteins and DR share causal genetic variants within the same genomic regions. This step is crucial for eliminating potential interference due to LD. We tested the posterior probability of hypothesis 4 (PPH4), which examines the likelihood of both the protein and DR sharing variants in the same region. Interpretation of PPH4 values is critical; a PPH4 greater than 0.5 suggests a likely colocalization, while a value exceeding 0.75 indicates a high probability of sharing causal variants.

The results of the colocalization analysis were instrumental in categorizing the identified proteins into tiers based on the strength of their causal evidence with DR. Proteins that showed consistent results in replication analyses and had strong supporting evidence of colocalization (PPH4 greater than 0.75) were classified as Tier 1 targets. This classification underscores a robust association with DR, suggesting a higher likelihood of being genuine disease biomarkers. Proteins with only high support evidence of colocalization (PPH4 greater than 0.75) were categorized as Tier 2 targets. These proteins, while showing potential association with DR, may require further validation. The remaining proteins, which did not meet these stringent criteria, were classified as Tier 3 targets. This tier-based system allows for a nuanced interpretation of the data, guiding future research and development efforts towards the most promising disease biomarkers for DR.

3 Results

3.1 MR analysis

In our MR analysis, we assessed 4657 plasma proteins to explore their potential link with DR, employing a methodology previously explicated. After applying an adjustment for the FDR, we identified five proteins with significant associations with DR (Figure 2A). Specifically, we found that higher genetically predicted levels of the proteins WARS (OR = 1.16; 95% CI = 0.095-0.208, FDR = 1.31×10^{-4}), KLK8 (OR = 1.22; 95% CI = 0.105-0.288, FDR = 1.10×10^{-2}), SIRPG (OR = 1.15; 95% CI = 0.071-0.201, FDR = 1.46×10^{-2}), and KLK11 (OR = 1.58; 95% CI = 0.222-0.696, FDR = 4.35×10^{-2}) were associated with an increased risk of DR. In contrast, an increase in HSPA1A levels (OR = 0.466; 95% CI = -1.067 to -0.46, FDR = 4.96×10^{-4}) was linked to a decreased risk of DR (Supplementary Table 1).

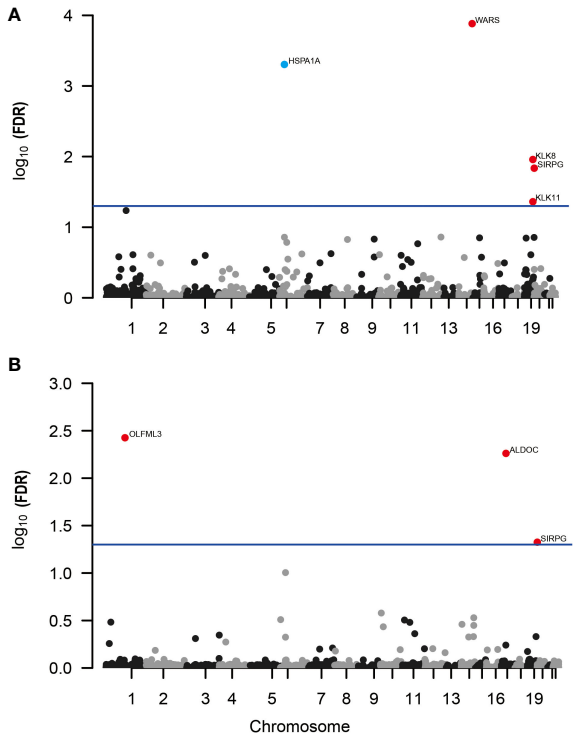

FIGURE 2
Manhattan plots for associations of genetically predicted 4657 plasma proteins levels with DR and PDR in MR analysis. **(A)** Associations of genetically predicted plasma protein levels with DR; **(B)** associations of genetically predicted plasma protein levels with PDR. Labelled and color genes refer to MR findings with FDR-corrected p < 0.05. Red genes indicate the positive effect of the plasma proteins on outcomes; blue genes indicate the negative effect of the plasma proteins on outcomes.

Further, when investigating PDR, our analysis revealed three proteins associated with a higher risk of developing PDR (Figure 2B; Supplementary Table 2). These include OLFML3 (OR = 1.51; 95% CI = 0.238-0.591, FDR = 3.75×10^{-3}), ALDOC (OR = 1.56; 95% CI = 0.246-0.637, FDR = 5.48×10^{-3}), and SIRPG (OR = 1.15; 95% CI = 0.068-0.208, FDR = 4.73×10^{-2}). Notably, SIRPG showed a consistent association with both DR and PDR.

3.2 Replication analyses

In the replication phase of our study, we re-examined five proteins initially identified as associated with DR. Out of these, two proteins, WARS and SIRPG, showed consistent results in the Icelandic deCODE genetics study. The analysis indicated an increased risk of DR with higher levels of WARS (OR = 1.39; 95% CI = 0.21-0.45; p-value = 5.50×10^{-8}) and SIRPG (OR = 1.39; 95% CI = 0.18-0.62; p-value = 3.32×10^{-4}), as shown in

Supplementary Table 3. Our sensitivity analysis, which included tests for heterogeneity (p-value for Cochran's Q = 0.442) and pleiotropy (p-value for MR-Egger intercept = 0.479), found no significant discrepancies in the association between WARS and DR. It's important to note that for SIRPG, due to the availability of only one IV (rs6043409), we couldn't perform heterogeneity and pleiotropy tests (Supplementary Table 4).

For PDR, our analysis replicated the associations for all three identified proteins: OLFML3, ALDOC, and SIRPG. Specifically, increased levels of OLFML3 (OR = 1.82; 95% CI = 0.09-1.12; p-value = 2.19×10^{-2}), ALDOC (OR = 1.83; 95% CI = 0.34-0.87; p-value = 9.28×10^{-6}), and SIRPG (OR = 1.58; 95% CI = 0.23-0.68; p-value = 6.65×10^{-5}) were associated with a higher risk of developing PDR. These results are detailed in Supplementary Table 5. Based on Cochran's Q statistics, there was little evidence of heterogeneity between OLFML3 and PDR (p-value for Cochran's Q = 0.108). Similar to SIRPG in DR analysis, due to the presence of only one IV for both SIRPG (rs6043409) and ALDOC (rs141921160), heterogeneity and pleiotropy analyses were not conducted.

3.3 Colocalization analyses

In our study, we conducted detailed colocalization analyses to further understand the relationship between certain plasma proteins and both DR and PDR. Our findings showed significant colocalization for three of the five analyzed proteins (KLK8, SIRPG, and WARS) with DR. The evidence for colocalization was strong, as indicated by the PPH4, which were 78.3%, 80.7%, 94.3%, and 87.6% respectively for these proteins (Supplementary Table 6). Similarly, for PDR, two proteins, ALDOC and SIRPG, also showed high evidence of colocalization with PPH4 values of 99.1% and 93.4%, respectively.

To classify the identified proteins based on the strength of evidence supporting their role in DR and PDR, we organized them into tiers. We considered several factors for this classification, including the consistency of results in replication analyses, the presence of heterogeneity or horizontal pleiotropy, and the strength of colocalization evidence. Based on this approach, WARS and SIRPG were categorized as Tier 1 evidence proteins for DR, indicating a strong link. For PDR, ALDOC and SIRPG were also classified as Tier 1 evidence proteins, underscoring their potential significance in the disease's development. These categorizations and the detailed evidence supporting them are presented in Table 1.

4 Discussion

In human genetics research, the focus on identifying disease biomarkers, especially for conditions like DR, is crucial. A large portion of FDA-approved drugs in recent years are supported by genetic research, highlighting the role of genetics in medical advancements (22). Our study, employing MR and colocalization analysis, identified four plasma proteins (WARS, KLK8, SIRPG, ALDOC) as potential markers for DR and PDR. Three of these proteins, WARS, SIRPG, and ALDOC, were validated in multiple MR analyses against an independent pQTL database. This validation strengthens our findings. Our study paves the way for further research to explore the direct histological links of these proteins to DR. It highlights the potential of these proteins as targets for future therapeutic interventions, given their relative ease of detection.

Our study highlights SIRPG as a significant marker for DR and its advanced form, PDR, supported by strong evidence. SIRPG, a member of the SIRP protein family, is primarily found on T cells and a subset of B cells (23). Genomic studies have linked two specific genetic variations of SIRPG, rs2281808 (C > T; intronic) and rs6043409 (G > A; A263 V), to type 1 diabetes (24, 25). The association of the T allele of rs2281808 with an increased risk of type 1 diabetes suggests a genetic predisposition (26). Further analysis using two-sample MR indicates a correlation between higher levels of SIRPG and an increased risk of type 1 diabetes (27). These findings suggest a potential link between elevated SIRPG levels and diabetes susceptibility. However, the direct role of SIRPG in the development and progression of DR and PDR needs further investigation. This research opens avenues for exploring SIRPG as a biomarker in diabetic eye diseases and understanding its underlying mechanisms in DR pathogenesis.

In our research, we identified WARS as another potential risk factor for DR. WARS, a fundamental enzyme in protein synthesis, links tryptophan to its corresponding transfer RNA (28). Previous studies have shown increased levels of WARS in the tears of patients

TABLE 1 Summary of levels of evidence for target proteins for DR and PDR.

Disease	Protein	Discovery	Replication	Heterogenity	Pleiotropy	Colocalization	Targets
DR	WARS	1.31E-04	3.01E-07	4.42E-01	4.80E-01	94.4%	Tier 1 Target
	HSPA1A	4.96E-04	8.89E-01	1.45E-147	NA	0.0%	Tier 3 Target
	KLK8	1.10E-02	5.78E-01	1.45E-147	4.91E-02	78.3%	Tier 2 Target
	SIRPG	1.46E-02	3.32E-04	NA	NA	80.7%	Tier 1 Target
	KLK11	4.35E-02	4.94E-01	1.30E-01	6.01E-01	1.0%	Tier 3 Target
PDR	OLFML3	3.75E-03	2.19E-02	1.08E-01	NA	0.0%	Tier 3 Target
	ALDOC	5.48E-03	9.28E-06	NA	NA	99.2%	Tier 1 Target
	SIRPG	4.73E-02	6.65E-05	NA	NA	93.4%	Tier 1 Target

with PDR, suggesting its involvement in the disease (29). Our findings support this link, establishing a causal relationship between WARS and DR. Interestingly, PDR is characterized by abnormal blood vessel growth, yet WARS is known to have anti-angiogenic effects. This includes its influence in ocular angiogenesis (30) and tumor growth (31). When WARS is broken down, it produces several smaller molecules, such as mini-WARS and T2-WARS, known to inhibit blood vessel growth (30–34). Specifically, T2-WARS interacts with VEGF pathways, reducing endothelial cell movement and angiogenesis (33, 35). Additionally, WARS acts as a natural trigger for Toll-like receptors (TLR) 2 and 4, known to play a role in inflammatory responses. The engagement of WARS with these receptors leads to the production of various inflammatory substances (36). Considering the known role of inflammation in DR, exploring the pathological implications of WARS in this context is of great importance (37). This further establishes WARS not only as a marker for DR but also as a potential target for understanding and managing the disease.

Our study highlighted ALDOC, a member of the class I fructose-bisphosphate aldolase gene family, as a key protein associated specifically with proliferative diabetic retinopathy (PDR). ALDOC's primary function involves critical steps in glycolysis, where it aids in breaking down sugars (38). We observed that increased levels of ALDOC align with elevated plasma free fatty acid concentrations. This correlation could influence insulin secretion and potentially lead to type 2 diabetes mellitus, a known risk factor for PDR (39, 40).

Furthermore, research by Michal et al. has uncovered the significant role of aldolase proteins, including ALDOC, in enhancing Wnt signaling (41). This signaling pathway, implicated in various cellular processes, is critical in the development of diabetic retinopathy. Specifically, ALDOC and its family members can modify Wnt signaling by interacting with key molecular components, thereby influencing cell behavior related to PDR (42). Although these findings position ALDOC as a potential risk marker for PDR, its direct role in the disease's pathogenesis is yet to be fully understood. More detailed studies are necessary to clarify the exact relationship between ALDOC levels and PDR, which could open new avenues for therapeutic interventions.

Our study has limitations, particularly in using blood-derived proteins, which may not completely reflect changes in DR-specific tissues like the retina. Future research should explore proteins from these ocular tissues for deeper insights into DR. Additionally, our use of SOMAmers technology, while advanced, may not capture the full range of proteins involved in DR. Exploring diverse proteomic methods and sample types could uncover more relevant proteins. Importantly, our focus on European ancestry limits the study's broader applicability. Future research must include diverse populations to understand how genetic differences affect DR across ethnicities. This is crucial for developing treatments and prevention strategies effective for a global population.

In summary, our study identifies strong causal connections between three plasma proteins (SIRPG, WARS, ALDOC) and DR. This finding opens new avenues for therapeutic research in DR. Future studies are essential to confirm these links and explore their underlying mechanisms. This work sets the stage for developing targeted treatments for DR, addressing a significant health challenge.

Data availability statement

The original contributions presented in the study are included in the article/Supplementary Material. Further inquiries can be directed to the corresponding author.

Author contributions

XZ: Conceptualization, Data curation, Formal analysis, Writing – original draft. SY: Writing – original draft, Writing – review & editing, Formal analysis, Resources. YT: Project administration, Resources, Writing – review & editing.

Funding

The author(s) declare financial support was received for the research, authorship, and/or publication of this article. This study was supported by the National Funded Postdoctoral Researcher Program of China (GZC20233180).

Acknowledgments

The authors would like to acknowledge the participants and investigators of the FinnGen study, as well as the valuable data provided by the deCODE genetics and Atherosclerosis Risk in Communities study.

Conflict of interest

The authors declare that the research was conducted in the absence of any commercial or financial relationships that could be construed as a potential conflict of interest.

Publisher's note

Supplementary material

The Supplementary Material for this article can be found online at: https://www.frontiersin.org/articles/10.3389/fendo.2023.1339374/full#supplementary-material

References

1. Tan TE, Wong TY. Diabetic retinopathy: Looking forward to 2030. *Front Endocrinol* (2022) 13:1077669. doi: 10.3389/fendo.2022.1077669

2. Yau JW, Rogers SL, Kawasaki R, Lamoureux EL, Kowalski JW, Bek T, et al. Global prevalence and major risk factors of diabetic retinopathy. *Diabetes Care* (2012) 35 (3):556–64. doi: 10.2337/dc11-1909

3. Duh EJ, Sun JK, Stitt AW. Diabetic retinopathy: current understanding, mechanisms, and treatment strategies. *JCI Insight* (2017) 2(14). doi: 10.1172/jci.insight.93751

4. Zhao Y, Singh RP. The role of anti-vascular endothelial growth factor (anti-VEGF) in the management of proliferative diabetic retinopathy. *Drugs Context* (2018) 7:212532. doi: 10.7573/dic.212532

5. Simo R, Hernandez C. Novel approaches for treating diabetic retinopathy based on recent pathogenic evidence. *Prog Retinal Eye Res* (2015) 48:160–80. doi: 10.1016/j.preteyeres.2015.04.003

6. Furino C, Boscia F, Reibaldi M, Alessio G. Intravitreal therapy for diabetic macular edema: an update. *J Ophthalmol* (2021) 2021:1–23. doi: 10.1155/2021/6654168

7. Zheng J, Haberland V, Baird D, Walker V, Haycock PC, Hurle MR, et al. Phenome-wide Mendelian randomization mapping the influence of the plasma proteome on complex diseases. *Nat Genet* (2020) 52(10):1122–31. doi: 10.1038/s41588-020-0682-6

8. Meleth AD, Agrón E, Chan CC, Reed GF, Arora K, Byrnes G, et al. Serum inflammatory markers in diabetic retinopathy. *Invest Ophthalmol Vis Sci* (2005) 46 (11):4295–301. doi: 10.1167/iovs.04-1057

9. Polat SB, Ugurlu N, Yulek F, Simavli H, Ersoy R, Cakir B, et al. Evaluation of serum fibrinogen, plasminogen, α2-anti-plasmin, and plasminogen activator inhibitor levels (PAI) and their correlation with presence of retinopathy in patients with type 1 DM. *J Diabetes Res* (2014) 2014:317292. doi: 10.1155/2014/317292

10. Sasongko MB, Wong TY, Jenkins AJ, Nguyen TT, Shaw JE, Wang JJ. Circulating markers of inflammation and endothelial function, and their relationship to diabetic retinopathy. *Diabetic Med J Br Diabetic Assoc* (2015) 32(5):686–91. doi: 10.1111/dme.12640

11. Lu CH, Lin ST, Chou HC, Lee YR, Chan HL. Proteomic analysis of retinopathy-related plasma biomarkers in diabetic patients. *Arch Biochem Biophys* (2013) 529 (2):146–56. doi: 10.1016/j.abb.2012.11.004

12. Gopalakrishnan V, Purushothaman P, Bhaskar A. Proteomic analysis of plasma proteins in diabetic retinopathy patients by two dimensional electrophoresis and MALDI-Tof-MS. *J Diabetes Its Complications* (2015) 29(7):928–36. doi: 10.1016/j.jdiacomp.2015.05.021

13. Smith GD, Ebrahim S. 'Mendelian randomization': can genetic epidemiology contribute to understanding environmental determinants of disease? *Int J Epidemiol* (2003) 32(1):1–22. doi: 10.1093/ije/dyg070

14. Chen J, Xu F, Ruan X, Sun J, Zhang Y, Zhang H, et al. Therapeutic targets for inflammatory bowel disease: proteome-wide Mendelian randomization and colocalization analyses. *EBioMedicine* (2023) 89:104494. doi: 10.1016/j.ebiom.2023.104494

15. Ou YN, Yang YX, Deng YT, Zhang C, Hu H, Wu BS, et al. Identification of novel drug targets for Alzheimer's disease by integrating genetics and proteomes from brain and blood. *Mol Psychiatry* (2021) 26(10):6065–73. doi: 10.1038/s41380-021-01251-6

16. Ferkingstad E, Sulem P, Atlason BA, Sveinbjornsson G, Magnusson MI, Styrmisdottir EL, et al. Large-scale integration of the plasma proteome with genetics and disease. *Nat Genet* (2021) 53(12):1712–21. doi: 10.1038/s41588-021-00978-w

17. Zhang J, Dutta D, Köttgen A, Tin A, Schlosser P, Grams ME, et al. Plasma proteome analyses in individuals of European and African ancestry identify cis-pQTLs and models for proteome-wide association studies. *Nat Genet* (2022) 54(5):593–602. doi: 10.1038/s41588-022-01051-w

18. Kurki MI, Karjalainen J, Palta P, Sipilä TP, Kristiansson K, Donner KM, et al. FinnGen provides genetic insights from a well-phenotyped isolated population. *Nature* (2023) 613(7944):508–18. doi: 10.1038/s41586-022-05473-8

19. Burgess S, Davey Smith G, Davies NM, Dudbridge F, Gill D, Glymour MM, et al. Guidelines for performing Mendelian randomization investigations: update for summer 2023. *Wellcome Open Res* (2019) 4:186. doi: 10.12688/wellcomeopenres.15555.1

20. Bowden J, Hemani G, Davey Smith G. Invited commentary: detecting individual and global horizontal pleiotropy in Mendelian randomization-A job for the humble heterogeneity statistic? *Am J Epidemiol* (2018) 187(12):2681–5. doi: 10.1093/aje/kwy185

21. Giambartolomei C, Vukcevic D, SChadt EE, Franke L, Hingorani AD, Wallace C, et al. Bayesian test for colocalisation between pairs of genetic association studies using summary statistics. *PloS Genet* (2014) 10(5):e1004383. doi: 10.1371/journal.pgen.1004383

22. Ochoa D, Karim M, Ghoussaini M, Hulcoop DG, McDonagh EM, Dunham I. Human genetics evidence supports two-thirds of the 2021 FDA-approved drugs. *Nat Rev Drug Discov* (2022) 21(8):551. doi: 10.1038/d41573-022-00120-3

23. Sinha S, Renavikar PS, Crawford MP, Steward-Tharp SM, Brate A, Tsalikian E, et al. Altered expression of SIRPγ on the T-cells of relapsing remitting multiple sclerosis and type 1 diabetes patients could potentiate effector responses from T-cells. *PloS One* (2020) 15(8):e0238070. doi: 10.1371/journal.pone.0238070

24. Sinha S, Borcherding N, Renavikar PS, Crawford MP, Tsalikian E, Tansey M, et al. An autoimmune disease risk SNP, rs2281808, in SIRPG is associated with reduced expression of SIRPγ and heightened effector state in human CD8 T-cells. *Sci Rep* (2018) 8(1):15440. doi: 10.1038/s41598-018-33901-1

25. Brooke G, Holbrook JD, Brown MH, Barclay AN. Human lymphocytes interact directly with CD47 through a novel member of the signal regulatory protein (SIRP) family. *J Immunol (Baltimore Md 1950)* (2004) 173(4):2562–70. doi: 10.4049/jimmunol.173.4.2562

26. Barrett JC, Clayton DG, Concannon P, Akolkar B, Cooper JD, Erlich HA, et al. Genome-wide association study and meta-analysis find that over 40 loci affect risk of type 1 diabetes. *Nat Genet* (2009) 41(6):703–7. doi: 10.1038/ng.381

27. Yazdanpanah N, Yazdanpanah M, Wang Y, Forgetta V, Pollak M, Polychronakos C, et al. Clinically relevant circulating protein biomarkers for type 1 diabetes: evidence from a two-sample Mendelian randomization study. *Diabetes Care* (2022) 45(1):169–77. doi: 10.2337/dc21-1049

28. Kwon NH, Fox PL, Kim S. Aminoacyl-tRNA synthetases as therapeutic targets. *Nat Rev Drug Discov* (2019) 18(8):629–50. doi: 10.1038/s41573-019-0026-3

29. Amorim M, Martins B, Caramelo F, Gonçalves C, Trindade G, Simão J, et al. Putative biomarkers in tears for diabetic retinopathy diagnosis. *Front Med* (2022) 9:873483. doi: 10.3389/fmed.2022.873483

30. Otani A, Slike BM, Dorrell MI, Hood J, Kinder K, Ewalt KL, et al. A fragment of human TrpRS as a potent antagonist of ocular angiogenesis. *Proc Natl Acad Sci U States A* (2002) 99(1):178–83. doi: 10.1073/pnas.012601899

31. Tzima E, Schimmel P. Inhibition of tumor angiogenesis by a natural fragment of a tRNA synthetase. *Trends Biochem Sci* (2006) 31(1):7–10. doi: 10.1016/j.tibs.2005.11.002

32. Wakasugi K, Slike BM, Hood J, Otani A, Ewalt KL, Friedlander M, et al. A human aminoacyl-tRNA synthetase as a regulator of angiogenesis. *Proc Natl Acad Sci USA* (2002) 99(1):173–7. doi: 10.1073/pnas.012602099

33. Tzima E, Reader JS, Irani-Tehrani M, Ewalt KL, Schwartz MA, Schimmel P. VE-cadherin links tRNA synthetase cytokine to anti-angiogenic function. *J Biol Chem* (2005) 280(4):2405–8. doi: 10.1074/jbc.C400431200

34. Kise Y, Lee SW, Park SG, Fukai S, Sengoku T, Ishii R, et al. A short peptide insertion crucial for angiostatic activity of human tryptophanyl-tRNA synthetase. *Nat Struct Mol Biol* (2004) 11(2):149–56. doi: 10.1038/nsmb722

35. Tzima E, Reader JS, Irani-Tehrani M, Ewalt KL, Schwartz MA, Schimmel P. Biologically active fragment of a human tRNA synthetase inhibits fluid shear stress-activated responses of endothelial cells. *Proc Natl Acad Sci USA* (2003) 100(25):14903–7. doi: 10.1073/pnas.2436330100

36. Nguyen TTT, Yoon HK, Kim YT, Choi YH, Lee WK, Jin M. Tryptophanyl-tRNA synthetase 1 signals activate TREM-1 *via* TLR2 and TLR4. *Biomolecules* (2020) 10 (9):1283. doi: 10.3390/biom10091283

37. Bayan N, Yazdanpanah N, Rezaei N. Role of toll-like receptor 4 in diabetic retinopathy. *Pharmacol Res* (2022) 175:105960. doi: 10.1016/j.phrs.2021.105960

38. Wang CF, Yuan CZ, Wang SH, Zhang H, Hu XX, Zhang L, et al. Differential gene expression of aldolase C (ALDOC) and hypoxic adaptation in chickens. *Anim Genet* (2007) 38(3):203–10. doi: 10.1111/j.1365-2052.2007.01605.x

39. Camps SG, Verhoef SP, Roumans N, Bouwman FG, Mariman EC, Westerterp KR. Weight loss-induced changes in adipose tissue proteins associated with fatty acid and glucose metabolism correlate with adaptations in energy expenditure. *Nutr Metab* (2015) 12:37. doi: 10.1186/s12986-015-0034-1

40. Kashyap S, Belfort R, Gastaldelli A, Pratipanawatr T, Berria R, Pratipanawatr W, et al. A sustained increase in plasma free fatty acids impairs insulin secretion in nondiabetic subjects genetically predisposed to develop type 2 diabetes. *Diabetes* (2003) 52(10):2461–74. doi: 10.2337/diabetes.52.10.2461

41. Caspi M, Perry G, Skalka N, Meisel S, Firsow A, Amit M, et al. Aldolase positively regulates of the canonical Wnt signaling pathway. *Mol Cancer* (2014) 13:164. doi: 10.1186/1476-4598-13-164

42. Chen Y, Hu Y, Zhou T, Zhou KK, Mott R, Wu M, et al. Activation of the Wnt pathway plays a pathogenic role in diabetic retinopathy in humans and animal models. *Am J Pathol* (2009) 175(6):2676–85. doi: 10.2353/ajpath.2009.080945

frontiers | Frontiers in Endocrinology

TYPE Original Research
PUBLISHED 26 January 2024
DOI 10.3389/fendo.2024.1295745

OPEN ACCESS

EDITED BY
Grigorios L. Kyriakopoulos,
National Technical University of Athens, Greece

REVIEWED BY
Navneet Mehrotra,
Retina Foundation and Retina Care, India
Francesco Maria D'Alterio,
Imperial College Healthcare NHS Trust, United Kingdom

*CORRESPONDENCE
Honghua Yu
yuhonghua@gdph.org.cn
Ling Yuan
yuanling8061@163.com
Yijun Hu
huyijun2014@163.com

†These authors have contributed equally to this work and share first authorship

RECEIVED 17 September 2023
ACCEPTED 02 January 2024
PUBLISHED 26 January 2024

CITATION
Lawali DJAM, Wu G, Adam ND, Lin Z, Kong H, Yi L, Fang Y, Niu Y, Tang C, Amza A, Zhang H, Yu H, Yuan L and Hu Y (2024) Difference of central foveal thickness measurement in patients with macular edema using optical coherence tomography in different display modes.
Front. Endocrinol. 15:1295745.
doi: 10.3389/fendo.2024.1295745

Difference of central foveal thickness measurement in patients with macular edema using optical coherence tomography in different display modes

Dan Jouma Amadou Maman Lawali[1†], Guanrong Wu[1†], Nouhou Diori Adam[2], Zhangjie Lin[1], Huiqian Kong[1], Liaohui Yi[1], Ying Fang[1], Yongyi Niu[1], Changting Tang[3], Abdou Amza[2], Hongyang Zhang[1], Honghua Yu[1,4*], Ling Yuan[5*] and Yijun Hu[1*]

[1]Guangdong Eye Institute, Department of Ophthalmology, Guangdong Provincial People's Hospital (Guangdong Academy of Medical Sciences), Southern Medical University, Guangzhou, China, [2]Department of Ophthalmology, Amirou Boubacar Diallo National Hospital, Abdou Moumouni University of Niamey, Niamey, Niger, [3]Affiliated Hospital of Guilin Medical University, Guilin, China, [4]Guangdong Provincial Key Laboratory of Artificial Intelligence in Medical Image Analysis and Application, Guangzhou, China, [5]Department of Ophthalmology, The First Affiliated Hospital of Kunming Medical University, Kunming, China

Purpose: To assess the differences in the measurement of central foveal thickness (CFT) in patients with macular edema (ME) between two display modes (1:1 pixel and 1:1 micron) on optical coherence tomography (OCT).

Design: This is a retrospective, cross-sectional study.

Methods: Group A consisted of participants with well-horizontal OCT B-scan images and group B consisted of participants with tilted OCT B-scan. We manually measured the CFT under the two display modes, and the values were compared statistically using the paired *t*-test. Spearman's test was used to assess the correlations between the OCT image tilting angle (OCT ITA) and the differences in CFT measurement. The area under the curve (AUC) was calculated to define the OCT ITA cutoff for a defined CFT difference.

Results: In group A, the mean CFT in the 1:1 pixel display mode was 420.21 ± 130.61 μm, similar to the mean CFT of 415.27 ± 129.85 μm in the 1:1 micron display mode. In group B, the median CFT in the 1:1 pixel display mode is 409.00 μm (IQR: 171.75 μm) and 368.00 μm (IQR: 149.00 μm) in the 1:1 micron display mode. There were significant differences between the two display modes with the median (IQR) absolute difference and median (IQR) relative difference of 38.00 μm (75.00 μm) and 10.19% (21.91%) (all $p = 0.01$). The differences in CFT measurement between the two display modes were correlated with the OCT ITA (absolute differences, $r = 0.88$, $p < 0.01$; relative differences, $r = 0.87$, $p < 0.01$). The AUC for a predefined CFT difference was 0.878 (10 μm), 0.933 (20 μm), 0.938 (30 μm), 0.961 (40 μm), 0.962 (50 μm), and 0.970 (60 μm).

Conclusion: In patients with DM, when the OCT B-scan images were well-horizontal, manual CFT measurements under the two display modes were similar, but when the B-scan images were tilted, the CFT measurements were different under the two display modes, and the differences were correlated to the OCT ITA.

KEYWORDS

optical coherence tomography, optical coherence tomography image tilting angle, central foveal thickness, display mode, macular edema

Introduction

Macular edema (ME) is one of the major causes of vision impairment in patients suffering from metabolic, vascular, and inflammatory retinal disorders (1–5). The etiology of ME includes diabetes, retinal vein occlusion (RVO), epiretinal membrane (ERM), and age-related macular degeneration (AMD) (3, 6–11). ME affects approximately 7 million people worldwide due to diabetes and approximately 3 million people due to venous occlusions. In developed countries, neovascular age-related macular degeneration represents 5% of ME among subjects over the age of 60 (12).

Spectral-domain optical coherence tomography (SD-OCT) is a non-invasive and standard diagnostic tool for detecting ME, as well as for monitoring and follow-up after treatment. As a result, SD-OCT has a considerable influence on decisions about the management of ME, particularly in common disorders such as DME and AMD (13–16). It allows the measurement of individual retinal layers, the determination of retinal thickness and macular volume, and the qualitative assessment of fluid distribution. Even though this was done manually before, several recent studies employing machine learning aim to automate the quantification of fluid and other distinctive factors (10, 14, 17). Although central macular thickness (CMT) measurements automatically evaluate the average retinal thickness within a 1-mm concentric circle (14, 18–20), clinicians are still using SD-OCT's central foveal thickness (CFT) manual measurements to assess ME, which represents a fundamental marker for diagnosing ME in different retinal diseases (21–23).

It is known that there are two display modes on OCT: the 1:1 pixel display mode and the 1:1 micron display mode. The 1:1 pixel display mode represents the most commonly used display mode for OCT images in daily clinical practice. The ratio between vertical and horizontal scales is 3.775 in the 1:1 pixel display mode and 1.0 in the 1:1 micron display mode. Previously, we found significant differences in CFT measurements between the two OCT display modes in myopic patients, and the differences were correlated to the OCT image tilting angle (OCT ITA) (24). However, whether our findings can be applied to patients with ME is yet to be confirmed.

The aim of the current study was to evaluate the differences in manual measurements of the CFT under the two display modes (1:1 pixel display mode and 1:1 micron display mode) in patients with ME. In addition, we investigated the OCT ITA cutoff for some predefined CFT differences between the two OCT display modes.

Materials and methods

Participants

In this retrospective, cross-sectional study, we recruited subjects with ME treatment-naive and post-treatment of different origins who visited the Ophthalmology Department of Guangdong Provincial People's Hospital (GDPH) and who received the SD-OCT scanning. The subjects' characteristics included age, gender, lens status eyes with ME, BCVA between 0.01 and 1.0 logMAR, and CFT more than 300 μm on SD-OCT.

We excluded eyes with severe cataracts, IOP >21 mmHg, and eyes that could not be scanned using SD-OCT due to poor patient cooperation. All subjects underwent comprehensive ophthalmic examinations, including best-corrected visual acuity with a decimal chart, slit-lamp biomicroscope examination of the anterior segment and the fundus, intraocular pressure, and SD-OCT scanning.

This study was approved by the Institutional Review Board (IRB) of GDPH and followed the Helsinki Declaration. Furthermore, the necessity for informed consent was waived by the same IRB because no specific subject can be identified from the data.

Imaging

Before SD-OCT scanning, 0.5% tropicamide (Santen Pharmaceutical Co., Ltd. Shiga Plant) was used to achieve adequate pupillary dilation. Participants were directed to look at the machine's fixation light, and the foveolar fixation was confirmed by visualizing the retinal image through the infrared monitoring camera.

We performed a high-resolution horizontal B-scan for each eye through the central fovea using SD-OCT (Spectralis, Heidelberg Engineering GmbH, Heidelberg, Germany), and an OCT image of

the right eye was selected for manual measurement. If the right eye image was not accessible, the left eye image was used. We divided the participants into two groups. Group A included patients with well-horizontal OCT B-scan images, and group B included patients with tilted OCT B-scan images. Manual measurement was accomplished by the same experienced ophthalmologist (D.M.). All measurements were conducted in both display modes, i.e., 1:1 pixel display mode and 1:1 micron display mode (Figures 1, 2). SD-OCT's caliper measuring tool was used to manually measure the CFT in the two display modes.

We defined CFT as the vertical distance between the surface of the internal limiting membrane and the outer border of the retinal pigment epithelium (RPE) (Figure 3). We used the ImageJ software (US National Institutes of Health, Bethesda, USA; https://imagej.net/software/fiji/) to assess the OCT ITA. To measure the OCT ITA, we first drew a line tangent to the RPE line below the foveola. The angle between this line and the bottom edge of the OCT image was designated as the OCT ITA (Figure 3).

Statistical analysis

The data are presented as mean and standard deviation (mean ± SD) for the data not normally distributed; otherwise, they are presented as median and interquartile range (IQR). The statistical analyses were performed using SPSS 26.0 (SPSS. Inc., Chicago, IL, USA). The Shapiro–Wilk test was used to assess the normality of the data. The OCT measurement in the two display modes was compared using the paired *t*-test. The absolute difference in CFT measurement was calculated by CFT in 1:1 pixel mode minus CFT in 1:1 micron mode, and the relative difference in CFT measurement was defined as the absolute difference divided by the retinal thickness in 1:1 micron mode. Spearman correlation tests and linear regressions were used to assess the correlations between the OCT ITA and the differences in OCT measurement under the two display modes. For all the tests, p <0.05 was considered statistically significant.

Results

Baseline demographic characteristics and underlying pathologies of ME in the two groups

Table 1 shows the baseline demographic characteristics and the underlying pathologies of ME in group A and group B. We recruited 52 participants in group A, consisting of 29 (55.8%) patients with

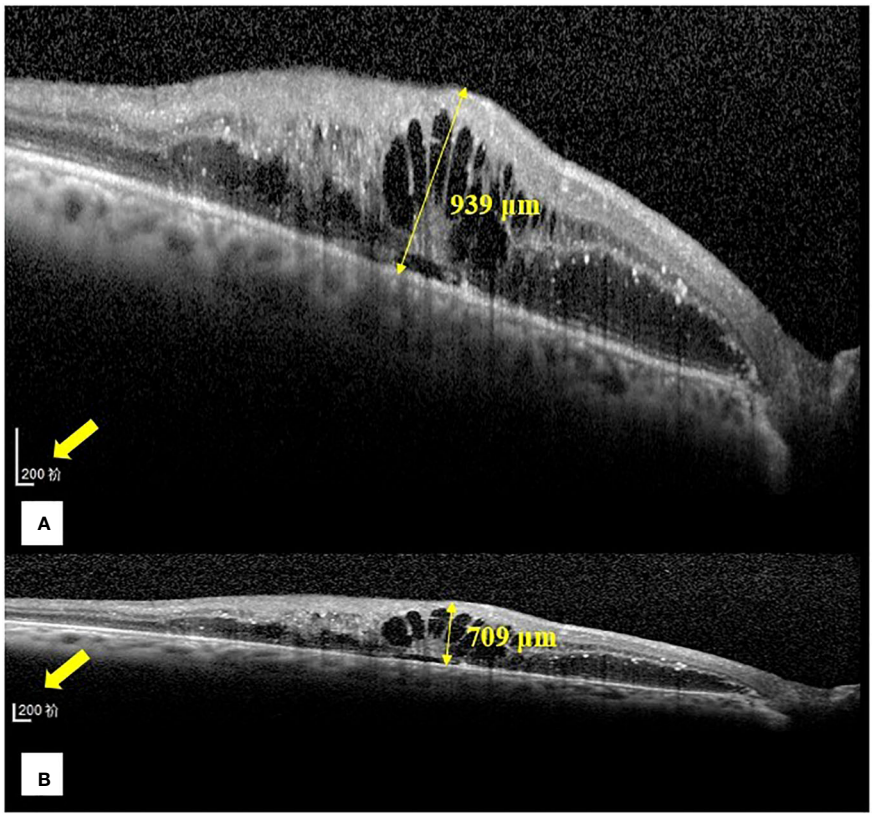

FIGURE 1
Representative images of the central foveal thickness manual measurement in the two optical coherence tomography display modes (1:1 pixel display mode and 1:1 micron display mode) in group **(B)**. **(A)** Central foveal thickness manual measurement in the 1:1 pixel display mode. **(B)** Central foveal thickness manual measurement in the 1:1 micron display mode. In the 1:1 pixel display mode, the central foveal thickness is 939 μm, and in the 1:1 micron display mode, it is 709 μm.

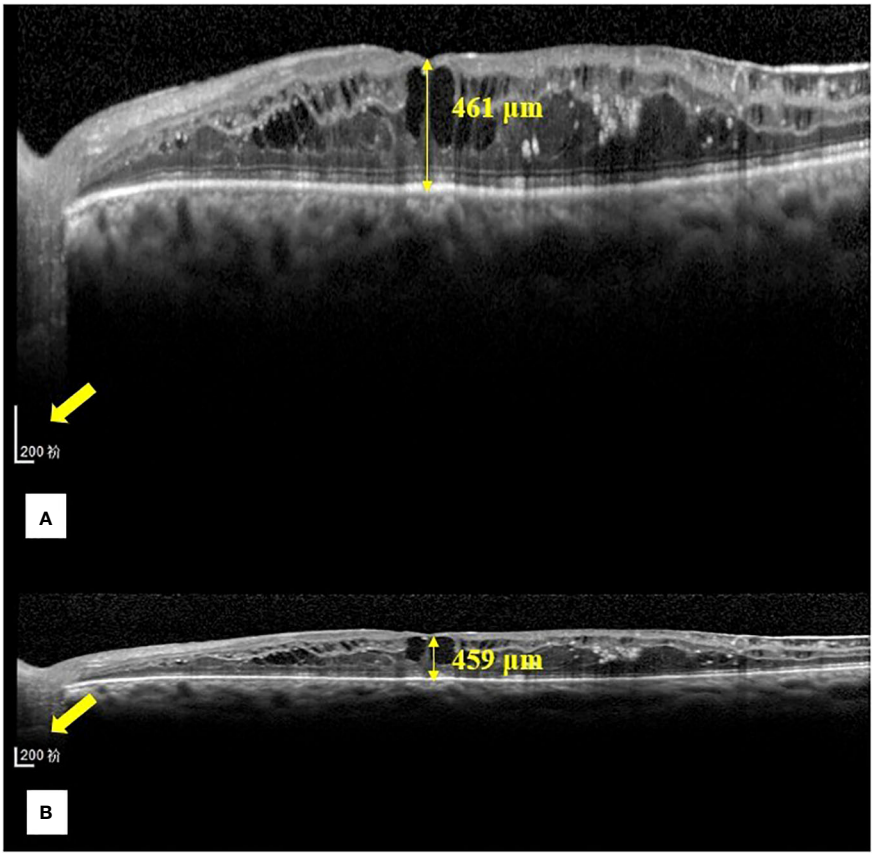

FIGURE 2
Representative images of the central foveal thickness manual measurement in the two OCT display modes (1:1 pixel display mode and 1:1 micron display mode) in group **(A)**. **(A)** Central foveal thickness manual measurement in the 1:1 pixel display mode. **(B)** Central foveal thickness manual measurement in the 1:1 micron mode. In the 1:1 pixel display mode, the central foveal thickness is 461 µm, and in the 1:1 micron display mode, it is 459 µm.

DME, 3 (5.8%) patients with RVO, 19 (36.5%) patients with ERM, and 1 (1.9%) patient with AMD, with a mean age of 63.15 ± 12.13 years, lens status ratio (phakic/pseudophakic) of 42/10, and mean BCVA of 0.43 ± 0.32. We recruited 112 participants in group B, consisting of 40 (35.5%) patients with DME, 14 (12.5%) patients with RVO, 54 (48.2%) patients with ERM, and 4 (3.6%) patients with AMD, with a median age of 66.00 years (IQR: 15.00 years), lens status ratio of 74/38, and median BCVA of 0.30 (IQR: 0.40).

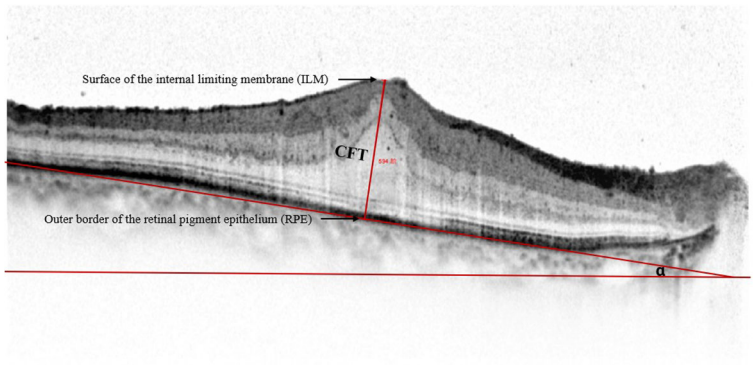

FIGURE 3
Representative spectral-domain optical coherence tomography image of the central foveal thickness and the optical coherence tomography image tilting angle. Central foveal thickness is defined as the distance between the surface of the internal limiting membrane and the outer border of the retinal pigment epithelium at the foveal zone. Optical coherence tomography image tilting angle is the angle alpha between the line parallel to the edge of the optical coherence tomography image and the line tangent to the retinal pigment epithelium.

TABLE 1 Baseline demographic characteristics and the underlying pathologies of macular edema in group A and group B.

Characteristics*	Group A	Group B
Age of the patients (years)	63.15 ± 12.13	66.00 (15.00)
Lens status (phakic/pseudophakic)	42/10	74/38
BCVA	0.43 ± 0.32	0.30 (0.40)
Etiology		
DME	29 (55.8%)	40 (35.7%)
RVO	3 (5.8%)	14 (12.5%)
ERM	19 (36.5%)	54 (48.2%)
AMD	1 (1.9%)	4 (3.6%)
Total number of eyes	52 (100%)	112 (100%)

Best-corrected visual acuity (BCVA) measurement at the logarithm of the minimum angle of resolution (logMAR) scale.
*The data are statistically normally distributed. The data are presented as mean and standard deviation for the data not normally distributed; otherwise, they are presented as median and interquartile range.
**The data are presented as numbers and the percentage of eyes.

Evaluation of the differences in CFT manual measurement between the two display modes

The evaluation of the differences (absolute and relative) between the two display modes in CFT manual measurement in group A and group B is shown in Table 2. In group A, the differences between the two display modes in CFT measurement are not statistically significant, with a mean CFT of 420.21 ± 130.61 μm in the 1:1 pixel display mode and a mean CFT of 415.27 ± 129.85 μm in the 1:1 micron display mode. The mean differences (absolute and relative) were 4.94 ± 4.14 μm and 1.23% ± 0.83% with p >0.05. In group B, we found statistically significant differences between the two display modes in the CFT manual measurement, with a median (IQR) in the 1:1 pixel display mode of 409.00 μm (171.75 μm) and 368.00 μm (149.00 μm) in the 1:1 micron display mode and a median (IQR) absolute and relative difference of 38.00 μm (75.00 μm) and 10.19% (21.91%) (all $p < 0.05$).

Correlations between the CFT differences in the two display modes and the OCT ITA

Table 3 shows the correlations between the CFT differences in the two display modes and the OCT ITA. The differences in the CFT manual measurement between the two display modes were significantly correlated with the OCT ITA (absolute differences, $r = 0.88$, $p < 0.01$; relative differences, $r = 0.87$, $p < 0.01$).

The OCT ITA cutoff for a predefined CFT difference and regression equations to correct the CFT differences

Since the CFT differences between the two display modes were correlated to the OCT ITA, we further analyzed the OCT ITA cutoff for a predefined CFT difference using a receiver operating characteristic (ROC) curve. As shown in Figure 4, the area under the curve (AUC) of OCT ITA for a predefined CFT difference was 0.878 (10 μm), 0.933 (20 μm), 0.938 (30 μm), 0.961 (40 μm), 0.962 (50 μm), and 0.970 (60 μm).

Linear regressions of the OCT ITA and the differences in CFT measurement between the two display modes are shown in Figures 5, 6 along with the regression equations. The regression equations of the OCT ITA are Y1 = −17.7 + 6.95x (R^2 = 0.69, $p < 0.001$) to correct the absolute CFT differences and Y2 = −0.0634 + 0.02x (R^2 = 0.75, $p < 0.001$) to correct the relative CFT differences.

Discussion

In the present study, we found significant differences in the manual measurement of CFT in patients with ME under the two OCT display modes when the OCT B-scan image is tilted. In addition, we found that the differences were correlated to the OCT ITA. To avoid measurement errors and misinterpretations of OCT B-scan images, it is beneficial to consider the differences between the two OCT display modes.

TABLE 2 Evaluation of the differences (absolute and relative) between the two display modes in group A as well as in group B.

CFT*	1:1 pixel (μm)	1:1 micron (μm)	Differences (absolute and relative)	p-value
Group A	420.21 ± 130.61	415.27 ± 129.85	4.94 μm ± 4.14 μm† 1.23% ± 0.85%††	>0.05
Group B	409.00 (171.75)	368.00 (149.00)	38.00 μm (75.00 μm)† 10.19% (21.91%)††	≤0.01

†Indicates the absolute difference.
††Indicates the relative difference.
*The data are statistically normally distributed. The data are presented as mean and standard deviation for the data not normally distributed; otherwise, they are presented as median and interquartile range.

TABLE 3 Correlation coefficients between the absolute and relative differences in the two OCT display modes and the OCT image tilting angle.

Differences	Angle (*r*)	*p*-value
ΔCFT (μm)*	0.88	≤0.01
ΔCFT (%)*	0.87	≤0.01

*The data are statistically not normally distributed.
**Spearman's test was performed to predict the correlation between the absolute and the relative differences and the mean angle of measurement with r representing the correlation coefficient. Significant if p <0.05.

Kim et al. found differences between the two display modes for choroidal thickness measurement, and the subfoveal choroidal thickness (SFCT) was overestimated when it was measured in 1:1 pixel display mode. Consequently, they suggested that choroidal thickness should be estimated according to the 1:1 micron display mode, mainly when the estimation line is not vertical. Furthermore, they concluded that a similar measurement error can arise when measuring the thickness of other structures when the OCT B-scan image is tilted, as demonstrated in some eyes for foveal retinal thickness, which is exactly the case in our current study. However, Kim et al. did not determine the specific cause of the tilted images, but they suspected eye curvature, particularly in the case of myopia, poor fixation, head tilt, or tilt OCT camera (18). Consistently, in our previous study, we demonstrated in myopic patients that the CFT was different between the two display modes, and the differences were correlated to the OCT ITA (24).

Cho et al. found that 1:1 micron images had slightly higher interobserver measurement errors for SFCT and that choroidal thickness measurements should be evaluated with caution, particularly for a thick choroid. The SFCT measurement did not differ substantially among the observers in their study for both image display modes (p = 0.5663 for the 1:1 pixel mode and p = 0.2839 for the 1:1 micron mode, respectively). However, their investigation revealed substantially poorer repeatability from the thick CT group for the 1:1 pixel images (0.747) than the 1:1 micron images (0.75) (25). Although Kim et al. observed an overestimation in 1:1 pixel images, these errors did not appear to have a significant impact on the reproducibility (18).

While the 1:1 pixel mode displays OCT images in a ratio of 3.775 between the vertical and horizontal scales, the 1:1 micron mode displays the OCT images in a ratio of 1.0. As a result, the 1:1 micron display mode must be vertically compressed approximately three-fold in the resolution of the retinal layers. Even though the 1:1 pixel display mode can more clearly depict a precise structural change, caution should be taken when the OCT B-scan image is titled. In our study, the absolute and the relative differences between the two display modes in group B represented, respectively, 38.00 μm (75.00 μm) and 10.19% (21.91%). According to previous studies, the interobserver repeatability of manual CFT measurement is 10% (26, 27). The differences in CFT manual measurement in tilted OCT B-scan images are more significant than the interobserver repeatability stated in the previous studies. Therefore, it is necessary to correct such

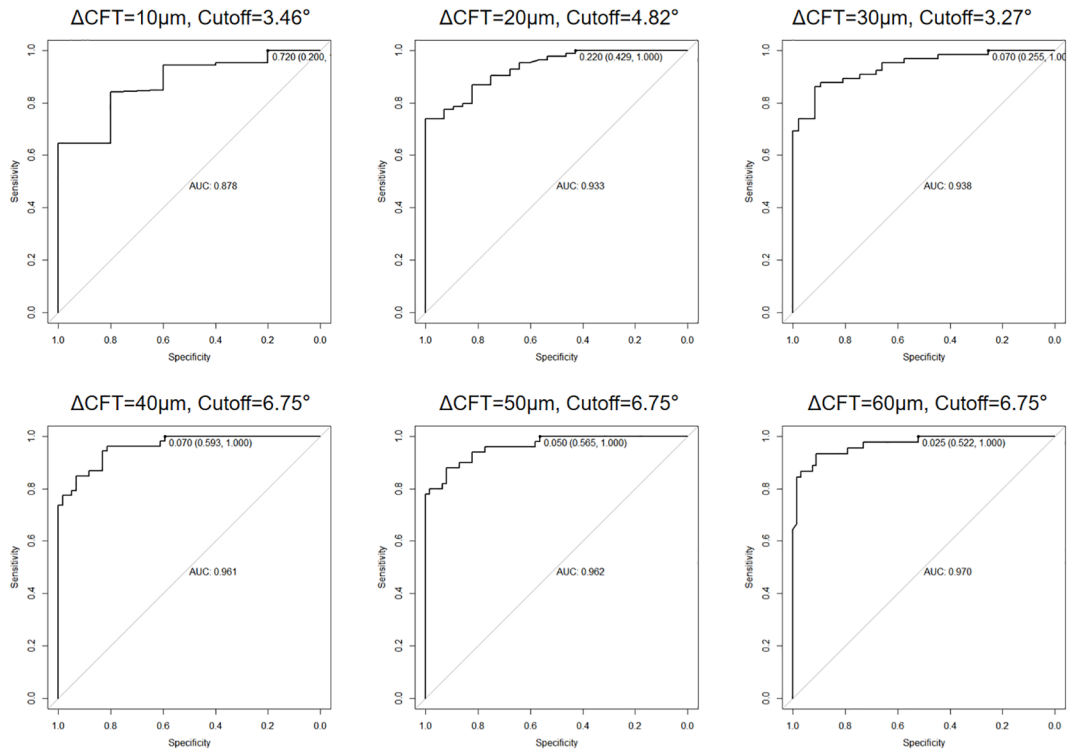

FIGURE 4
Area under the receiver operating characteristic (ROC) curve (AUC) and optical coherence tomography image tilting angle (OCT ITA) cutoff for a predefined central foveal thickness difference. As a result, the AUC of OCT ITA for a predefined central foveal thickness difference was 0.878 (10 μm), 0.933 (20 μm), 0.938 (30 μm), 0.961 (40 μm), 0.962 (50 μm), and 0.970 (60 μm).

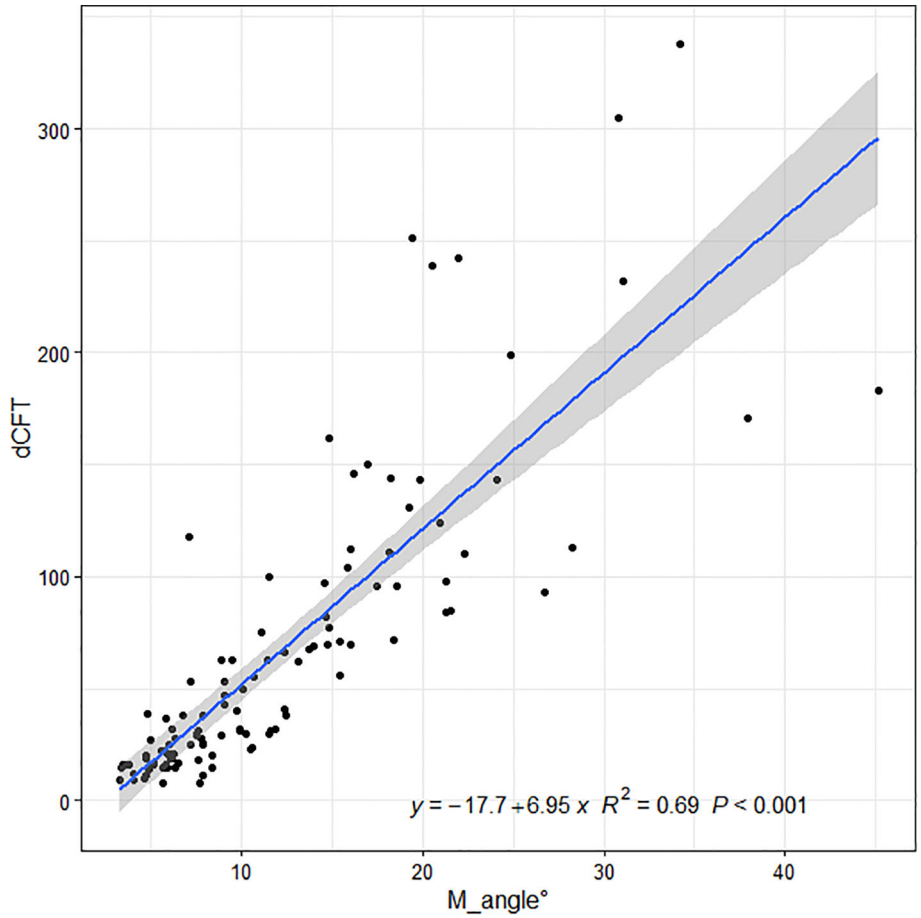

FIGURE 5
Linear regressions of the optical coherence tomography image tilting angle and the absolute differences in central foveal thickness manual measurement between the two display modes along with the regression equations. As a result, the regression equation of the optical coherence tomography image tilting angle and the absolute difference in central foveal thickness manual measurement are Y1 = −17.7 + 6.95*x* (R^2 = 0.69, p < 0.001).

differences in clinical practice. Moreover, we also provided the solution for when to correct the CFT differences. The AUC was 0.878 to 0.970, depending on the cutoff value of the CFT difference used. The sensitivity of the AUC calculated was 100% for all cutoff values, indicating that it is a highly accurate tool to predict when to correct the differences. The specificity of the AUC ranged from 20.0% to 59.3%, depending on the cutoff value used, and the cutoff OCT ITA ranged from 3.27 to 6.75. These results are consistent to predict when exactly to correct the differences between the two OCT display modes.

In patients with ME, the size of macular cysts is correlated to disease severity and treatment outcomes (28–30). Thus, many clinicians use OCT manual measurement to measure the size of macular cysts in clinical practice (31–33). It is important to accurately measure the size of macular cysts for assessing ME severity and the effectiveness of treatment (30, 34). Furthermore, accurate measurement of the cyst size can also help to identify the need for further investigation, such as fluorescein angiography, which can offer more detailed information about the cyst and the underlying pathology (30, 35). According to the results of our study, it is also important to pay attention to the tilted OCT B-scan images when manually measuring the size of macular cysts because the size of the cysts may be overestimated in the 1:1 pixel mode if the OCT B-scan images are tilted.

In the case of well-horizontal OCT B-scan images, there was no significant difference in CFT measurements between the two display modes. Therefore, it is unnecessary to correct the CFT difference in these cases, and it is important for the technicians to bear in mind that well-horizontal OCT B-scan images are obtained during OCT examinations.

In our current study, after demonstrating the differences between the two OCT display modes in patients with ME and their correlation with the OCT ITA, we proposed regression equations with the OCT ITA cutoff to correct the differences

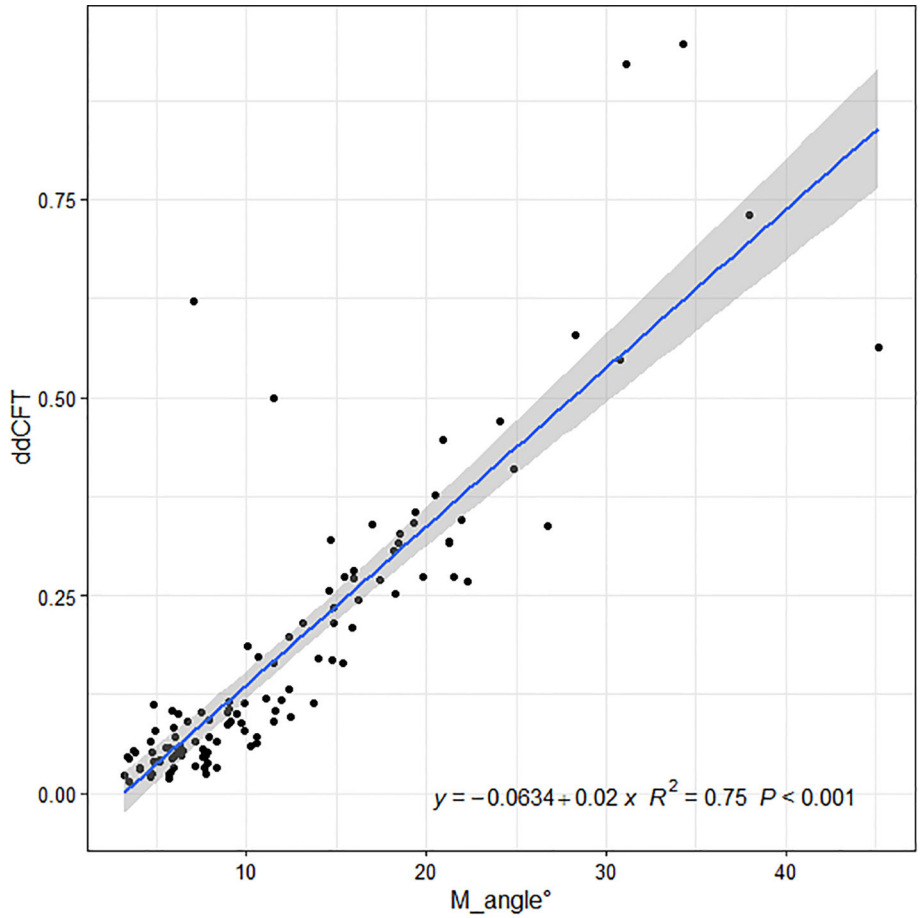

FIGURE 6
Linear regressions of the optical coherence tomography image tilting and the relative differences in central foveal thickness manual measurement between the two display modes along with the regression equations. As a result, the regression equation of the optical coherence tomography image tilting angle and the relative difference in central foveal thickness manual measurement are Y2 = −0.0634 + 0.02*x* (R^2 = 0.75, p < 0.001).

because neither the product's manufacturer nor previous literature recommended a scale of measurement.

Conclusion

Our study found that when the OCT B-scan images were well-horizontal, manual CFT measurements in ME patients were similar under the two display modes. However, when the B-scan images were tilted, the CFT measurements in patients with ME differed under the two display modes, and these differences were correlated to the OCT ITA. We were able to correct the discrepancies between the two display modes by using the regression equations.

Data availability statement

The raw data supporting the conclusions of this article will be made available by the authors, without undue reservation.

Ethics statement

The studies involving humans were approved by Institutional Review Board (IRB) of GDPH and followed the Helsinki Declaration. The studies were conducted in accordance with the local legislation and institutional requirements. Written informed consent for participation was not required from the participants or the participants' legal guardians/next of kin in accordance with the national legislation and institutional requirements.

Author contributions

DL: Conceptualization, Data curation, Formal analysis, Investigation, Methodology, Resources, Software, Supervision, Validation, Writing – original draft, Writing – review & editing. GW: Data curation, Formal analysis, Methodology, Software, Validation, Writing – review & editing. NA: Investigation, Methodology, Supervision, Validation, Writing – review & editing. ZL: Formal analysis, Investigation, Methodology, Supervision,

Validation, Writing – original draft, Writing – review & editing. HK: Validation, Writing – review & editing. LY: Data curation, Methodology, Validation, Writing – review & editing. YF: Data curation, Methodology, Validation, Writing – review & editing. YN: Conceptualization, Investigation, Methodology, Validation, Writing – review & editing. CT: Investigation, Methodology, Validation, Writing – review & editing. AA: Investigation, Methodology, Supervision, Validation, Writing – review & editing. HZ: Conceptualization, Investigation, Methodology, Validation, Writing – review & editing. HY: Conceptualization, Data curation, Formal analysis, Funding acquisition, Methodology, Project administration, Resources, Supervision, Validation, Visualization, Writing – review & editing. LY: Conceptualization, Formal analysis, Investigation, Methodology, Supervision, Validation, Visualization, Writing – original draft, Writing – review & editing. YH: Conceptualization, Data curation, Formal analysis, Investigation, Methodology, Project administration, Resources, Software, Supervision, Validation, Visualization, Writing – original draft, Writing – review & editing.

Funding

The author(s) declare financial support was received for the research, authorship, and/or publication of this article. This work was supported by the National Natural Science Foundation of China (81870663 and 82171075), the Science and Technology Program of Guangzhou (20220610092), the Outstanding Young Talent Trainee Program of Guangdong Provincial People's Hospital (KJ012019087), the GDPH Scientific Research Funds for Leading Medical Talents and Distinguished Young Scholars in Guangdong Province (KJ012019457), the Talent Introduction Fund of Guangdong Provincial People's Hospital (Y012018145), the launch fund of Guangdong Provincial People's Hospital for NSFC (8217040546, 8227041127), the Medical Scientific Research Foundation of Guangdong Province, China (A2021378). National Natural Science Foundation of China (82260207), Basic Research Program of Yunnan Province (202201AY070001-036). The sponsors or funding organizations had no role in the design or conduct of this research.

Conflict of interest

The authors declare that the research was conducted in the absence of any commercial or financial relationships that could be construed as a potential conflict of interest.

Publisher's note

References

1. Yau JW, Rogers SL, Kawasaki R, Lamoureux EL, Kowalski JW, Bek T, et al. Global prevalence and major risk factors of diabetic retinopathy. *Diabetes Care* (2012) 35 (3):556–64. doi: 10.2337/dc11-1909

2. Wang Z, Zhong Y, Yao M, Ma Y, Zhang W, Li C, et al. Automated segmentation of macular edema for the diagnosis of ocular disease using deep learning method. *Sci Rep* (2021) 11(1):13392. doi: 10.1038/s41598-021-92458-8

3. Forrester JV, Kuffova L, Delibegovic M. The role of inflammation in diabetic retinopathy. *Front Immunol* (2020) 11:583687. doi: 10.3389/fimmu.2020.583687

4. Bae JH, Al-Khersan H, Yannuzzi NA, Hasanreisoglu M, Androudi S, Albini TA, et al. Surgical therapy for macular edema: What we have learned through the decades. *Ocul Immunol Inflamm* (2019) 27(8):1242–50. doi: 10.1080/09273948.2019.1672194

5. Tang F, Qin X, Lu J, Song P, Li M, Ma X. Optical coherence tomography predictors of short-term visual acuity in eyes with macular edema secondary to retinal vein occlusion treated with intravitreal conbercept. *Retina* (2020) 40(4):773–85. doi: 10.1097/iae.0000000000002444

6. Grzybowski A, Markeviciute A, Zemaitiene R. Treatment of macular edema in vascular retinal diseases: A 2021 update. *J Clin Med* (2021) 10(22):5300. doi: 10.3390/jcm10225300

7. Costa JV, Moura-Coelho N, Abreu AC, Neves P, Ornelas M, Furtado MJ. Macular edema secondary to retinal vein occlusion in a real-life setting: a multicenter, nationwide, 3-year follow-up study. *Graefes Arch Clin Exp Ophthalmol* (2021) 259 (2):343–50. doi: 10.1007/s00417-020-04932-0

8. Das A, McGuire PG, Rangasamy S. Diabetic macular edema: Pathophysiology and novel therapeutic targets. *Ophthalmology* (2015) 122(7):1375–94. doi: 10.1016/j.ophtha.2015.03.024

9. Rittiphairoj T, Mir TA, Li T, Virgili G. Intravitreal steroids for macular edema in diabetes. *Cochrane Database Syst Rev* (2020) 11(11):Cd005656. doi: 10.1002/14651858.CD005656.pub3

10. Zur D, Iglicki M, Busch C, Invernizzi A, Mariussi M, Loewenstein A. OCT biomarkers as functional outcome predictors in diabetic macular edema treated with dexamethasone implant. *Ophthalmology* (2018) 125(2):267–75. doi: 10.1016/j.ophtha.2017.08.031

11. Johnson MW. Etiology and treatment of macular edema. *Am J Ophthalmol* (2009) 147(1):11–21.e1. doi: 10.1016/j.ajo.2008.07.024

12. Daruich A, Matet A, Moulin A, Kowalczuk L, Nicolas M, Sellam A, et al. Mechanisms of macular edema: Beyond the surface. *Prog Retin Eye Res* (2018) 63:20–68. doi: 10.1016/j.preteyeres.2017.10.006

13. de Azevedo AGB, Takitani G, Godoy BR, Marianelli BF, Saraiva V, Tavares IM, et al. Impact of manual correction over automated segmentation of spectral domain optical coherence tomography. *Int J Retina Vitreous* (2020) 6:4. doi: 10.1186/s40942-020-0207-6

14. Dysli M, Rückert R, Munk MR. Differentiation of underlying pathologies of macular edema using spectral domain optical coherence tomography (SD-OCT). *Ocul Immunol Inflamm* (2019) 27(3):474–83. doi: 10.1080/09273948.2019.1603313

15. Mowatt G, Hernández R, Castillo M, Lois N, Elders A, Fraser C, et al. Optical coherence tomography for the diagnosis, monitoring and guiding of treatment for neovascular age-related macular degeneration: a systematic review and economic evaluation. *Health Technol Assess* (2014) 18(69):1–254. doi: 10.3310/hta18690

16. Wolf S, Wolf-Schnurrbusch U. Spectral-domain optical coherence tomography use in macular diseases: a review. *Ophthalmologica* (2010) 224(6):333–40. doi: 10.1159/000313814

17. Yiu G, Welch RJ, Wang Y, Wang Z, Wang PW, Haskova Z. Spectral-domain OCT predictors of visual outcomes after ranibizumab treatment for macular edema resulting from retinal vein occlusion. *Ophthalmol Retina* (2020) 4(1):67–76. doi: 10.1016/j.oret.2019.08.009

18. Kim JH, Kang SW, Ha HS, Kim SJ, Kim JR. Overestimation of subfoveal choroidal thickness by measurement based on horizontally compressed optical coherence tomography images. *Graefes Arch Clin Exp Ophthalmol* (2013) 251 (4):1091–6. doi: 10.1007/s00417-012-2147-9

19. Tekin K, Inanc M, Kurnaz E, Bayramoglu E, Aydemir E, Koc M, et al. Quantitative evaluation of early retinal changes in children with type 1 diabetes mellitus without retinopathy. *Clin Exp Optometry* (2018) 101(5):680–5. doi: 10.1111/cxo.12667

20. Querques G, Lattanzio R, Querques L, Triolo G, Cascavilla ML, Cavallero E, et al. Impact of intravitreal dexamethasone implant (Ozurdex) on macular morphology and function. *RETINA* (2014) 34(2):330–41. doi: 10.1097/IAE.0b013e31829f7495

21. Shah AR, Williams S, Baumal CR, Rosner B, Duker JS, Seddon JM. Predictors of response to intravitreal anti-vascular endothelial growth factor treatment of age-related macular degeneration. *Am J Ophthalmol* (2016) 163:154–66.e8. doi: 10.1016/j.ajo.2015.11.033

22. Kim M, Park YG, Jeon SH, Choi SY, Roh YJ. The efficacy of selective retina therapy for diabetic macular edema based on pretreatment central foveal thickness. *Lasers Med Sci* (2020) 35(8):1781–90. doi: 10.1007/s10103-020-02984-6

23. Sandberg MA, Pearce EN, Harper S, Weigel-DiFranco C, Hart L, Rosner B, et al. The relationship of central foveal thickness to urinary iodine concentration in retinitis pigmentosa with or without cystoid macular edema. *JAMA Ophthalmol* (2014) 132 (10):1209–14. doi: 10.1001/jamaophthalmol.2014.1726

24. Lawali D, Wu G, Guo Y, Lin Z, Wu Q, Amza A, et al. Measurement of foveal retinal thickness in myopic patients using different display modes on optical coherence tomography: A retrospective, cross-sectional study. *Ophthalmol Ther* (2023) 12(1):167–78. doi: 10.1007/s40123-022-00584-x

25. Cho AR, Choi YJ, Kim YT. Influence of choroidal thickness on subfoveal choroidal thickness measurement repeatability using enhanced depth imaging optical coherence tomography. *Eye (Lond)* (2014) 28(10):1151–60. doi: 10.1038/eye.2014.197

26. Verma G. Standardization of cone penetrometer test method. *Int J Eng Advanced Technol (IJEAT)* (2018).

27. Kawasaki R UM, Ueno S, et al. Repeatability of manual central foveal thickness measurement using optical coherence tomography. *Jpn J Ophthalmol* (2006). doi: 10.1007/s10384-006-0223-2

28. Ruia S, Saxena S, Gemmy Cheung CM, Gilhotra JS, Lai TYY. Spectral domain optical coherence tomography features and classification systems for diabetic macular edema: A review. *Asia-Pacific J Ophthalmology* (2016) 5(5):360–7. doi: 10.1097/apo.0000000000000218

29. Koleva-Georgieva DN, Sivkova NP. Types of diabetic macular edema assessed by optical coherence tomography. *Folia Med (Plovdiv)* (2008) 50(3):30–8.

30. Markan A, Agarwal A, Arora A, Bazgain K, Rana V, Gupta V. Novel imaging biomarkers in diabetic retinopathy and diabetic macular edema. *Ther Adv Ophthalmology* (2020) 12:2515841420950513. doi: 10.1177/2515841420950513

31. Helmy YM, Atta Allah HR. Optical coherence tomography classification of diabetic cystoid macular edema. *Clin Ophthalmol* (2013) 7:1731–7. doi: 10.2147/opth.S47987

32. Sahin M, Cingü AK, Gözüm N. Evaluation of cystoid macular edema using optical coherence tomography and fundus autofluorescence after uncomplicated phacoemulsification surgery. *J Ophthalmol* (2013) 2013:376013. doi: 10.1155/2013/376013

33. Ozdek SC, Erdinç MA, Gürelik G, Aydin B, Bahçeci U, Hasanreisoğlu B. Optical coherence tomographic assessment of diabetic macular edema: comparison with fluorescein angiographic and clinical findings. *Ophthalmologica* (2005) 219(2):86–92. doi: 10.1159/000083266

34. Yalçın G, Özdek Ş, Baran Aksakal FN. Defining cystoid macular degeneration in diabetic macular edema: An OCT-based single-center study. *Turk J Ophthalmol* (2019) 49(6):315–22. doi: 10.4274/tjo.galenos.2019.22687

35. Antcliff RJ, Stanford MR, Chauhan DS, Graham EM, Spalton DJ, Shilling JS, et al. Comparison between optical coherence tomography and fundus fluorescein angiography for the detection of cystoid macular edema in patients with uveitis. *Ophthalmology* (2000) 107(3):593–9. doi: 10.1016/S0161-6420(99)00087-1

frontiers | Frontiers in Public Health

TYPE Original Research
PUBLISHED 30 January 2024
DOI 10.3389/fpubh.2024.1347671

OPEN ACCESS

EDITED BY
Kai Jin,
Zhejiang University, China

REVIEWED BY
Li Dong,
Capital Medical University, China
Jingjing Zhao,
University of Louisville, United States
Yedi Zhou,
The Second Xiangya Hospital of Central South University, China

*CORRESPONDENCE
Liang Li
liliang2925184@126.com
Tongdao Xu
xutongdao830130@163.com

†These authors have contributed equally to this work

RECEIVED 01 December 2023
ACCEPTED 17 January 2024
PUBLISHED 30 January 2024

CITATION
Wang Z, Chen D, Peng L, Wang X, Ding Q, Li L and Xu T (2024) Exposure to volatile organic compounds is a risk factor for diabetes retinopathy: a cross-sectional study. *Front. Public Health* 12:1347671. doi: 10.3389/fpubh.2024.1347671

Exposure to volatile organic compounds is a risk factor for diabetes retinopathy: a cross-sectional study

Zhi Wang[1†], Dongjun Chen[2†], Lingling Peng[1], Xian Wang[3], Qun Ding[1], Liang Li[3*] and Tongdao Xu[1*]

[1]Department of Endocrinology, The Second People's Hospital of Lianyungang, Lianyungang, China, [2]Department of Cardiac Function Examine, The Second People's Hospital of Lianyungang, Lianyungang, China, [3]Department of Ultrasonography, The Second People's Hospital of Lianyungang, Lianyungang, China

Introduction: A few past experimental studies have indicated that exposure to volatile organic compounds (VOCs) might be a potential risk factor for diabetes retinopathy (DR). However, these findings lack substantial support from extensive epidemiological research. This large-scale cross-sectional study aimed to examine whether exposure to low levels of VOCs in the general population is associated with diabetes mellitus (DM) and DR.

Methods: The analytical data was from the National Health and Nutrition Examination Survey (NHANES) dataset (2011–2018). To minimize the potential impact of gender and age on the findings, propensity score matching was utilized to align the data selection. Relationships between blood VOCs and DM and DR were assessed in a sample of 2,932 adults using the logistic regression models. Additionally, Bayesian kernel machine regression (BKMR) models and Weighted Quantile Sum (WQS) were conducted for mixture exposure analysis.

Results: The result shows VOCs were positive associated with DM and DR in US adults, as assessed by WQS model, and the calculated odd ratios (ORs) [95% confidence interval (C.I)] were 53.91(34.11~85.22) and 7.38(3.65~14.92), respectively. Among the components of VOCs, 1,2-Dibromoethane, Carbon Tetrachloride and 2,5-Dimethylfuran were positive related with the DR, and ORs (95%C.I) were 2.91(2.29~3.70), 2.86(2.25~3.65) and 2.19(1.79~2.94), respectively. BKMR model shows that there was a dose–response relationship between combined VOCs and DR, although the relationship was non-linearly.

Conclusion: This study suggested that exposure to VOCs may increase the risk of DR, which had important public health implications.

KEYWORDS

diabetes mellitus, diabetic retinopathy, volatile organic compounds, epidemiology, NHANES

1 Introduction

Diabetes mellitus (DM) is a chronic metabolic disorder characterized by high levels of blood glucose due to insufficient insulin production or impaired insulin action (1). According to the World Health Organization (WHO) and the International Diabetes Federation (IDF), in 2021, approximately 537 million adults aged 20 to 79 worldwide are affected by DM, directly contributing to 1.5 million deaths annually (2). The most prevalent complications associated with DM include diabetic nephropathy (DN) (3), diabetic retinopathy (DR) (4), and cardiovascular diseases. These complications have a significant impact on the quality of life and increase the risk of mortality in individuals with diabetes. DR, which is a common complication of DM, can cause visual impairment and blindness on a global scale (5). As the incidence of DM rapidly grows, the prevalence of DR also increases accordingly. Previous studies have shown that the occurrence rate of DR in DM patients worldwide is 34.6% (6). In China, the prevalence of DR is 1.7% in the general population and 22.4% among diabetics (7). The growing population of individuals affected by DR not only demands a substantial allocation of medical resources but also imposes a significant burden on society. Consequently, the prevention and control of DR assume paramount importance in the current era of heightened diabetes prevalence.

In recent years, there has been a surge in awareness regarding the correlation between environmental pollution and human health (8). Extensive scientific research has firmly established that DR is intricately connected to environmental changes. Notably, a study conducted by Fan Cao et al. (9) revealed that exposure to air pollution, such as $PM_{2.5}$/$PM_{0.1}$ and environmental tobacco smoke, significantly increased the occurrence of autoimmune eye diseases, including DR and Graves' ophthalmopathy. Furthermore, a comprehensive scoping review involving 27 studies found compelling evidence suggesting that air pollution could be a modifiable risk factor for chronic eye diseases (10).

Volatile organic compounds (VOCs) encompass a wide array of chemicals extensively employed as solvents, degreasers, and cleaning agents in both industrial and consumer applications (11). It has been revealed through numerous investigations that a significant number of these VOCs have contaminated groundwater, drinking water sources and indoor areas such as homes, offices and classroom where person spend most her/his time. Previous studies have highlighted the adverse effects of exposure to VOCs on human health (11, 12). A perspective review summarized the impacts of VOCs and considered that prolonged exposure to VOCs might have an effect on various physiological functions of the body, including prostate function, respiratory system, lung function levels, and sex hormone levels (11). Some studies have found that VOCs are a risk factor for DM in the US population (13, 14). However, few study was to investigate the association between VOCs and DR, and there is a lack of epidemiological evidence to support the correlation between DR and VOCs.

The National Health and Nutrition Examination Survey (NHANES) is a cross-sectional study conducted by the Centers for Disease Control and Prevention of the United States. This study collects data on the status of DR, concentrations of VOCs, and the presence of DM in the participants. By analyzing this data, we can investigate the relationship between VOCs and DR.

2 Methods

2.1 Study design and participants

The data of this cross-sectional was from the National Health and Nutrition Examination Survey (NHANES, https://www.cdc.gov/nchs/nhanes) 2011–2018. A total of 39,156 participants were recruited from four rounds of NHANES, and all participants was divided into two groups based on whether participants were diagnosed with diabetes: 3,194 cases of diabetes patients and 33,749 cases of non-diabetes patients, with 2,213 missing cases. Among all individuals, a total of 6,186 participants under the age < 20 years old, 201 women with pregnant, and 17,547 participants who had not completed the volatile organic compound metabolites (mVOCs) detection were excluded. Ultimately, 1,479 cases of diabetes patients and 11,530 cases of non-diabetes patients were included. Considering that age and gender are influencing factors for diabetes, this study utilized the PSM score method to match 1,479 cases of diabetes patients with 11,530 non-diabetes participants. A successful match was made for 1,466 pairs of patients. Therefore, a total of 2,932 patients were included in this study, with 1,466 cases of diabetes patients and 1,466 cases of non-diabetes patients (Figure 1). Among the diabetes patients, 321 individuals with diabetes and DR. All participants with this cross-section study were more than 20 years old, and the informed consents and ethical approval could be found on the web of NHANES.

2.2 Measurement of whole blood mVOCs

The measurement of mVOCs in human whole blood was carried out by capillary gas chromatography and mass spectrometry with selected-ion monitoring detection and isotope-dilution. This method quantifies levels of individual mVOCs and Trihalomethanes and methyl tert-butyl ether in whole blood to low-parts-per-trillion range. Because non-occupationally exposed individuals have blood mVOC concentrations within this range, this method is applicable for determining these quantities and investigating cases of sustained or recent low-level exposure. Detailed methods and information of mVOCs could be found on the web of NHANES. To ensure data integrity and sufficient sample size, we carefully selected 22 mVOCs (In the NHANES surveys conducted between 2011 and 2018, a total of 32 mVOCs were detected in the 2011–2012 cycle, 39 VOCs in the 2013–2014 cycle, 40 VOCs in the 2015–2016 cycle, and 40 VOCs in the 2017–2018 cycle. To increase the sample size, we combined the data from all four cycles and focused on VOCs that were consistently detected across all four cycles. As a result, a total of 22 VOCs were identified in the intersection of the four cycles, and these 22 VOCs were chosen for further analysis). The 22 mVOCs included 2,5-Dimethylfuran, 1,1,1,2-Tetrachloroethane, Hexane, 1,2-Dichlorobenzene, 1,2-Dichloroethane, 1,3-Dichlorobenzene, Tetrachloroethene, Benzene, Chlorobenzene, Carbon Tetrachloride, 1,4-Dichlorobenzene, 1,2-Dibromoethane, Ethylbenzene, Furan, Isopropylbenzene, Methylene Chloride, Nitrobenzene, o-Xylene, Trichloroethene, 1,1,1-Trichloroethane, 1,2,3-Trichloropropane and m−/p-Xylene.

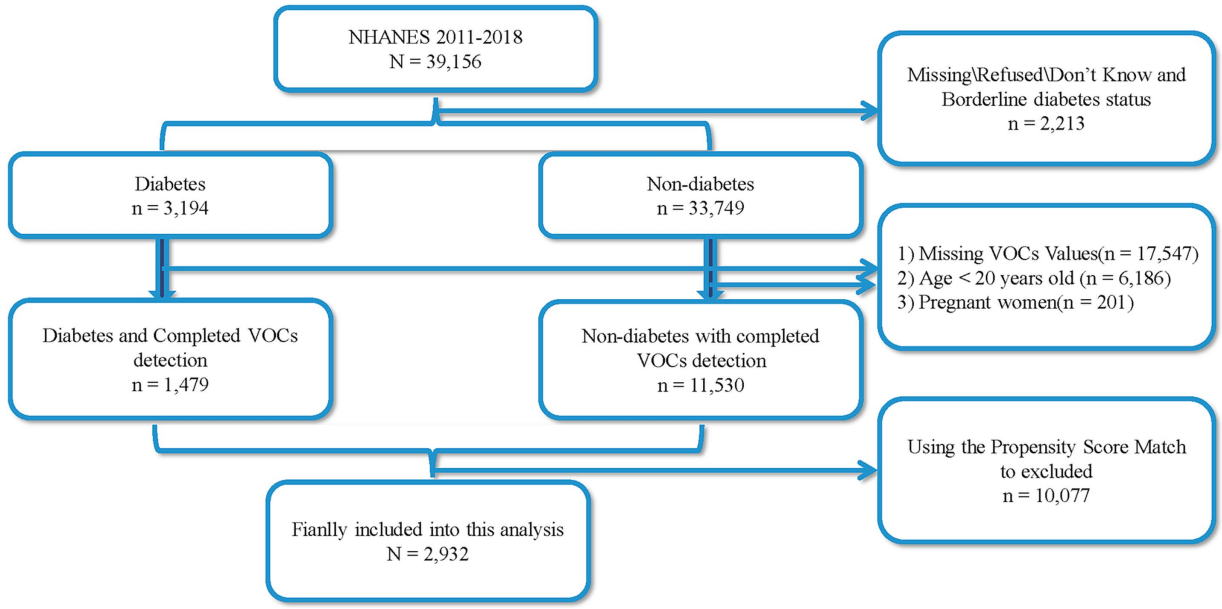

FIGURE 1
The flowchart of finally analysis participants.

2.3 Measurements of DM and DR

In the NHANES survey, there is a questionnaire specifically designed to inquire whether the participants have diabetes. The question is as follows: "{Have you/Has SP} ever been told by a doctor or health professional that {you have/{he/she/SP} has} diabetes or sugar diabetes?" If the participants respond affirmatively with a "yes," they are considered individuals with diabetes. Another question pertaining to diabetes-related complications is as follows: "Has a doctor ever told {you/SP} that diabetes has affected {your/his/her} eyes or that {you/s/he} had retinopathy?." This question aims to identify if diabetic individuals have experienced any eye-related issues. If the participants respond positively with a "yes," they are considered individuals with diabetic retinopathy.

2.4 Covariable

In this cross-sectional study, covariates, that were included in the finally analysis, were based on previous studies associated with diabetes. Age, sex, race/ethnicity and education levels were from the demographic data, body mass index (BMI) was collected from examination data.

2.5 Statistical analysis

In this study, we utilized propensity score matching (PSM) to select our study subjects. We included a total of 1,479 diabetic patients from NHANES 2011–2018. Considering the impact of age and gender on both VOCs concentrations and diabetes, we carefully matched non-diabetic patients with the diabetes group in terms of age and gender at a comparable ratio. Descriptive analysis of the data was conducted to describe the mean, proportions, and median of demographic information, mVOCs concentrations, BMI, FPG, and fasting insulin levels across different groups. The difference between the three groups was analyzed using the Chi-square test, Mann–Whitney test, and one-way ANOVA. Univariate logistic regression and weighted quantile sum (WQS) were employed to explore the association between DM and DR and individual or combined mVOCs. To investigate the joint effects of mixed pollutants between mVOCs and DM and DR, the study introduced the Bayesian kernel machine regression (BKMR) model to explore the dose–response functions. All data analyses were performed using R software (Version 4.1.3), and p-values <0.05 were considered statistically significant.

3 Results

3.1 The basic characteristic of participants

In Table 1, the characteristics of the participants and the levels of mVOCs were examined in NHANES 2011–2018. The total number of participants was 2,932, consisting of 1,466 non-diabetic individuals, 1,145 individuals with diabetes but without diabetic Retinopathy (DR), and 321 individuals with diabetes and DR. Individuals with diabetes exhibited higher body mass index (BMI) and fasting insulin levels compared to non-diabetic individuals. However, there were no significant differences in these aspects between individuals with diabetes and those with DR. Additionally, race and education levels showed significantly variations among the three groups. Regarding the mVOCs, certain components including 2,5-Dimethyfuran, 1,1,1,2-Tetrachloroethane, Benzene, Carbon Tetrachloride, 1,2-Dibromoethane, Isopropylbenzene, Nitrobenzene, and 1,2,3-Trichloropropane exhibited significant differences among the

TABLE 1 The clinical characteristic of participants.

Variables	Non-diabetes	Diabetes with non-diabetic retinopathy	Diabetes with diabetic retinopathy	*p*
n	1,466	1,145	321	
Sex (male)	770	583	187	0.067
Age (years)	61.80 ± 12.61	61.50 ± 12.81	62.85 ± 11.80	0.237
Diabetic duration (years)	~~	8.00 (4.00 ~ 15.00)	15.00 (7.50 ~ 24.50)	<0.001
BMI (kg/m2)	28.08 ± 6.17	32.34 ± 7.43	31.67 ± 6.88	<0.001
FPG (mmol/L)	5.78 ± 1.19	8.72 ± 3.42	9.03 ± 4.23	<0.001
Fasting insulin (uU/mL)	9.63 (6.15 ~ 14.79)	12.92 (7.94 ~ 22.33)	10.73 (7.74 ~ 23.24)	<0.001
Race				
Mexican American	127 (8.7%)	196 (17.1%)	52 (16.2%)	<0.001
Other Hispanic	129 (8.8%)	104 (9.1%)	37 (11.5%)	
Non-Hispanic White	614 (41.9%)	370 (32.3%)	100 (31.2%)	
Non-Hispanic Black	378 (25.8%)	306 (26.7%)	83 (25.9%)	
Non-Hispanic Asian	193 (13.2%)	133 (11.6%)	38 (11.8%)	
Other race	25 (1.7%)	36 (3.1%)	11 (3.4%)	
Education level				
Less than 9th grade	177 (12.1%)	184 (16.1%)	54 (16.8%)	0.001
9-11th grade	195 (13.3%)	160 (14.0%)	51 (15.9%)	
High school graduate	329 (22.4%)	267 (23.3%)	82 (25.5%)	
Some college or AA degree	384 (26.2%)	303 (26.5%)	78 (24.3%)	
College graduate or above	381 (26.0%)	231 (20.2%)	56 (17.4%)	
Volatile organic compounds				
2,5-Dimethylfuran (ng/L)	7.80 (7.80 ~ 26.80)	8.00 (7.80 ~ 8.00)	8.00 (7.80 ~ 8.00)	0.036
1,1,1,2-Tetrachloroethane (ng/L)	28.30 (28.30 ~ 28.30)	28.00 (28.00 ~ 28.30)	28.00 (28.00 ~ 28.30)	<0.001
Hexane (ng/L)	86.30 (86.30 ~ 86.30)	86.20 (86.00 ~ 86.30)	86.20 (86.00 ~ 86.30)	0.638
1,2-Dichlorobenzene (ng/L)	17.70 (17.70 ~ 17.70)	18.00 (17.70 ~ 18.80)	18.00 (17.70 ~ 18.00)	0.926
1,2-Dichloroethane (ng/L)	7.10 (7.10 ~ 7.10)	7.08 (7.00 ~ 7.10)	7.08 (7.00 ~ 7.10)	0.631
1,3-Dichlorobenzene (ng/L)	17.70 (17.70 ~ 17.70)	18.00 (18.00 ~ 18.00)	18.00 (17.70 ~ 18.00)	0.074
Tetrachloroethene (ng/L)	33.90 (33.90 ~ 55.00)	34.00 (33.90 ~ 34.00)	34.00 (33.90 ~ 34.00)	0.392
Benzene (ng/L)	17.00 (17.00 ~ 57.39)	17.00 (17.00 ~ 52.00)	17.00 (17.00 ~ 44.00)	0.023
Chlorobenzene (ng/L)	7.80 (7.80 ~ 7.80)	8.00 (7.80 ~ 8.00)	8.00 (7.80 ~ 8.00)	0.126
Carbon Tetrachloride (ng/L)	3.50 (3.50 ~ 3.50)	4.00 (3.50 ~ 4.00)	4.00 (3.50 ~ 4.00)	<0.001
1,4-Dichlorobenzene (ng/L)	65.50 (28.30 ~ 633.50)	42.00 (28.00 ~ 273.00)	63.00 (28.30 ~ 542.00)	0.366
1,2-Dibromoethane (ng/L)	10.60 (10.60 ~ 10.60)	11.00 (10.60 ~ 11.00)	11.00 (10.60 ~ 11.00)	<0.001
Ethylbenzene (ng/L)	17.00 (17.00 ~ 48.65)	17.00 (17.00 ~ 36.00)	17.00 (17.00 ~ 28.00)	0.470
Furan (ng/L)	17.00 (17.00 ~ 27.14)	18.00 (17.70 ~ 18.00)	18.00 (17.70 ~ 18.00)	0.129
Isopropylbenzene (ng/L)	28.30 (28.30 ~ 28.30)	28.00 (28.00 ~ 28.30)	28.00 (28.00 ~ 28.32)	0.007
Methylene Chloride (ng/L)	176.80 (176.80 ~ 176.80)	177.00 (176.80 ~ 177.00)	177.00 (176.80 ~ 177.00)	0.451
Nitrobenzene (ng/L)	226.30 (226.30 ~ 226.30)	226.00 (226.00 ~ 226.30)	226.00 (226.00 ~ 266.30)	<0.001
o-Xylene (ng/L)	17.00 (17.00 ~ 38.58)	17.00 (17.00 ~ 32.00)	17.00 (17.00 ~ 28.00)	0.410
Trichloroethene (ng/L)	8.50 (8.50 ~ 8.50)	8.00 (8.00 ~ 8.50)	8.00 (8.00 ~ 8.50)	0.658
1,1,1-Trichloroethane (ng/L)	7.10 (7.10 ~ 7.10)	7.06 (7.00 ~ 7.10)	7.00 (7.00 ~ 7.10)	0.553
1,2,3-Trichloropropane (ng/L)	28.30 (28.30 ~ 28.30)	28.00 (28.00 ~ 28.30)	28.00 (28.00 ~ 28.30)	<0.001
m−/p-Xylene (ng/L)	72.00 (40.50 ~ 123.78)	49.00 (24.00 ~ 110.00)	50.00 (24.00 ~ 96.00)p	0.219

BMI, body mass index; FPG, fasting plasma glucose.

three groups. While, the levels of 14 other components did not show any noticeable distinctions.

3.2 Association of the risk of DM and DR with single VOCs levels and union mVOCs

In the initial step, we observed distinct levels of eight VOC components among the three groups. Subsequently, logistic regression was employed to examine the relationship between individual VOCs and the risk of DM and DR. Additionally, the WQS was utilized to assess the association between combined VOC levels and the risk of DM and DR development. Prior to analysis, the data type of VOCs was transformed into a binary variable based on the respective median values. In Figure 2A, we observed a negative correlation between the risk of DM and the presence of 1,2,3-Trichloropropane, Nitrobenzene, Isopropylbenzene, and 1,1,1,2-Tetrachloroethane, and the odds ratios (ORs) and 95% confidence interval (C.I) were 0.02(0.01 ~ 0.03), 0.02(0.01 ~ 0.03), 0.59(0.47 ~ 0.75) and 0.02(0.01 ~ 0.03), respectively. Conversely, we found a positive association between the risk of DM and the presence of 1,2-Dibromoethane, Carbon Tetrachloride, and 2,5-Dimethylfuran, and ORs and 95%C.I were 7.85(6.59 ~ 9.37), 7.15(6.04 ~ 8.50) and 4.18(3.58 ~ 4.89), respectively. Furthermore, the WQS indicated that higher levels of combined mVOCs were positively associated with an increased risk of DM after adjusting for sex, age, education levels, race/ethnicity and BMI, with an OR of 53.91 (95% C.I,34.11 ~ 85.22). In Figure 2B, we found that there was a negative association of the risk of DR with the presence of 1,2,3-Trichloropropane, Nitrobenzene and 1,1,1,2-Tetrachloroethane, and ORs (95%C.I) were 0.31(0.24 ~ 0.39), 0.30(0.23 ~ 0.38) and 0.30(0.24 ~ 0.38), respectively. 1,2-Dibromoethane, Carbon Tetrachloride and 2,5-Dimethylfuran were positive related with the risk of DR, and ORs (95%C.I) were 2.91(2.29 ~ 3.70), 2.86(2.25 ~ 3.65) and 2.19(1.79 ~ 2.94), respectively. There was no significant relationship of Benzene and Isopropylbenzene with the risk of DR. We also explored the association between the combined mVOCs and the risk of DR using WQS after adjusting for sex, age, education levels, race/ethnicity and BMI, and found that there was a positive association with OR of 7.38 (95%CI,3.65 ~ 14.92).

3.3 The exposure-response effect of VOCs on DM and DR

The BKMR model was utilized to examine the relationship between mVOCs and the development of DM or DR. The model was

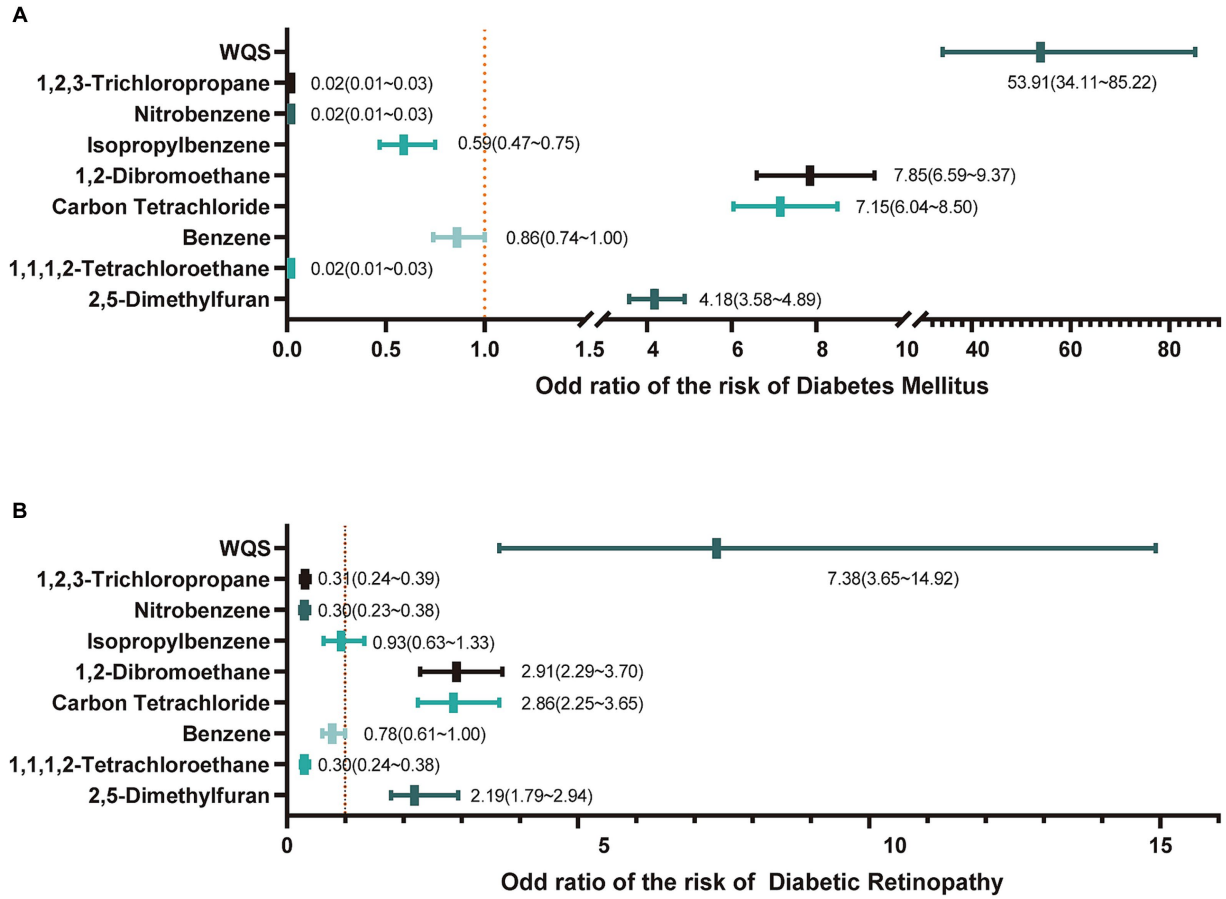

FIGURE 2
The relationship of mVOCs with diabetes mellitus and diabetic retinopathy. **(A)** The odd ratio of mVOCs on the risk of diabetes mellitus. WQS, weighted quantile sum; **(B)** The odd ratio of mVOCs on the risk of diabetic retinopathy.

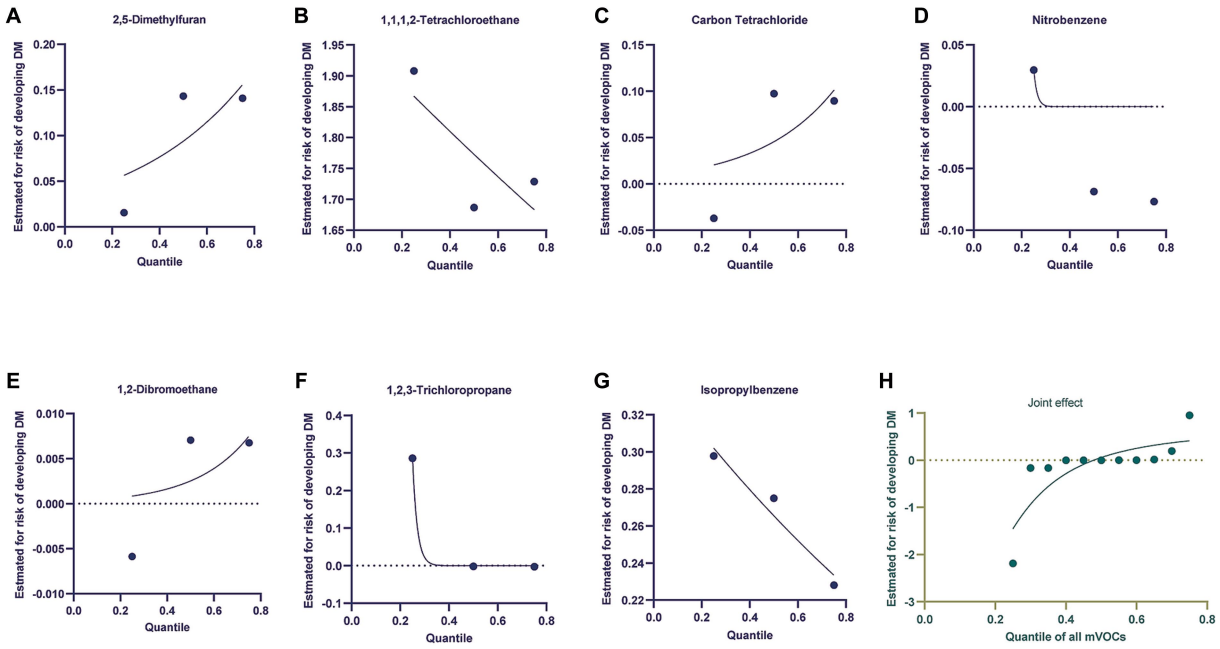

FIGURE 3
Using the Bayesian kernel machine regression (BKMR) model to investigate the exposure-response functions between mVOCs and diabetes mellitus. **(A–G)** Depicted the individual VOCs and their corresponding exposure-response functions in relation to diabetes mellitus. **(H)** The joint effect of mVOCs on diabetic mellitus.

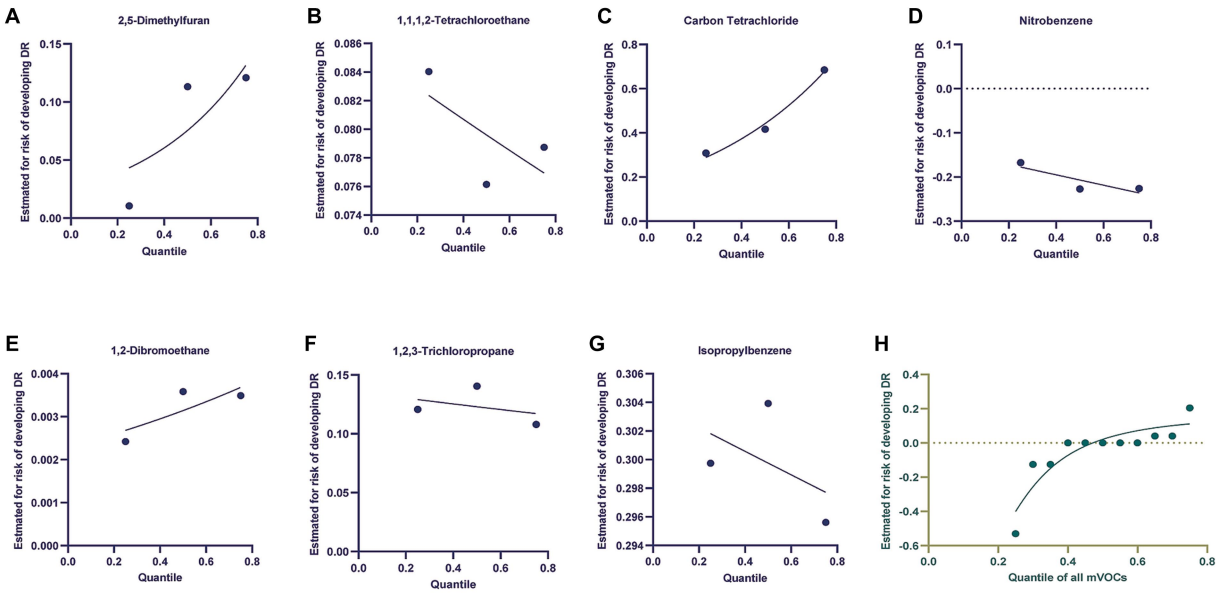

FIGURE 4
Using the Bayesian kernel machine regression (BKMR) model to investigate the exposure-response functions between mVOCs and diabetic retinopathy. **(A–G)** Depicted the individual VOCs and their corresponding exposure-response functions in relation to diabetic retinopathy. **(H)** The joint effect of mVOCs on diabetic retinopathy.

adjusting for sex, age, BMI, education levels and race/ ethnicity. When observing Figure 3, it was discovered that the likelihood of DM escalated as the level of mVOCs increased. Furthermore, the individual exposures to 2,5-Dimethylfuran, Carbon Tetrachloride, and 1,2-Dibromoethane exhibited a positive correlation with the risk of DM. Negative exposure-response association was observed between 1,1,1,2-Tetrachloroethane, Nitrobenzene, 1,2,3-Trichloropropane, Isopropylbenzene and the risk of DM. Figure 4 showed the univariate and joint exposure-response functions of mVOC and DR. A significant positive exposure-response relationship was observed

between 2,5-Dimethylfuran, Carbon Tetrachloride, 1,2-Dibromoethane and the risk of DR. Negative exposure-response association was observed between 1,1,1,2-Tetrachloroethane, Nitrobenzene, 1,2,3-Trichloropropane, Isopropylbenzene and the risk of DR.

4 Discussion

In this comprehensive cross-sectional epidemiological study, we have identified an exposure-response relationship between VOCs and both DM and DR. The findings of this study provide epidemiologic evidence supporting a significant association between VOCs and the increased risk of DR. Although VOCs are widely recognized as common environmental pollutants with known adverse effects on the body, their connection to diabetes and its related DR has remained unclear, necessitating further investigation. In this present study, the WQS regression and BKMR model were suggested that the joint effect of VOCs was positive associated with DM and DR.

Several prior studies have attempted to elucidate the particular mechanisms through which environmental pollutants impact DM and its complications (15), insulin resistance (16) and plasma fasting glucose levels (17). However, numerous unexplored mechanisms still remain in need of investigation. Specifically, how environmental pollutants contribute to retinal microvascular changes and neuropathy in individuals with diabetes. A review conducted by Rao et al. summarized the relationship between air pollution and type 2 diabetes. It highlighted the experimental studies supporting this association, specifically focusing on tissues involved in the pathogenesis of T2DM, such as the immune system, adipose tissue, liver, and central nervous system (18). The development of DR is an intricate process involving a multitude of molecules and biochemical mechanisms (19). Research has indicated that the activation of protein kinase C (20), small GTP-binding proteins (21), and the mitogen-activated protein kinase pathway (22), along with the responses of oxidative stress (23) and endoplasmic reticulum stress, are all mechanisms associated with and contributing to the onset of DR. In these mechanisms, oxidative stress should be given sufficient attention. Research shows that the retina is rich in polyunsaturated fatty acids, has a high capacity for oxygen intake and glucose consumption, and is more susceptible to damage from oxidative stress compared to other tissues (24). Chen et al. (25) conducted a study involving 454 patients diagnosed with gestational diabetes mellitus (GDM) and 454 healthy controls. The researchers measured the concentrations of urinary VOCs as well as oxidative stress markers (8-OHdG, 8-OHG, and HNEMA) for each participant and the findings unveiled a noteworthy positive association between VOCs and oxidative stress markers, implying the involvement of VOCs in the body's response to oxidative stress.

In fact, numerous components of VOCs exhibit a strong correlation with oxidative stress (26). In several experimental settings, Carbon Tetrachloride (CCl4) is commonly employed as an agent to induce liver injury (27). This is attributed to CCl4 undergoing metabolism in the liver through cytochrome P450 superfamily monooxygenases (CYP family), resulting in the generation of trichloromethyl free radical (CCl3*). Subsequently, those free radical initiates lipid peroxidation reactions, leading to the production of peroxides that specifically target mitochondria and inflict damage upon hepatocyte membranes. Ultimately, this damaging process contributes to the development of liver fibrosis (28). In our current study, we have discovered a positive correlation between CCl4 and the risk of DR. This finding indicates that CCl4 induces oxidative stress in the retina and elevates the likelihood of DR. The European Food Safety Authority (29) conducted an assessment on the safety of furan and methylfurans in food. Their findings revealed that 2,5-Dimethylfuran exhibits hepatotoxicity in rats, with various mechanisms being implicated including oxidative stress, gene expression modifications, epigenetic fluctuations, inflammation, and enhanced cell proliferation. Pal et al. (30). conducted a comprehensive study to assess the fluctuations in the concentrations of 38 VOCs in urine samples collected from a group of 19 healthy individuals over a 44-day period. Their findings revealed significant and positive correlations between the concentrations of VOCs and oxidative stress biomarkers, including lipid, protein, and DNA damage. However, in our findings, some compounds of VOCs have a negative relationship with the risk of DR, such as 1,1,1,2-Tetrachloroethane, Nitrobenzene, 1,2,3-Trichloropropane and Isopropylbenzene. This phenomenon suggests that the association between VOCs and DR is not a straightforward one. As the concentration of a particular pollutant rises within the body, the body initiates compensatory responses to counteract and mitigate the adverse impacts brought about by that pollutant. Moreover, it is inadequate to assess the individual effects of VOCs components on the human body separately, given that people in the real world are exposed to a myriad of pollutants. Instead, it is essential to evaluate the cumulative impact of a specific category of pollutants on human health. In this study, we observed a positive correlation between the concentration of VOCs extracted from blood samples and the risk of DR, and our study employed propensity score matching to mitigate the influence of age and gender on the findings, and the analysis of the overall impact of VOCs using WQS and BKRM models is also deemed reliable. In our results, we found that race and education levels were significantly difference among three groups. It is well known that race was a risk factor of DM and DR. DM is a multifaceted condition that is influenced by a combination of environmental and genetic factors. The diverse genetic backgrounds present in different ethnic groups can contribute to varying incidence rates of DM (31). In general, there is a positive correlation between educational background, economic income, and cultural level (32). Individuals with higher levels of education are more likely to be aware of the potential risks that diseases can pose and have greater resources to prevent and control them.

Some previous studies reported the association between VOCs and the risk of DM using NHANES dataset (13, 14), however, few study was to explore the relationship between VOCs and the risk of DR. We hypothesize that there could be multiple factors contributing to this observation. Firstly, the number of individuals with DR in the NHANES database is relatively limited compared to the overall diabetic population, which is a constraint of this study. Secondly, DR is recognized as a complication of diabetes, and if there is evidence linking VOCs to diabetes, it is plausible that VOCs may indirectly influence the occurrence and progression of DR through their impact on blood glucose levels. Nevertheless, we acknowledge that susceptibility to DR may also play a role, necessitating further comprehensive investigation.

Some limitations should be stated in this study. Firstly, it should be noted that this is a cross-sectional analysis, which means

we cannot verify the causal association between exposure to VOCs and the risk of DR. Secondly, it is to mention that the participants in this study were solely Americans, and thus our findings need further validation in other countries. Finally, we used the propensity score matching to reduce the confounding effect of sex and age, but this method may result in sample attrition. Nonetheless, we believe that using propensity score matching in cross-sectional studies is still necessary.

5 Conclusion

We conducted a comprehensive investigation into the relationship between multiple blood VOCs and DM and DR using data from the NHANES 2011–2018. A total of 2,932 US adults with complete data participated in this study. Our analyses, utilizing WQS and BKMR models, revealed a positive association between multiple blood VOCs and both diabetes and DR. Notably, increased concentrations of CCl4 were significantly and positively correlated with the presence of DR. Furthermore, co-exposure to multiple VOCs exhibited a positive correlation with DR, with the majority of VOCs demonstrating a nonlinear relationship with diabetes and DR. While our study suggests a connection between VOCs exposure and DR, more evidence is required to substantiate these findings.

Data availability statement

The original contributions presented in the study are included in the article/supplementary material, further inquiries can be directed to the corresponding authors.

Ethics statement

The studies involving humans were approved by the ethics committee of the second people's hospital of Lianyungang. The studies were conducted in accordance with the local legislation and institutional requirements. The participants provided their written informed consent to participate in this study.

Author contributions

ZW: Investigation, Methodology, Writing – original draft. DC: Data curation, Software, Validation, Visualization, Writing – review & editing. LP: Formal analysis, Visualization, Writing – review & editing. XW: Investigation, Software, Visualization, Writing – review & editing. QD: Investigation, Software, Visualization, Writing – review & editing. LL: Conceptualization, Methodology, Project administration, Visualization, Writing – original draft, Writing – review & editing. TX: Conceptualization, Project administration, Writing – review & editing.

Funding

The author(s) declare that no financial support was received for the research, authorship, and/or publication of this article.

Acknowledgments

The authors would like to thank all participants for their cooperation and sample contributions and all the reviewers who participated in the review.

Conflict of interest

The authors declare that the research was conducted in the absence of any commercial or financial relationships that could be construed as a potential conflict of interest.

Publisher's note

References

1. Soares Andrade CA, Shahin B, Dede O, Akpeji AO, Ajene CL, Albano Israel FE, et al. The burden of type 2 diabetes mellitus in states of the European Union and United Kingdom at the national and subnational levels: a systematic review. *Obes Rev*. (2023) 24:e13593. doi: 10.1111/obr.13593

2. Aschner P, Karuranga S, James S, Simmons D, Basit A, Shaw JE, et al. The international diabetes Federation's guide for diabetes epidemiological studies. *Diabetes Res Clin Pract*. (2021) 172:108630. doi: 10.1016/j.diabres.2020.108630

3. Jadawji C, Crasto W, Gillies C, Kar D, Davies MJ, Khunti K, et al. Prevalence and progression of diabetic nephropathy in south Asian, white European and African Caribbean people with type 2 diabetes: a systematic review and meta-analysis. *Diabetes Obes Metab*. (2019) 21:658–73. doi: 10.1111/dom.13569

4. Simo R, Stitt AW, Gardner TW. Neurodegeneration in diabetic retinopathy: does it really matter? *Diabetologia*. (2018) 61:1902–12. doi: 10.1007/s00125-018-4692-1

5. Simo-Servat O, Hernandez C, Simo R. Diabetic retinopathy in the context of patients with diabetes. *Ophthalmic Res*. (2019) 62:211–7. doi: 10.1159/000499541

6. Sun XJ, Zhang GH, Guo CM, Zhou ZY, Niu YL, Wang L, et al. Associations between psycho-behavioral risk factors and diabetic retinopathy: NHANES (2005–2018). *Front Public Health*. (2022) 10:966714. doi: 10.3389/fpubh.2022.966714

7. Song P, Yu J, Chan KY, Theodoratou E, Rudan I. Prevalence, risk factors and burden of diabetic retinopathy in China: a systematic review and meta-analysis. *J Glob Health*. (2018) 8:010803. doi: 10.7189/jogh.08.010803

8. Liu Y, Xiao M, Huang K, Cui J, Liu H, Yu Y, et al. Phthalate metabolites in breast milk from mothers in southern China: occurrence, temporal trends, daily intake, and risk assessment. *J Hazard Mater*. (2024) 464:132895. doi: 10.1016/j.jhazmat.2023.132895

9. Cao F, Liu ZR, Ni QY, Zha CK, Zhang SJ, Lu JM, et al. Emerging roles of air pollution and meteorological factors in autoimmune eye diseases. *Environ Res*. (2023) 231:116116. doi: 10.1016/j.envres.2023.116116

10. Millen AE, Dighe S, Kordas K, Aminigo BZ, Zafron ML, Mu L. Air pollution and chronic eye disease in adults: a scoping review. *Ophthalmic Epidemiol*. (2023) 31:1–10. doi: 10.1080/09286586.2023.2183513

11. Zhou X, Zhou X, Wang C, Zhou H. Environmental and human health impacts of volatile organic compounds: a perspective review. *Chemosphere*. (2023) 313:137489. doi: 10.1016/j.chemosphere.2022.137489

12. Liu N, Bu Z, Liu W, Kan H, Zhao Z, Deng F, et al. Health effects of exposure to indoor volatile organic compounds from 1980 to 2017: a systematic review and meta-analysis. *Indoor Air*. (2022) 32:e13038. doi: 10.1111/ina.13038

13. Wang X, He W, Wu X, Song X, Yang X, Zhang G, et al. Exposure to volatile organic compounds is a risk factor for diabetes: a cross-sectional study. *Chemosphere*. (2023) 338:139424. doi: 10.1016/j.chemosphere.2023.139424

14. Duan X, Chen Z, Xia C, Zhong R, Liu L, Long L. Increased levels of urine volatile organic compounds are associated with diabetes risk and impaired glucose homeostasis. *J Clin Endocrinol Metab*. (2023) 109:e531–42. doi: 10.1210/clinem/dgad584

15. Liu XK, Si SW, Ye Y, Li JY, Lyu HH, Ma YM, et al. The link between exposure to phthalates and type 2 diabetes mellitus: a study based on NHANES data and Bioinformatic analysis. *Biomed Environ Sci*. (2023) 36:892–6. doi: 10.3967/bes2023.115

16. Letellier N, Yang JA, Cavaillès C, Casey JA, Carrasco-Escobar G, Zamora S, et al. Aircraft and road traffic noise, insulin resistance, and diabetes: the role of neighborhood socioeconomic status in San Diego County. *Environ Pollut*. (2023) 335:122277. doi: 10.1016/j.envpol.2023.122277

17. Tan Q, Wang B, Ye Z, Mu G, Liu W, Nie X, et al. Cross-sectional and longitudinal relationships between ozone exposure and glucose homeostasis: exploring the role of systemic inflammation and oxidative stress in a general Chinese urban population. *Environ Pollut*. (2023) 329:121711. doi: 10.1016/j.envpol.2023.121711

18. Rao X, Patel P, Puett R, Rajagopalan S. Air pollution as a risk factor for type 2 diabetes. *Toxicol Sci*. (2015) 143:231–41. doi: 10.1093/toxsci/kfu250

19. Sadikan MZ, Abdul Nasir NA, Lambuk L, Mohamud R, Reshidan NH, Low E, et al. Diabetic retinopathy: a comprehensive update on in vivo, in vitro and ex vivo experimental models. *BMC Ophthalmol*. (2023) 23:421. doi: 10.1186/s12886-023-03155-1

20. Yumnamcha T, Guerra M, Singh LP, Ibrahim AS. Metabolic dysregulation and neurovascular dysfunction in diabetic retinopathy. *Antioxidants (Basel)*. (2020) 9:9. doi: 10.3390/antiox9121244

21. Lu Q, Lu L, Chen W, Chen H, Xu X, Zheng Z. RhoA/mDia-1/profilin-1 signaling targets microvascular endothelial dysfunction in diabetic retinopathy. *Graefes Arch Clin Exp Ophthalmol*. (2015) 253:669–80. doi: 10.1007/s00417-015-2985-3

22. Zhang H, Zhang X, Li H, Wang B, Chen P, Meng J. The roles of macrophage migration inhibitory factor in retinal diseases. *Neural Regen Res*. (2024) 19:309–15. doi: 10.4103/1673-5374.379020

23. Zhang SM, Fan B, Li YL, Zuo ZY, Li GY. Oxidative stress-involved Mitophagy of retinal pigment epithelium and retinal degenerative diseases. *Cell Mol Neurobiol*. (2023) 43:3265–76. doi: 10.1007/s10571-023-01383-z

24. Hussain A, Ashique S, Afzal O, Altamimi MA, Malik A, Kumar S, et al. A correlation between oxidative stress and diabetic retinopathy: an updated review. *Exp Eye Res*. (2023) 236:109650. doi: 10.1016/j.exer.2023.109650

25. Chen S, Wan Y, Qian X, Wang A, Mahai G, Li Y, et al. Urinary metabolites of multiple volatile organic compounds, oxidative stress biomarkers, and gestational diabetes mellitus: association analyses. *Sci Total Environ*. (2023) 875:162370. doi: 10.1016/j.scitotenv.2023.162370

26. Sambiagio N, Berthet A, Wild P, Sauvain JJ, Auer R, Schoeni A, et al. Associations between urinary biomarkers of oxidative stress and biomarkers of tobacco smoke exposure in smokers. *Sci Total Environ*. (2022) 852:158361. doi: 10.1016/j.scitotenv.2022.158361

27. Teschke R, Xuan TD. Heavy metals, halogenated hydrocarbons, phthalates, glyphosate, Cordycepin, alcohol, drugs, and herbs, assessed for liver injury and mechanistic steps. *Front Biosci (Landmark Ed)*. (2022) 27:314. doi: 10.31083/j.fbl2711314

28. Lin Y, Chen XJ, Li JJ, He L, Yang YR, Zhong F, et al. A novel type lavandulyl flavonoid from *Sophora flavescens* as potential anti-hepatic injury agent that inhibit TLR2/NF-κB signaling pathway. *J Ethnopharmacol*. (2023) 307:116163. doi: 10.1016/j.jep.2023.116163

29. EFSA Panel on Contaminants in the Food Chain (CONTAM)Knutsen HK, Alexander J, Barregård L, Bignami M, Brüschweiler B, et al. Risks for public health related to the presence of furan and methylfurans in food. *EFSA J*. (2017) 15:e05005. doi: 10.2903/j.efsa.2017.5005

30. Pal VK, Li AJ, Zhu H, Kannan K. Diurnal variability in urinary volatile organic compound metabolites and its association with oxidative stress biomarkers. *Sci Total Environ*. (2022) 818:151704. doi: 10.1016/j.scitotenv.2021.151704

31. Brannon GE, Kindratt TB, Boateng GO, Sankuratri BYV, Brown KK. Racial and ethnic disparities in patient experience and diabetes self-management among nonpregnant women of childbearing age with diabetes in the United States: a scoping review, 1990 to 2020. *Womens Health Issues*. (2024) 34:26–35. doi: 10.1016/j.whi.2023.08.004

32. Chen Y, Du J, Zhou N, Song Y, Wang W, Hong X. Prevalence, awareness, treatment and control of dyslipidaemia and their determinants: results from a population-based survey of 60 283 residents in eastern China. *BMJ Open*. (2023) 13:e075860. doi: 10.1136/bmjopen-2023-075860

frontiers | Frontiers in Endocrinology

TYPE Clinical Trial
PUBLISHED 22 February 2024
DOI 10.3389/fendo.2024.1286736

OPEN ACCESS

EDITED BY
Wenbin Wei,
Capital Medical University, China

REVIEWED BY
Tingting Liu,
Shandong Eye Institute, China
John Vincent Forrester,
University of Aberdeen, United Kingdom
Changzheng Chen,
Renmin Hospital of Wuhan University, China

*CORRESPONDENCE
Hong Wang
dr.wanghong@163.com

†These authors have contributed equally to this work and share first authorship

RECEIVED 31 August 2023
ACCEPTED 25 January 2024
PUBLISHED 22 February 2024

CITATION
Li S, Tao Y, Yang M, Zhao H, Si M, Cui W and Wang H (2024) Aflibercept 5+PRN with retinal laser photocoagulation is more effective than retinal laser photocoagulation alone and aflibercept 3+PRN with retinal laser photocoagulation in patients with high-risk proliferative diabetic retinopathy and diabetic macular edema: a 12-month clinical trial. *Front. Endocrinol.* 15:1286736. doi: 10.3389/fendo.2024.1286736

Aflibercept 5+PRN with retinal laser photocoagulation is more effective than retinal laser photocoagulation alone and aflibercept 3+PRN with retinal laser photocoagulation in patients with high-risk proliferative diabetic retinopathy and diabetic macular edema: a 12-month clinical trial

Shuting Li[1†], Yuan Tao[2†], Mengyao Yang[1], Hui Zhao[1], Mingwei Si[1], Wenxuan Cui[1] and Hong Wang[1*]

[1]Department of Ophthalmology, Qilu Hospital of Shandong Province, Jinan, China, [2]Department of Ophthalmology, The Second People's Hospital of Jinan, Jinan, China

Objective: This study aimed to investigate and compare the efficacy and safety of retinal laser photocoagulation (PRP) alone, PRP with aflibercept 3+PRN, and PRP with aflibercept 5+PRN in patients with both high-risk proliferative diabetic retinopathy (PDR) and diabetic macular edema (DME).

Methods: Overall, 170 patients with high-risk PDR and DME (170 eyes from 170 patients) who visited our ophthalmology clinic from December 2018 to December 2020 were divided into the PRP (n=58), aflibercept 5+PRN with PRP (n=53), and aflibercept 3+PRN with PRP (n= 59) groups. General information, such as age, sex, and eye category, was obtained. Moreover, best-corrected visual acuity (BCVA), baseline central macular foveal thickness (CFT), microaneurysm (MA), area of neovascularization (NV), area of hard exudate (HE), and cytokine levels in atrial fluid before and after treatment, were assessed. The χ^2 test was used for comparison between groups for statistical data. Analysis of variance was used for the statistical description of measurement data, independent samples were analyzed using Student's *t*-test, and Student–Newman–Keuls test was used for group comparisons. Differences were considered statistically significant at $P < 0.05$.

Results: After treatment, no significant improvement in the BCVA (logMAR) of patients in the PRP group was observed. The BCVA (log MAR) decreased from 0.72 ± 0.17 and 0.74 ± 0.17 to 0.50 ± 0.13 and 0.53 ± 0.17 in PRP with aflibercept 5+PRN and PRP with aflibercept 3+PRN groups, respectively, with a statistically significant difference compared to those in the PRP group ($P<0.05$ in all cases).

However, no statistically significant difference was observed between the combined treatment groups (P>0.05). The CFT in the PRP-only group decreased slightly from 361.80 ± 36.70 μm to 353.86 ± 40.88 μm, with no statistically significant difference (P>0.05), whereas the CFT in the aflibercept 5+PRN with PRP and aflibercept 3+PRN with PRP groups decreased from 356.57 ± 37.57 μm and 358.17 ± 44.66 μm to 284.87 ± 31.52 μm and 303.19 ± 37.00 μm, respectively, with statistically significant differences before and after treatment (P<0.05 for both groups). Statistically significant differences were observed in CFT between the three groups after treatment (P<0.05 in all cases). The number of MA (pcs) in the PRP, aflibercept 5+PRN with PRP, and aflibercept 3+PRN with PRP groups decreased from 118.34 ± 27.96, 118.60 ± 33.34, and 116.59 ± 28.95 to 92.95 ± 29.04, 44.60 ± 20.73, and 54.26 ± 25.43, respectively. The two-way comparison of the three groups revealed statistically significant differences in MA (P<0.05 in all cases). In the three groups, NV decreased from 1.00 ± 0.21 mm^2, 1.01 ± 0.18 mm^2, and 0.98 ± 0.20 mm^2 before treatment to 0.49 ± 0.17 mm^2, 0.31 ± 0.16 mm^2, and 0.38 ± 0.14 mm^2, respectively, with statistically significant differences (P<0.05 in all cases). After 12 months of treatment, 13, 18, and 18 patients had reduced HE area in the PRP-only, aflibercept 5+PRN with PRP, and aflibercept 3+PRN with PRP groups, respectively, with statistically significant differences (P<0.05 in all cases). After 12 months of treatment, vascular endothelial growth factor, monocyte chemoattractant protein-1, and glial fibrilliary acidic protein levels (pg/mL) in the aqueous humor decreased in both combined treatment groups compared with that at baseline, with statistically significant differences; however, no significant difference was observed between the two combined treatment groups (P>0.05).

Conclusion: Aflibercept 5+PRN combined with PRP was safe and effective in treating patients with high-risk PDR and DME, and was more effective than PRP-only and aflibercept 3+PRN with PRP in improving CFT and MA.

KEYWORDS

aflibercept, retinal laser photocoagulation, diabetic retinopathy, cytokines, microaneurysm

1 Introduction

Diabetes mellitus (DM) is a metabolic disease predominantly characterized by hyperglycemia. Generally, DM is caused by insufficient insulin secretion in the body; however, the other biological mechanisms remain unclear. Long-term illness in patients with DM damages various organs in the body, such as the eyes, kidneys, and heart, seriously affecting organ function. Nowadays, the quality of life of people has improved significantly, eating habits have changed, sugar intake is increasing, and the number of patients with DM is increasing. Statistics show that in 2017, the number of patients with DM worldwide reached 425 million (aged 20–79 years), which will exceed 600 million in 30 years; moreover, patients in low- and middle-income countries, such as China and India, account for 80 percent of the total DM population (1). According to the WHO, patients with DM worldwide increased to 366 million in 2011, which is expected to increase to 500 million in 2025, with more than 150 million patients experiencing ocular complications, such as diabetic retinopathy (DR) (2, 3). DR is a form of ocular microangiopathy and the most serious DM-related complication; it seriously endangers the health of patients with DM (4). DR pathogenesis includes increased endothelial cells in the eye capillaries, increased intimal thickness, damaged pericytes, microangioma, and damaged blood-retina barrier due to increased permeability of the blood vessels, microvascular obstruction, and neovascularization (NV) (5, 6). Currently, the prevalence of DR is 34.6% worldwide; however, it is higher in some developed countries, reaching 40.3% (7). The proportion of patients with type 1 and 2 DM suffering from blindness due to DR is 3.6% and 1.6%, respectively (8). DR is associated with significantly reduced living standards, huge medical costs, and increased social burden (9, 10).

Many anti-vascular endothelial growth factor (VEGF) drugs exist; however, the use of therapeutic drugs is strictly controlled. The main drugs recommended for treating DM-related visual complications are ranibizumab and aflibercept. However, the

aflibercept 3 + PRN or 5 + PRN program is less effective for treating DR worldwide. Determining a standardized loading dose and administration interval for the intravitreal injection of aflibercept for DR treatment is challenging. In cases of deteriorated retinal anatomy and function, the administration interval needs to be shortened. Therefore, this study aimed to compare the safety and efficacy of retinal laser photocoagulation (PRP) and PRP with intravitreal injection of aflibercept (3 + PRN or 5 + PRN) for patients with high-risk proliferative DR (PDR).

2 Materials and methods

2.1 Study participants

2.1.1 Population data statistics

This study included 170 ophthalmology outpatients diagnosed with high-risk PDR through detection techniques, such as visual acuity, intraocular pressure, slit lamp, fundus photography, ocular B ultrasound, optical coherence tomography (OCT), and fundus fluorescence angiography at the Qilu Hospital of Shandong University between December 2018 and December 2020. According to their treatment regimen, the patients were divided into the laser (n=58; men: women=30:28; mean age=66.7 ± 3.9 years; right eye=29 [50%]; left eye=29 [50%]), aflibercept 5 + PRN intravitreal injection with PRP (n=53; men: women=28:25; mean age=65.2 ± 4.5 years), and aflibercept 3 + PRN intravitreal injection with PRP (n=59; men: women=28:31; age=67.8 ± 3.7 years; right eye=27 [50.9%]; left eye= 26 [49.1%]) groups. Each group was followed up for 12 months (Table 1). This study was conducted in accordance with the Declaration of Helsinki and approved by the Medical Ethical Review Committee of Qilu Hospital of Shandong University (Approval Letter No.: 2019091). All the patients provided written informed consent.

2.1.2 Diagnostic criteria for high-risk PDR

The concept of high-risk PDR emerged in 1991 and was proposed by the early treatment diabetic retinopathy study (ETDRS) research group [104]. According to DR treatment guidelines in China, high-risk PDR is defined as NV of the disc of > 1/4–1/3 disc diameter (DD) or NV elsewhere in the retina of > 1/2 DD, accompanied by pre-retinal or vitreous hemorrhage. High-risk PDR should be treated timely with PRP [105]. This study used the definition of high-risk PDR in the 2014 Chinese guidelines for clinical diagnosis and treatment of DR.

2.1.3 Inclusion criteria

The inclusion criteria included: patients with DR at high risk of PDR; patients whose OCT showed a central retinal thickness (CRT) of 250 μm or a best-corrected visual acuity (BCVA) 25~73 ETDRS letters; no vitreous hemorrhage, retinal detachment, and other surgical indications; and patients compliant with the treatment follow-up plan.

2.1.4 Exclusion criteria

The exclusion criteria included: DR caused by age-related macular degeneration and retinal vein occlusion; history of using other anti-VEGF drugs within 3 months; patients with a history of laser treatment within 6 months, affecting macular function; history of intraocular hormone therapy within 6 months; history of vitreoretinal surgery; patients with unclear refractive media affecting the measurement results; and patients with poor general condition.

2.2 Study methods

2.2.1 Data collection

Data on the medical history and examination results of the patients were obtained from the hospital's electronic case management system, and relevant follow-up indicators were obtained by telephone. At the monthly follow-up, all patients were examined using BCVA, intraocular pressure, fundus photography, OCT, and fundus fluorography. BCVA was observed using the EDTRS visual chart and converted into LogMAR. CRT was measured using OCT (model Cirrus HD-OCT

TABLE 1 General Patient Data.

	PRP group (n =58)	Aflibercept 5 + PRN with PRP group (n =53)	Aflibercept 3 + PRN with PRP group (n =59)	t, χ^2	P
Man	30 (51.7%)	28 (52.8%)	28 (47.5%)	0.368	0.832
Woman	28 (48.3%)	25 (47.2%)	31 (52.5%)		
Age (year)	66.7 ± 3.9	65.2 ± 4.5	67.8 ± 3.7	2.550	0.081
O. D	29 (50.0%)	27 (50.9%)	29 (49.2%)	0.036	0.982
L. E	29 (50.5%)	26 (49.1%)	30 (50.8%)		
Mean time (s) after fluorescein dye injection when counting microangiomas	30.24 ± 2.41	29.51 ± 2.95	30.43 ± 3.06	1.632	0.199
Mean time (s) after fluorescein dye injection during calculation of retinal neovascular area	40.10 ± 3.94	40.53 ± 3.90	40.97 ± 3.59	0.761	0.468

PRP, retinal laser photocoagulation; O. D, right eye; L. E, left eye.

5000, Carl Zeiss) and hard exudation (HE) area was observed using VISUCAM224 fundus camera. Data processing analysis was performed. CRT was defined as the average of three measurements of the mean thickness from the inner to the outer central 1 mm of retinal tomography, measured by the same experienced technician. A boundary line between the HE area and NV vessels was drawn from the edge of the optic disc to the temporal 2PD of all HE areas and NV vessels to capture the area of each HE and NV vessel, which were added to obtain the total area. Observations in the peripheral retina were excluded to unify the results before and after examination within and between the patient groups. All results were reviewed by professional ophthalmologists (Figure 1).

Macular area (MA) and hemorrhage were distinguished by comparing the results of color fundus photography and fundus fluorescein angiography. Fundus fluorescence imaging (FFA) was performed using a Spectralis HRA laser device, aimed at the patient's eye. Fluorescein sodium diluent (3 mL) was injected into the antecubital vein and the patient was observed for any discomfort 10 min later. Patients that showed no adverse events were administered 5 mL of 20% fluorescein sodium diluent, and the retina of the optic disc, posterior pole, and MA were captured and recaptured after 10 min, 15 min, and 20 min using the same shooting range, and all photos were archived.

In addition, adverse events during treatment were recorded. Four patients in the PRP group discontinued treatment owing to massive vitreous accumulation and were switched to treatment by vitrectomy, while those receiving aflibercept and PRP were tested as expected.

2.2.2 Treatment methods

2.2.2.1 Pre-operative laser preparation

The naked eye, corrected far and near vision, intraocular pressure, cornea, pupil, anterior chamber, iris, and lens were checked, and color fundus image and fundus fluorescein angiography were performed. Patients and their family members were informed that the laser therapy was designed to enhance or improve existing vision and reduce the risk of deterioration, which may cause visual fluctuations and mild eye pain during processing, and that there will be repeated postoperative and photocoagulation examinations. Patients were required to sign an informed consent form before the operation. Except for angle-closure glaucoma, pupil dilation drugs were used to widen the pupil. Furthermore, contact lenses were cleaned and disinfected. The laser equipment was checked. Generally, argon ion, argon green, or argon blue-green lasers were used more frequently. The patient was positioned appropriately, and surface anesthesia was applied to the eye. Whole PRP was performed according to the scheme recommended by ETDRS, with the external optic disc connected to

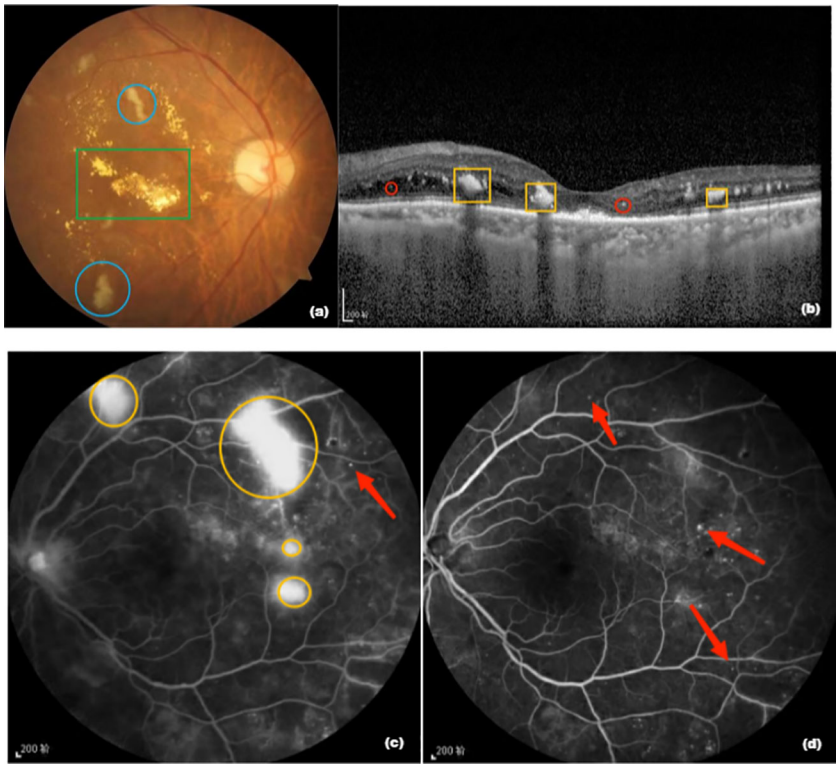

FIGURE 1
(A) Fundus photograph. The green box is a hard exudate, yellowish-white, and the area shown in blue circle is an absorbent cotton spot, also called "soft exudate"; **(B)** Optical coherence tomography image. The yellow box is a hard exudate and the structure shown in red circle is a highly reflective point; **(C)** Fundus fluorescence image before treatment. The yellow circle is the neovascularization area and the red arrow points to the microvascular tumor; **(D)** Fluorescence imaging image of the fundus of the patient after 12 months of aflibercept treatment showing that neovascularization has disappeared and the microvascular tumor is still partially present.

the equator, 2 DD from the macular center and temporal side, and the disseminated laser photocoagulation outside the formed oval range. Photocoagulation was performed on the nasal, lower, upper, and temporal sides, and the interval between each photocoagulation was 1 week. The size of the light dots was 200–500 microns, and the energy consumption was 200–300 uW over an exposure time of 0.2 – 0.3 s. The number of spots in this treatment was not more than 500, and the diameter of the two rooms was 1–1.5 spots. During the follow-up procedure, PRP salvage therapy was allowed. In addition, the patients receiving PRP with aflibercept received a vitreous injection of aflibercept before PRP, which effectively prevented macular swelling caused by short-term laser photocoagulation and the interruption of vitreous hemorrhage treatment. Changes in intraocular pressure and the presence of vitreous hemorrhage were monitored.

Intravitreal injection and aqueous humor collection were performed in the ophthalmic operating room. Before administering the injection, the conjunctiva sac and lacrimal duct were cleaned, disinfected, and covered. Surface anesthesia was applied to the patient's eye in the conjunctiva sac. Aqueous humor samples were collected from all patients and rinsed continuously before treatment with aflibercept intraocular injection.

2.2.2.2 Operation procedure

All patients had their aqueous humor collected before treatment with the intraocular injection. After surface anesthesia was applied to the affected eye, the operator opened the eyelid and used an insulin needle to collect 100 μL of aqueous humor in the anterior chamber, 1.0 mm of the limbal ring. Immediately after collection, the aqueous humor was placed in a sterile Eppendorf tube and kept in the refrigerator at -80°C for further tests.

Intravitreal injection of 2 mg aflibercept was administered into the angular scleral margin with a spacing of 3.5 mm. After the injection, the needle was gently pressed with a cotton swab for approximately 10–15 s. After observing the eye, tobramycin-dexamethasone eye ointment was applied and covered with gauze. The patients in the 5 + PRN and 3 + PRN groups initially received 5 and 3 monthly 2 mg intravitreal aflibercept injections, respectively, according to the following conditions: 5 ETDRS letters decrease in BCVA and 100 μ m increase in CRT. During the initial treatment period, follow-up was performed once a month, followed by once every other month for 1 year.

2.2.3 Sample testing

At baseline and 12 months of follow-up, the aqueous humor was extracted for testing. During the study, the immediate segment, intraocular pressure, and fundus were carefully observed, and changes were recorded. During the follow-up, the equipment and methods used before and after treatment were the same for BCVA, intraocular pressure, fundus photography, OCT, and FFA measurements, which were performed by three professional eye technicians.

The aqueous humor was tested using the flow-through liquid-phase multiplex protein quantification technique to determine VEGF and monocyte chemoattractant protein-1(MCP-1) content. The operation was as follows: aqueous humor samples were centrifuged at 4°C and 1000 g for 15 min. Subsequently, 50 uL of MCP-1 supernatant was obtained and tested for VEGF. Next, 45 μL capture bead diluent was injected into a 1.5 ml centrifugation tube, and MCP-1 and VEGF beads were violently shaken using the oscillator for 15 s. Thereafter, 1 μL of the solution was mixed with 45 μL of bead diluent and finally mixed with shock. Next, 50 uL of aqueous humor was added to the solution, fully mixed using the oscillometer, and finally placed in a dark environment for 1 h. In a 1.5 ml centrifugation tube, 45 μ ml of detection reagent diluent solution, hand-flicked MCP-1 PE, and VEGF PE, were mixed with gentle shaking. The configured PE solution was placed in a dark centrifugal pipe in the second step for 2 h, and 1 ml BD wash buffer was added to the completely covered and clean centrifugal tube. The cap of the centrifugal tube was poured two times, and centrifuged at 200 g. The liquid was discharged, and 300 micro LBD aqueous solution was added. The centrifugal tube was covered and rotated with a finger to suspend the beads completely and placed into the flow falcon injection tube. After cleaning and starting the software, the software was operated by inserting the injection needle, setting the parameters, and reading the data. The value of each index was calculated using the standard curve expression rather than reading. Glial fibrillary acidic protein (GFAP) content of the aqueous humor was determined by the enzyme-linked immunosorbent assay (ELISA) (1). Detection protein and the corresponding buffer agent were selected. On the day of the test, the aqueous humor samples were removed from the refrigerated room of -80^{0}C into the refrigerated room of 4^{0}C for thawing, to determine the number of samples and verify the identity of the experimenter. (2) A standard solution was made by adding 20 μl of aqueous humor to 380 microliters of diluent. We made 3000 pg/ml of the top standard solution and repeated it twice to obtain seven gradually diluted standard solutions. For sample preparation, 50 μl of aqueous humor was required for each sample, which was added to the microplate and incubated with 50 μl of antibody for 1 h. The microplate was washed with the washing liquid thrice after incubation, and 100 μl of TMB was added to the microplate and incubated for 10 min. Thereafter, 100 μl of the termination solution was added (8). Using the microplate reader set at 450 nm, OD was determined. The standard curve was compared with that of the OD and OD of the standard, and the sample OD was introduced into the standard curve to obtain the GFAP content of the sample.

2.3 Statistical methods

Statistical analysis was performed using SPSS software version 23.0 (Armonk, NY: IBM Corp). The χ^2 test was used to compare count data, analysis of variance was used for statistical description of measurement data, Student's *t*-test was used to analyze independent samples, and the Student–Newman–Keuls test was used for group comparisons. A P-value of less than 0.05 was considered statistically significant.

3 Results

3.1 Changes in the BCVA before and after treatment

Post-treatment, the BCVA (log MAR) increased slightly in the PRP group from 0.69 ± 0.17 to 0.71 ± 0.17, with no significant difference

10.3389/fendo.2024.1286736

(P>0.05). However, in the aflibercept 5 + PRN with PRP and aflibercept 3 + PRN with PRP groups, the BCVA (log MAR) decreased from 0.72 ± 0.17 and 0.74 ± 0.17 to 0.50 ± 0.13 and 0.53 ± 0.17, respectively, with statistically significant differences (all P<0.05). Statistically significant differences were observed between the aflibercept 5 + PRN with PRP and aflibercept 3 + PRN with PRP groups and PRP alone group (Q=9.794, P<0.05; Q=8.388, P<0.05, respectively). However, no significant difference was observed between the two combined treatment groups (Q=1.638, P>0.05) (Table 2).

3.2 Changes in central macular foveal thickness before and after treatment

Central macular foveal thickness (CFT) slightly decreased in the PRP group from 361.80 ± 36.70 μm to 353.86 ± 40.88 μm, with no significant difference (P>0.05). In the aflibercept 5 + PRN with PRP and aflibercept 3 + PRN with PRP groups, CFT decreased from 356.57 ± 37.57 μ m and 358.17 ± 44.66 μ m to 284.87 ± 31.52 μ m and 303.19 ± 37.00 μ m, respectively, with statistically significant differences observed before and after treatment (P<0.05 in both groups). There were significant differences between the three groups after treatment (Q=13.947, P<0.05 for PRP vs. aflibercept 5 + PRN and PRP alone; Q=10.528, P<0.05 for aflibercept 3 + PRN and PRP vs. aflibercept 5 + PRN with PRP; Q=3.718, P<0.05). In the aflibercept 5 + PRN with PRP group, the decrease in CFT was significantly better than that in the aflibercept 3 + PRN with PRP and PRP-only groups (Table 3).

3.3 Changes in the number of MA before and after treatment

The number of MA (one) in the PRP, aflibercept 5 + PRN with PRP, and aflibercept 3 + PRN with PRP groups decreased from 118.34 ± 27.96, 118.60 ± 33.34, and 116.59 ± 28.95 to 92.95 ± 29.04, 44.60 ± 20.73, and 54.26 ± 25.43, respectively (P<0.05 in all groups). For the three pairwise comparisons, the differences were all statistically significant (Q=14.156, P<0.05 for PRP vs. aflibercept 5 + PRN; Q=11.643, P<0.05 for aflibercept 3 + PRN with PRP vs. aflibercept 5 + PRN with PRP). In the aflibercept 5 + PRN with PRP, the decrease in the number of MA was significantly better than that in the aflibercept 3 + PRN with PRP and PRP groups (Table 4).

3.4 Changes in the retinal NV area before and after treatment

The retinal NV area in the PRP, aflibercept 5+PRN with PRP, and aflibercept 3+PRN with PRP groups decreased from 1.00 ± 0.21 mm^2, 1.01 ± 0.18 mm^2, and 0.98 ± 0.20 mm^2 to 0.49 ± 0.17 mm^2, 0.31 ± 0.16 mm^2, and 0.38 ± 0.14 mm^2, respectively. All the differences were statistically significant before and after treatment (P<0.05 in all groups). Pairwise comparisons showed statistically significant differences between the PRP and aflibercept 5 + PRN with PRP groups and between the PRP and aflibercept 3 + PRN with PRP groups (Q=8.627, P<0.05 and Q=5.725, P<0.05, respectively). However, no significant difference was observed between aflibercept 5 + PRN with PRP and aflibercept 3 + PRN with PRP groups (Q=3.068, P>0.05) (Table 5).

3.5 Changes in the HE area before and after treatment

After 12 months of treatment, in the PRP group, patients without HE increased from two to nine, patients with an HE area of less than 0.5 mm^2 increased from 23 to 29, patients with an HE area of 0.5 mm^2–2.5 mm^2 reduced from 22 to 13, and patients with an HE area of more than 2.5 mm^2 decreased from 11 to seven. In the 5 + PRN with PRP group, patients with no HE area increased from two to 20. The number of patients with an HE area of less than 0.5 mm^2 remained unchanged, patients with an HE area of 0.5 mm^2–2.5 mm^2 reduced from 20 to eight, and patients with an HE area of more than 2.5 mm^2 reduced from eight to two. Patients without HE before treatment In the 3 + PRN with PRP group increased from three to 21, patients with an HE area of less than 0.5 mm^2 decreased from 25 to

TABLE 2 Changes in the BCVA (LogMAR) before and after treatment.

	Pretherapy BCVA (log MAR)	BCVA (log MAR) after 12 months of treatment	T	P
PRP group (n=58)	0.69 ± 0.17	0.71 ± 0.17	0.440	0.661
Aflibercept 5 + PRN combination group (n=53)	0.72 ± 0.17	0.50 ± 0.13	7.514	0.000
Aflibercept 3 + PRN combined group (n=59)	0.74 ± 0.17	0.53 ± 0.17	6.795	0.000
F	1.203	28.210		
P	0.305	0.000		

Q =9.794, P <0.05 for PRP-only; Q =8.388, P <0.05 for PRP vs. aflibercept 3 + PRN with PRP and PRP vs. aflibercept 5 + PRN with PRP. Q =1.638 for pairwise comparison of the three samples (Newman–Keuls method), BCVA: best-corrected visual acuity.

10.3389/fendo.2024.1286736

TABLE 3 Changes in the CFT before and after treatment.

	Pre-treatment CFT (μ m)	CFT after treatment (μ m)	T	P
PRP group (n=58)	361.80 ± 36.70	353.86 ± 40.88	1.110	0.270
Aflibercept 5 + PRN combined group (n=53)	356.57 ± 37.57	284.87 ± 31.52	10.645	0.000
Aflibercept 3 + PRN combined group (n=59)	358.17 ± 44.66	303.19 ± 37.00	7.282	0.000
F	0.261	53.134		
P	0.771	0.000		

Q =13.947, P <0.05 for PRP vs. aflibercept 5 + PRN with PRP; Q =10.528, P <0.05 for aflibercept 3 + PRN with PRP vs. aflibercept 5 + PRN with PRP, P <0.05; q-wise comparison of three samples (Newman–Keuls method); CFT, central foveal thickness.

19, patients with an HE area of 0.5 mm^2–2.5 mm^2 decreased from 21 to 16, and patients with an HE area of more than 2.5 mm^2 reduced from 10 to three. The differences were all statistically significant (χ^2 = 8.3500, 23.4701, and 18.7631, respectively; P<0.05) (Table 6).

3.6 Changes in VEGF levels in the aqueous humor before and after treatment

VEGF in the aflibercept 3 + PRN with PRP group and aflibercept 5 + PRN with PRP decreased from 156.33 ± 11.30 pg/mL and 154.46 ± 9.67 pg/mL to 8.81 ± 4.28 pg/mL and 8.44 ± 4.85 pg/mL, respectively (P<0.05 in both groups). After treatment, no statistical difference was observed between aflibercept 5 + PRN with PRP and aflibercept 3 + PRN with PRP (P>0.05) (Table 7).

3.7 Changes in the levels of MCP-1 in the aqueous humor before and after treatment

MCP-1 levels in the aflibercept 3 + PRN with PRP and aflibercept 5 + PRN with PRP groups significantly increased from 978.05 ± 96.93 pg/mL and 997.00 ± pg/mL to 237.57 ± 93.31 and 2222.78 ± 86.79 pg/mL, respectively (P<0.05 in both groups). However, no significant difference was observed between the MCP-1 level in the aflibercept 5 + PRN with PRP and aflibercept 3 + PRN with PRP groups (P>0.05) (Table 8).

3.8 Changes in the level of GFAP in the aqueous humor before and after treatment

GFAP levels in the aflibercept 3 + PRN with PRP and aflibercept 5 + PRN with PRP groups significantly reduced from 1.39 ± 0.20 (t=0.18) and 0.26 ± 0.18) pg/mL to 0.26 ± 0.11 and 0.28 ± 0.13, respectively (P<0.05 in both groups). However, no significant difference was observed in GFAP levels between aflibercept 5 + PRN with PRP and aflibercept 3 + PRN with PRP groups (P>0.05) (Table 9).

4 Discussion

4.1 Research background

In the early 1990s, through extensive study of the mechanisms underlying DR, a classification of DR based on severity was proposed which is still widely used. In the absence of NV, DR is classified as non-proliferative (NPDR), ranging from mild to severe. In the presence of NV, DR is classified as proliferative (PDR). The risk of progression to advanced PDR is highly dependent on baseline disease levels; compared with severe NPDR, moderate NPDR progresses to PDR after 1 year, with a 12–27% risk and a 52% risk of PDR over the same period (11). By analyzing the mechanism underlying DR, four factors affecting DR were

TABLE 4 Changes in MA before and after treatment.

	Number of MA before treatment	MA number after 12 months of treatment	T	P
PRP group (n=58)	118.34 ± 27.96	92.95± 29.04	4.797	0.000
Aflibercept 5 + PRN with PRP group (n=53)	118.60 ± 33.34	44.60 ± 20.73	13.102	0.000
Aflibercept 3 + PRN with PRP group (n=59)	116.59 ± 28.95	54.26 ± 25.43	12 426	0.000
F	0.084	57.361		
P	0.927	0.000		

Q =14.156, P <0.05 for PRP vs. aflibercept 5 + PRN with PRP; P <0.05 for PRP versus PRP; Q =11.643 for aflibercept 3 + PRN with PRP vs. aflibercept 5 + PRN with PRP, P <0.05; q-test (Newman–Keuls method), MA, Microhemangioma.

10.3389/fendo.2024.1286736

TABLE 5 Changes in NV area before and after treatment.

	Pretherapy New vessel area	After 12 months of treatment New vessel area	T	P
PRP group (n=58)	1.00 ± 0.21	0.49 ± 0.17	14.359	0.000
Aflibercept 5 + PRN with PRP group (n=53)	1.01 ± 0.18	0.31 ± 0.16	27.866	0.000
Aflibercept 3 + PRN with PRP group (n=59)	0.98 ± 0.20	0.38 ± 0.14	19.415	0.000
F	0.121	19.340		
P	0.891	0.000		

Q =8.627, P <0.05 for PRP vs. aflibercept 5 + PRN with PRP; Q =5.725 for aflibercept 3 + PRP with PRP, P> 0.05; the q-wise comparison of three samples (Newman–Keuls method), NV: neovascularization; PRP, retinal laser photocoagulation.

identified. The patient's vision is severely impaired within 2 years (defined as a 5/200 diagnosis of no less than twice every 5 months) (12). As the number of risk factors increased from two to three, the risk of severe visual loss increased from 8.5% to 26.7%.

In patients with diabetes, impaired retinal pigment epithelium pumping capacity and choroidal blood flow limit the migration of water and lipids from the outer retinal layer to the choroid. Thus, HE's are formed, expanded, and deposited, and are more likely to occur in the macular fovea, accompanied by a rapid decrease in CFT in patients with macular edema. Several additional studies reported that diabetic macular edema (DME) with subretinal fluid (SRF) may be associated with the formation of hyper-reflective foci that may precede and extravasate the deposition of plasma lipids and/or proteins comprising HE. The longer the duration of cystoid macular edema, the higher the risk of HE deposition in the macular region during follow-up. We speculate that long-term macular edema may increase the concentration of inflammatory cytokines and VEGF in the vitreous fluid, which is significantly associated with the presence of SRF (13), whereas more exudates were deposited within the macular retina to form a clinical HE. However, there is still controversy about whether the origin of the hyper-reflective foci is a precursor of HE (14, 15). Therefore, the relationship between SRF and HE deposition in the macula must be further explored.

Cytokines are small molecule proteins with strong biological functions. Studies have shown that cytokines can be divided into interleukins (ILs), interferons, tumor necrosis factor superfamily, colony-stimulating factors, chemokines, and growth factors. Cytokines are closely associated with various ocular diseases, such as DME, neovascular glaucoma, DR, and other immune diseases. A validation experiment using ELISA showed that ANG-1, ANG-2, IL-6, VEGF, MMP-9, hepatocyte growth factor (HGF), placental growth factor (PIGF), depolin and metalloproteinase (ADAM) -11, chemokines (CXCL) -10, IL-8, and platelet-derived growth factor (PDGF) -A were higher than the control group (16). However, few

TABLE 6 Changes in HE areas before and after treatment.

	HE area	Before therapy	At 12 months after the treatment	x^2	P
PRP group (n=58)	no HE	2	9	8.350	0.039
	<0.5 mm^2	23	29		
	0.5 mm^2–2.5 mm^2	22	13		
	>2.5 mm^2	11	7		
Aflibercept 5 + PRN with PRP group (n=53)	no HE	2	20	23.470	0.000
	<0.5 mm^2	23	23		
	0.5 mm^2–2.5 mm^2	20	8		
	>2.5 mm^2	8	2		
Aflibercept 3 + PRN with PRP group (n=59)	no HE	3	21	18.763	0.000
	<0.5 mm^2	25	19		
	0.5 mm^2–2.5 mm^2	21	16		
	>2.5 mm^2	10	3		
x^2		0.610	13.160		
P		0.996	0.041		

HE, hard exudate area; PRP, retinal laser photocoagulation.

TABLE 7 Changes in VEGF levels in the atrial fluid before and after treatment.

	Pre-treatment (pg/mL)	After 12 months of treatment (pg/mL)	T	P
Aflibercept 3 + PRN with PRP group (n=59)	156.33 ± 11.30	8.81 ± 4.28	95.780	0.000
Aflibercept 5 + PRN with PRP group (n=53)	154.46 ± 9.67	8.44 ± 4.85	93.965	0.000
t	0.935	0.430		
P	0.352	0.668		

Comparison of changes in VEGF levels in the aqueous humor before and after treatment using the t-test. VEGF: vascular endothelial growth factor; PRP, retinal laser photocoagulation.

clinical studies exist on the relationship between cytokines, such as MCP-1 and GFAP, and disease progression in patients with PDR and the changes after anti-VEGF treatment. We collected the concentrations of VEGF, MCP-1, GF, and GFAP in the aqueous humor before and after treatment, observed the changes in the cytokine level after PRP and aflibercept with PRP treatment, and explored the prognostic relationship among patients with high-risk PDR.

We found that some patients with good vision already fulfilled the criteria for high-risk PDR at the first visit, and the new blood vessels appearing in the inner retina had ruptured, resulting in vitreous hemorrhage, and severe decline in vision. To reduce this risk, PRP must be administered strictly as prescribed. Anti-VEGF drugs are now used in clinical practice. However, based on the economic situation in some poor areas in China, some patients choose PRP treatment alone because they cannot afford the cost of anti-VEGF drugs.

Among various anti-VEGF drugs, aflibercept is an emerging drug, and its effect has been fully confirmed after phase VIVID and VISTA III clinical trials (17). Chen Zhen, a Chinese medical expert (18) and Lu Qianyi (19) have verified its efficacy. However, the previous research was conducted among Caucasians. Domestically, research knowledge is limited to the short-term treatment of DME for 1 or 2 months, and its long-term effects have not been elucidated.

Therefore, this study used PRP alone, aflibercept 3 + PRN and PRP, and followed expert consensus (20). Aflibercept 5 + PRN with PRP regimen was recommended for patients with both high-risk PDR and DME. At baseline and after 12 months of treatment, BCVA (Log MAR), CFT, MA, NV area, and HE changed. The treatment regimen of the combined treatment group comprised an intravitreal injection before performing PRP. The reasons were as follows (1): compared with the half-life of anti-VEGF drugs, such as ranezumab and comaccept, the intravitreal half-life of aflibercept is usually more than 10 days (21); (2) macular edema caused by retinal laser photocoagulation mostly occurs during photocoagulation or 1 month after treatment (22). Thus, an intravitreal aflibercept injection was administered 1 week before PRP.

4.2 Factors influencing the efficacy of anti-VEGF therapy in DR treatment

We found that the BCVA was better in the PRP group. The BCVA (log MAR) in the PRP alone group did not improve after treatment; however, it increased from 0.69 ± 0.17 to 0.71 ± 0.17, indicating that PRP alone could not delay or prevent further decline in visual acuity. This is also consistent with previous studies. Rebecca et al. (23) reported that after PRP, patients showed lower BCVA in the 1st and 3rd months compared with that before PRP. Moreover, Zhao et al. (24) showed that the incidence of BCVA was significantly decreased at 1 and 3 months after PRP compared with that before PRP in patients with DR. Lorusso et al. (25), reported lower BCVA than the basal levels 6 months after PRP in patients with DR.

In this study, intravitreal aflibercept injection had no significant effect on the NV and HE area (P>0.05); hence, we speculated that it may be related to the distribution of HE and NV in different locations in the retina of the patients. In 2020, Li Xiaoli et al. (26) analyzed the distribution of patients with DR using FFA and color fundus photography FP and found that HE occurs mostly in the posterior pole (69.7%). In severe NPDR and hyperplastic DR, intraretinal microvascular abnormality, NPA, and NV were more

TABLE 8 Changes in monocyte chemotactic protein (MCP-1) levels in the atrial fluid before and after treatment.

	Pre-treatment (pg/mL)	After 12 months of treatment (pg/mL)	T	P
Aflibercept 3 + PRN with PRP group (n=59)	978.05 ± 96.93	237.57 ± 93.31	42.841	0.000
Aflibercept 5 + PRN with PRP group (n=53)	997.00 ± 108.74	222.78 ± 86.79	47.319	0.000
T	0.975	0.866		
P	0.332	0.389		

Changes in MCP-1 levels in aqueous humor before and after treatment were compared using the t-test. MCP-1: monocyte chemoattractant protein; retinal laser photocoagulation.

10.3389/fendo.2024.1286736

TABLE 9 Changes in glial fibrillary acidic protein (GFAP) levels in the atrial fluid before and after treatment.

	Pre-treatment (pg/mL)	After 12 months of treatment (pg/mL)	T	P
Aflibercept 3 + PRN with PRP group (n=59)	1.39 ± 0.20	0.26 ± 0.11	39.403	0.000
Aflibercept 5 + PRN with PRP group (n=53)	1.32 ± 0.18	0.28 ± 0.13	36.418	0.000
T	1.961	0.818		
P	0.052	0.415		

Comparison of changes in GFAP levels in the aqueous humor before and after treatment was performed using the t-test. GFAP: glial fibrillary acidic protein; PRP, retinal laser photocoagulation.

common on the nasal side, especially in the inferior nasal region (60.3%, 38.7%, and 76.0%, respectively). Although our study participants were all patients with high-risk PDR, their blood glucose control and disease progress were not used to classify the location of HE and NV within the groups, which may have led to inconsistent responses to anti-VEGF drugs and, thus, affected the prognosis of retinal anatomical structure and function.

In addition, we found that the concentration of cytokines, VEGF, MCP-1, and GFAP in the aqueous humor improved after treatment compared with that before treatment; however, no statistical difference was observed in the aflibercept 5 + PRN group (P>0.05). This may have been due to the patient's genotype, blood pressure level, blood sugar level, blood lipid level, renal function, smoking history, insomnia, and the interaction between cytokines affecting the expression of Muller cells. The reasons are given as follows:

Several studies have shown that smoking duration and blood pressure can affect the concentration of MCP-1 in patients. Komiyama et al. (27), in a large sample analysis of serum MCP-1 concentrations, after adjusting for sex differences, found that serum MCP-1 concentration was positively associated with smoking duration in smokers and that smoking duration was an independent determinant of serum MCP-1 concentration in smokers. They also found that in smokers, serum MCP-1 concentrations were significantly higher than that in normotensive patients, systolic blood pressure was an independent determinant of serum MCP-1 concentration in smokers, and ACS was more likely to occur in long-term smokers. Unlike in smokers, serum MCP-1 concentration was not associated with systolic or diastolic blood pressure. The study found that the serum MCP-1 concentration in patients with hypertension was significantly higher than that in patients without hypertension. MCP-1 concentration gradually increased with increased hypertension grade, and the gap between the levels was statistically significant (P<0.05). Notably, MCP-1 concentration is related to genotype. A domestic study showed that MCP-1 c.2518G/G is a susceptibility gene for DR, especially high-risk PDR among patients with type 2 diabetes in the Han population in Northern China. The G allele was associated with DR severity in the A/G polymorphism, while the G allele showed no obvious correlation with DR, requiring further studies (28).

In addition to MCP-1, VEGF expression is associated with genotype. Increasing evidence suggests that miR-126 is involved in the regulation of genes closely related to angiogenesis and inflammation. Studies have detected significantly high expressions of miR-126 in the vitreous tissue, proliferative membrane tissues, and the plasma of the affected eyes of patients with PDR compared with patients without PDR. Furthermore, miR-126 expression was significantly higher in the vitreous and proliferation membrane tissues in patients with stage VI DR than in patients with stage V and IV DR. In other words, miR-126 expression increased with increasing PDR severity. It is suggested that miR-126 is abnormally highly expressed in patients with PDR and may be a potential mechanism underlying PDR development (29).

Since there are two large glial cell populations in the retina, namely the astrocytes and Muller cells, which can all express cytokines, such as VEGF, GFAP, and MCP-1, we cannot determine the source of cytokines in the aqueous humor. Alternatively, the expression of other inflammatory cytokines may have an impact on the function of Muller cells. Previous studies have demonstrated that IL-17A promotes functional impairment in the Muller cells through Act 1 signaling. Th 22 cells are involved in DR pathogenesis by directly promoting retinal Muller-cell activation and dysfunction as well as BRB disruption and inflammatory response via IL-22 production. In addition, Th 22 cells can secrete IL-22, IL-22, and IL-22 R α 1 to activate the Act 1/TRAF 6 pathway and promote an inflammatory response in Muller cells (30). However, whether they could further affect the expression of VEGF, MCP-1, and GFAP by Muller cells is unknown and needs to be investigated.

In this study, the differences in CFT and MA number between the aflibercept 5 + PRN with PRP and aflibercept 3+PRN with PRP groups were significant before and after treatment (P<0.05, in all groups); the efficacy of aflibercept 5 + PRN with PRP was significantly better than PRP alone and aflibercept 3 + PRN with PRP. This suggests that increasing the aflibercept loading dose can significantly reduce CFT and MA for the same treatment time. We speculated that by increasing the loading dose, we could significantly improve vascular permeability, reduce inflammation and oxidative stress, reduce the generation of microhemangiomas, reduce retinal ischemia and hypoxia, increase blood flow, and reduce vascular leakage, which can help DR regress at an earlier date. Therefore, although there was no statistically significant difference between aflibercept 5+PRN with PRP and aflibercept 3 +PRN with PRP in BCVA after 12 months of treatment, in the long run, it may reduce the destruction of the retinal structure and visual function in patients with DR. Therefore the aflibercept 5+PRN with PRP regimen is necessary for patients with DR.

As for BCVA, NV, and HE area, and whether the observation indicators, such as cytokines in the aqueous humor, will predict a better prognosis based on our treatment strategy and follow-up

period, further investigation is needed to clarify the role of MA, HE, genotype, smoking history, sleep quality, blood pressure level, blood sugar level, blood lipid level, and hemoglobin level through long-term observation and detailed statistical analysis.

4.3 Safety of intravitreal aflibercept injection

In this study, no serious adverse events occurred except that a few patients experienced subconjunctival hemorrhage and transient elevated intraocular pressure after intravitreal injection. Intravitreal aflibercept administration is safe and well tolerated, with a few side effects; however, strict clinical evaluation of poor systemic conditions, such as advanced age, patients with a recent history of cardiovascular and cerebrovascular disease, and poor blood glucose control, should be performed before intravitreal aflibercept administration.

4.4 Strengths and limitations of the study

The main objective of this study was to observe the effectiveness and safety of different dosage regimens of intravitreal aflibercept injection with PRP in patients with high-risk PDR and DME. Although the patients chose the treatment plan independently, their choice may be somewhat related to their economic level, living standard, and other factors. However, the baseline data of the patients in the three groups were not significantly different, except for the number of injections they received ($P>0.05$), indicating that the three groups were comparable, and selection bias was reduced to some extent. In addition, based on previous studies on anti-VEGF treatment after MCP-1, GFAP, and the relationship between the concentration and DR, previous animal studies showed the occurrence and development of DR; therefore, we hope that we can observe the severity of DR, as a clinical prediction of patient prognosis index in the future. However, this study had some limitations. First, the general condition of the patients, such as genotype, body mass index, blood pressure level, blood glucose level, blood lipid level, microalbumin level, smoking history, and sleep status, were not considered nor evaluated. These factors may affect the prognosis of the disease. Future studies should consider these factors when performing data collection and analysis. Second, NV and HE areas were all measured manually, which is prone to inevitable statistical errors. Developing automatic measurement tools, such as through artificial intelligence, is required to provide a higher detection accuracy. Third, only three cytokines, VEGF, MCP-1, and GFAP, were observed, and the levels of other inflammatory cytokines and chemokines, which may have an effect on the expression of Muller cells, were not monitored. Finally, the long-term effect and safety of multiple aflibercept injections was not determined.

In conclusion, aflibercept 5 + PRN intravitreal injection with PRP was safe and effective in treating patients with both PDR and DME, and it improved CFT better than in 3 + PRN (MA); however, BCVA, NV, and HE area, and VEGF, MCP-1, GFAP cytokines in aqueous aflibercept 3 + PRN group were not improved. CFT and MA can be used as early indicators for observing the improvement and regression of DR; however, their long-term clinical efficacy needs further investigation.

Data availability statement

The original contributions presented in the study are included in the article/supplementary material. Further inquiries can be directed to the corresponding authors.

Author contributions

SL: Writing – original draft. YT: Formal analysis, Writing – review & editing. SY: Data curation, Writing – review & editing. MY: Resources, Writing – review & editing. HZ: Formal analysis, Writing – review & editing. MS: Investigation, Writing – review & editing. WC: Resources, Writing – review & editing. HW: Supervision, Writing – review & editing.

Funding

The author(s) declare financial support was received for the research, authorship, and/or publication of this article. This study was supported by Shandong Province medical health science and technology project (202307020900).

Acknowledgments

We would like to thank the Editor (www.editage.cn) for English language editing.

Conflict of interest

The authors declare that the research was conducted in the absence of any commercial or financial relationships that could be construed as a potential conflict of interest.

Publisher's note

References

1. Yeh HC, Brown TT, Maruthur N, Ranasinghe P, Berger Z, Suh YD, et al. Comparative effectiveness and safety of methods of insulin delivery and glucose monitoring for diabetes mellitus: a systematic review and meta-analysis. *Ann Intern Med* (2012) 157:336–47. doi: 10.7326/0003-4819-157-5-201209040-00508

2. Wong TY, Sabanayagam C. The war on diabetic retinopathy: where are we now? *Asia Pac J Ophthalmol (Phila)* (2019) 8:448–56. doi: 10.1097/APO.0000000000000267

3. Chen XD, Gardner TW. A critical review: psychophysical assessments of diabetic retinopathy. *Surv Ophthalmol* (2021) 66:213–30. doi: 10.1016/j.survophthal.2020.08.003

4. Ruta LM, Magliano DJ, Lemesurier R, Taylor HR, Zimmet PZ, Shaw JE. Prevalence of diabetic retinopathy in Type 2 diabetes in developing and developed countries. *Diabetes Med* (2013) 30:387–98. doi: 10.1111/dme.12119

5. Giuliari GP, Sadaka A, Chang PY, Cortez RT. Diabetic papillopathy: current and new treatment options. *Curr Diabetes Rev* (2011) 7:171–5. doi: 10.2174/157339911795843122

6. Masser DR, Otalora L, Clark NW, Kinter MT, Elliott MH, Freeman WM. Functional changes in the neural retina occur in the absence of mitochondrial dysfunction in a rodent model of diabetic retinopathy. *J Neurochem* (2017) 143:595–608. doi: 10.1111/jnc.14216

7. Avidor D, Loewenstein A, Waisbourd M, Nutman A. Cost-effectiveness of diabetic retinopathy screening programs using telemedicine: a systematic review. *Cost Eff Resour Alloc* (2020) 18:16. doi: 10.1186/s12962-020-00211-1

8. Thapa R, Bajimaya S, Sharma S, Rai BB, Paudyal G. Systemic association of newly diagnosed proliferative diabetic retinopathy among type 2 diabetes patients presented at a tertiary eye hospital of Nepal. *Nepal J Ophthalmol* (2015) 7:26–32. doi: 10.3126/nepjoph.v7i1.13163

9. Samadi Aidenloo N, Mehdizadeh A, Valizadeh N, Abbaszadeh M, Qarequran S, Khalkhali H. Optimal glycemic and hemoglobin A1c thresholds for diagnosing diabetes based on prevalence of retinopathy in an Iranian population. *Iran Red Crescent Med J* (2016) 18:e31254. doi: 10.5812/ircmj.31254

10. Pranata R, Vania R, Victor AA. Statin reduces the incidence of diabetic retinopathy and its need for intervention: A systematic review and meta-analysis. *Eur J Ophthalmol* (2021) 31:1216–24. doi: 10.1177/1120672120922444

11. Fundus pathology group of ophthalmology Society of Chinese Medical Association. Clinical guidelines for the diagnosis and treatment of diabetic retinopathy in China. *Chin J Ophthalmol* (2014) 50:851–65.

12. Lin S, Ramulu P, Lamoureux EL, Sabanayagam C. Addressing risk factors, screening, and preventative treatment for diabetic retinopathy in developing countries: a review. *Clin Exp Ophthalmol* (2016) 44:300–20. doi: 10.1111/ceo.12745

13. Four risk factors for severe visual loss in diabetic retinopathy. The third report from the Diabetic Retinopathy Study. The diabetic retinopathy study research group. *Arch Ophthalmol* (1979) 97:654–5. doi: 10.1001/archopht.1979.01020010310003

14. Chung YR, Lee SY, Kim YH, Byeon HE, Kim JH, Lee K. Hyperreflective foci in diabetic macular edema with serous retinal detachment: association with dyslipidemia. *Acta Diabetol* (2020) 57:861–6. doi: 10.1007/s00592-020-01495-8

15. Do JR, Park SJ, Shin JP, Park DH. Assessment of hyperreflective foci after bevacizumab or dexamethasone treatment according to duration of macular edema in patients with branch retinal vein occlusion. *Retina* (2021) 41:355–65. doi: 10.1097/IAE.0000000000002826

16. Yu Y, Zhang J, Zhu R, Zhao R, Chen J, Jin J, et al. The profile of angiogenic factors in vitreous humor of the patients with proliferative diabetic retinopathy. *Curr Mol Med* (2017) 17:280–6. doi: 10.2174/1566524017666171106111440

17. Schreur V, Altay L, Van Asten F, Groenewoud JMM, Fauser S, Klevering BJ, et al. Hyperreflective foci on optical coherence tomography associate with treatment outcome for anti-VEGF in patients with diabetic macular edema. *PloS One* (2018) 13:e0206482. doi: 10.1371/journal.pone.0206482

18. Do DV, Nguyen QD, Vitti R, Berliner AJ, Gibson A, Saroj N, et al. Intravitreal aflibercept injection in diabetic macular edema patients with and without prior anti-vascular endothelial growth factor treatment: outcomes from the Phase 3 program. *Ophthalmology* (2016) 123:850–7. doi: 10.1016/j.ophtha.2015.11.008

19. Zhen C, Amin X, Qinyun X. Efficacy of intravitreal abiercept in the treatment of diabetic macular edema. *J Wuhan Univ (Med Ed)* (2019) 40:842–4.

20. Qianyi L. Clinical efficacy of abiercept via intravitreal injection in diabetic macular edema. *New Adv Ophthalmol* (2019) 39:340–2.

21. Avitabile T, Azzolini C, Bandello F, Boscia F, De Falco S, Fornasari D, et al. Aflibercept in the treatment of diabetic macular edema: a review and consensus paper. *Eur J Ophthalmol* (2017) 27:627–39. doi: 10.5301/ejo.5001053

22. Lu L, Jun LJ, Changzheng C. Long-term follow-up of continuous intravitreal injection of diabetic macular edema. *J Wuhan Univ (Med Ed)* (2020) 41:819–23.

23. Rebecca SFF, Shaikh FF, Jatoi SM. Comparison of efficacy of combination therapy of an intravitreal injection of bevacizumab and photocoagulation versus Pan Retinal Photocoagulation alone in High risk Proliferative Diabetic Retinopathy. *Pak J Med Sci* (2021) 37:157–61. doi: 10.12669/pjms.37.1.3141

24. Zhao T, Chen Y, Liu D, Stewart JM. Optical coherence tomography angiography assessment of macular choriocapillaris and choroid following panretinal photocoagulation in a diverse population with advanced diabetic retinopathy. *Asia Pac J Ophthalmol (Phila)* (2020) 10:203–7. doi: 10.1097/APO.0000000000000345

25. Lorusso M, Milano V, Nikolopoulou E, Ferrari LM, Cicinelli MV, Querques G, et al. Panretinal photocoagulation does not change macular perfusion in eyes with proliferative diabetic retinopathy. *Ophthalmic Surg Lasers Imaging Retina* (2019) 50:174–8. doi: 10.3928/23258160-20190301-07

26. Li X, Xie J, Zhang L, Cui Y, Zhang G, Wang J, et al. Differential distribution of manifest lesions in diabetic retinopathy by fundus fluorescein angiography and fundus photography. *BMC Ophthalmol* (2020) 20:471. doi: 10.1186/s12886-020-01740-2

27. Komiyama M, Takanabe R, Ono K, Shimada S, Wada H, Yamakage H, et al. Association between monocyte chemoattractant protein-1 and blood pressure in smokers. *J Int Med Res* (2018) 46:965–74. doi: 10.1177/0300060517723415

28. Dong L, Lv XY, Wang BJ, Wang YQ, Mu H, Feng ZL, et al. Association of monocyte chemoattractant protein-1 (MCP-1)2518-A/G polymorphism with proliferative diabetic retinopathy in northern Chinese type 2 diabetes. *Graefes Arch Clin Exp Ophthalmol* (2014) 252:1921–6. doi: 10.1007/s00417-014-2651-1

29. Ambros V. MicroRNA pathways in flies and worms: growth, death, fat, stress, and timing. *Cell* (2003) 113:673–6. doi: 10.1016/s0092-8674(03)00428-8

30. Liu R, Liu CM, Cui LL, Zhou L, Li N, Wei XD. Expression and significance of MiR-126 and VEGF in proliferative diabetic retinopathy. *Eur Rev Med Pharmacol Sci* (2019) 23:6387–93. doi: 10.26355/eurrev_201908_18518

Frontiers in Endocrinology

Explores the endocrine system to find new therapies for key health issues

The second most-cited endocrinology and metabolism journal, which advances our understanding of the endocrine system. It uncovers new therapies for prevalent health issues such as obesity, diabetes, reproduction, and aging.

Discover the latest Research Topics

See more →

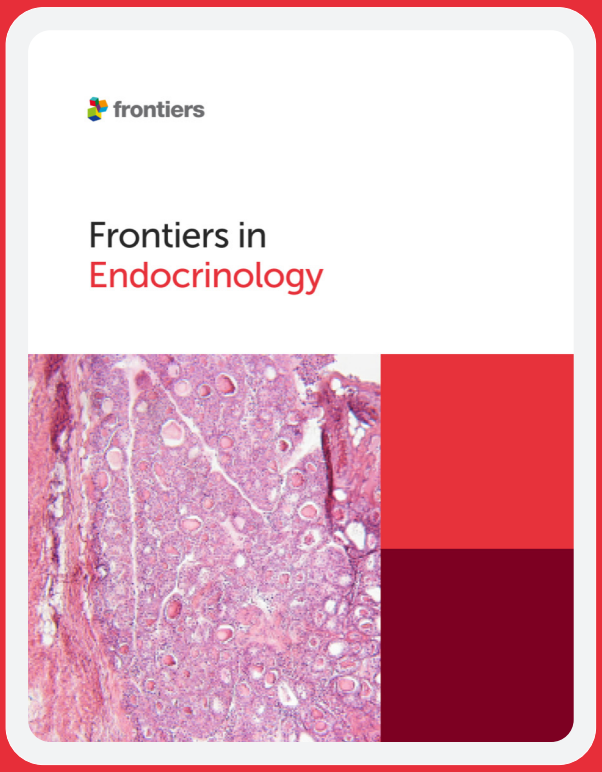

Frontiers

Avenue du Tribunal-Fédéral 34
1005 Lausanne, Switzerland
frontiersin.org

Contact us

+41 (0)21 510 17 00
frontiersin.org/about/contact